2012

Trap Efficiency of a Silted Prairie Reservoir: Rapidan Reservoir, Blue Earth County, Minnesota

Katherine Brosch Rassmussen
Minnesota State University - Mankato

Trap Efficiency of a Silted Prairie Reservoir: Rapidan Reservoir, Blue Earth County, Minnesota

By
Katherine Brosch Rassmussen

A Thesis Submitted in Partial Fulfillment of the Requirements for the Master of Science degree in Geography

Minnesota State University, Mankato
Mankato, Minnesota
May 2012

Trap Efficiency of a Silted Prairie Reservoir:
Rapidan Reservoir, Blue Earth County, Minnesota

Katherine Brosch Rassmussen

This thesis has been examined and approved by the following members of the thesis committee.

Dr. Forrest Wilkerson, Advisor
Associate Professor of Geography

Dr. Bryce Hoppie
Professor of Geology

Dr. Ginger Schmid
Assistant Professor of Geography

Trap Efficiency of a Silted Prairie Reservoir: Rapidan Reservoir, Blue Earth County, Minnesota

Katherine Brosch Rassmussen

ABSTRACT

Rapidan Dam and Reservoir are located along the Blue Earth River south of Mankato, Minnesota. The dam was constructed in 1911 as a source of hydroelectric power to supplement the surroundings communities. Currently, the reservoir is heavily silted and provides little hydroelectric benefit while proving costly to maintain. This study (1) defines the sedimentary, geomorphic, stream flow and suspended load characteristics of the reservoir for 2008-2009 and (2) compares these parameters with those available from 1985 (23 years prior).

Stream gauging and sediment sampling took place in 2008 and 2009 at three monitoring locations (two upstream and one downstream of the dam) to assess the mass balance through the reservoir. Fifty reservoir bottom sediment samples were collected for sieve and settling tube particle size analyses of grain size distributions. Multiple years of aerial photographs were also obtained to evaluate the surface area lost to siltation since 1939.

Results indicate that the trap efficiency is altered. Currently Rapidan Reservoir cannot retain the silt and clay fraction of the Blue Earth River's suspended load. In the 23 year period, the average grain size within the reservoir increased from silt to medium sand. The average maximum velocity required to deposit that sediment has also increased by more than a factor of ten, (i.e., from 0.27 to 3.20 cm/sec). The increase in velocity corresponds to the accumulation of numerous sandbars that decrease the area for water to spread out in the reservoir. This association of cause and effect is supported by the analyses of eight aerial photographs dating from 1939 to 2006 that show that the overall surface area in the reservoir has decreased by 56% since the late 1930's. Increased velocities also provide the mechanism to incise and channelize the Blue Earth River through the reservoir and remobilize previously deposited sediment. Stream flow and loading results from 2008 and 2009 show that the reservoir serves as a source for suspended sediment to downstream reaches of the Blue Earth and Minnesota Rivers.

A study of this nature paired with follow up studies could inform decision making processes for either removal or further rehabilitation. Removal would provide an excellent opportunity for researchers to study a large scale experiment in river restoration, both the positive and negative effects from reopening a waterway that has been segmented for over a century.

Acknowledgements

First and foremost, I would like to graciously thank Dr. Bryce Hoppie of the Geology Department. This project could not have been completed without his continued help, oversight and support, for which I am very much appreciative.

A very special thank you to Dr. Forrest Wilkerson (advisor) and Dr. Ginger Schmid of the Geography Department for serving as members of my committee, answering many of my numerous questions and for pushing the finalization of my thesis forward while also dealing with the loss of a family loved one.

Many thanks go out to those who assisted with the data collection and analyses related to this project; undergraduate students Scott Hommerding, Ryan Beuc and Jonathan Stoltman and fellow graduate student Mike Merlini. Thank you also to Rick Moore of the Water Resources Center at Minnesota State Mankato for sharing his expertise and insight on GIS and IDW interpolations.

Finally, I would like to thank my entire family for their continued support through this long process. To my husband Luke, thank you for maintaining the household and taking care of our dog while I stayed late after work night-after-night to finish my paper. Thanks also to my mother Rosemary, who would not let me walk away and who continuously supported and encouraged me along the way.

TABLE OF CONTENTS

LIST OF FIGURES

LIST OF TABLES

LIST OF APPENDICES

ACRONYMS

BEC	Blue Earth County
BER	Blue Earth River
cfs	Cubic feet per second
CSAH	County State-Aid Highway (county road)
GIS	Geographic Information System
IDW	Inverse Distance Weighting
lbs	Pounds
mg/L	Milligrams per liter
MPCA	Minnesota Pollution Control Agency
MSU	Minnesota State University, Mankato
MVTL	Minnesota Valley Testing Laboratory (in New Ulm, Minnesota)
TSS	Total Suspended Solids
USACOE	United States Army Corps of Engineers
USDOI	United States Department of the Interior
USGS	United States Geological Survey
WRC	Water Resources Center, at Minnesota State University, Mankato

CHAPTER 1: INTRODUCTION

1.1 Regional Overview

1.1.1 Lake Pepin, a Threatened Water Body Downstream of the Rapidan Reservoir

Lake Pepin is a naturally impounded lake along the Mississippi River on the Minnesota-Wisconsin border, 80 km (50 miles) downstream from the twin cities of Minneapolis and St. Paul (Figure 1.0). Formed approximately 10,000 years ago by an alluvial fan of the Chippewa River in Wisconsin, the lake is an important commercial and recreational resource for the surrounding region. Recent studies reveal that the rate of sedimentation is greatly accelerated compared to pre-settlement land use conditions (Engstrom and Almendinger 2000, Engstrom et al. 2008). Although natural processes would completely fill the lake within 3,000-4,000 years (MPCA 2005, Kelley and Nater 2000), sediment is currently depositing on the lake bottom ten times faster than pre-settlement rates and will completely fill the natural reservoir within 340 years. Consequently, the lake will lose all economic and recreational value in less than 100 years (Sekely 2002). Since 1830, approximately 17% of the lake's volume has been replaced by deposited sediment (Engstrom et al. 2008). The increase in sediment is attributable to significant land use

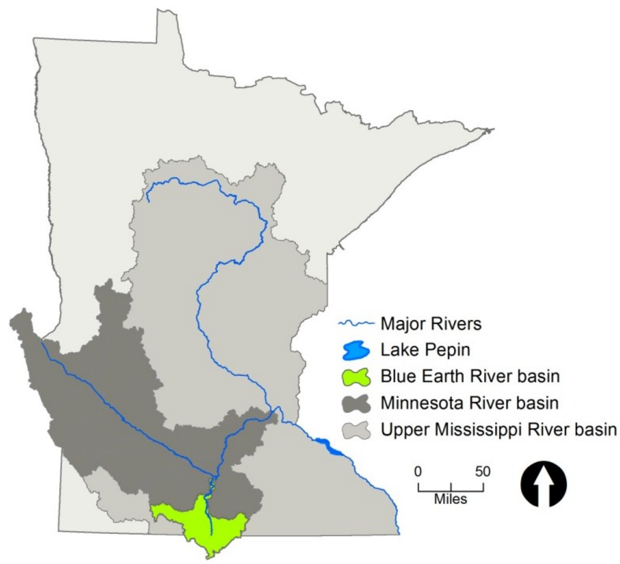

Figure 1.0: Location of Lake Pepin in relation to the Blue Earth and Minnesota River basins

changes over the past 180 years including the transformation from natural prairies to agriculturally dominated landscape as well as increases in population and municipalities. Once Lake Pepin fills in, its natural function as a downstream filter of suspended solids will diminish (MPCA 2005).

To assess state water bodies, the state of Minnesota developed expected ranges for sediment concentrations in addition to state-wide water quality standards. However, because Lake Pepin is dissimilar from the typical glacially sculpted lakes throughout Minnesota, state and citizen groups have pushed for site-specific standards for Lake Pepin. The proposed draft standards require sediment in the channel upstream from Lake Pepin to be reduced by 50%. Meeting this goal will require significant reductions from the Minnesota River (LPLA 2009), a tributary of the Mississippi River that supplies 85-90% of the sediment to Lake Pepin (Kelley and Nater 2000; MPCA 2005).

1.1.2 The Minnesota River, a Contributor to Lake Pepin and Receiver of Blue Earth River Waters

The Minnesota River is 540 km (335 mile) long and is ranked as one of twenty rivers in the nation seriously threatened by pollution (MRBJPB 2002). Pathogens, sediment, phosphorus and nitrogen all contribute to reduced water quality in the basin (Mulla and Mallawatantri 1999). Every year, 566,990 metric tons (625,000 tons) of total suspended sediment (TSS) are transported by the river and transferred to Mississippi River near Fort Snelling, Minnesota (Senjem et al. 2002). While research shows that the Minnesota River delivers the majority of the sediment load to Lake Pepin (MPCA 2005), it disproportionally contributes only about 25% of the flow (Sekely 2002). Over a five-year period, the cumulative total suspended solid (TSS) load at Judson, Minnesota (above the confluence with the Blue Earth River) was calculated at 1.6 million metric tons (1.8 million tons), while it increased downstream to 4.9 million metric tons (5.4 million tons) at St. Peter (Figure 1.1). This increase, over 300% total, results from contributions of TSS from the Greater Blue Earth River watershed which discharges between the two gauges, as well as near-channel sources within the Middle Minnesota watershed (MPCA 2009).

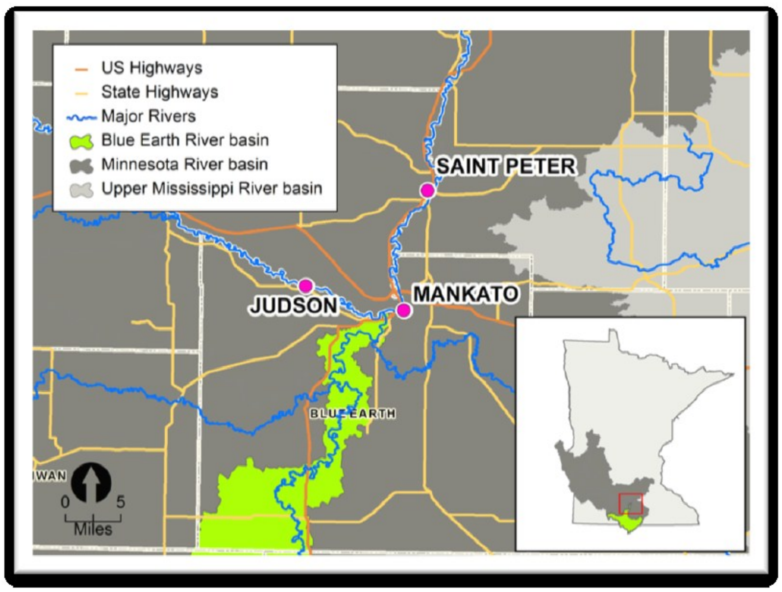

Figure 1.1: Location of Blue Earth River outlet to the Minnesota River at Mankato with respect to the towns of Judson and St. Peter, Minnesota upstream and downstream along the Minnesota River

1.1.3 Blue Earth River, an Impaired Waterway with an Ineffectual Dam

The Greater Blue Earth River is a major sub-watershed of the Minnesota River Basin and is comprised of the Watonwan, Le Sueur and Blue Earth Rivers. The Greater Blue Earth is the source of 55% of the suspended solids load to the Minnesota River

(Mulla and Mallawatantri 1999). The Blue Earth River ecosystem is degraded by transformations in the natural geomorphology and changes to the land use that modify its hydrologic and sediment transport regimes, most notably the conversion from a wetland dominated prairie landscape to row-crop agriculture (WRC 2000). Agricultural land use practices currently account for 92% of the basin's land-use (Boone 2000), which in turn led to the loss of 86% of wetlands within the once natural prairie pothole landscape (USACOE 2009).

Water moves through the watershed by an intricate network of artificial drainage made up of public and private ditches and subsurface tile systems (USACOE 2006, USACOE 2009). Along with the complex web of subsurface drainage, numerous small natural streams were straightened and deepened to help with row crop productivity and to control water from tile runoff.

In addition to agriculture, the regional geology significantly influences the hydrology of the Greater Blue Earth River watershed. With the final retreat of the Des Moines lobe of the Wisconsin ice sheet approximately 13,400 years ago, melt water from the receding ice became impounded by a natural dam created by a low moraine in Western Minnesota (Gran et al. 2011, Matsch 1983). The impounded water created a vast lake called Glacial Lake Agassiz (Figure 1.2) which covered north western Minnesota, eastern North Dakota, Manitoba and western Ontario. Around 11,500 radiocarbon years B.P., the Minnesota River valley was catastrophically excavated following failure of the natural impoundment on the southern end of Glacial Lake Agassiz (Gran et al. 2011). The sudden flush of the glacial River Warren carved a deep and wide valley in that the now under fit Minnesota River now resides (Matsch 1983). Many existing low-gradient tributaries were left abandoned and elevated on the landscape and have since been incising through the fine-grained glacial till and lacustrine sediments to once again reach equilibrium (Gran et al. 2011). Headwater streams are typically incised 12 to 23 meters (40 to 75 feet), while the channel of the Blue Earth River has eroded nearly 46 to 61 meters (150 to 200 feet) of the post-glacial till plain near the mouth of the river at Mankato (MPCA 2005).

Figure 1.2: Extent of Glacial Lake Agassiz across Minnesota, North Dakota, Manitoba and Ontario. The outflow of Glacial Lake Agassiz was through the Glacial River Warren, now occupied by the Minnesota River. Map from the Minnesota Historical Society.

While agriculture and geology are significant, there are additional anthropogenic effects. Developed urbanized areas account for 286 km^2 (70,600 acres) of impervious surfaces (concrete, pavements, roofs) within the Blue Earth River watershed (Boone 2000). In addition, thirteen wastewater treatment plants and two water treatment plants exist along with eleven major agriculturally related industries. Furthermore, there are 36 small unsewered communities and subdivisions and an unknown quantity of straight pipes to ditches, and ravines that discharge organic waste directly into the river (WRC 2000). The construction of Rapidan Dam and resulting reservoir along the main stem of the Blue Earth River has also played a role in altering the sediment transport throughout the basin over the past 100 years.

This thesis project focuses in on the Rapidan Dam and reservoir in an attempt to compare and contrast the sediment characteristics with similar data collected in 1985. The 1985 results, originally presented in Quade et al. (2004) are reinterpreted with statistical measures to more fully characterize the distribution of sedimentary particle sizes throughout the reservoir. Comparable sedimentary samples from the reservoir were collected in the fall of 2008 and winter of 2009 and subsequently analyzed for their particle size distribution. The samples were also subjected to loss on ignition (LOI) analyses to determine the fraction of sediment that was composed of detrital organic matter. Discharge and suspended solids samples were collected above and below the reservoir during the monitoring seasons of 2008 and 2009 to assess the mass balance of sedimentary load through the reservoir and thus, determine if the reservoir acts as a sink or source of sediments to downstream reaches. Finally, multiple aerial images of the reservoir from 1939 through 2006 were analyzed using Geographic Information System (GIS) tools to assess the loss of reservoir capacity due to the growth of sandbars and floodplain within the reservoir by low-gradient fluvial processes.

1.2 Problem Statement

Rapidan Dam is an aging structure that provides few hydroelectric or recreational benefits at ever-increasing costs. For example, in a typical year the dam's hydroelectric plant will produce approximately $200,000 in revenue while repairs to the dam can exceed $300,000 (Linehan 2007). Emergency repairs to correct undermining of the dam's structural integrity have previously totaled as much as $2 million (Fischenich 2007). Further illustrating this point, the dam generated $2.04 million dollars from 2002 to 2009, but cost the public $2.05 million dollars in repair and maintenance (Linehan 2009).

Given the lack of economic benefit and increasing costs, Blue Earth County, the governmental organization responsible for the dam's maintenance recently explored options for permanently repairing or removing the dam (Linehan 2007). As part of this exploration, the United States Army Corps of Engineers (USACOE) studied the cost of rehabilitating the dam for the next fifty years and found the cost to be $10.4 million dollars. A majority of those dollars are associated with building a stilling basin, a depressed area downstream of the dam that is needed to reduce the velocity and energy of water passing over the dam. The stilling basin would allow the dam to accommodate roughly 28,500 cubic feet per second (cfs) of water (just less than the 100 year flood level). Without a stilling basin, a peak flood event (such as in 1965) could cause extensive downstream undermining of the dam and eventually lead to its catastrophic loss (USACOE 2009). If the dam failed suddenly, a massive, unrestrained release of water and sediment would occur and have significant deleterious public safety and environmental repercussions to downstream reaches. The study estimates the cost of alleviating those threats by completely removing the dam and restoring the original stream channel to be $29 million dollars (USACOE 2009).

Selecting the most prudent corrective action for the dam and reservoir relies on accurate estimates of cost versus benefit associated with repairing the dam, removing it, or taking no-action. While considerable time and effort was used to estimate the costs of dam repair and/or removal (see above), far less effort was expended on determining the benefits of maintaining the dam and reservoir. Specifically, the benefits to downstream water quality provided by the dam and reservoir are currently undefined and cannot be reasonably estimated from existing studies. This important limitation is implied by the easily recognized, significant changes in reservoir area and sand bar size and shape since the last time a study of sedimentary loads and reservoir characteristics was completed in 1985 (Figure 1.3). Consequently, there is currently no way of knowing whether or not the reservoir removes or contributes sediment to the Blue Earth River, how the reservoir influences hydrologic and geomorphic processes in the watershed, or if modifying the structure of the dam would impact the size, shape, and composition of the vast stores of sediment currently residing behind the dam.

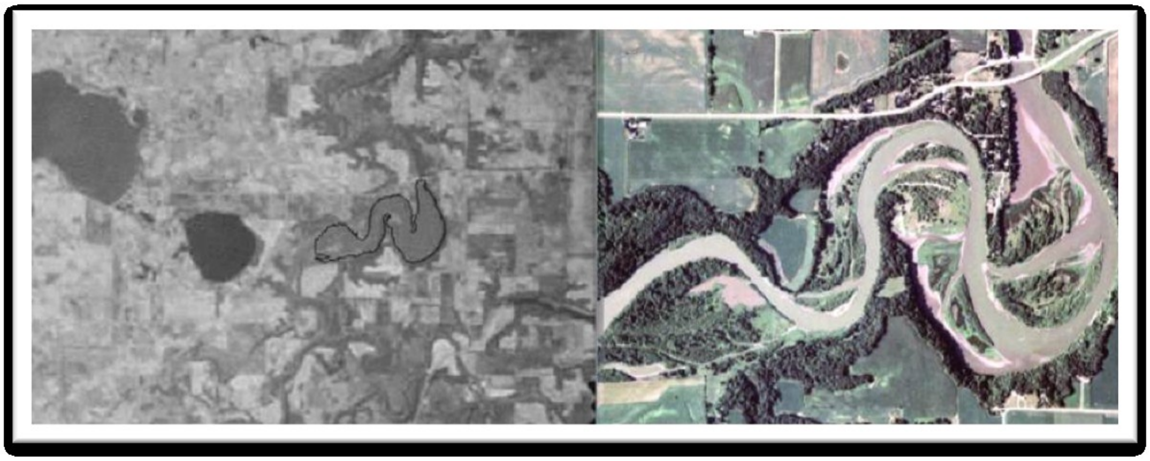

Figure 1.3: Aerial view of Rapidan Reservoir in 1985 (left) and 2006 (right). The 1985 image is the only available for that year. Note the obvious geomorphic variability between the two years.

1.3 Hypotheses

The sediment loading characteristics of Rapidan Reservoir are unknown as to whether the reservoir serves as a sink (trap) or source of suspended solids to the Blue Earth River and downstream reaches. Further study is warranted. The principle problems addressed in the problem statement can be answered by testing the following hypotheses.

H_0: Sedimentary characteristics and the ability to retain particles within Rapidan Reservoir are consistent with a previous study conducted in 1985.

H_1: Due to settling and landform evolution, additional trap efficiency is built into the reservoir. Rapidan Reservoir will serve as a trap for suspended solids to downstream reaches. The summed contribution of upstream TSS loads will be greater than TSS loads out of the reservoir. Fine clay, silt and sand fractions will be retained within deposited sediments.

H_2: The reservoir has lost trap efficiency and serves as a pass through intermediate base level or additional source of sedimentary material moving through the Blue Earth River. TSS loads downstream from Rapidan Reservoir will be equal to or greater than the summed contributions from upstream reaches. The reservoir will no longer be able to retain the fine clay, silt and sand size fractions.

1.4 Outcomes

This project will produce the following outcomes:

1. A total load, flow-weighted-mean concentration, yield and runoff will be calculated for two sites upstream and one site downstream from Rapidan Reservoir to assess if the reservoir is acting as a sink or source for sediment.
2. Particle size analysis will be completed along randomly selected transects within Rapidan Reservoir to characterize the particle size distribution of sediment within the reservoir under current (2008-09) conditions. In addition, 1985 results will be further interpreted using the same methodologies as the 2008-09 data. Differences between the two datasets will confirm if the reservoir is acting under similar conditions or if it has increased or lost trap efficiency.
3. Loss on ignition will be completed on the collected reservoir samples to determine the percentage of sediments that are organic versus inorganic. A high percentage of organic content within the samples could indicate long residence times within the deposited sediments.

4. Various aerial photographs will be digitized using ArcGIS to show the distribution and surface extent of sandbars within Rapidan Reservoir over time.

5. Analyses of deposited particles within Rapidan Reservoir in both 1985 and 2008-09 will provide insight into the maximum velocities required to deposit those sediments based on Hjulstrom's Diagram. Comparison of the two datasets will validate if the average velocities within the reservoir have remained constant, increased or decreased.

CHAPTER 2: LITERATURE REVIEW

2.1 Rapidan Dam History

Humans have built dams for 5,000 years (Poff and Hart 2002). At the turn of the 20th century, hydropower use was at a peak and made up nearly 60% of the electrical power demand in the United States (Halacy 1977). Today, hydroelectric power provides 10% of the total electrical power for the nation (Heintz Center 2002). Many of these structures are now deteriorating and maintenance is costly (USACOE 2001). With changing societal needs, there is now an increased demand for further study and removal of historic dams.

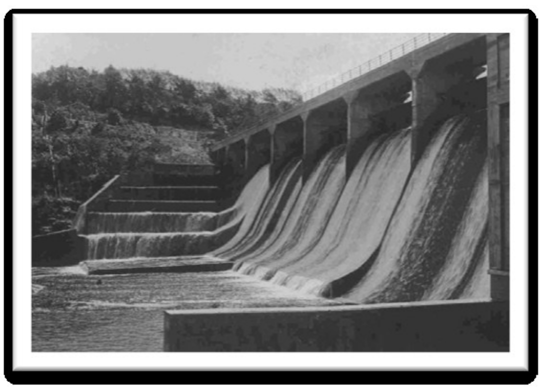

Figure 2.0: Rapidan Dam, 1911. Photo from the Minnesota Historical Society

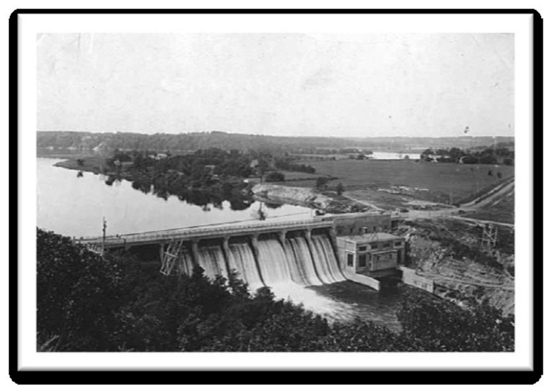

Figure 2.1: Rapidan Dam, 1920. Photo from the Minnesota Historical Society

Construction of Rapidan Dam (Figures 2.0 and 2.1) began in 1910, and operation commenced on March 11, 1911 (Quade et al. 2004). Its intended use was for hydroelectric power to supplement electricity supplies to the surrounding communities of Rapidan, Mankato, Lake Crystal and Kasota. The dam impounds the Blue Earth River twelve miles upstream from its mouth at Mankato, Minnesota. The dam was built by the

Amburson Company and was overseen by the H.M. Billesby Company of Chicago, who also owned Consumer Power Company (CPC). CPC ultimately became Northern States Power Company (Ruff 1987). The dam spans 414 feet (126 m) wide and 82.5 feet (25 m) tall, with a reservoir capable of holding a surface water area of 415 acres (1,679,445 m^2). Sluice gates (for water level control) were originally installed to help regulate the buildup of silt and sediment behind the dam, however, due to rapid sedimentation behind the gates, they failed to operate properly from the first attempt in 1911 (Quade et al. 2004). In April of 1965, significant rainfall led to an early ice breakup that resulted in a peak flow of 43,100 cubic feet per second (cfs) (1,206 m^3/sec). In comparison, the USACOE calculated the 100 year flood event to be 30,000 cfs (USACOE 2009). The rapid influx of water that occurred in 1965 caused extensive damage, rendering the dam inoperable. The dam lay unrepaired due to the lack of interest in hydroelectric power until 1975 when Blue Earth County overtook ownership (Ruff 1987). In 1983, after 18 years of hydroelectric inactivity, the dam was rehabilitated with an upgrade to the power house, reinforced structure, new tainter (water control) gates, and dredging immediately upstream of the turbine intakes. By 1984, the dam returned to full peaking operation (Quade et al. 2004). Peaking refers to inflow and outflow water rates that are not necessarily equal above and below the dam and reservoir. Peaking allows for the storage of water behind the dam and subsequent release when electrical generation is desired. Today, the hydroelectric operations at the dam are managed by North American Hydro under a lease agreement with Blue Earth County. Approximately 5% (or roughly $37,000) of the annual revenue generated by the dam is returned to the county, which also receives an additional, but temporary, $189,000 annual credit from Minnesota's Renewable Energy Production Incentive Program (USACOE 2009). Rapidan Dam has been a historic landmark to the locals for over a century. A county park with tent camping, historic Dam Store restaurant, popular fishing spot and an excellent paddling access point are adjacent to the dam itself. While the agriculturally defined southern Minnesota is not known as a tourist hotspot, this area draws in hoards of people every year for the recreation, site seeing and eatery. Many locals may feel that the dam is a historically significant structure, while others may clash and feel that the river should be restored to its natural, free flowing, unobstructed environment.

2.2 The Rapidan Dam Research Project Study

The Rapidan Research Project was a three-year study conducted by Minnesota State University, Mankato (formerly Mankato State) from 1983 to 1985 and was overseen by Professor Henry Quade. The purpose of the project was to determine "the effects of converting a run-of-the-river, unstratified reservoir, hydroelectric dam into a peaking operation." Water quality, sediment transport, synthetic organics and aquatic macro-invertebrates were the four components studied as part of the project since these organisms could be impacted by the dam conversion (Quade et al. 2004). As part of the project, a master's degree was undertaken by graduate student Greg Ruff in 1984-1985. Ruff (1987) concluded that total suspended solid (TSS) and total suspended volatile solid (TSVS) concentrations were greater at sites above the reservoir and dam than at sites below the dam. Based on his findings, Rapidan Reservoir was acting as a trap for sediment in 1985, except during brief peaking intervals lasting less than a few hours. All analyses by Ruff involved a review of concentration data alone (above, within and downstream from the reservoir) and did not involve a mass balance of flow into and out of the reservoir. More recently, research shows that 8,410,103 m^3 or 11 million cubic yards of sediment exists behind the dam (Barr et al. 2000). Payne (1994) attempted a mass balance study of TSS in the Blue Earth River upstream and downstream of Rapidan Reservoir. The downstream monitoring location was not immediately below the dam, but rather was located at the outlet near Mankato, Minnesota after the Le Sueur River joins the Blue Earth River. His study involved the analyses of three separate runoff events. The first event occurred during snowmelt runoff in March 1991. Results showed that 16 percent more sediment was delivered to the mouth of the Blue Earth River than was delivered to the reservoir by the Watonwan and Blue Earth Rivers upstream from Rapidan Reservoir. As the event receded, less TSS was observed at the Greater Blue Earth River outlet than was delivered to the reservoir. It was hypothesized that the reservoir could have served as a source for sediment with increased flows and then acted a trap for sediment as flows subsided. The two following events analyzed by Payne in May and July of that same year showed an equal balance of TSS loads delivered to the reservoir and downstream to the Minnesota River (Payne 1994).

As part of the Rapidan Dam Research Project taken on by Quade et al. (2004), sediment samples were collected along 21 transects within Rapidan Reservoir during July 1985. As a general rule, the top two centimeters were collected and analyzed. In the lab, the samples were mechanically split with half being utilized for percent organic determination and half being used for grain size. All deposited reservoir bottom sediments were classified to grain sizes based on Quade (2004) (Table 2.0). Coarse grained sands and gravels were observed near the mouth of the Watonwan River and further upstream in the Blue Earth River with sand being the dominant sediment. A general decrease in sand and increase in silts and clays was detected from transect U through N (Figure 2.2). Transects M through C (closest to the dam) had nearly no gravel or very coarse sand. Areas outside of the main river channel within the reservoir had coarser sediment than within the natural thalweg. An increase in grain size was observed from transect F through transect C and was attributed to the suction effect caused by the turbines. Due to the low-energy environment found throughout most of the reservoir, limited differences or trends were seen in the dispersal of fines within the overall reservoir.

Table 2.0: Particle size class breakdown utilized by the Rapidan Research Project in 1985.

CLASS	PARTICLE DIAMETER (mm)
Pebble or larger	> 4
Gravel	2 - 4
Sand	0.062 – 2
Very Coarse Sand	1 – 2
Coarse Sand	0.5 – 1
Medium Sand	0.25 – 0.5
Fine and Very Fine Sand	0.06 – 0.25
Silts and Clays	< 0.062
Coarse and Medium Silt	0.016 – 0.062
Fine and Very Fine Silt	0.004 – 0.016
Clay	< 0.004

Total Non-Filterable Residue (TNFR), now referred to as Total Suspended Solids (TSS) were collected at sites above and below the reservoir in 1985 to characterize the effects of the peaking operation. General observations were made regarding lower TSS concentrations during lower flows and elevated concentrations with storm events or with the initial surge of the peaking operation (which acted much like a natural event). Three separate peaking events were sampled; August 9th, August 26th and August 30th. The August 9th event followed a period with many consecutive days of no power generation, compared to the August 26th and 30th events which were preceded by a run-of-the-river mode. The August 9th event concentrations were higher than the later events and it was hypothesized that the increased source was from scouring and re-suspension of bank material and deposited sediment immediately upstream from the dam. Figures 2.3, 2.4 and 2.5 illustrate the different particle size fractions within the reservoir and upstream channel. A dominance of silt and clay exists within the reservoir samples.

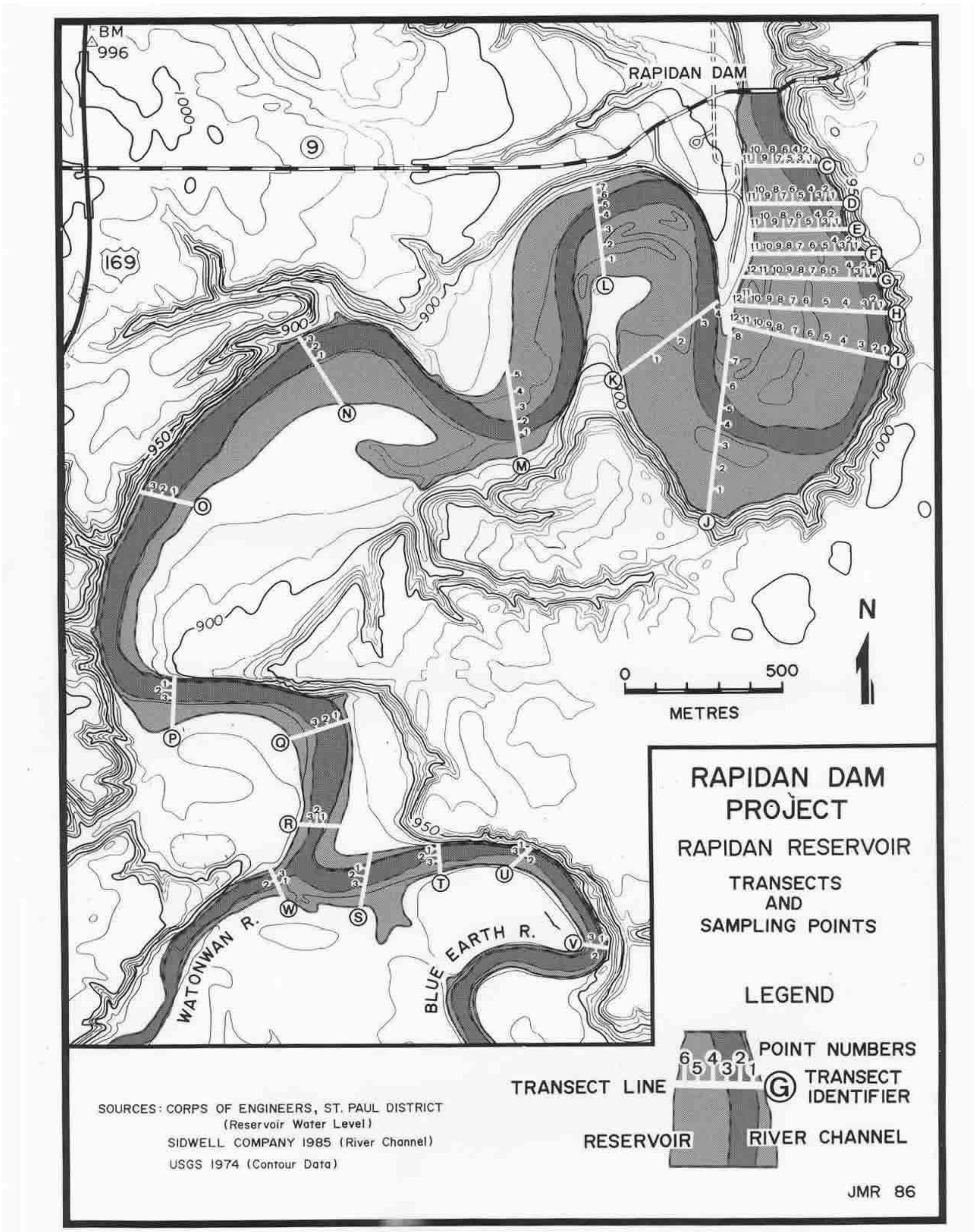

Figure 2.2: Reservoir transects and sampling sites, July 1985 (Quade 2004).

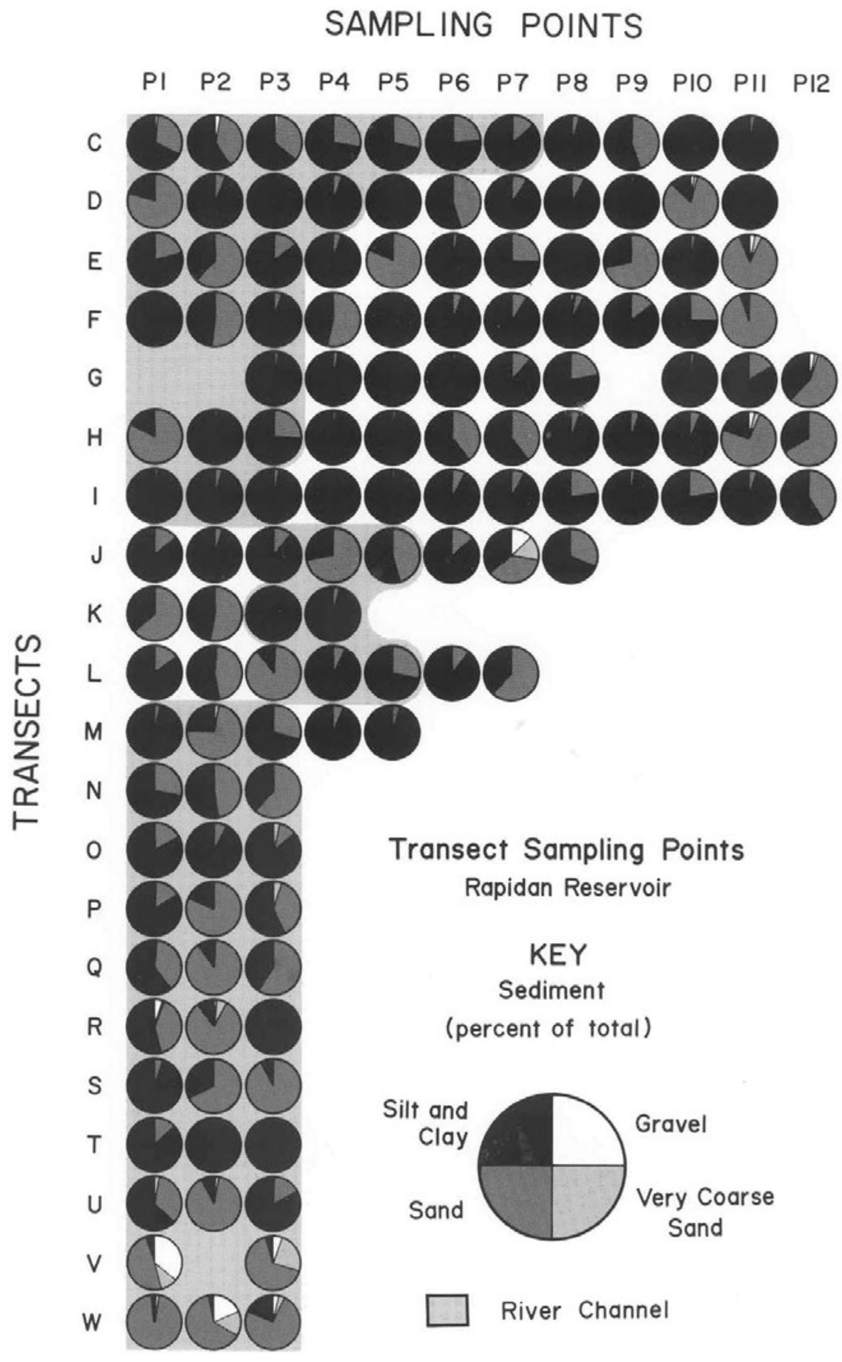

Figure 2.3: Sediment analyses of reservoir samples collected in 1985. Percent total fraction for silt and clay, sand, very coarse sand, and gravel. Further divisions of sizes are presented in Figures 2.4 and 2.5. All samples were acquired from submerged water locations, though some (background shaded gray) were collected from deeper depths indicating where the natural river channel existed prior to dam rehabilitation in 1984-85. Figure reproduced from Quade et al. (2004).

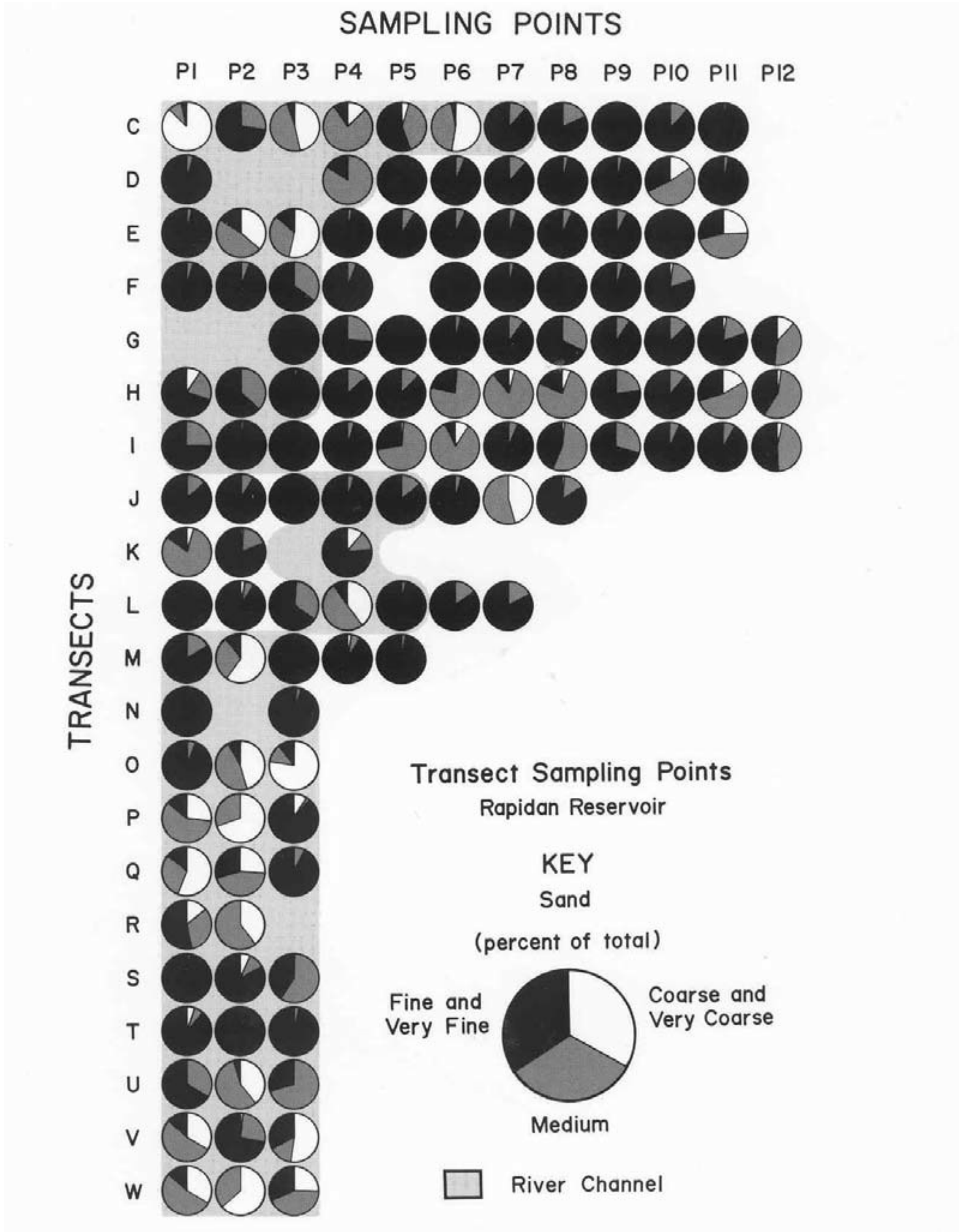

Figure 2.4: Sand analyses of reservoir sediment samples collected in 1985. Percent total fractions for fine and very fine sand, medium sand and coarse and very coarse sand. All samples were acquired from submerged water locations, though some (background shaded gray) were collected from deeper depths indicating where the natural river channel existed prior to dam rehabilitation in 1984-85. Figure from Quade et al. (2004).

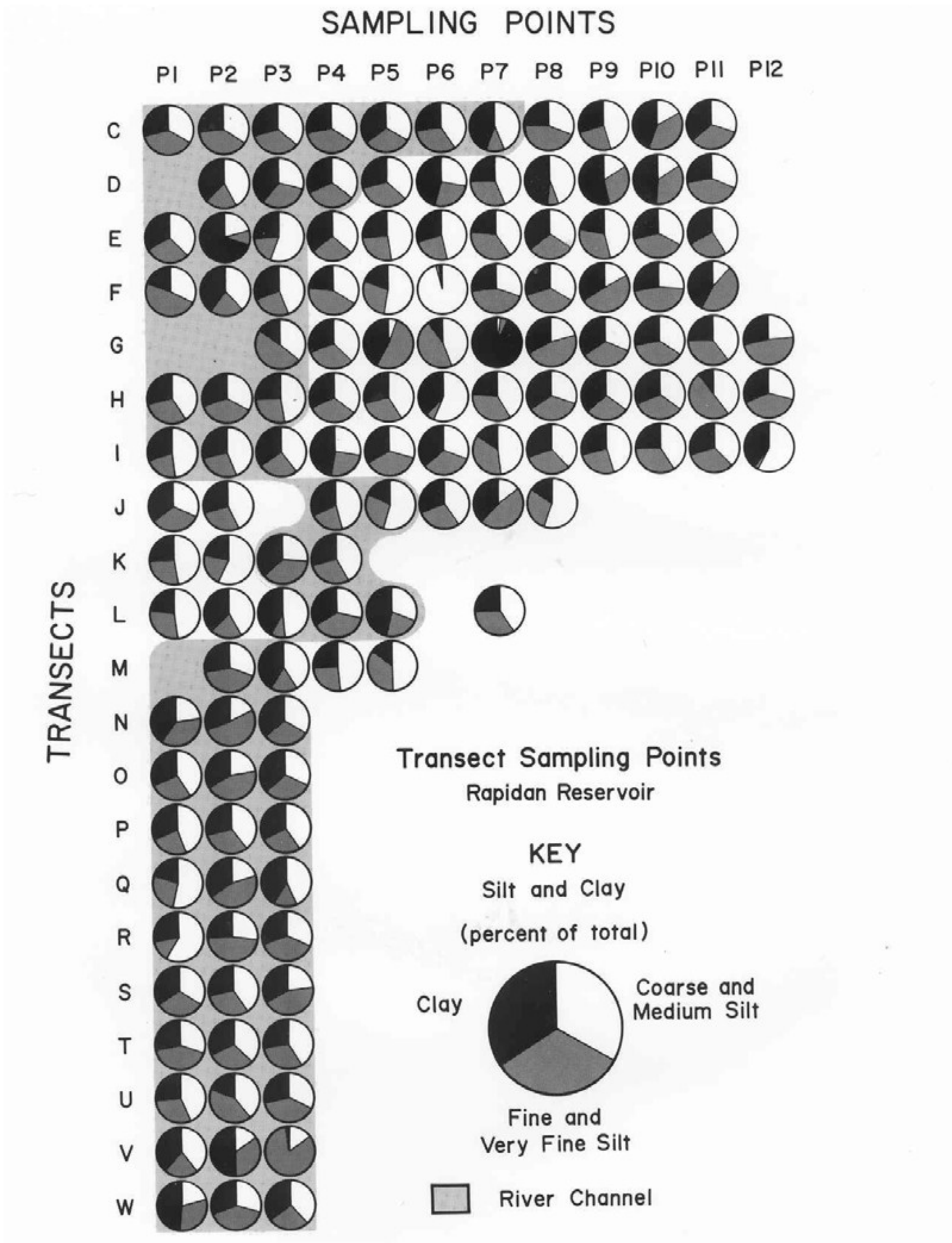

Figure 2.5: Silt and clay analyses of reservoir sediment samples collected in 1985. Percent fractions for clay, fine and very fine silt, coarse and medium silt. All samples were acquired from submerged water locations, though some (background shaded gray) were collected from deeper depths indicating where the natural river channel existed prior to dam rehabilitation in 1984-85. Figure from Quade et al. (2004).

2.3 Upland versus Stream Bank Erosion

Exposed soil from cultivated farm fields is often blamed as the primary source for sediment in the Greater Blue Earth River Basin and in downstream Lake Pepin. However, agricultural producers who manage fields adjacent to streams, ditches and ravines often share accounts of productive land lost to stream bank erosion, mass wasting and slumping. In the Dominican Republic, contrary to historic beliefs, it was believed that the majority of erosion problems stemmed from the cultivation of steep slopes. A study using Cesium-137 found that only 17% of sediment could be attributed to agricultural erosion in the uplands (Nagle 2002). A study conducted by the Minnesota Pollution Control Agency (MPCA) on the Maple River (a tributary stream of the Le Sueur and subsequently Greater Blue Earth River) found that 40% (arithmetic 5 year average) of the seasonal TSS load was from stream bank erosion. The same study found similar results for the Watonwan River (41%) and a range of 20-38% at other tributary sites within the Minnesota River basin. Using airborne laser scanning on the Blue Earth River, Thoma et al. (2005) found the mass wasting from stream bank erosion ranged from 23-56%. Furthermore, Sekely (2002) studied seven major stream banks along the Blue Earth River from 1997 to 2000. Findings showed that TSS loading contributions ranged from 31% to 44%. This range in values represents the maximum and minimum extents based on two different area calculation methods. The wide range of stream bank contribution results suggests that different techniques provide varied outcomes. In addition, most studies are based on limited river sections due to the difficulty in accessing suitable study sites. Each individual stream bank erodes under different conditions

(Gupta et al. 2001) and pattern tiling may be leading to further incision of the channel (Blann et al. 2009).

A sediment budget was completed on the adjacent Le Sueur River basin in June 2011 (Gran et al. 2011). Geomorphology and geologic history between the Blue Earth and Le Sueur River basins are very similar with methods and results likely being transferable. The Le Sueur River sediment budget study found that roughly 50,000 metric tons per year (110,231,131 pounds) of sediment was delivered to the mouth of the Le Sueur River in pre-settlement times. Currently, with an extensive transformation of land use, vegetation and hydrology over the past 200 years, the sediment delivery rate has increased four to five fold to nearly 225,000 metric tons per year (496,040,090 pounds). This is based on a measured average from 2000-2010 (Gran et al. 2011).

The largest sediment sources to the river are identified as near-channel sediment sources from bluffs, stream banks, channel widening and incision. Ravines and uplands, once widely thought to be the main sediment contributors account for an average of 9% (ravines) and 27% (uplands), although of all the contributing factors, upland contributions had the highest percent increase since pre-settlement times (Gran et al. 2011). To reduce sediment erosion rates, the following has been suggested: Water retention should be increased in the upland areas to delay the delivery of the water to the channel. This will in turn reduce stream bank and bluff erosion. Vulnerable bluffs along the main stem of the river should be armored, direct discharges to the river should be minimized and adequate buffers should be installed. The spatial extent of ravines is small as compared to bluffs, but they are still capable of delivering sediment at high rates (Gran et al. 2011).

2.4 Dam Removal

In addition to the cost of maintenance, studies, repair and removal, dams are historically known to degrade adjacent environments. Rapidan Dam obstructs aquatic navigation from the Mississippi and Minnesota River systems to nearly 1,200 miles of tributary streams above the dam. While the current reservoir has limited holding capacity for hydroelectric generation, it does provide some value for recreational use (fishing and boating) as well as conservation (waterfowl and aquatic habitat) (USACOE 2009).

Dams modify the normal hydrologic behaviors of a river and ultimately transform the river's physical and chemical dynamics. Reservoirs inundate natural channels, floodplain habitats, and existing ecosystems while fragmenting river corridors and trapping sediment sources from downstream locations. Water concentrated with nutrients, pesticides, herbicides and heavy metals can transport these contaminants where they will accumulate within sediment on the bed of the reservoir (Heintz Center 2002). Once a dam structure is removed, the river segments and aquatic ecosystems will be reconnected and re-established. However, the sediment and any attached contaminants could be remobilized to downstream locations. When a reservoir is initially established, it will have a tendency to improve downstream water quality, acting as a trap for sediments and other contaminants (Heintz Center 2002). As water from a river enters a reservoir, its cross sectional area increases while its velocity decreases. This action allows some suspended solids to settle out of the water column. An example of this process, called siltation, is provided in Chinese rivers and reservoirs where sediment deposition has led to the loss of 66% of that nation's reservoir capacity (Wang and Hu 2009). Specifically, the Manwan Dam on the Upper Mekong River in China lost 21.5-22.8% of its storage capacity over an 11-year period (1993-2003) (Fu et al. 2008). Furthermore, a regional study conducted by Crowder estimated that 0.22% of the storage provided by both lakes and reservoir in the nation is lost annually, of which 24% is from cropland erosion and subsequent siltation (Crowder 1987). Reservoir sediments are easily eroded, and are not stabilized by roots and vegetation unless the accumulated sandbar has been exposed above the water surface for multiple growing seasons.

Dams have a working life span. After years of accumulation from the constant influx of sediment, reservoirs gradually fill in becoming less efficient at trapping sediment. Once a dam is removed, there will be an initial sediment flush until a state of equilibrium is reached (Heintz Center 2002). Prior to removal, important analysis of sediment within the reservoir should take place such as a calculation of the total volume, grain size analysis to indicate erodibility and transport potential, the potential for excess nutrients and contaminants and extensive modeling to predict the fluvial response to the dam removal (Quinn 1999).

According to Sawaske and Freyberg (2012), there are over 700 documented dam removals in the past century, 350 of which were in the last decade alone. Water quality considerations in the decision making process to remove dams are very important from a regulatory standpoint. The stream that replaces the dam is subject to evaluation against standards laid out by the Clean Water Act (Heintz Center 2002). If the downstream reach is already listed as impaired on the state of Minnesota 303d impaired waters list, additional sediment could have great implications for total maximum daily load (TMDL) studies. Although there is no Clean Water Act provision or regulation that specifically addresses dam removal, if the dam removal prompts changes to pollutant loading in the river, the US Environmental Protection Agency's TMDL requirements may apply (Heintz Center 2002). Other considerations such as biologic, economic and social outcomes all need to be well understood and evaluated as well before removal decision making occurs.

2.4.1 Biologic aspects of dam removal

In addition to the fragmentation of a river corridor, dams can completely alter area habitat characteristics (Blann et al. 2009). The overall area or length of the river that is affected by the placement of the dam is relatively small compared to the length of river upstream and downstream of the reservoir and dam that are affected biologically. Consequently, the species that depend on the river and riparian area are also influenced. Dams can create wetlands upstream over a long period of time. Removal of a structure, may create some wetlands downstream (dependent on accessibility to floodplains, terrain topography and land use), but may also be at the expense of losing the created wetlands upstream. With removal of the dam, the river may erode down through the fine sediment, disconnecting the water source from the valuable wetlands.

2.4.2 Economic aspects of dam removal

From an economic standpoint, cost versus benefit analysis should always be completed prior to approving plans for dam removal (USDOI 2003). This type of analysis can be used to put an actual measurement, whether positive or negative on the outcome of the entire removal. It can be a very complicated task, because of the difficulty in establishing environmental outcomes in a monetary scenario (Heintz Center 2002).

2.4.3 Social aspects of dam removal

Aesthetics of the dam itself and the adjacent river reaches are two social aspects when considering removal. Reservoirs may provide recreational opportunities for boating and fishing. Locals may be attached to the structure and its history. On the other hand, other interested parties may want to see the river restored to a natural, free-flowing, unobstructed state.

When considering the pros and cons, social, economic, environmental, aesthetic and recreational aspects of removing a dam and reservoir structure, numerous questions should be addressed and carefully analyzed. The answers to the questions presented below are beyond the scope of this thesis project and are provided merely to broaden the extent of this work. Results presented will provide additional information that complements socio-economic studies implied by these questions but the decision for dam removal will be based on a complete set of facts.

1) Would removal lead to unwanted invasive species, or could it potentially restore native species?

2) Are there any problems associated with potentially contaminated sediment held behind the dam?

3) Will there be a net gain or loss in wetland or habitat area?

4) In the long run, will it be more profitable to remove or repair the dam?

5) What draw would the county park have if the dam were removed?

6) Would fishing, canoeing, kayaking activities resume if the dam no longer existed?

7) Could newly created rapids in place of the existing structure actually cause a hazard or be a liability?

8) Will the groundwater table be affected at all?

9) Will there be any conflicts with current laws and regulations – EPA's TMDL or Clean Water Act?

10) What would offset the loss in hydrologic electricity production?

11) How will dam removal affect aesthetic property value in the surrounding area?

2.5 Flux Model and Pollutant Load Calculations

FLUX is a numerical model designed by William Walker of the USACOE in the mid-1980's. It is an interactive program and model intended calculate and estimate the pollutant loading of nutrients and sediment in a gauged stream over a predetermined time period (Walker 1996). During 2007-08, the MPCA provided funding to the USACOE to convert the dated DOS-based version of FLUX into a Windows-based version. This new system, $Flux_{32}$, is still undergoing minor modifications but has increased the usability of the model (MPCA personal communication, 2010).

Required input data for the $Flux_{32}$ model includes water quality results with corresponding instantaneous discharge values and a complete flow record (instantaneous or mean daily flows) over the specific period of interest. $Flux_{32}$ includes six calculation techniques (Walker 1996):

- Method 1 is for direct load averaging and is useful in watersheds with known point sources and for when flow and concentration are inversely related.
- Method 2 is an averaging method and multiplies the flow-weighted mean concentration (FWMC) by the mean flow over the specified time period(s). Method 3 is the same as method 2, but adjusts for bias where concentration varies with flow.
- Methods 4 through 6 are regression methods. Methods 4 and 5 are not best for data sets with a significant amount of zero flows present. These methods account for differences between the average sampled flow and the average total flow. Method 6 is also a regression method that is for use when there is a strong relationship and correlation between concentration and flow.

$Flux_{32}$ is utilized after flow and water chemistry data have been collected to interpret load results between sampling events. Continuous sampling for both flow gauging and particulates or solutes is cost-prohibitive and typically does not fall within project budgets; therefore, periodic discrete samples can be collected throughout a monitoring season over a range of flows to assist with estimating pollutant loading (MPCA personal communication, 2010). Correlations can exist between concentration and flow for some solutes. $Flux_{32}$ uses concentration versus low regression equations to estimate the pollutant load and concentration on days when samples were not collected. The output from the model is a total load and FWMC over the period of data (Walker 1996). Results can then be used to calculate a sediment yield for all pollutants based on watershed acreage.

CHAPTER 3: STUDY AREA

3.1 Climate, Landscape and the Blue Earth River Basin

The Blue Earth River watershed has a humid continental climate, defined by hot, wet summers and cold winters which falls under the Koppen climate classification zone of Dfa. Spring and fall precipitation tends to favor widespread, persistent accumulation events whereas summer precipitation is more convection-driven. During summer, the region can experience brief, intensive, localized high-volume precipitation events. Annual precipitation totals within the watershed range from 27-33 inches, with 4-5.5 inches of runoff being generated on average. Approximately 84% of precipitation falling within the watershed is utilized as transpiration or leaves as evaporation while 16% exits the watershed as runoff through the Blue Earth River (MPCA 2005). Long term precipitation records show increasing rainfall totals, including intensity and duration (Seeley 2008). Figure 3.0 shows a overall increase in precipitation totals from northwest to southeast in the Minnesota River basin.

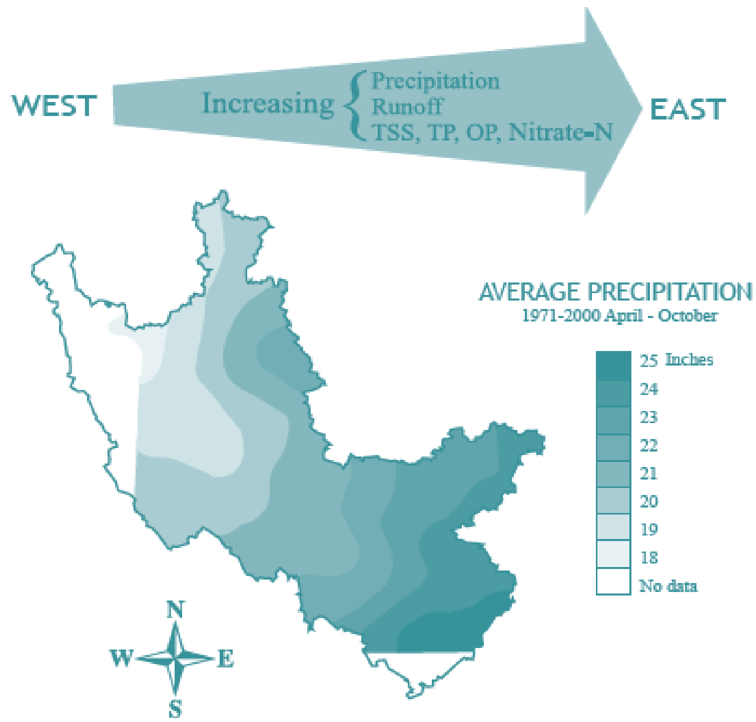

Figure 3.0: Increasing average precipitation from west to east in the Minnesota River Basin. Graphic: Minnesota River Trends Report, November 2009.

Monthly sediment loading for the twelve major watersheds of the Minnesota River basin generally increases from west to east across the basin. Differences among the water quality of the basin are primarily due to the mean annual precipitation ranging from 22 inches on the western portion of the basin to 33 inches on the eastern side. The Greater Blue Earth River Basin drains the area of highest rainfall and runoff in the Minnesota River Basin (Payne 1994). Mean annual runoff therefore ranges from two inches to eight inches from east to west. Moreover, a steeper landscape and wetter climate, along with more erodible soils in the eastern portions are also responsible (Mulla and Mallawatantri 1999). Due to the inconsistency in climate differences, runoff intensity is also variable, along with pollutant loads from west to east. During the 2002 monitoring season, runoff varied from one inch to over eleven inches across the basin (WRC 2003) and in 2003 runoff ranged between one to six inches from west to east (WRC 2004).

The Greater Blue Earth River watershed consists of discharge from the Blue Earth, Watonwan and Le Sueur Rivers (Figures 3.1 and 3.2). The watershed encompasses five Minnesota counties: Faribault (39.3%), Martin (39.3%), Blue Earth (10.1%), Jackson (7.1%) and Freeborn (4.0%) (Figure 3.1). The four largest towns in the basin are Mankato, Blue Earth, Fairmont and St. James with a total population of roughly 95,000 inhabitants in 51 municipalities (MPCA 2006).

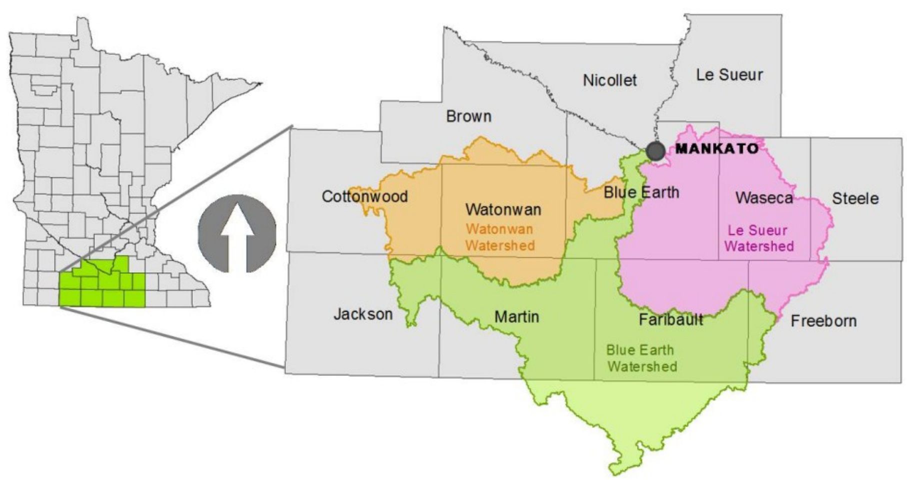

Figure 3.1: Counties located within the Greater Blue Earth River Basin. Map created by author using ArcMap 9.2.

Originating in Kossuth County, Iowa and flowing north to its confluence with the Minnesota River at Mankato, the Blue Earth River (BER) basin covers nearly 3,476 square miles (9,003 km^2), with 3,152 square miles (8,164 km^2) residing within Minnesota borders. The main stem of the river is nearly 140 miles (225 kilometers) in length and erodes through a valley of glacial drift and till, creating steep sided ravines at dispersed locations as the river gradually cuts down closer to the elevation of the Minnesota River (MPCA 2000, Waters 1977). Land use within the Blue Earth River basin consists of 85.3% cultivated crops, 6.9% developed, 2.1% grassland, 2.6% wetlands and 1.5% open water. The remaining percentage comprises pasture/hay and barren lands (WRC 2012).

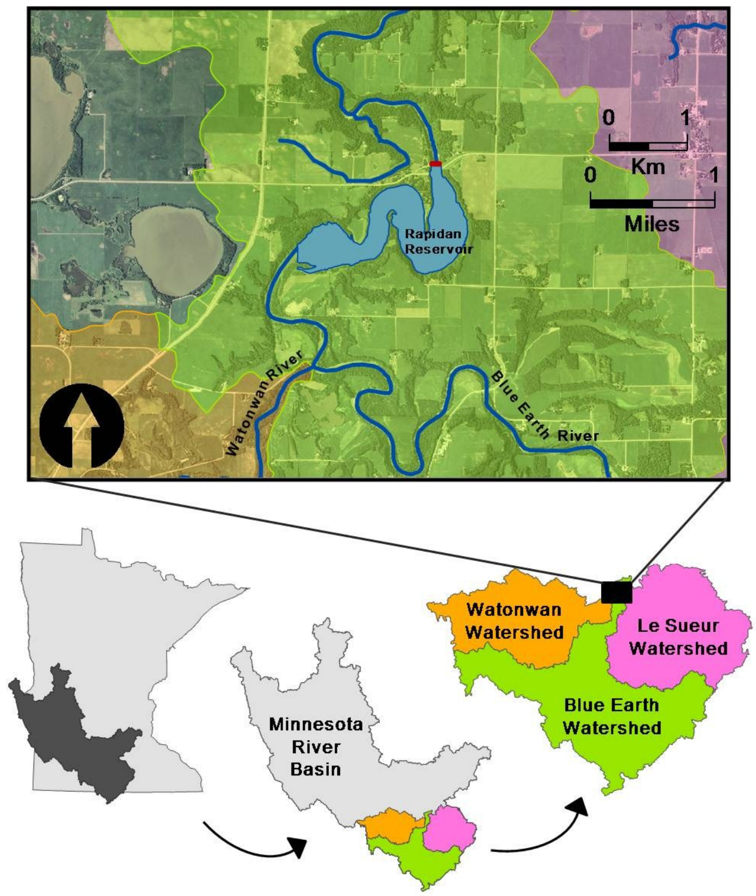

Figure 3.2: Location of Rapidan Reservoir. Map created by author using ArcMap 9.2.

Upstream of Rapidan Reservoir, the slope of the river is three feet per mile (0.56 m/km); while downstream of the reservoir it is five feet per mile (0.95 m/km) (Quade et al. 2004); the overall gradient is 0.6 m/km (Waters 1977). The Watonwan River empties into the BER 16.3 miles upstream, and the Le Sueur River merges 3.3 miles upstream from the confluence with the Minnesota River at Mankato (WRC 2000). Collectively, the Greater Blue Earth River watershed accounts for 46% of the flow in the Minnesota River at Mankato. Rapidan Dam is located 12.0 river miles upstream from the mouth of the Blue Earth River at Mankato and 1.7 miles (2.8 km) west of the small rural town of Rapidan, Minnesota (Section 7 and 8, T107N, R27W and R28W). The reservoir as it existed in 1911 was capable of covering 415 acres. The majority of inundated land reached from the dam to three river miles upstream, with some effects of water level alteration evident to over five miles upstream. The widest span of the valley containing Rapidan Reservoir is approximately 0.3 miles.

The landscape in the western portion of the Blue Earth River watershed is level to gently rolling till deposits that are a blend of poorly drained loamy soils of 0-2% slope with well drained loamy soils of 2-6% slope. In the eastern half, a nearly level terrain of very poorly drained clay or silty soils is present where the glacial Lake Minnesota was once situated. A mixture of till plains and moraines (2-12%) also dot the landscape (MPCA 2005).

3.2 Sampling Locations

Three sampling locations were chosen to effectively study contributions to and from the reservoir, two upstream from the reservoir and one immediately downstream (Figure 3.3). One of the two monitoring locations upstream from the reservoir is located on the main stem of the Blue Earth River (BEC34). This site is situated upstream from where the Watonwan River enters the Blue Earth River. The second upstream monitoring station is located near the outlet of the Watonwan River (BEC13W). The third monitoring station is just downstream from Rapidan Dam at an existing USGS gauging station (BEC9).

- **<u>BEC9</u>**: Blue Earth River, 900 feet downstream from Rapidan Dam (downstream left bank), off of CSAH 9. Access to the site is via Rapidan Dam County Park at the established USGS gauging station.
    - Latitude: 44.0931 °N
    - Longitude: -94.1080 °W

- **<u>BEC13W</u>**: Watonwan River, 7.75 river miles upstream from the confluence with the Blue Earth River at CSAH 13, 1 mile west of Garden City, Minnesota. This site is located at the established USGS station.
    - Latitude: 44.0462 °N
    - Longitude -94.1947 °W

- **<u>BEC34:</u>** Blue Earth River, 7.5 river miles upstream from Rapidan Dam, at CSAH 34, 2.5 miles south west of Rapidan, Minnesota.
    - Latitude: 44.0682 °N
    - Longitude: -94.1003 °W

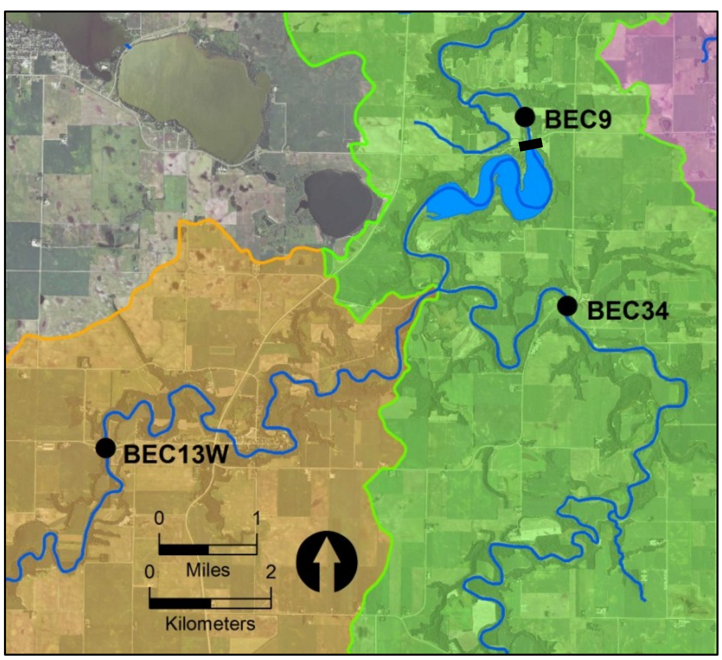

Figure 3.3: Sampling site locations with respect to Rapidan Reservoir.

CHAPTER 4: METHODS

4.1 Field Methods

4.1.1 Collection of Water Samples for TSS Analyses

The following section will explain the methods of collecting water samples for use in determining the mass balance of TSS in Rapidan Reservoir. All three monitoring locations were sampled on the same date, in the order of BEC34, BEC13W, and BEC9 last. The need and intensity of sample collection was conducted based on the amount of flow. Ideally, samples were collected and spread evenly throughout the entire range of flows over a monitoring season (from peak storm events to base flow conditions). In order to calculate the most accurate load at the end of the monitoring season, 20-25 samples were collected between March (when the river became ice free) and October or November, depending on autumn rain events. Grab samples were collected at sites BEC13W and 34 by lowering a one gallon pail into the river underlying the downstream (northern) guardrails of county highway bridges at each site. The bucket was rinsed at least three times with river water prior to acquiring a representative sample. At both locations, the pail was lowered into the river at three to four locations, allowed to become fully submerged, and then vigorously stirred prior to having a portion of the retrieved water transferred into a four-liter glass amber bottle.

Because BEC9 does not have a bridge, samples at this location were acquired by utilizing a “swing sampler”. The apparatus consisted of a 750mL polyethylene bottle attached to the end of 12-foot long pole. The bottle dipped into the BER at BEC9 from the west bank of the river and/or multiple times to acquire 4L samples similar to those obtained from BEC13W and 34.

Samples were chilled on ice and refrigerated to minimize post-sampling biologic activity until they could be analyzed for TSS per standard methods (SM2540D, see below). Date and time were documented as well as observations about the physical appearance of the river, the recreational suitability and recent weather patterns during each sampling event. In addition, a bridge-to-water measurement (or tape down) was taken from the USGS wire-weight gage to assure that the pressure transducer (stage measurement device) was tracking correctly at site BEC34. Rainfall data were available from a long term network rain gauge at Mankato, Minnesota.

Flow measurements were taken roughly every five weeks at various flow regimes to produce accurate results for rating curve development. Standard USGS stream gauging methods (Rantz 1982) were followed. During high flow conditions (i.e., water depth >1m), flow measurements were collected using a Price type AA current meter affixed to a 30 pound sounding weight whose depth in the stream was controlled by a USGS standard sounding reel mounted to the Rickly Hydrologic bridge board. During low flow conditions, the current meter was attached to a wading rod and measurements were acquired by fording the river. Calculated continuous flow records were produced by linking the gauging results with continuous stream stages recorded by a Solinst Levelogger (datalogging submersible pressure transducer) installed in a stilling well immediately downstream of the BER Blue Earth County CSAH 34 bridge crossing. Finalized flows for BEC13W and 9 were obtained from the existing USGS gauging stations located on site. Gauging methods at those sites also follow protocols outlined in Rantz (1982).

4.1.2 Rapidan Reservoir Sediment Samples

Reservoir sediment samples were collected in the fall and winter months at varying times: November 2007, January and February 2008, November 2008 and February 2009. In November 2007, the Minnesota State University Biology Department motor boat was used to collect samples in open water. The remaining majority of samples were collected when significant ice (up to 1 meter thick) covered the reservoir and therefore were able to be accessed by foot. A gas powered Jiffy ice auger with a 10" diameter cutting blade was used to cut through the ice to open water.

Figure 4.01: Minnesota State University Water Resources Center boat on Rapidan Reservoir, November 2007.

The sampling apparatus consisted of a 500 mL metal can that was bolted and hinged to a steel sampling rod. When lowered to the reservoir bottom, the can would rotate into a horizontal position and then it would be dragged for a short distance to capture a portion of the upper two inches of river bottom at each sampling site. The can was rotated into a vertical position and raised slowly through the water column to eliminate any washing and loss of fine particles from the sample. This process was repeated multiple times in the same location to ensure an adequate amount of sample was obtained (between 200-2,000 g). Samples, including water from the sampling can were poured into large Ziploc™ freezer bags and labeled appropriately. Latitude and longitude coordinates for each sample location were collected using a handheld Garmin GPS device. An 18-lb pry bar and Estwing Gad Pry bar were used to collect samples of frozen sediment through the augered holes that were drilled in shallow locations where ice was grounded on the river/reservoir bottom.

Figure 4.02: Augering sampling holes on the Rapidan Reservoir, January 2008.

4.2 Total Suspended Solids Analyses

Standard method 2540D was used to determine TSS on water samples from BEC 9, 13W, and 34. Each analysis required the preparation of a 47 mm diameter Pall glass fiber filter paper by firing at 550° Celsius for at least 15 minutes. The paper was cooled, weighed, and placed in a laboratory oven at 105° Celsius for at least one hour before being allowed to cool and reweighed. The temperature of 105° Celsius was chosen because higher temperatures could pull water out of the clay layer and artificially reduce grain sizes which would not accurately represent the mass of solids suspended in the river. If the filter paper was within 5% or 0.5 mg of the original weight, the paper could be used. If not, the procedure was repeated.

The field water samples were shaken vigorously for at least one minute to allow all particles to become resuspended. A volume of 100 to 400 mL of sample (lower volumes were used for visibly turbid samples whereas larger volumes correspond to visibly clear samples) was then slowly drawn through paper by vacuum filtration. Once filtered, the paper was placed in the oven at 105˚C for at least one hour, removed and weighed. This step was repeated. The final weight, subtracted from the initial weight of the filter paper and divided by the amount of water, gave a TSS result in mg/l.

Prior to completing the 2008 and 2009 monitoring season, some analyses were run in duplicate to show consistency. In addition, Minnesota State University Water Resources Center staff and the Blue Earth County Soil and Water Conservation District collected water quality samples at BEC13W and BEC9 for other projects associated with the MPCA. Review of results between the projects on the same day show reproducibility and consistency.

4.3 Particle Size Analyses

The particle size of sediment in the Rapidan Reservoir is important because it shows the distribution and availability of grain sizes in the surrounding exposed bedrock, glacial till or other Quaternary sediments in the localized watershed area. Also, it demonstrates the sizes of particles that are resistant to weathering and erosion and that may be available for transportation and deposition.

4.3.1 Sieve Analyses

The first step to determining the particle size distribution of the reservoir samples was to place the entire saturated sediment sample and any muddy water stored in each Ziploc bag into an aluminum baking pan. After proper labeling, samples were air-dried and then placed in a laboratory oven at 105˚C until completely void of water (typically 24-48 hours). This temperature was not high enough to begin burning particulate organic matter in the sediment.

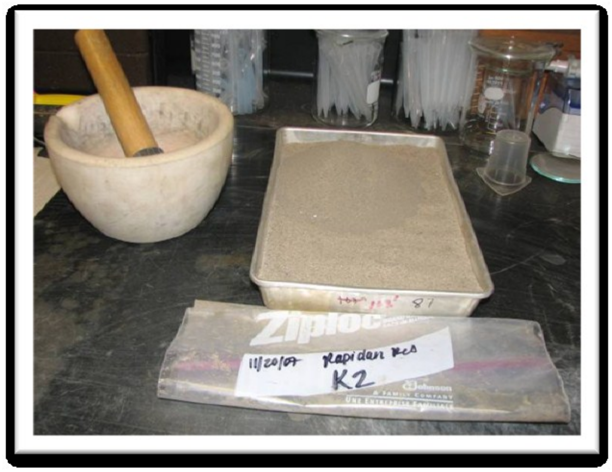

Figure 4.03: Pulverized sediment sample from Rapidan Reservoir.

Once the samples were dried, they were pulverized using a rubber pestle (mallet) and mortar to disaggregate any aggregated particles (Figure 4.03). A rubber mallet was used with care so as not to actually break apart individual grain sizes from their natural form. The pulverized sediment was split using a mechanical sample splitter (Figure 4.04) to obtain a representative sub-sample of the field sample. Once split, two identical samples were created. One of the split samples was then run through the splitter a second time, and one of the sub-samples was chosen at random for analysis. This process was done to eliminate any bias (Friedman and Sanders 1978).

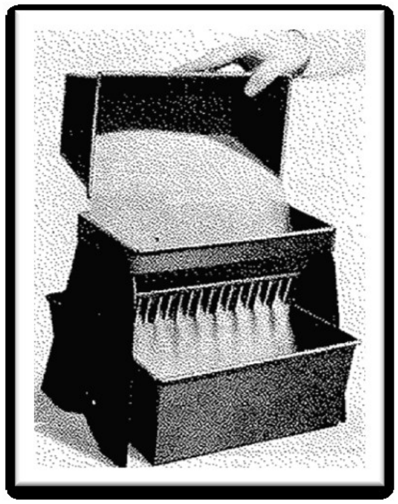

Figure 4.04: Example of mechanical sample splitter used to generate unbiased sample selection. Photo from Friedman and Sanders 1978.

A final sample size of 100-350g, depending on the visual appearance of the overall particle size, was selected for continuing study and analysis. If the sample appeared very fine, a smaller weight was used since it was likely to produce at least 15.0g of sediment from the finest sieve (sizes less than 0.0625mm) once the entire sieving process was complete. If the sample appeared coarse grained with cobbles and pebbles but also contained a significant amount of fine sand, then a larger fraction was used to attempt to get the 15.0 g of fines necessary to accurately estimate the full range of particle sizes in the (poorly sorted) sample.

The samples were weighed using a digital balance to the nearest 0.1g and poured into the uppermost or coarsest sieve (pan # ½ or a 12.7mm wire mesh opening). Table 4.0 highlights the sieves used for analysis and the associated mesh size opening or particle size. On numerous occasions, after manually shaking by hand, more pulverizing had to be done with the mortar and pestle if particles were noticeably still aggregated.

Sieving was done for at least 10 to 20 minutes for each sample with a Gilson Ro-Tap Test Sieve Shaker (Figure 4.05).

Figure 4.05: The Gilson Ro-Tap Sieve Shaker prepared for an analysis with a stack of Tyler brass sieves.

Table 4.0: Sieve screen size key.

SIEVE SCREEN #	PARTICLE SIZE / OPENING (mm)	SIZE CLASS	
½	12.7	Medium	Gravel
3½	5.66	Fine	
14	1.40	Very Coarse	Sand
45	0.354	Medium	
80	0.180	Fine to Medium	
120	0.125	Fine	
230	0.0625	Very Fine	
Bottom Pan	<0.0625	--	Silt

The contents of the sediment retained on each sieve were carefully poured one by one onto high-gloss wax paper (the wax paper was used to reduce loss by adhesion due to static electricity). It was apparent that some material did still remain on the paper as a very fine dust, and was recombined with the contents of the finest screened material. Angular grains often remained lodged in the mesh opening of the sieves. A horsehair paintbrush was used to gently brush material out of each pan and into pre-weighed beakers (Figure 4.06). If particles remained wedged, the pan was tapped evenly against a clean, smooth solid surface to dislodge the individual grains. The sediment fraction from each sieve was then weighed to the nearest 0.1 g and summed. The difference between this weight and the initial weight was used to estimate how much material was lost during sieving. The "fines" (particles less than $^{1}/_{16}$ or 0.0625 mm) were saved for further size analysis of silt and clay fractions using settling tubes.

Figure 4.06: Sieve size fractions split into separate beakers.

4.3.2 Pipette Analysis (Settling Tubes) of Fines

Sieving is not practical for particles sizes below 0.0625 ($^{1}/_{16}$) mm due to the electrostatic attraction of particles. The pipette analysis (also referred to as the settling tubes method) is a widely used method for determining the fraction of fines in a sample based on the rates at which the different particles fall in a fluid (Friedman and Johnson 1982). Each sample of fines was weighed to the nearest 15.001g and added to 5.5+/-0.001g of the chemical dispersant sodium hexametaphosphate, ($(NaPO_4)_6$). The dispersant, also known by its commercial name Calgon™, Coty, Inc., was used to eliminate fine particles from sticking together to form larger aggregates that are not individual grains. If 15g of fines were not present in a particular sample, then further analysis of the silt and clay fraction was not completed. Each sample was added to a 1,000mL glass or plastic graduated cylinder and then filled with deionized water exactly to the 1,000mL line.

Figure 4.07: Settling tubes analysis.

The sample was agitated and inverted multiple times for one minute to evenly distribute the sample particles. It was then left to sit for 24 hours to assure that flocculation (lumps) did not occur. After the 24 hours, the sample was again shaken vigorously for one minute to re-suspend all particles uniformly in the column. The time the cylinder was placed back on a flat surface was recorded as 00:00 for the analysis. After exactly one minute, the first 20 mL aliquot of water was removed and further aliquots were removed at times and depths found in Table 4.3, and placed in pre-weighed beakers.

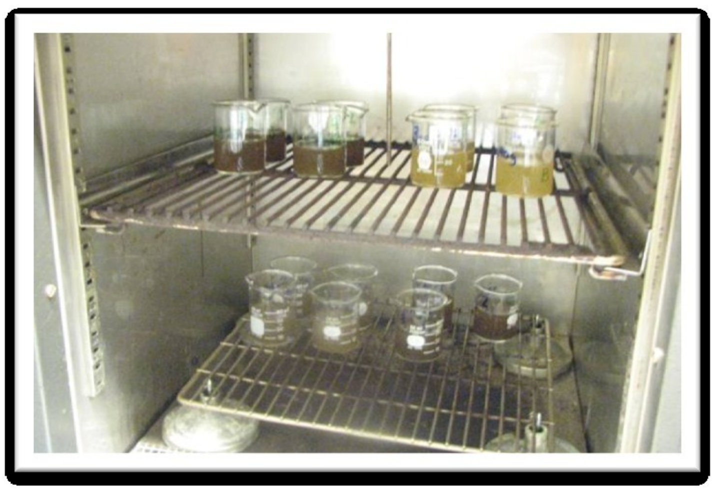

Figure 4.08: 50mL beakers derived from settling tube analysis, placed in 105˚C oven to eliminate water content and leave measurable sample fraction.

After each subsequent aliquot, the pipette was rinsed three times with deionized water and the rinse water was added to the same 50mL beaker that held the original aliquot. This method assured that all particles adhering to the inner walls of the pipette were transferred into the beaker. After each aliquot of water was collected for each sample, the labeled beakers were placed in an oven (Figure 4.08) at 105˚C until all water was driven off of the sample (at least 24 hours).

Weights of the beaker plus the dried sample were recorded to the nearest 0.001g. The weight of the dispersant (Calgon™) was accounted for by adding $^{1}/_{50}$ of the total dispersant weight to the beaker weight for each aliquot. The fraction weight was then calculated for each class size. Table 4.2 shows particle diameters from the smallest clay through boulders. Table 4.1 shows the time, depth and associated particle size diameter for the settling tube analysis.

Table 4.1: Time, velocity and particle size diameter taken from Friedman and Johnson 1982. Settling times are according to the Wadell Modification of Stokes' Law (at temperatures near 20˚C).

BEAKER #	**TIME** (Hours)	**VELOCITY** (cm/sec)	**DEPTH** (cm)	**PARTICLE SIZE DIAMETER** (mm)		**SIZE CLASS**	
1	0:01:00	0.223	20	0.062500	1/16	Very Coarse	Silt
2	0:02:59	0.0558	10	0.031250	1/32	Coarse	
3	0:11:59	0.0139	10	0.015625	1/64	Medium	
4	0:47:51	0.00349	10	0.007813	1/128	Fine	
5	3:12:00	0.00087	10	0.003906	1/256	Very Fine	
6	8:58:00	0.000217	7	0.001953	1/512	---	Clay
7	25:43:00	0.000054	5	0.000977	1/1024		
8	106:50:00	0.000013	5	0.000488	1/2048		

Table 4.2: Particle Grade-Size scale (Freidman and Sanders, 1978).

PARTICLE DIAMETER (mm)	SIZE CLASS		
2048	Very Large	Boulder	Gravel
1024	Large		
512	Medium		
256	Small		
128	Large	Cobble	
64	Small		
32	Very Coarse	Pebbles	
16	Coarse		
8	Medium		
4	Fine		
2	Very Fine		
1	Very Coarse	Sand	Sand
1/2	Coarse		
1/4	Medium		
1/8	Fine		
1/16	Very Fine		
1/32	Very Coarse	Silt	Mud
1/64	Coarse		
1/128	Medium		
1/256	Fine		
1/512	Very Fine		
< 1/512	---	Clay	

4.4 Loading Calculation

Version 3.10 (8/29/11) of $Flux_{32}$ was used to calculate TSS loads. The periods of investigation included April 1st through October 31st (7 months) for 2008, and March 1st through October 31st (8 months) for 2009 and were based on the availability of TSS results. Instantaneous (hourly) and daily average flows for BEC9 and BEC13W were obtained from the USGS long term gauging station data, available online (http://water.usgs.gov). BEC34 flow data was gauged and computed by Minnesota State University Geology professor, Bryce Hoppie, as part of this project.

Water chemistry results that were below the laboratory minimum limit of detection were represented as <2 mg/L. For the purpose of load calculations in FLUX, the value was approximated as 1 mg/L which is consistent with how MPCA staff computes loads (MPCA personal communication).

$Flux_{32}$ allows users to compute loads based on six different methods (Chapter 2.5) and allows stratification of results based on the correlations between flow or time of the year. For the purpose of this project, numerous options were attempted. Without any strata breaks entered, the data were graphically reviewed by flow and date to see where natural breaks would make sense, e.g., at the end of a large runoff event, or during base flow periods later in the season. Stratifications by flow and date were entered with two or three different strata breaks to view the range of different outcomes. The selected stratification schemes and methods were chosen with the lowest coefficient of variation values (CV) and the best agreement between methods (i.e., different methods were estimating similar total loads and FWMC). The CV is a measure of error and equals the standard error of the estimate expressed as a fraction of the predicted value (Walker 1996). A FWMC is the average concentration of the analyte passing a monitoring station over a set time period weighted by the total flow. Finalized results included the total load (kg and lbs) and the FWMC (mg/L). Results were paired with total volume of water, and total runoff based on the upstream contributing watershed.

4.5 Loss on Ignition Analyses

The percent of organic material was determined for each of the dried river bottom sediment samples collected in Rapidan Reservoir. Each sample was previously dried at 105˚C to remove any water content before the particle size analysis procedure could take place. The organic content of each sample was found by loss-on-ignition (LOI), following the procedure outlined by Dean (1974). Roughly 10 g of sediment were weighed using an analytical balance to the nearest 0.001 g. The sample was placed in a clean, pre-weighed crucible and combusted in a muffle furnace at 550˚C for one hour. Once removed from the furnace, the crucible and sample were immediately placed in a vacuum desiccator and allowed to cool for 30 minutes. Once cool, the crucible was reweighed in triplicate to find an average value which was then subtracted from the original dry sample weight. A constant sample size of 10 g was used. Samples were kept in the furnace for at least 1 hour and temperature remained consistent through each run. A simple calculation was made to find the percent of organic matter lost on ignition of the sample (Dean 1974):

$$\left(\frac{\text{dry weight before ignition} - \text{dry weight after}}{\text{dry weight before ignition}} \right) \text{X } 100$$

4.6 Historical Sandbar Surface Area Analyses

To note the progression and deposition of sandbars in Rapidan Reservoir over time, historic aerial photographs were observed over different time periods. From the Minnesota Department of Natural Resources Landview website, historic photographs from 1939, 1949 and 1964 were obtained. A 1974 image was acquired from the Water Resources Center at Minnesota State University in Mankato and a 1:80,000 scale poor quality image from 1985 was found online at the USGS Earth Explorer website. More recent imagery from 1992, 2002 and 2006 were attained from the Blue Earth County Environmental Services office. No public aerial images were found for the time period between 1911 and 1939.

The 1939, 1949 and 1964 aerial images were downloaded as a JPEG photo format. The original images were not ortho-rectified for use with mapping software, meaning that they were not corrected to have the same dimensions and distortions as a projected map. Ortho-rectification was a necessity so an accurate area could be calculated when digitizing the sandbars. This process was completed using ERDAS IMAGINE 9.1. The 1992, 2002 and 2006 images were previously rectified by Blue Earth County Environmental Services staff (NAD83, UTM Zone 15 North) and were used as the reference images. Digitizing of sandbars was completed with the ArcMap 9.2 GIS software. Once the sandbars were digitized, the area in acres of all sandbars was determined. The total acreage was subtracted from the predetermined whole reservoir acreage (which was obtained from the 1939 aerial image) to calculate a percent surface area lost within the reservoir to deposition.

4.7 Statistical Analyses of Particle Size Analyses

Statistical measures used to describe particle size information for this project can be found in the Petrology of Sedimentary Rocks (Boggs 1992). Graphic mean, inclusive standard deviation, skewness and kurtosis were used for the purposes of this project and are calculated from percentile values of particle size distributions determined from reservoir sediment samples. In order to obtain percentile values, cumulative arithmetic curves needed to be created. Cumulative arithmetic curves show the cumulative weight percent of the sample by particle size, and illustrate the fraction of material that was coarser than each successive grain size. The data analysis and graphing software KaleidaGraph™ by Synergy Software, Inc., was used to extract 5th, 16th, 25th, 50th, 75th, 84th and 95th percentile values from the cumulative curves.

Particle sizes for natural sediments can have the potential to span many orders of magnitude. Because the range is so great, a useful method of representing particle size data for description and to show the distribution is by using a negative base two logarithmic scale, known in sedimentology as the phi (ϕ) (Boggs 1992). Phi values are calculated from the grain sizes measured in millimeters. In Microsoft Excel, the formula **–log(x,2)** computes the phi value, where “x” is the particle size diameter in millimeters.

Particle sizes were presented for 1985 in the Rapidan Research Project (Quade 2004) as pie charts. No appendices of hard numbers were found. To extract numbers for statistical analyses, the pie charts were enlarged and percentages were estimated. Once percentages of all available particle sizes were derived, 2008-09 results and 1985 results were used for statistical analyses following the same methodology.

4.7.1 Particle Size Graphic Mean

Graphic mean is the average particle size for a representative sample and is the measure of the 16th, 50th and 84th percentile (percent of the sample by weight) values by using the equation below (Boggs 1992). Table 4.3 interprets graphic mean values from coarse gravel down to fine clay.

$$M = \frac{\Phi 16 + \Phi 50 + \Phi 84}{3}$$

Where:
M = graphic mean of particle sizes
$\phi 16$ = 16th percentile
$\phi 50$ = 50th percentile
$\phi 84$ = 84th percentile

Table 4.3: Graphic mean particle size classification (Boggs 1992).

GRAPHIC MEAN VALUE		CLASSIFICATION
Values from	To	
∞	−1 ϕ	Gravel
-1	0 ϕ	Very Coarse Sand
0	+ 1 ϕ	Coarse Sand
1	+ 2 ϕ	Medium Sand
2	+ 3 ϕ	Fine Sand
3	+ 4 ϕ	Very Fine Sand
4	+ 8 ϕ	Silt
8	∞	Clay

4.7.2 Inclusive Standard Deviation

Inclusive standard deviation is a measure of the degree of sorting. Sorting is an indicator of the distribution of grain sizes within a sediment sample, and is a measure of how similar the grains are to the mean. A poorly sorted sample would show that the cumulative sediment sizes are mixed (highly variable with a range of sizes) while a well sorted sample indicates similar sediment sizes (low variability). Values were classified on a scale from very well sorted to extremely poorly sorted (Boggs 1992) (Table 4.4). Inclusive standard deviation is found by using the following equation.

$$\sigma_1 = \frac{\Phi 84 - \Phi 16}{4} + \frac{\Phi 95 - \Phi 5}{6.6}$$

Where:
σ_1 = inclusive standard deviation of particle sizes
$\phi 5$ = 5th percentile
$\phi 16$ = 16th percentile
$\phi 84$ = 84th percentile
$\phi 95$ = 95th percentile

Table 4.4: Sorting classes based on the inclusive standard deviation of grain sizes (Boggs 1992).

SORTING CLASS		CLASSIFICATION
Values from	To	
< 0.35		Very Well Sorted
0.35	0.50	Well Sorted
0.50	0.71	Moderately Well
0.71	1.00	Moderately Sorted
1.00	2.00	Poorly Sorted
2.00	4.00	Very Poorly Sorted
> 4.00		Extremely Poorly

4.7.3 Skewness

Skewness is defined as the degree of asymmetry (lop-sidedness) of a frequency curve (Boggs 1992). Symmetrical curves have a skewness of 0.00. Samples with a large proportion of fine material are positively skewed and samples with a greater amount of coarse material are negatively skewed (Figure 4.09). Skewness is determined by the following equation:

$$SK_1 = \frac{(^{\Phi}84 + {}^{\Phi}16 - (2 * {}^{\Phi}50))}{2 * (^{\Phi}84 - {}^{\Phi}16)} + \frac{(^{\Phi}95 + {}^{\Phi}5 - (2 * {}^{\Phi}50))}{2 * (^{\Phi}95 - {}^{\Phi}5)}$$

Where:
SK_1 = skewness of particle sizes
$^{\phi}5 = 5^{th}$ percentile
$^{\phi}16 = 16^{th}$ percentile
$^{\phi}50 = 50^{th}$ percentile
$^{\phi}84 = 84^{th}$ percentile
$^{\phi}95 = 95^{th}$ percentile

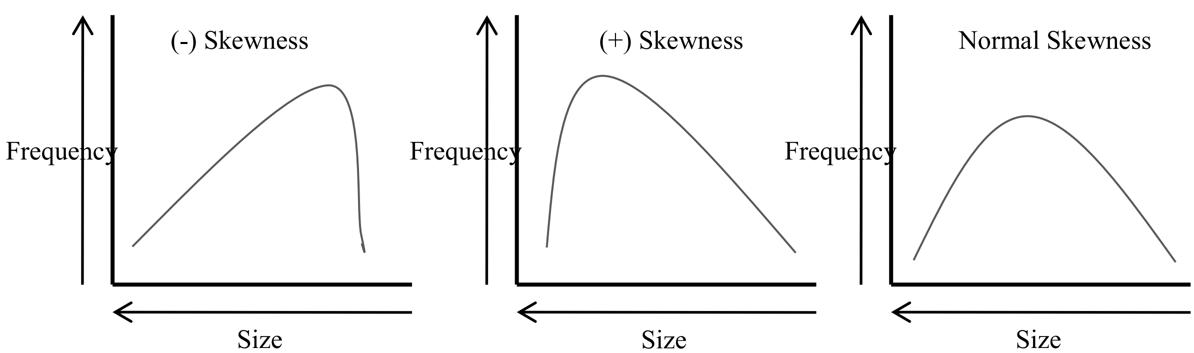

Figure 4.09: Examples of skewness measures.

Table 4.5: Skewness particle size classification (Boggs 1992).

SKEWNESS VALUE		CLASSIFICATION
Values from	To	
+0.30	+1.00	Strongly Positive Skewed
+0.10	+0.30	Positive Skewed
-0.10	+0.10	Near Symmetrical
-0.30	-0.10	Negative Skewed
-1.00	-0.30	Strongly Negative Skewed

4.7.4 Kurtosis

Kurtosis is defined as the degree of peakedness or the departure from "normal" in frequency curves. A normal distribution (mesokurtic) would have a kurtosis value of 1.00. If a sample tends to be better sorted in the middle of the curve rather than towards the edges, it is defined as more peaked (lepokurtic); if a sample is better sorted at the edges rather than the center of the curve, it is flat (platykurtic) (Boggs 1992) (Figure 4.10). Kurtosis values are classified using the breaks in Table 4.7 and are found by using the following equation:

$$K_G = \frac{{}^{\Phi}95 - {}^{\Phi}5}{2.44 * ({}^{\Phi}75 - {}^{\Phi}25)}$$

Where:
K_G = kurtosis of particle sizes
${}^{\phi}5 = 5^{th}$ percentile
${}^{\phi}25 = 25^{th}$ percentile
${}^{\phi}75 = 75^{th}$ percentile
${}^{\phi}95 = 95^{th}$ percentile

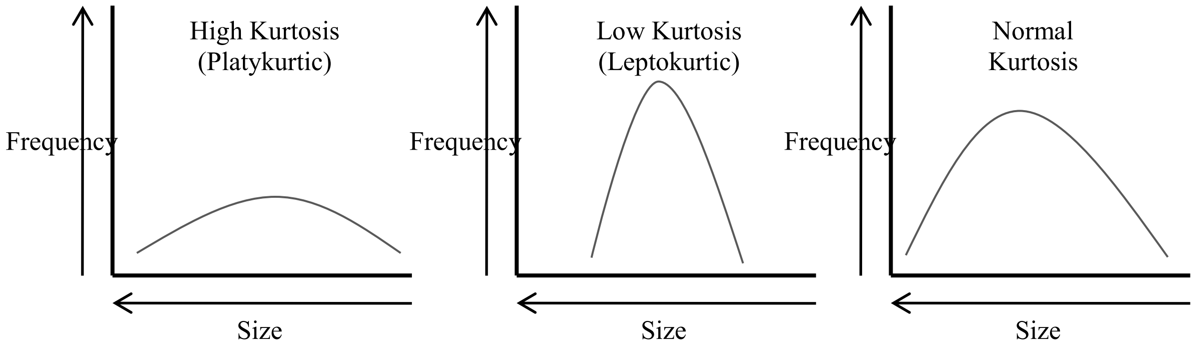

Figure 4.10: Examples of kurtosis measures.

Table 4.6: Kurtosis particle size classification (Boggs 1992).

KURTOSIS VALUE		CLASSIFICATION
Values from	To	
< 0.67		Very Platykurtic
0.67	0.90	Platykurtic
0.90	1.11	Mesokurtic
1.11	1.50	Leptokurtic
1.50	3.00	Very Leptokurtic
> 3.00		Extremely Leptokurtic

4.8 GIS Analyses and Interpolation

Sediment sample waypoints (latitude and longitude coordinates) were uploaded from the Garmin handheld GPS into ArcMap for the 2008-09 samples. For 1985 sample locations, a map provided in the Rapidan Dam Research Report was geo-referenced (assigned accurate location information). A new point shapefile was then created in ArcGIS 10.0 ArcCatalog and edited to include all the locations and appropriate names of each sample site in 1985. The reservoir boundary was digitized from the reservoir map provided in Quade et al (2004).

Sample graphic mean results were tabulated in an Excel spreadsheet and "joined" (a function available in ArcMap 10.0) to the same waypoint ID within the shapefile. To visually illustrate the particle size results throughout the reservoir, a GIS interpolation was completed using the Inverse Distance Weighted (IDW) method in ArcMap 10.0. An IDW interpolation assigns values to unknown areas that are not represented by physical sample results and operates under the assumption that values close to one another are more similar than those that are farther apart. Samples that are closer to the unknown interpolated points will have more influence and the influence will decrease with greater distance. IDW has a power (P) function where the P value is proportional to the inverse distance weight. The lower the P value, the less the weighting decreases with distance. With higher P values, only the nearest surrounding points will influence the calculation (ESRI 2007). Multiple P values (0.5, 2, 5, and 10) were studied; a power of 10 produced the most realistic results for the Rapidan Reservoir particle size data. To force the interpolation to calculate values within the confines of the desired sample area and not across non-flooded areas, a polygon of the reservoir was converted to a polyline feature and used as a Polyline Barrier within the IDW interpolation. Without the polyline barrier function, the interpolation was influenced by the nearest points, regardless of their physical relatedness within the Blue Earth River channel or flooded areas of the Rapidan Reservoir. This would have been true for transect N and O (Figure 4.11) Output values were reclassified to align with the mean grain size criteria ranges found in Table 4.4. The same methodology was applied to the 1985 data to extract an interpolation for the mean grain size within the reservoir.

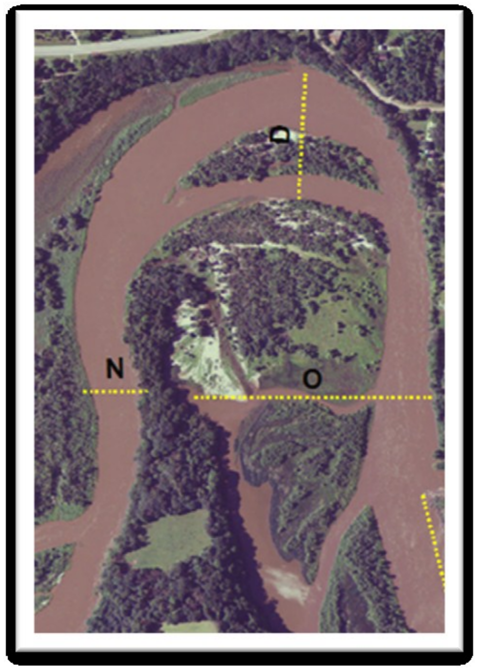

Figure 4.11: Aerial view of transect N and O which are physically separated by a ridge.

For comparison purposes, the whole reservoir mean and median grain size were found for both sets of data (1985 and 2008-09). To derive the whole reservoir mean and median from the interpolated output, each data set was first multiplied by a constant raster with a value of 1,000. The constant raster was used to maintain the precision of the data since the next step was to convert the raster into an integer format. Once the data was in an integer format, the Zonal Statistics tool (found under the Spatial Analyst extension) was used in ArcMap 10.0 to obtain the mean and median. Results were then divided by 1,000 to convert the data back to the original scale.

In addition to having the mean and median for comparison between the two datasets, the IDW interpolation values for each dataset were subtracted from one another (using the same extent) to gain the change in phi values (mean grain size). The Minus tool (under the Spatial Analyst extension) was utilized to figure out the difference between the two interpolations. The results were reclassified to fit the range of data from -3.0 to 8.0 in intervals of 1.0. The output of this process will show areas where there was a progression to finer material (lower numbers) and areas that became more coarse (higher numbers).

CHAPTER 5: RESULTS AND DISCUSSION

5.1 Precipitation, Flow and Runoff

5.1.1 Observed Precipitation Totals for 1984-85 and 2007-09 compared with 30 year Normal values

Precipitation is the main driver of water delivered to water bodies and therefore it plays a large role in studies involving water quantity and quality. Precipitation data were taken from the closest long-term network rain gauge located at Mankato, Minnesota (station ID# 215073). Area normals presented (Table 5.01 and 5.02) are also derived from the gauge at Mankato for a one-to-one comparison. Precipitation normals are the arithmetic mean of a climatological element computed over a 30-year consecutive period. Normals presented in this paper are calculated from 1971-2000. Updated normals are also available for the 1981-2010 period and do not differ greatly from the 1971-2000 values. It must be noted that rainfall totals can vary greatly over short distances (personal observation). Totals do not necessarily represent rainfall totals throughout the Greater Blue Earth River watershed that directly led to runoff and sedimentary loads determined at sites BEC 9, 13W, and 34. This section will provide context for conditions in 1984-85 and 2007-09.

Table 5.01: Observed rainfall versus normal precipitation values (1971-2000) at Mankato, Minnesota (#215073), 2007-09.

Month	**Observed Rainfall - inches -**			**#215073 30-Year Normal**	**Departure from Normal (1971-2000)**		
	2007	2008	2009	1971-2000	2007	2008	2009
JAN	1.62	0.30	0.63	1.07	0.55	-0.77	-0.44
FEB	1.82	0.30	1.12	0.62	1.2	-0.32	0.50
MAR	2.45	0.84	2.50	2.09	0.36	-1.25	0.41
APR	1.63	4.34	1.82	3.08	-1.45	1.26	-1.26
MAY	2.16	3.64	1.24	3.59	-1.43	0.05	-2.35
JUN	2.92	3.36	3.53	5.6	-2.68	-2.24	-2.07
JUL	2.50	3.90	1.63	4.38	-1.88	-0.48	-2.75
AUG	8.06	2.16	4.20	4.43	3.63	-2.27	-0.23
SEP	3.48	1.26	0.66	3.1	0.38	-1.84	-2.44
OCT	4.40	2.18	6.13	2.45	1.95	-0.27	3.68
NOV	0.20	1.87	1.45	2.02	-1.82	-0.15	-0.57
DEC	1.24	1.24	2.60	0.99	0.25	0.25	1.61
	32.48	**25.39**	**27.51**	**33.42**	**-0.94**	**-8.03**	**-5.91**

Table 5.02: Observed rainfall versus normal precipitation values (1971-2000) at Mankato, Minnesota (#215073), 1984-85.

Month	Observed Rainfall - inches -		#215073 30-Year Normal	Departure from Normal (1971-2000)	
	1984	1985	1971-2000	1984	1985
JAN	0.86	1.71	1.07	-0.21	0.64
FEB	0.66	0.33	0.62	0.04	-0.29
MAR	1.55	3.9	2.09	-0.54	1.81
APR	3.8	3.72	3.08	0.72	0.64
MAY	2.45	1.92	3.59	-1.14	-1.67
JUN	4.99	2.25	5.6	-0.61	-3.35
JUL	3.31	2.49	4.38	-1.07	-1.89
AUG	3.76	5.47	4.43	-0.67	1.04
SEP	2.89	5.01	3.1	-0.21	1.91
OCT	5.82	3.31	2.45	3.37	0.86
NOV	1.82	1.25	2.02	-0.2	-0.77
DEC	2.58	1.42	0.99	1.59	0.43
	34.49	**32.78**	**33.42**	**1.07**	**-0.64**

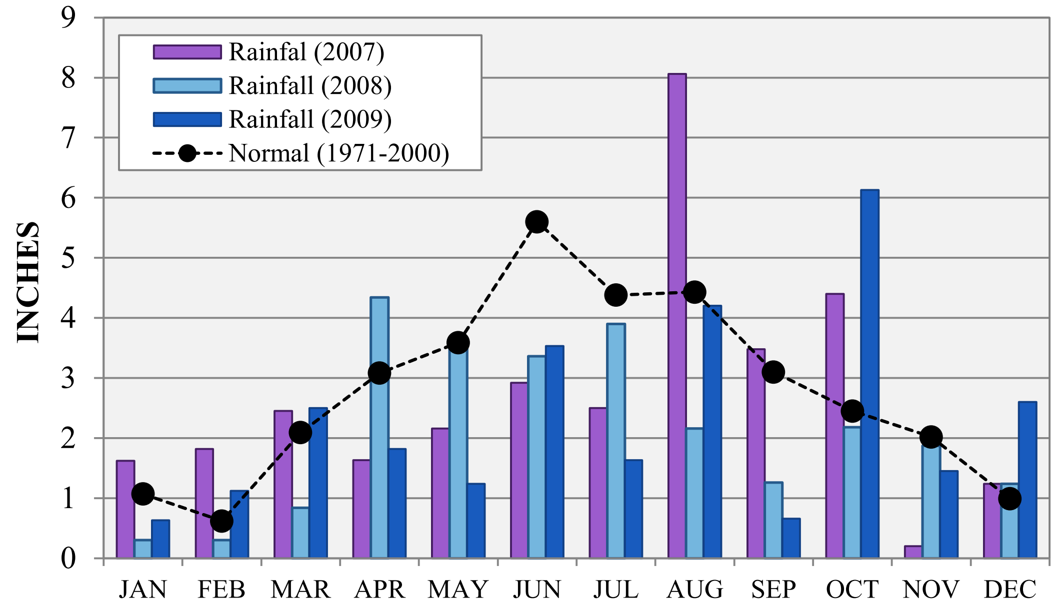

Figure 5.01: 2007-09 monthly precipitation totals for Mankato, Minnesota versus the 30 year normal (#215073).

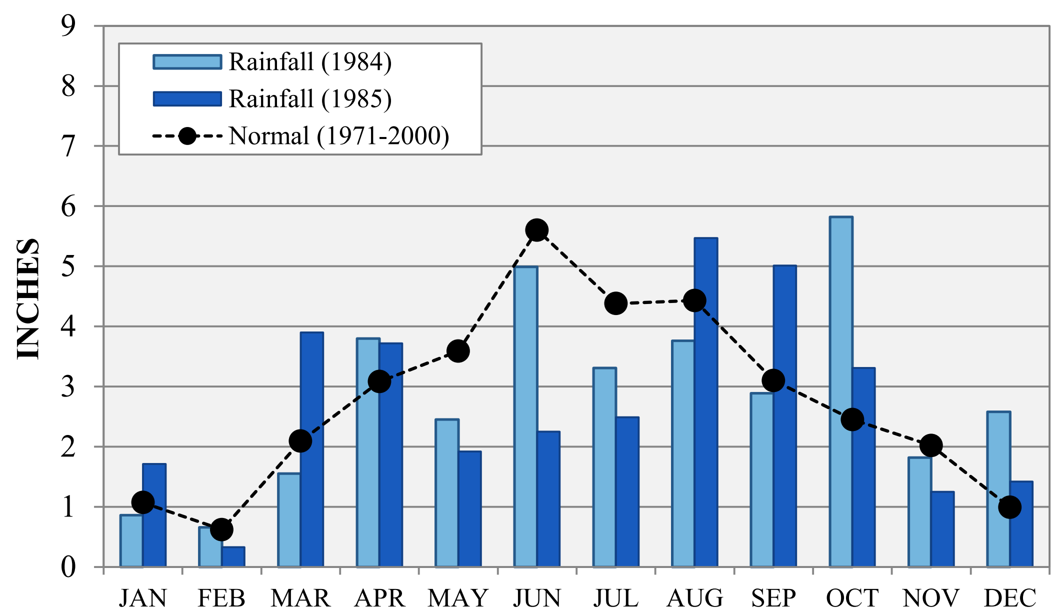

Figure 5.02: 1984-85 monthly precipitation totals for Mankato, MN versus the 30 year normal (#215073).

Cumulative monthly rainfall totals for 1984 and 1985 were near the 30-year normal with 1984 receiving 1.07” of excess precipitation and 1985 receiving slightly less than 0.64”. Monthly fluctuations above and below the normal were observed throughout the year. In 1984, May and July precipitation totals were shy by over an inch each, while in October and December, totals were above normal by 3.37” and 1.59” respectively. Other months had close to normal values, all falling within 0.7”. October 1984 saw the highest departure from normal with a surplus of 3.37”. In 1985, the annual precipitation total came close to the 30-year normal, falling short by only 0.64”. February, May, June, July and November were all below normal while other months exceeded normal. May through July experienced a cumulative deficit of 3.91” but August through October rebounded with an excess of 3.81” over normal conditions.

Annual rainfall totals in 2007 were slightly below normal by 0.94”, with drier conditions observed from April through July (-7.44”). Above normal conditions persisted from August through October (+5.96”) with significant rain events to help account for the summer deficit. Annual totals for both 2008 and 2009 fell significantly below the 30-year normal by 8.03” and 5.91” respectively. Only April, May and December totals exceeded the normal for 2008, by a mere 1.56” combined. June through November of 2008 saw a shortage of 7.25” of precipitation, while June and August were both over two inches short of normal conditions with September not falling far behind (-1.84”). 2009 consisted of a dry summer with a significant shortfall of 11.1” from April through September with May, June, July and September all falling short by over two inches each. Two large storm events in October 2009 (October 5-6th and October 18-

19th) helped to alleviate the drought-like conditions putting the cumulative total at an excess of 3.68" for the month.

Overall, comparing the two periods of interest, 1984 had the highest annual precipitation and was the year preceding collection of Rapidan Reservoir sediment samples. By contrast, 2008-09 were fairly dry years, falling 18-24% below normal for annual totals.

Monthly totals for 2007-09 are presented in Table 5.01 (as compared to the 1971-2000 normal values) along with the departure from normal. Monthly observed cumulative rainfall totals for 1984-85 are found in Table 5.02. Graphic bar charts of the monthly precipitation totals for the same years are presented in Figures 5.01 and 5.02.

5.1.2 Flow for 1984-85 and 2008-09 at BEC9, 13W and 34

BEC13W and BEC9 are two established, long-term USGS gauging stations on the Watonwan River near Garden City, Minnesota, and on the Blue Earth River near Rapidan, Minnesota, respectively. BEC13W has historical discharge data dating back to 1940 with complete available monthly data starting in 1977. BEC9 has scattered monthly discharge data available beginning in 1909 and continuous monthly data since 1950. Monthly discharge averages for both sites are presented in Tables 5.03 and 5.04. Observed monthly discharge values for BEC9 during 1984-85 and 2007-09 are presented in Tables 5.05 and 5.07 with departures from computed monthly averages in red. Observed monthly discharge values for BEC13W during 1984-85 and 2007-09 are available in Tables 5.06 and 5.08.

Table 5.03: Monthly discharge average (1950-2010) for the Blue Earth River gauging station downstream from Rapidan Dam (BEC9). Data is available from http://water.usgs.gov.

Blue Earth River near Rapidan, MN (USGS 05320000) Monthly Discharge Average -- cfs (1950-2010)											
JAN	FEB	MAR	APR	MAY	JUN	JUL	AUG	SEP	OCT	NOV	DEC
223	295	1,480	2,955	1,961	2,269	1,424	678	649	888	587	368

Table 5.04: Monthly discharge average (1977-2010) for the Watonwan River gauging station near Garden City, Minnesota (BEC13W). Data is available from http://water.usgs.gov.

Watonwan River near Garden City, MN (USGS 05319500) Monthly Discharge Average -- cfs (1977-2010)											
JAN	FEB	MAR	APR	MAY	JUN	JUL	AUG	SEP	OCT	NOV	DEC
81	118	616	1,029	696	844	487	222	263	343	242	145

Table 5.05: Average monthly discharge, 1984-1985, Blue Earth River downstream from Rapidan Dam (BEC9). Departures are derived from historic averages found in Table 5.03. Values in red indicate a deficit.

BEC9 - Average Monthly Discharge Over Monitored Period												
YEAR	JAN	FEB	MAR	APR	MAY	JUN	JUL	AUG	SEPT	OCT	NOV	DEC
1984	261	1,042	2,857	6,286	4,044	5,184	1,870	313	134	193	357	341
Departure	38	747	1,377	3,331	2,083	2,915	446	-366	-515	-695	-230	-26
1985	214	149	2,362	2,735	1,634	933	262	159	684	1,884	942	738
Departure	-9	-146	882	-220	-327	-1,335	-1,162	-519	35	996	356	370

Table 5.06: Average monthly discharge, 1984-1985, Watonwan River near Garden City, Minnesota (BEC13W). Departures are derived from historic averages found in Table 5.04. Values in red indicate a deficit.

BEC13W - Average Monthly Discharge Over Monitored Period												
YEAR	JAN	FEB	MAR	APR	MAY	JUN	JUL	AUG	SEPT	OCT	NOV	DEC
1984	52	134	708	2505	885	1349	477	103	60	106	145	101
Departure	-29	16	92	1476	190	505	-10	-119	-203	-237	-97	-44
1985	42	46	933	949	619	256	90	63	279	614	241	150
Departure	-39	-72	316	-80	-77	-588	-397	-160	17	271	-1	4

Table 5.07: Average monthly discharge, 2007-09, Blue Earth River downstream from Rapidan Dam. Departures are derived from historic averages found in Table 5.03. Values in red indicate a deficit.

BEC9 - Average Monthly Discharge Over Monitored Period												
YEAR	**JAN**	**FEB**	**MAR**	**APR**	**MAY**	**JUN**	**JUL**	**AUG**	**SEPT**	**OCT**	**NOV**	**DEC**
2007	610	237	4,259	3,811	1,760	1,073	187	686	677	3,848	1,303	551
Departure	387	-58	2,779	856	-201	-1,196	-1,237	8	28	2,960	716	183
2008	356	172	614	2,707	3,908	5,019	969	201	74	76	94	72
Departure	133	-123	-866	-248	1,947	2,750	-455	-477	-575	-812	-493	-296
2009	52	482	1,240	721	825	961	765	164	60	1,023	1,398	736
Departure	-171	187	-240	-2,234	-1,136	-1,308	-659	-514	-589	135	811	368

Table 5.08: Average monthly discharge, 2007-09, Watonwan River near Garden City, Minnesota. Departures are derived from historic averages found in Table 5.04. Values in red indicate a deficit.

BEC13W - Average Monthly Discharge Over Monitored Period												
YEAR	**JAN**	**FEB**	**MAR**	**APR**	**MAY**	**JUN**	**JUL**	**AUG**	**SEPT**	**OCT**	**NOV**	**DEC**
2007	90	35	1,296	892	504	258	36	172	129	1,021	388	164
Departure	9	-83	680	-137	-192	-586	-451	-50	-134	678	146	19
2008	92	61	150	718	1,422	1,510	189	50	22	33	44	28
Departure	11	-57	-466	-311	726	666	-298	-172	-241	-310	-198	-117
2009	15	130	356	229	210	286	98	20	13	153	209	115
Departure	-66	12	-260	-800	-486	-558	-389	-202	-250	-190	-33	-30

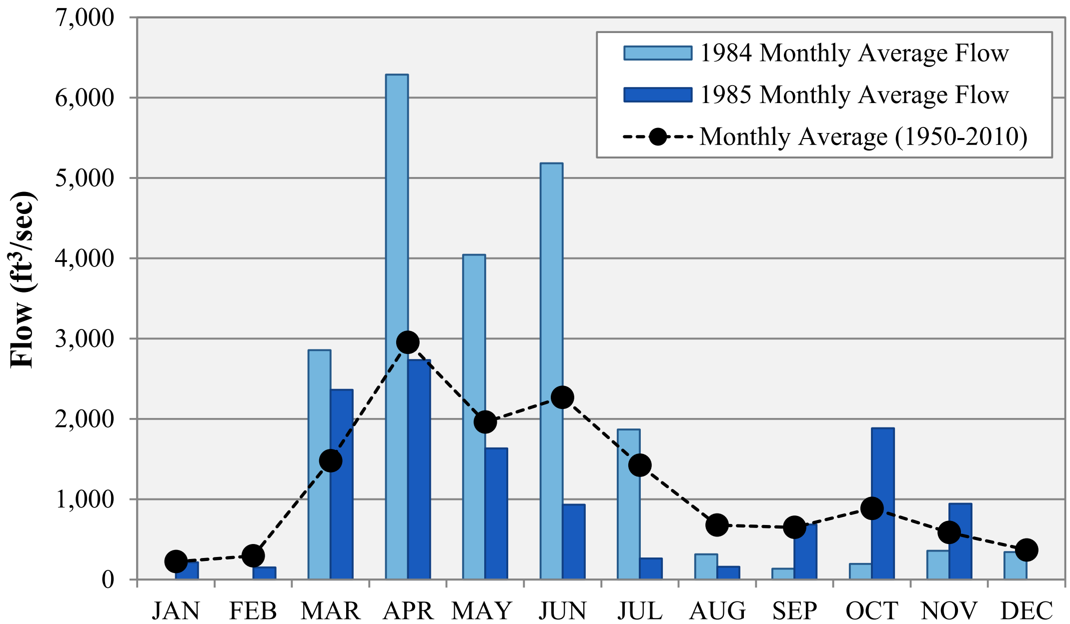

Figure 5.03: Blue Earth River downstream from Rapidan Dam (BEC9), monthly average discharge for 1984 and 1985 as compared to the monthly average from 1950-2010.

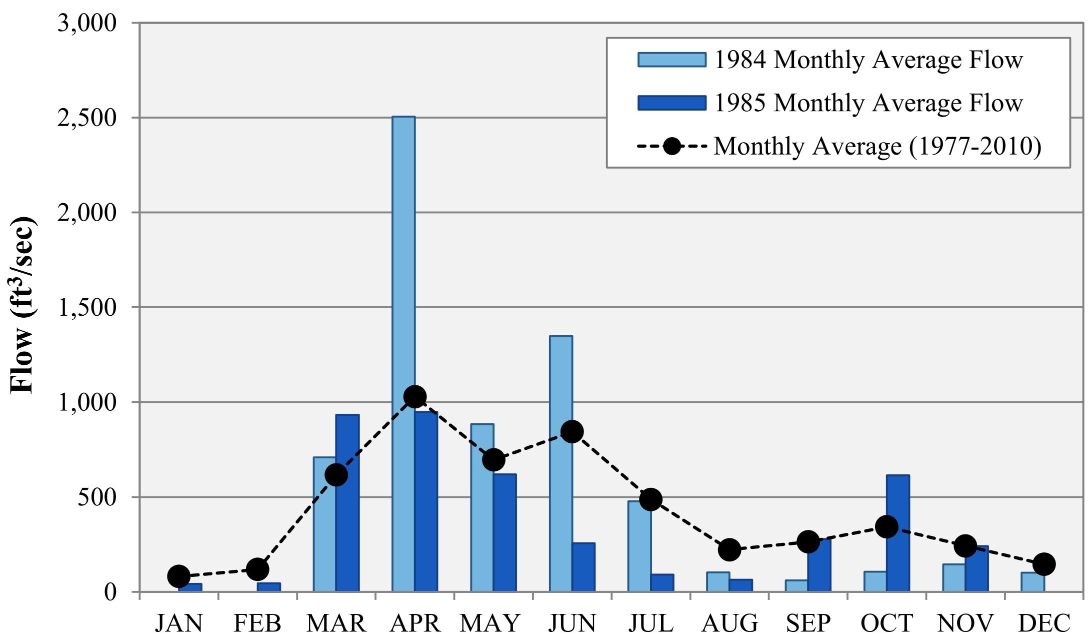

Figure 5.04: Watonwan River near Garden City, Minnesota (BEC13W), monthly average discharge for 1984 and 1985 as compared to the monthly average from 1977-2010.

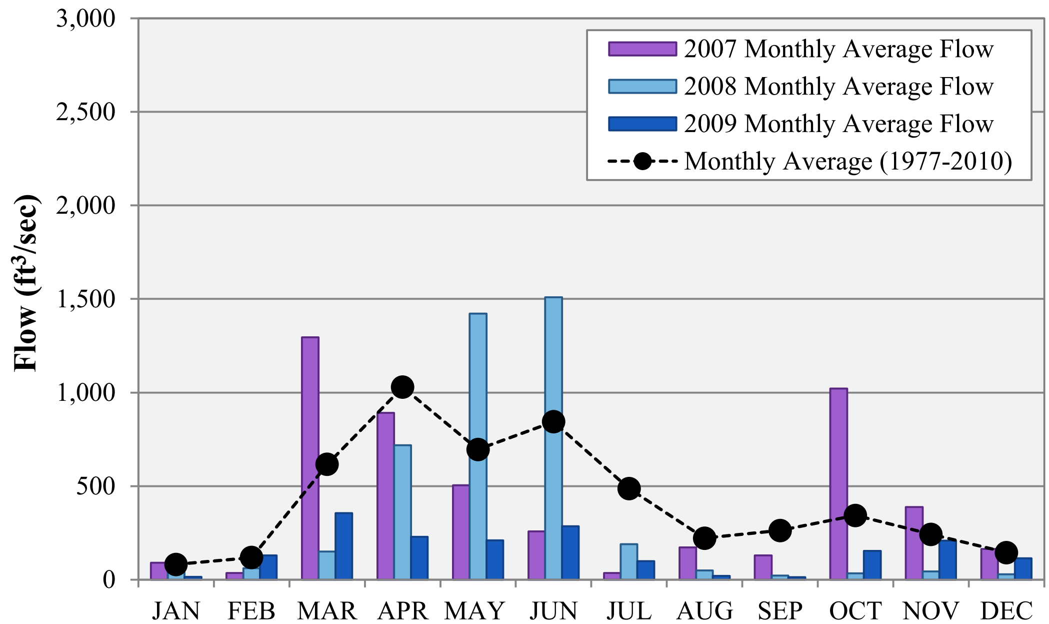

Figure 5.05: BEC13W, Watonwan River, observed (2007-2009) and long-term monthly flow averages.

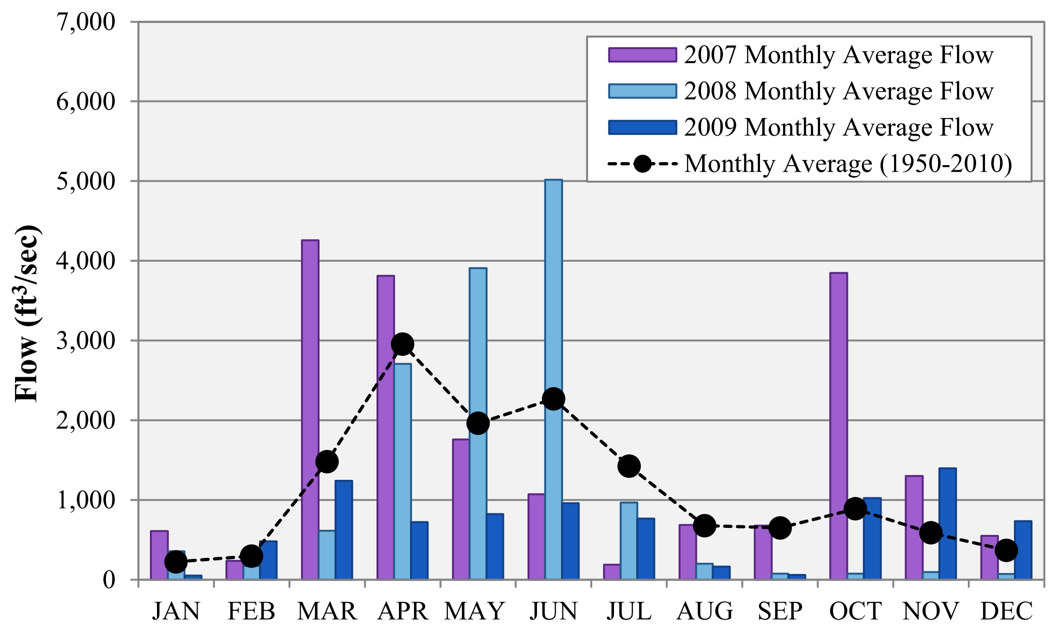

Figure 5.06: BEC9, Blue Earth River downstream from Rapidan Dam, observed (2007-2009) and long-term monthly flow averages.

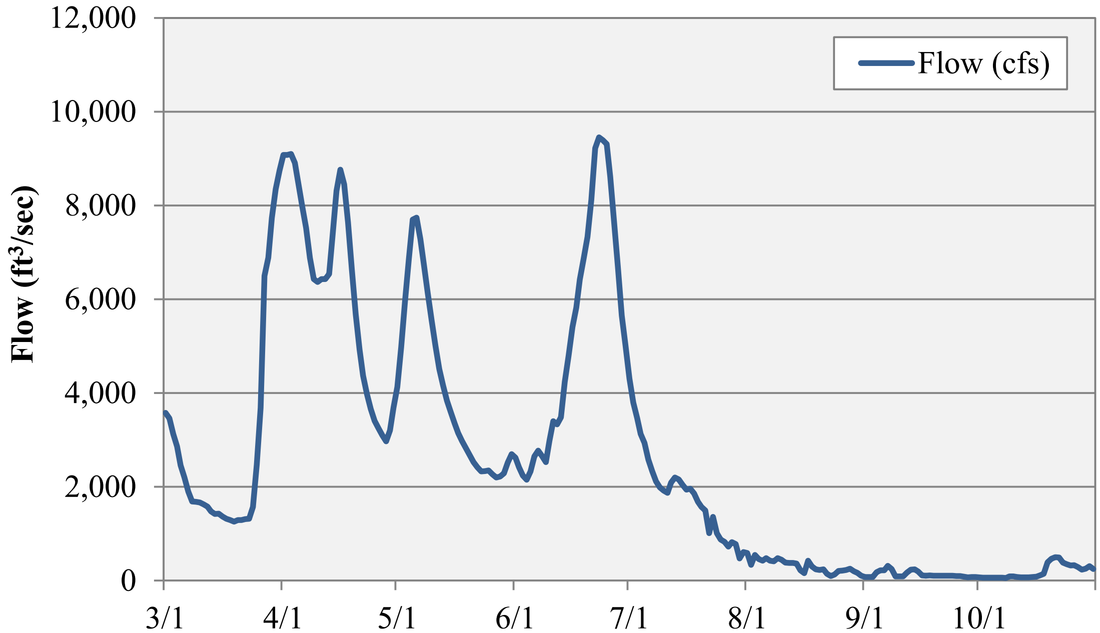

Figure 5.07: Blue Earth River hydrograph, downstream from Rapidan Dam (BEC9), 1984.

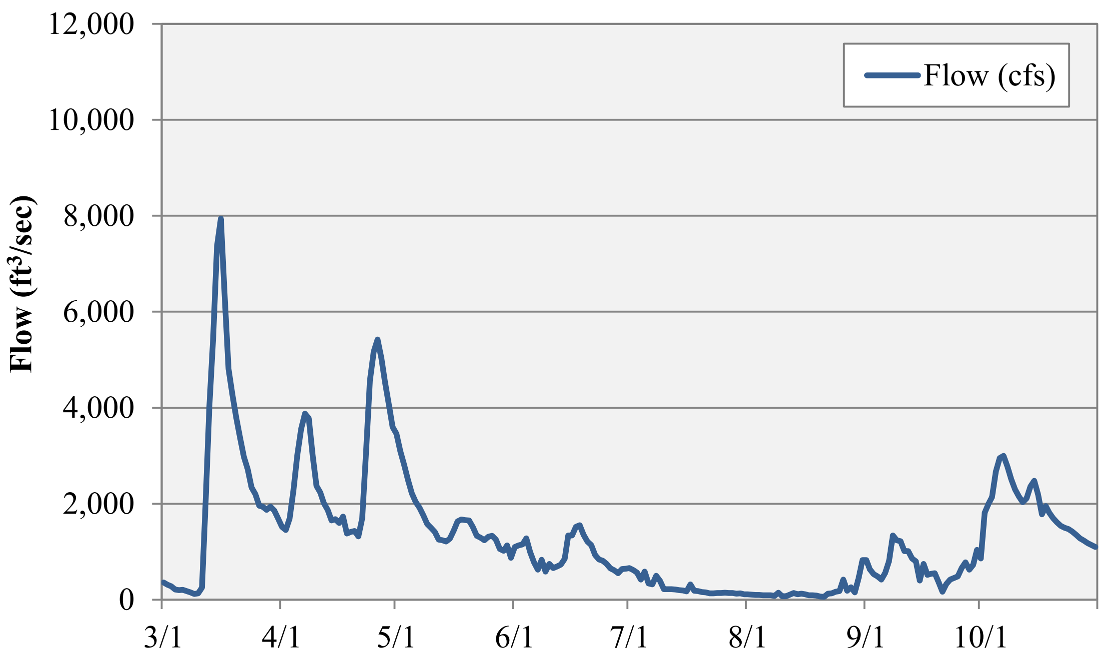

Figure 5.08: Blue Earth River hydrograph, downstream from Rapidan Dam (BEC9), 1985.

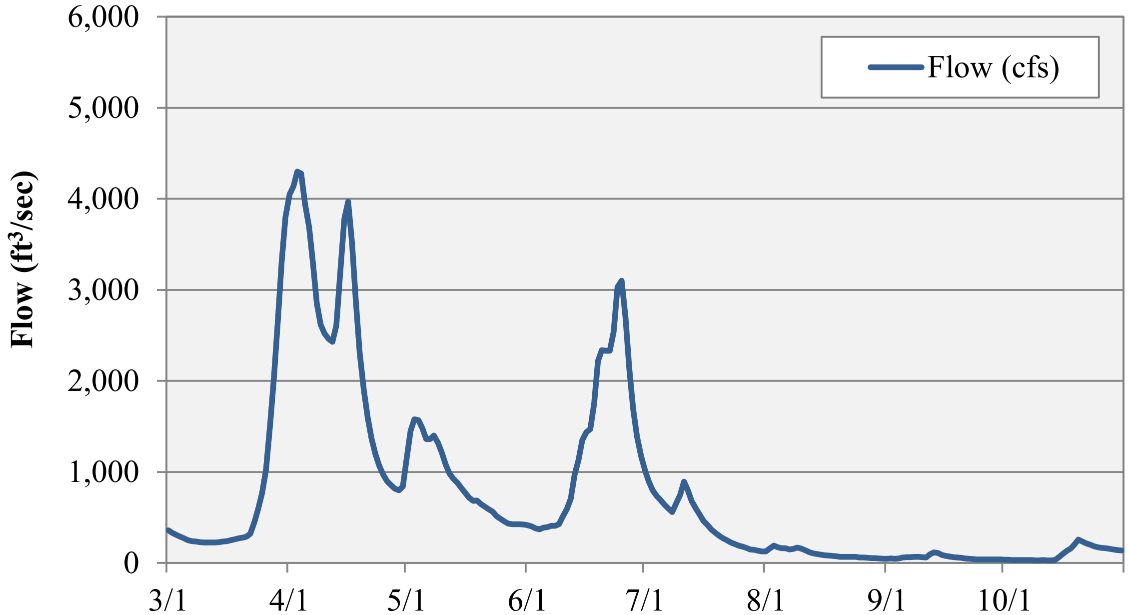

Figure 5.09: Watonwan River near Garden City, Minnesota hydrograph, (BEC13W), 1984.

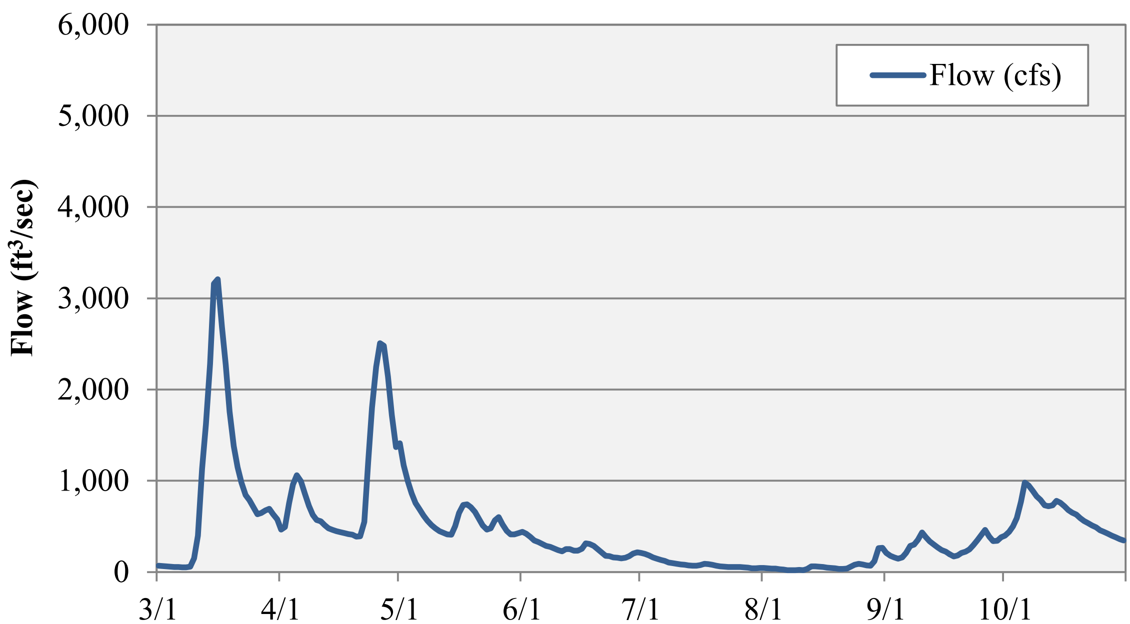

Figure 5.10: Watonwan River near Garden City, Minnesota hydrograph, (BEC13W), 1985.

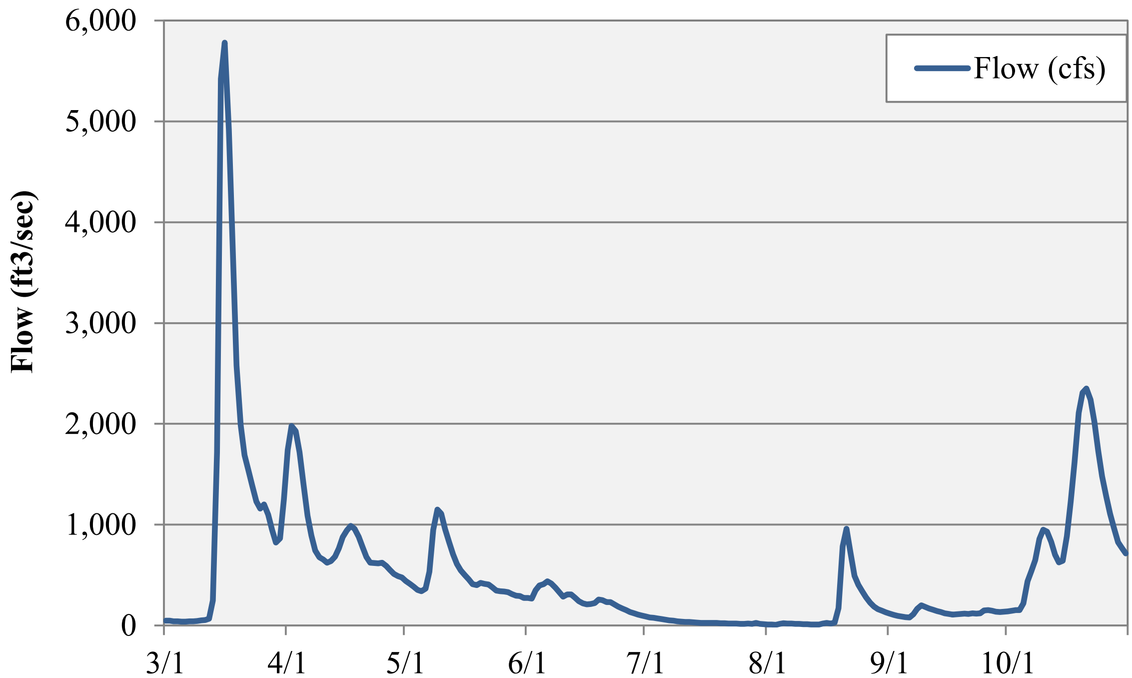

Figure 5.11: BEC13W, Watonwan River stream discharge, March - October 2007.

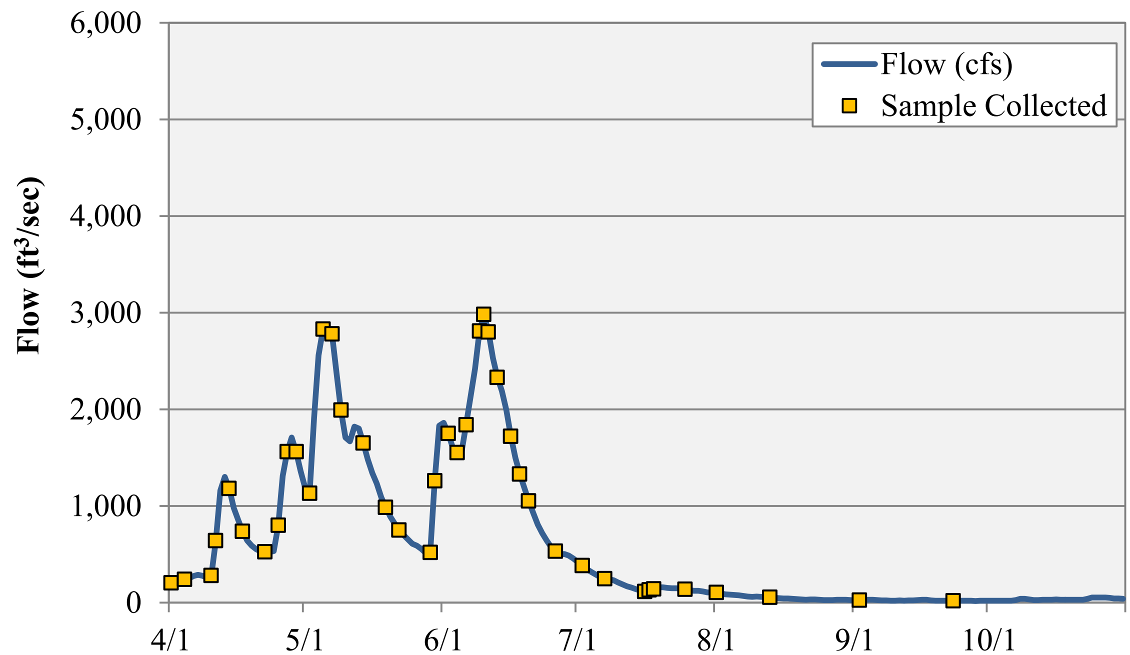

Figure 5.12: BEC13W, Watonwan River stream discharge and sample collection distribution, April - October, 2008.

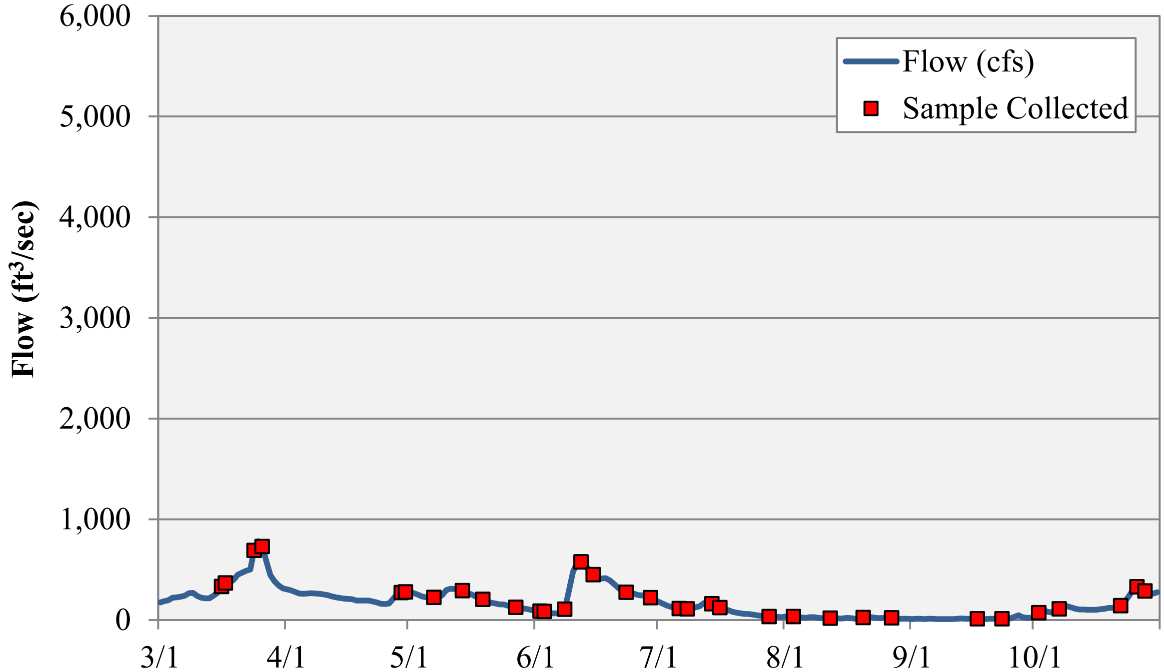

Figure 5.13: BEC13W, Watonwan River, stream discharge and sample collection distribution, March - October 2009.

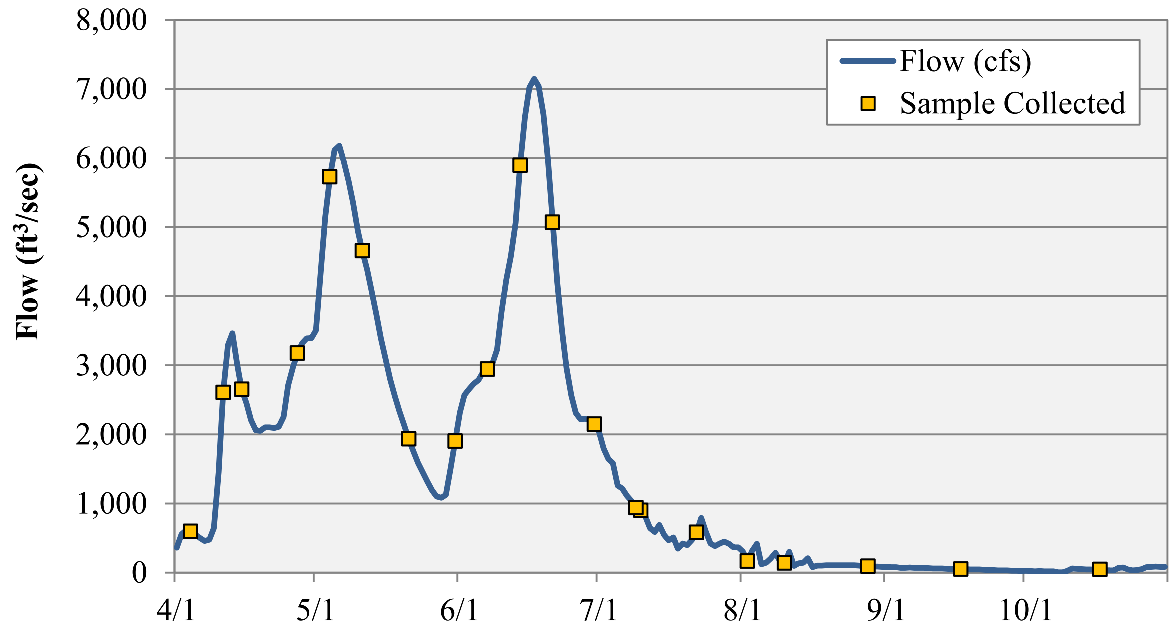

Figure 5.14: BEC34, Blue Earth River at Blue Earth County Road 34, stream discharge and sample collection distribution, April - October, 2008.

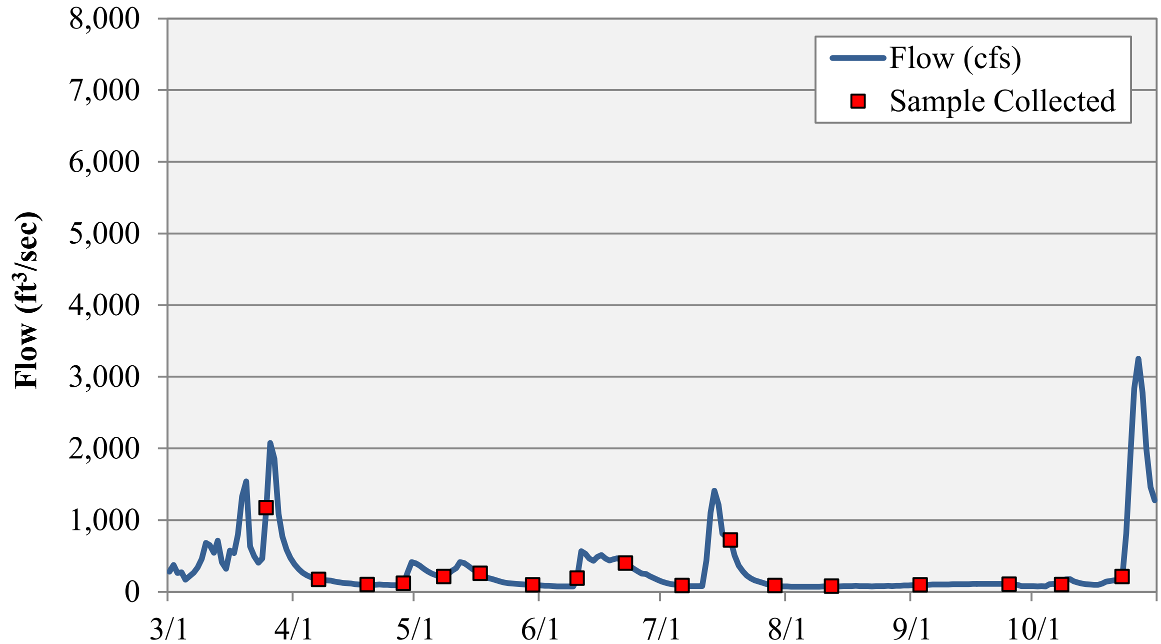

Figure 5.15: BEC34, Blue Earth River at Blue Earth County Road 34, stream discharge and sample collection distribution, March - October, 2009.

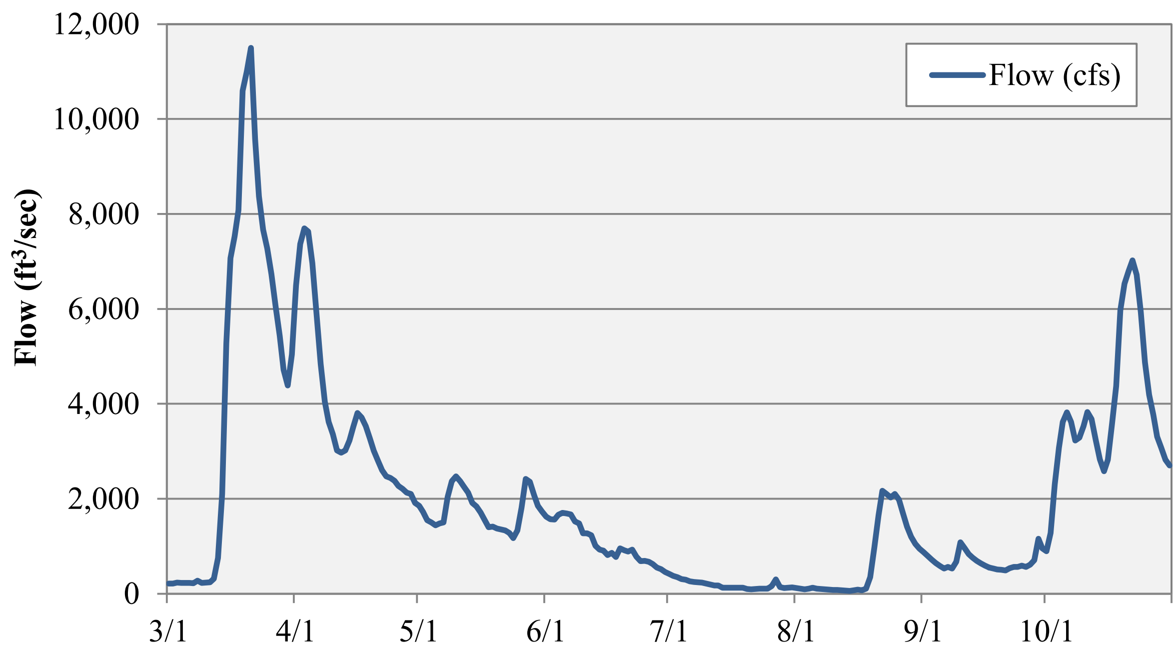

Figure 5.16: BEC9, Blue Earth River downstream from Rapidan Dam. Stream discharge, March - October, 2007.

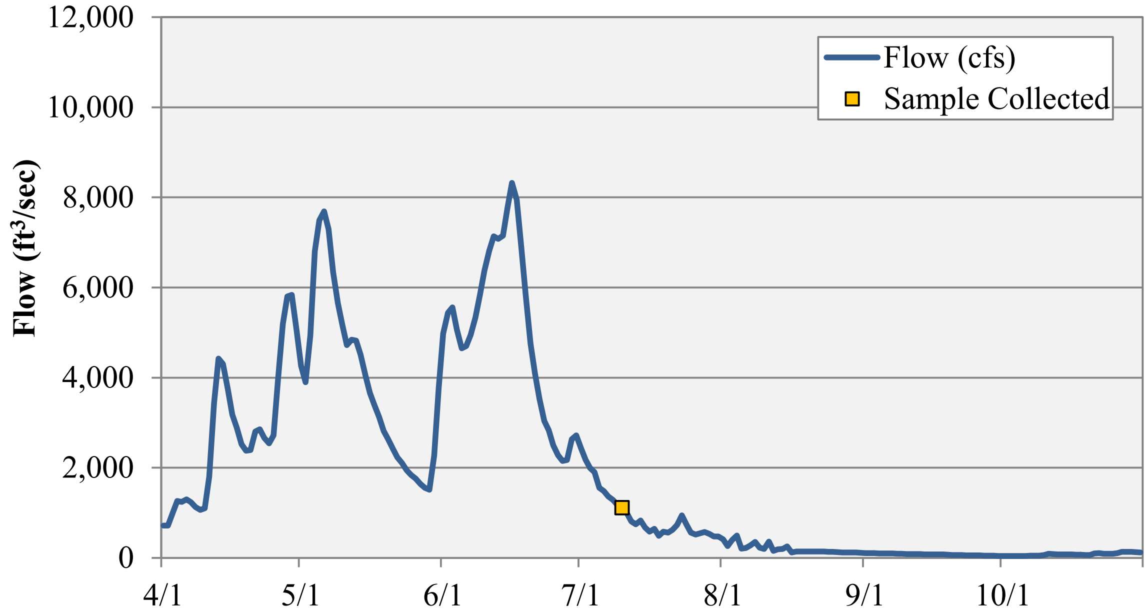

Figure 5.17: BEC9, Blue Earth River downstream from Rapidan Dam. Stream discharge and sample collection distribution, April - October, 2008.

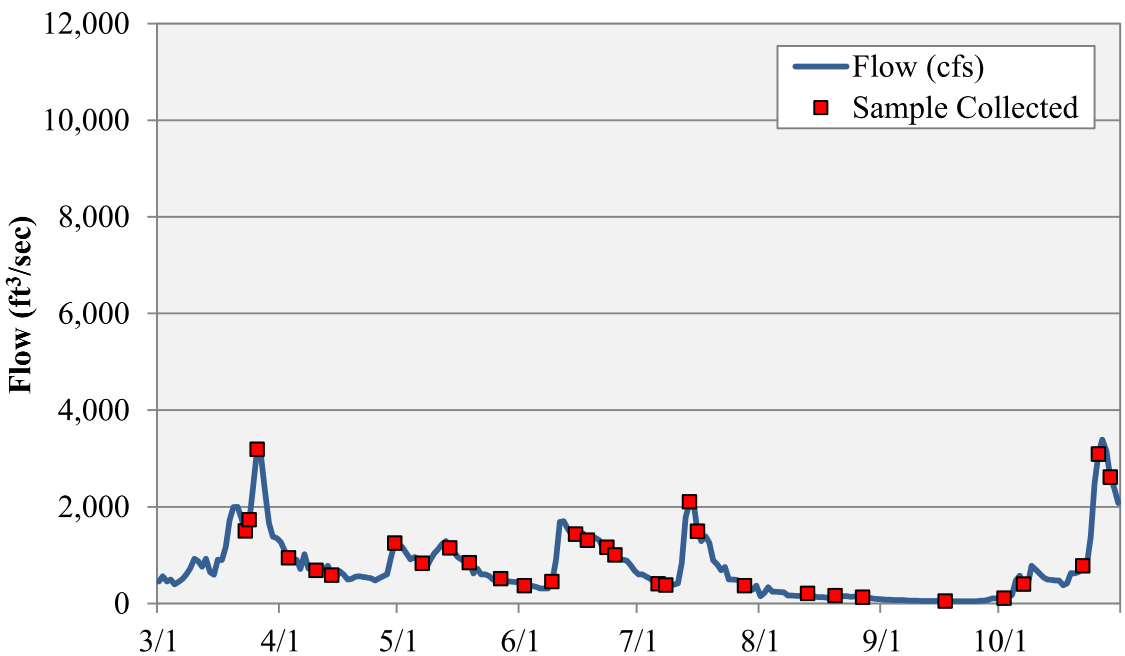

Figure 5.18: BEC9, Blue Earth River downstream from Rapidan Dam. Stream discharge and sample collection distribution, March - October 2009.

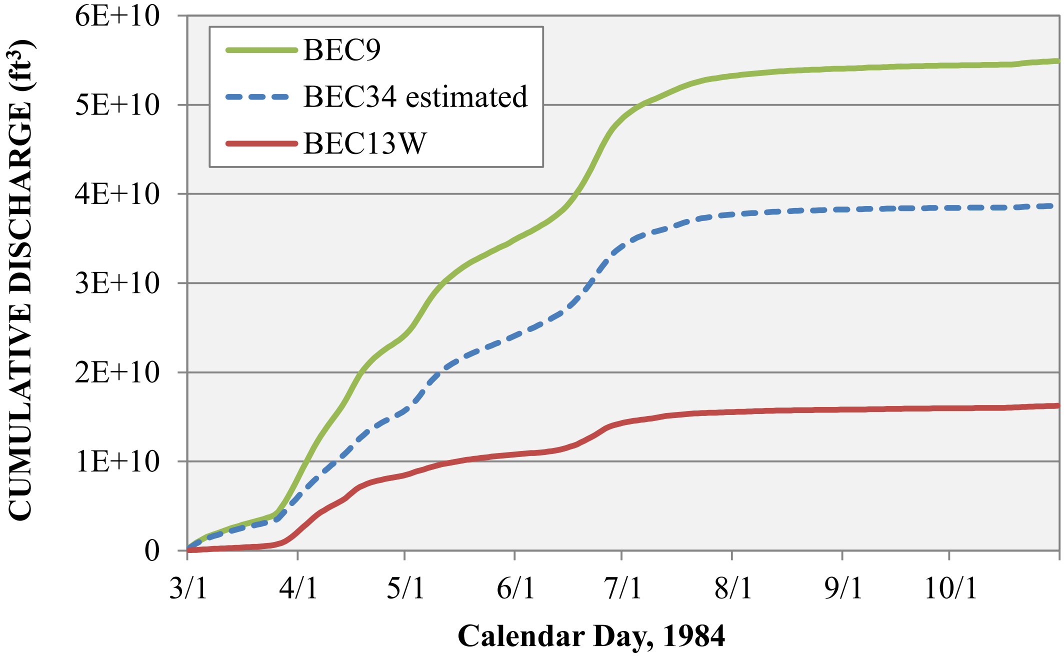

Figure 5.19: 1984 cumulative water volume (ft^3) for BEC9, BEC34 and BEC13W
Note: BEC34 cumulative water volume is estimate by subtracting BEC13W from BEC9

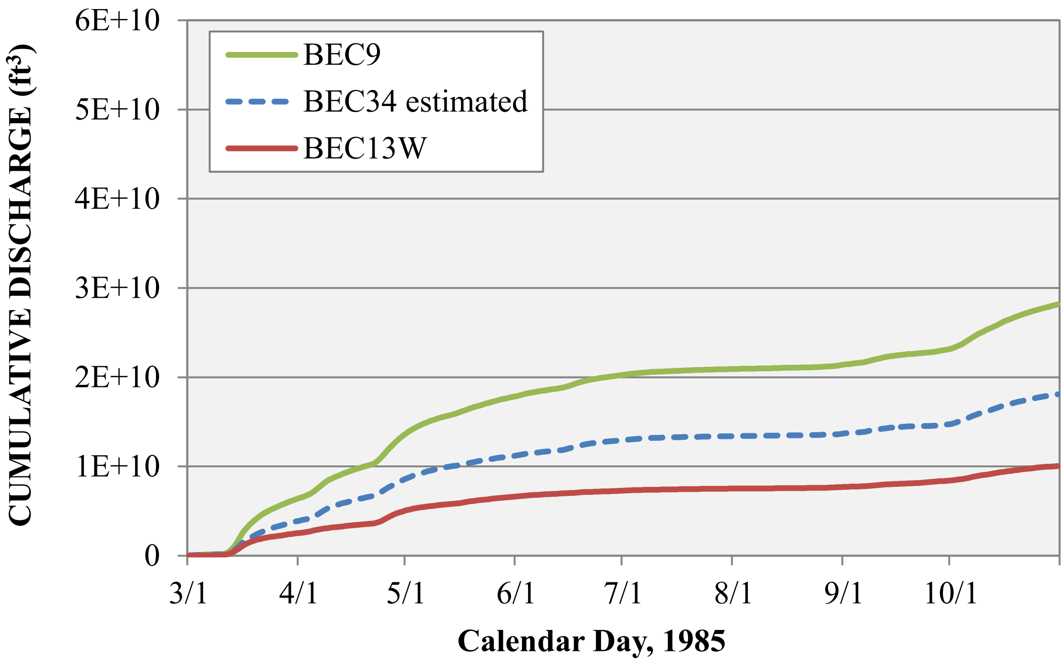

Figure 5.20: 1985 cumulative water volume (ft^3) for BEC9, BEC34 and BEC13W
Note: BEC34 cumulative water volume is estimate by subtracting BEC13W from BEC9

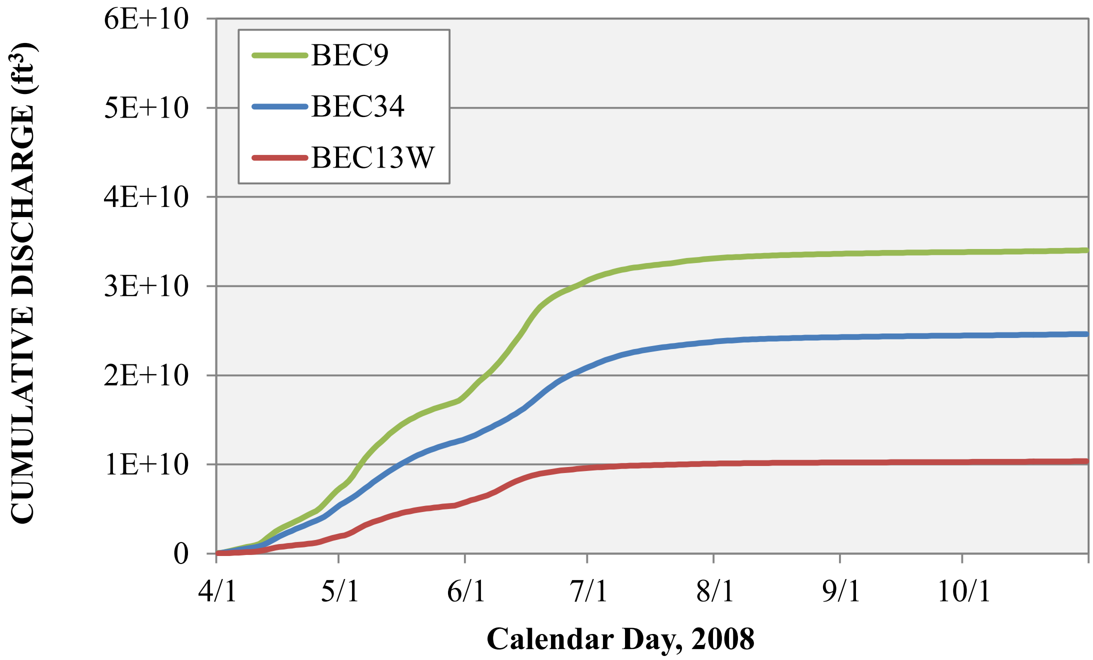

Figure 5.21: 2008 cumulative water volume (ft^3) for BEC9, BEC34 and BEC13W

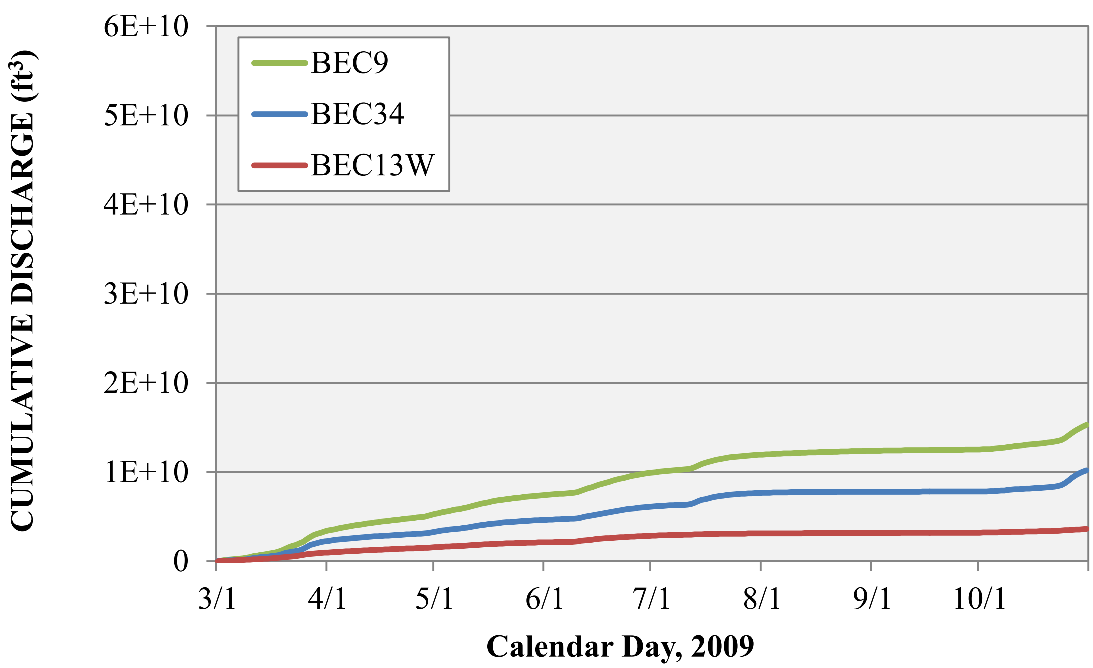

Figure 5.22: 2009 cumulative water volume (ft^3) for BEC9, BEC34 and BEC13W

On average, each monitoring season prior to and including the years for which particle size information is available (i.e., 1984, 1985, 2007, 2008 and 2009) had between three to five major runoff events with numerous smaller events scattered throughout the seven or eight month period of interest. Smaller events were either due to lesser rain accumulation amounts or timing of storm events in relation to the growing season and crop canopy development. It is possible for an "event" or large peak in the hydrograph to persist for long durations and could be the result of multiple rain events that continue feeding the system while maintaining elevated flows.

In 1984, three to four major events were prominent from April through June at BEC9 and BEC13W, but an uneventful July through October followed. Five out of twelve months had below normal flows at both BEC13W and BEC9. In general, March through July average flows were above normal and August through December were below normal. This does not correlate well over the same time period with observed monthly precipitation totals which were in excess in April and October, but were short in March, and May through September. October had an excess of 3.37" of precipitation but had a lower average monthly discharge which could be attributed to timing of rainfall events after dry conditions. Water could have been depleted in the soil from the preceding months allowing for more infiltration.

1985 had five large runoff events at the two sites with numerous minor responses to the hydrograph as well. Seven out of twelve months had below average monthly discharge. January, February and April through August were below normal while March and September through December were above normal. Monthly discharge averages compared well with observed monthly precipitation totals. March had excess precipitation and then May through July flows were below normal before going into a wet fall.

2007 was comprised of four to five large runoff events with snowmelt, an April and May event and two larger end-of-the-season events in August and October of that year. Four out of twelve months in 2007 at BEC9 had below average monthly discharge values (February and May through July) and seven out of twelve months were below average at BEC13W. In general, 2007 had a wet March followed by a dry late spring and summer. A significant rain event in mid-August followed by multiple October rain events helped to lighten the drought-like conditions.

2008 was dominated by three to four runoff events in April, May and June with a very quiet fall. Nine out of twelve months saw lower than average discharges. January and March through September were below average, while February and October through December were above average. Summer flow deficits associate well with observed precipitation deficits.

2009 possessed lower flows compared to other years but had three to five small runoff events in March, July and a late season fall event in October. Eight out of twelve months at BEC9 and eleven out of twelve months at BEC13W had lower than average monthly discharges. Largely, most of the season was at or below normal for 2009 until October rain events brought conditions almost back to normal. Even though 2008 received less precipitation compared to 2009, cumulative flows were much higher for

2008 due to timing of earlier season precipitation events. Cumulative flows were highest in 1984; similar for 1985 and 2008 and lowest in 2009 (Figures 5.19-5.22).

Hydrographs for each year (1984-85 and 2007-09) by site are presented in Figures 5.07-5.18). Hydrographs have the same Y-axis by site to show the variability over the years presented.

5.1.3 Runoff for 1984-85 and 2008-09 at BEC9, 13W and 34

The term runoff refers to depth of water spread out evenly over the entire watershed upstream of the monitoring station. To determine the water depth, the total water volume calculated for the period of interest flowing past a monitoring station is weighted to the watershed acreage. Runoff is calculated by using the following equation:

$$\underset{\text{(inches)}}{\textbf{RUNOFF}} = \frac{\textbf{TOTAL WATER VOLUME}\ (\text{ft}^3)}{\textbf{DRAINAGE AREA}\ (\text{ft}^2)} \times 12$$

Table 5.09: Watershed acreage, total water volume, and runoff for 1984-85 and 2007-09. Dates highlighted in red indicate a shorter calculation time period.

Year	Station	Watershed (acres)	Volume (ft^3)	Time Period	Runoff (inches)
1984	BEC13W	554,640	16,250,803,200	3/1-10/31	8.07
1985			10,054,972,800	3/1-10/31	4.99
2007			11,427,030,720	3/1-10/31	5.68
2008			10,367,395,200	4/1-10/31	5.15
2009			3,612,202,560	3/1-10/31	1.79
2008	BEC34	977,760	24,632,677,152	4/1-10/31	6.94
2009			10,195,490,502	3/1-10/31	2.87
1984	BEC9	1,542,400	54,924,480,000	3/1-10/31	9.81
1985			28,159,315,200	3/1-10/31	5.03
2007			43,179,264,000	3/1-10/31	7.71
2008			34,025,788,800	4/1-10/31	6.08
2009			15,273,100,800	3/1-10/31	2.73

Runoff values were calculated for 1984-85, 2007 and 2009 from March 1st – October 31st and from April 1st through October 31st for 2008 based on available data (Table 5.09). Results ranged from 1.79-8.07" for BEC13W, 2.87-6.94" for BEC34 and 2.73-9.81" for BEC9. 2009 had the lowest runoff depth out of the measured years and subsequently also experienced the lowest intensity of flows and second highest departure from normal precipitation. 1984 had the highest runoff depth for BEC13W and BEC9. To further that statement, 1984 was also the only year to have an annual precipitation total above the 30-year normal and also saw much higher average flows from March through July. BEC34 was not continually gauged in 1984-85 and therefore, runoff results are not available for comparison in those two years. Gauging equipment was also not installed until mid-August 2007 at BEC34. Since data was not obtainable over the same time period, it also was not available for comparison.

Despite just over two more inches of precipitation in 2009 versus 2008 (Table 5.01), 2008 had greater runoff (an additional 3.3 to 4.1" more per station) and saw higher peak flows (discharge). This was likely due to timing of the rain events during the agricultural growing season. If precipitation events occur in spring and early summer before the growing season is well established, water infiltrates through soil and runs off the land more readily. When crop canopies are well developed (July through September), water can be taken up by crops and the ground surface is also stabilized by root systems. If large storm events occur in late March to mid-June, the ground is more vulnerable to runoff. Other factors such as soil type and soil moisture also play a role. Similarly, 2007 had just over 7" of rain more than 2008, yet runoff values were not exceedingly higher by the same magnitude than 2008 likely due to drier spring and summer months when the ground is most susceptible to runoff and erosion.

5.2 Sediment Loading, Flow-weighted Mean Concentrations and Yields

A total of 17-40 TSS results were available per site per year for the three monitoring stations: BEC9, BEC13W and BEC34 (Appendix 1). Results were utilized for the loading calculation and were a mixture of results collected by this project, and publicly available results from the MPCA. TSS results utilized for each sites loading calculation were only from one lab for consistency (i.e. BEC34 was only from MSU's internal laboratory, while BEC9 was only from MVTL). Results from the MPCA were analyzed at a state certified laboratory and collected using standard operating procedures. BEC34 TSS results were collected and analyzed solely for the purpose of this project.

Table 5.10: 2008 and 2009 Total Suspended Solids loading for the three main stem monitoring sites, BEC9, BEC34 and BEC13W.

LOADING RESULTS	SITE	2008 TSS		2009 TSS	
		kg	lbs	kg	lbs
CONTRIBUTION TO RESERVOIR	BEC34	110,130,670	242,838,127	29,213,870	64,416,583
	BEC13W	22,286,595	49,141,942	5,628,430	12,410,689
TOTAL CONTRIBUTION *	BEC34+ BEC13W	132,417,265	291,980,069	34,842,300	76,827,272
TOTAL LOAD EXITING RESERVOIR	BEC9	269,296,020	593,797,724	42,627,768	93,994,228
DIFFERENCE		**136,878,755**	**301,817,655**	**7,785,468**	**17,166,956**
SINK OR SOURCE?		SOURCE		SOURCE	

* From Blue Earth and Watonwan River main stems. Ravines and direct overland contributions downstream from BEC13W and BEC34 are not accounted for.

Table 5.11: 2008 and 2009 load, flow-weighted-mean concentration, yield and runoff for BEC9, BEC34 and BEC13W.

Site ID		BEC34		BEC13W		BEC9	
Year		2008	2009	2008	2009	2008	2009
Date Range		4/1/08-10/31/08	3/1/09-10/31/09	4/1/08-10/31/08	3/1/09-10/31/09	4/1/08-10/31/08	3/1/09-10/31/09
Load	kg	110,130,670	29,213,870	22,286,595	5,628,430	269,296,020	42,627,768
	lbs	242,838,127	64,416,583	49,141,942	12,410,689	593,797,724	93,994,228
FWMC	mg/L	158	101	76	55	279	99
Yield	lbs/acre	248	66	89	22	385	61
Runoff	inches	6.94	2.87	5.15	1.79	6.08	2.73
Volume	ft^3	24,632,677,152	10,195,490,502	10,367,395,200	3,612,202,560	34,025,788,800	15,273,100,800
	liters	697,597,416,945	288,736,291,017	293,604,632,064	102,297,576,499	963,610,338,816	432,534,214,656
Watershed	acre	977,760		554,640		1,542,400	
	ft^2	42,591,225,600		24,160,118,400		67,186,944,000	

While BEC9 and BEC13W have ample historical data available (both discharge and water chemistry), BEC34 has very limited water quality results. Gauging flow is not an active practice by either the USGS or MPCA at the BEC34 bridge crossing, though it was gauged for two separate projects from 1989-92 and again in 1996 (Payne 1994, WRC 2000). However, in both studies, BEC9 was not concurrently monitored along with BEC13W and BEC34. Instead, a bridge crossing at the outlet of the Blue Earth River (on US Highway 169) in Mankato, Minnesota was monitored and sampled. Without water chemistry and gauging data simultaneously from all three stations, the true mass balance of Rapidan Reservoir is unknown. No other published loading data could be computed that included all three stations to truly decipher if the reservoir was acting as a sink or source for sediment. Samples associated with the Rapidan Research Project were collected in 1985 at BEC34, however, only a handful were collected and a majority were during lower flows which would underestimate and bias the loading results. Flow was not gauged at BEC34 during the 1984-85 study (Quade et al. 2004).

Total suspended solid concentrations ranged from 5 to 784 mg/L at BEC9 in 2008 and 13-515 mg/L in 2009. BEC13W had the lowest maximum concentrations ranging from 7 to 183mg/L in 2008 and 6 to 133 mg/L in 2009. Finally, TSS concentrations at BEC34 ranged from 10 to 418 mg/L in 2008 and 12-200 mg/L in 2009. In all cases, concentrations were higher in 2008 than 2009 which agrees with the FWMC for those years as well. FWMC ranged from 55 mg/L on the low end (BEC13W in 2009) to 279 mg/L on the high end (BEC9 2008).

Yield results show similar patterns to FWMC patterns. 2008 had higher yields than 2009 at all three sites, even though 2008 data represents a seven month period while 2009 results are reported over an eight month period. The highest yield calculated was 385 pounds per acre at BEC9 in 2008. The lowest yield observed was 22 pounds per acre at BEC13W in 2009. Because yield results are a direct measurement from the total TSS load, the same holds true for loading at the three monitoring stations. The Watonwan River contributed less suspended solids to Rapidan Reservoir than did the Blue Earth River at County Road 34 in both 2008 and 2009.

Based on 2008 and 2009 loading data, Rapidan Reservoir acted as a source for TSS to downstream reaches. In general terms, more sediment was leaving the reservoir than was being supplied to it by upstream contributions and indicates the trap efficiency of the reservoir is not sufficient to retain all particle sizes. Table 5.10 outlines the Blue Earth and Watonwan River loading contributions to the reservoir and the total load of suspended solids leaving the reservoir downstream. The sum of BEC13W and BEC34 loads is assumed to be the total load to the reservoir although those numbers do not account for ravine and direct overland contributions from locations downstream of the BEC13W and BEC34 gauging stations. Contributions are presumed to be small. Table 5.11 provides detailed loading information for 2008 and 2009 at each site, including total load, flow-weighted mean concentration, yield, runoff and total water volume. 2008 had lower precipitation totals than 2009, but saw higher water volumes, TSS loads, yields and FWMC. Higher concentrations, yields and runoff downstream from Rapidan Reservoir also coincide with showing the reservoir was acting as an overall source for sediment in 2008 and 2009.

5.3 Surface Reservoir Sandbar Distribution

Eight aerial photographs were obtained of Rapidan Reservoir spanning from 1939 to 2006. Photographs were analyzed using ArcGIS for the purpose of characterizing the extent of sandbar accumulation in the reservoir by digitizing exposed sandbars.

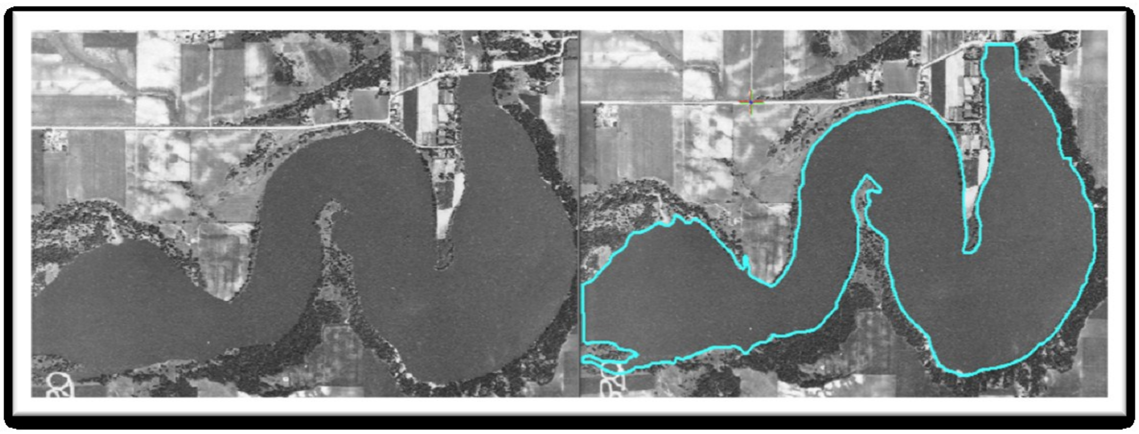

Figure 5.23: Aerial photograph of Rapidan Reservoir, 05-30-1939. Cyan color indicates outline of reservoir in 1939.

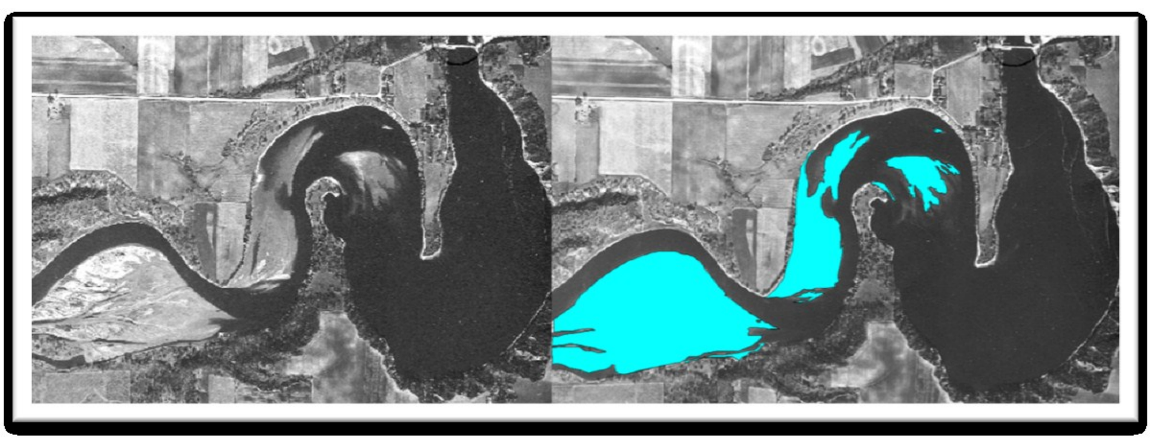

Figure 5.24: Aerial photograph of Rapidan Reservoir, 10-15-1949. Cyan color indicates digitized area of sandbars.

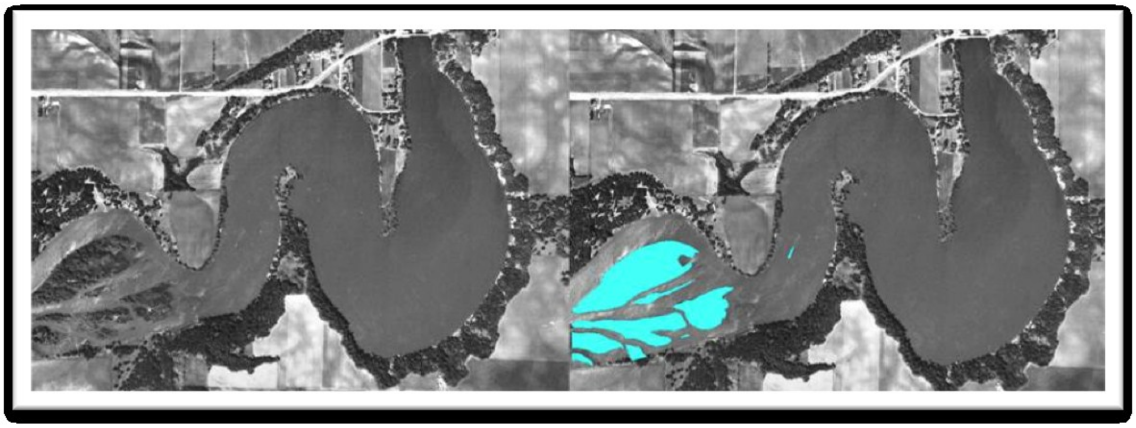

Figure 5.25: Aerial photograph of Rapidan Reservoir, 06-26-1964. Cyan color indicates digitized area of sandbars.

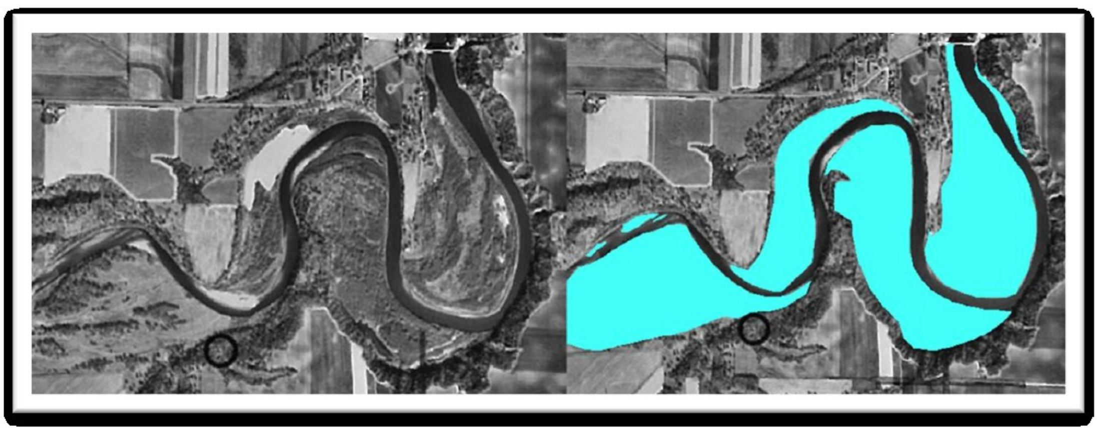

Figure 5.26: Aerial photograph of Rapidan Reservoir, 10-20-1974. Cyan color indicates digitized area of sandbars.

Figure 5.27: Rapidan Reservoir, 1985. Estimate off of map provided in the Rapidan Research Report (Quade et al. 2004). Cyan color indicates digitized area of sandbars.

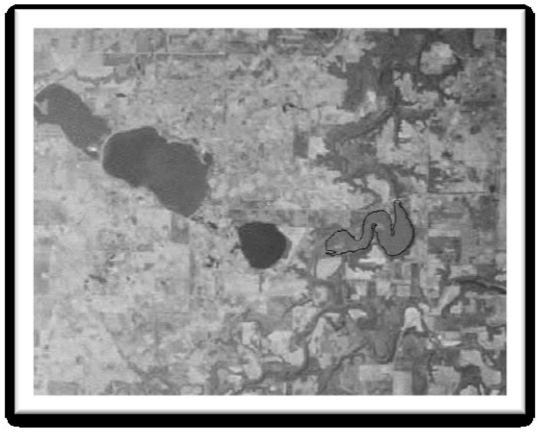

Figure 5.28: Rapidan Reservoir, 05-02-1985, after dam rehabilitation. The chain of lakes in the image are Crystal-Loon-Mills. Rapidan Reservoir is the kidney bean shaped reservoir to the right of the lakes. Low resolution, 1:80,000 scale.

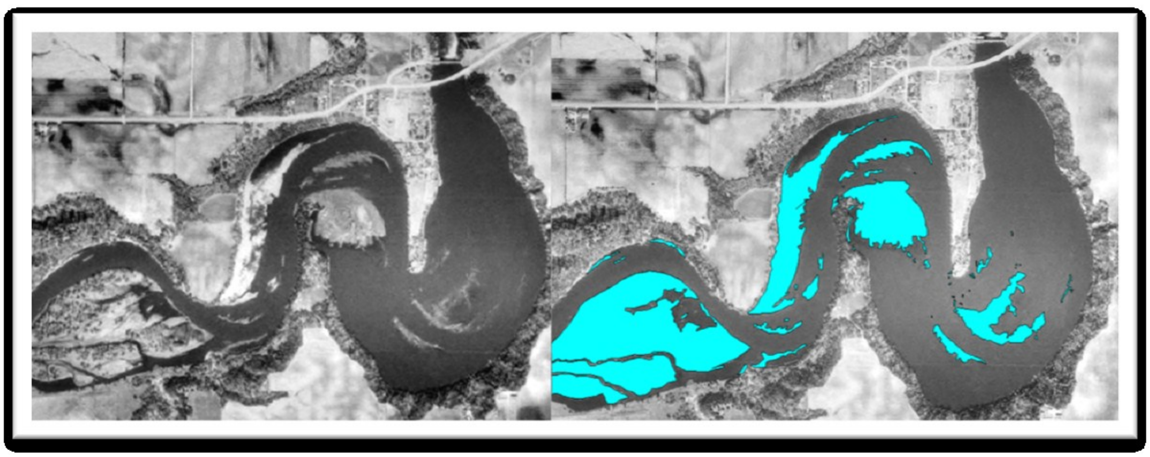

Figure 5.29: Aerial photograph of Rapidan Reservoir, 1992. Cyan color indicates digitized area of sandbars.

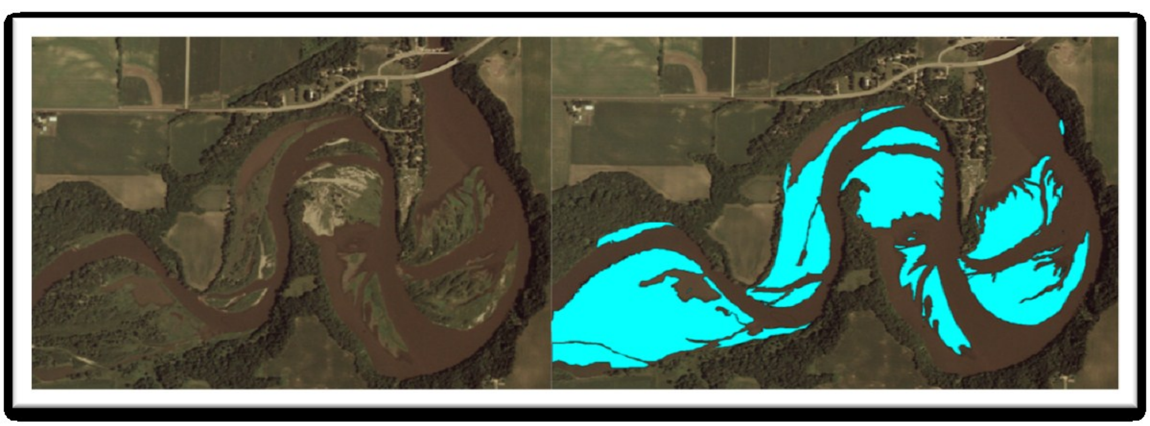

Figure 5.30: Aerial photograph of Rapidan Reservoir, 2002. Cyan color indicates digitized area of sandbars.

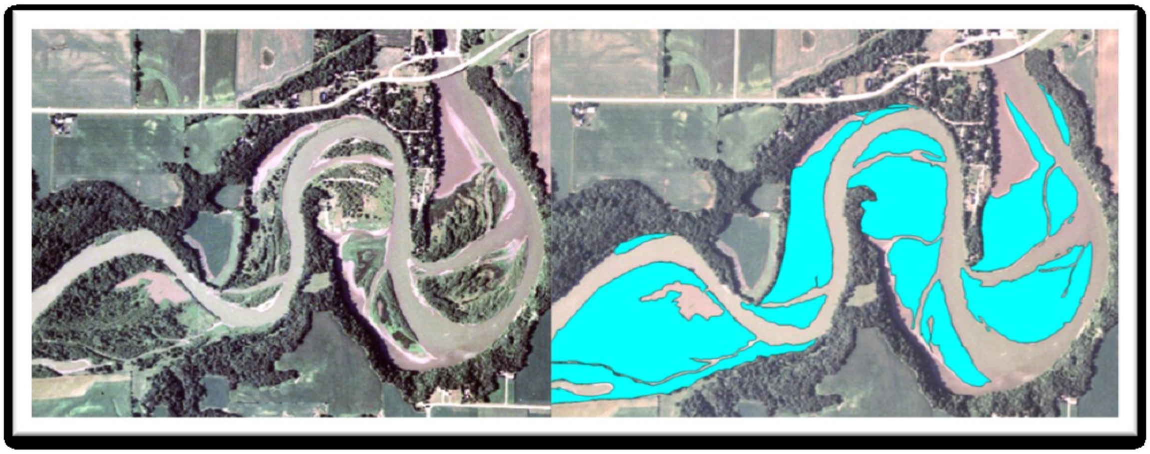

Figure 5.31: Aerial photograph of Rapidan Reservoir, 2006. Cyan color indicates digitized area of sandbars.

Table 5.12: Surface water area and sandbar coverage area calculated from multiple historic aerial photographs using ArcGIS 9.2.

YEAR	SURFACE WATER AREA (acres)	SANDBAR SURFACE AREA (acres)	PERCENT SANDBARS
1939	315.72	0	0 %
1949*	227.68	88.04	28 %
1964	281.68	34.04	11 %
1974**	62.98	252.74	80%
1985	278.05	37.67	12 %
1992	223.57	92.15	29 %
2002	171.80	143.92	46 %
2006	138.76	176.96	56 %

* 1949 reservoir water level was very low.

** Dam was inoperable from 1965-1984 and was in run-of-the-river mode.

The 1939 aerial photograph was used as the initial reservoir surface area reference due to it being the earliest aerial imagery available. A small portion of the true reservoir is cut out of the frame on the western border and the adjacent frame could not be found to complete the 1939 image. Each subsequent year was digitized using the same border as the 1939 image for consistency. Though sedimentation surely took place in the reservoir prior to 1939, it is assumed that from 1911 to 1939 that the surface area of the reservoir was not diminished by sandbars. No aerial photographs were found prior to 1939 or before the dam was completed in 1911. The 1949 image was taken when the water level was visibly low from normal conditions. A daily average flow was available for this day from the USGS database and showed that the discharge below the dam was 18 cfs. The low water level could have either been from a dry fall or from recent draining of the reservoir due to the peaking operation of the dam at that time. A majority of the visible sandbars in the 1949 photo do not show vegetation growth suggesting that they were not exposed for a long period of time and likely were submerged during normal flow conditions. The 1964 image was taken on 6/26/1964 and the daily average flow was 669 cfs which is well below the average (1909-2010) of 2,290 cfs for June 26th (USGS online database: http://waterdata.usgs.gov/mn/nwis). Visible sandbars, however, appear fairly vegetated with a well-established vegetation canopy signifying that the sandbars had existed for an extended amount of time. In 1965, a peak discharge significantly damaged the dam to the point that it remained out of operation until being repaired in 1984. During this period of the time, water was merely flowing unimpeded through the reservoir and over the dam. No impoundment of water was occurring. The 1974 image shows that the river had reverted to a natural channel through the deposited sediment as a result. Because the dam was out of operation in the 1974 image, it subsequently has the highest percentage of sandbars. If the dam had been in operation at the time, the preceding findings would not be true. A digital mapping image of the reservoir is available for 1985 from the 2004 Rapidan Research Report (Figure 2.3). The image specified shaded gray areas for river channel and reservoir. For the purpose of this paper, it is assumed that the areas shaded as reservoir were capable of being fully inundated with water under normal water levels. It can also be assumed that sandbars were present but not exposed except during low water levels. Some sandbars could have been excavated with the dredging associated with dam rehabilitation in the mid 1980's. A low resolution image from 05-02-1985 was available from the USGS Earth Explorer online database. It is difficult to decipher, but appears to support correlation between the aerial photograph and the map available from Quade et al. (2004) (Figures 5.27 and 5.28). The water level in the reservoir is unknown in the 1992, 2002 and 2006 images. The available aerial images represent one day in time and it is assumed that the surface expression and area of sandbars increases or decreases as water levels fluctuate throughout the season. Visual observations of aerial photos from 2007-2010 show little noticeable increase in the sandbar extent. The percent of surface exposed sandbars ranges from 0% in 1939 to 56% by 2006. Based on the geomorphologic evolution of the basin and current land use practices, the Blue Earth River is primed to transported large quantities of sediment. Findings by Gran et al. (2011) and Magner (2004) suggest that rivers have a natural tendency to incise and Thoma (2005) and Bauer (1998) show that incision leads to stream bank erosion and sloughing of banks which can supply large masses of sediment to the river.

Results of digitized sandbar polygons for each available year as compared to the original image are presented in Figures 5.23-5.31. Percentages for surface area lost in the area of interest are presented in Table 5.12.

5.4 Loss on Ignition of Rapidan Reservoir Sediment Samples

Loss on ignition (LOI) provides the percent organic material in a sample and can be indicative of highly suspended materials because the average density of organic matter is less than that of inorganic particles. It can also be an indicator for residence time especially in lower velocity backwater channel areas where sediment could be more susceptible to algal growth attachment from nutrient availability. All samples collected in Rapidan Reservoir for particle size analyses (Figure 5.43) were also run for LOI. Results of individual samples by transect (from downstream to upstream) are presented in Figures 5.32 to 5.41. Average LOI results by transect are provided in Table 5.13 and Figure 5.42.

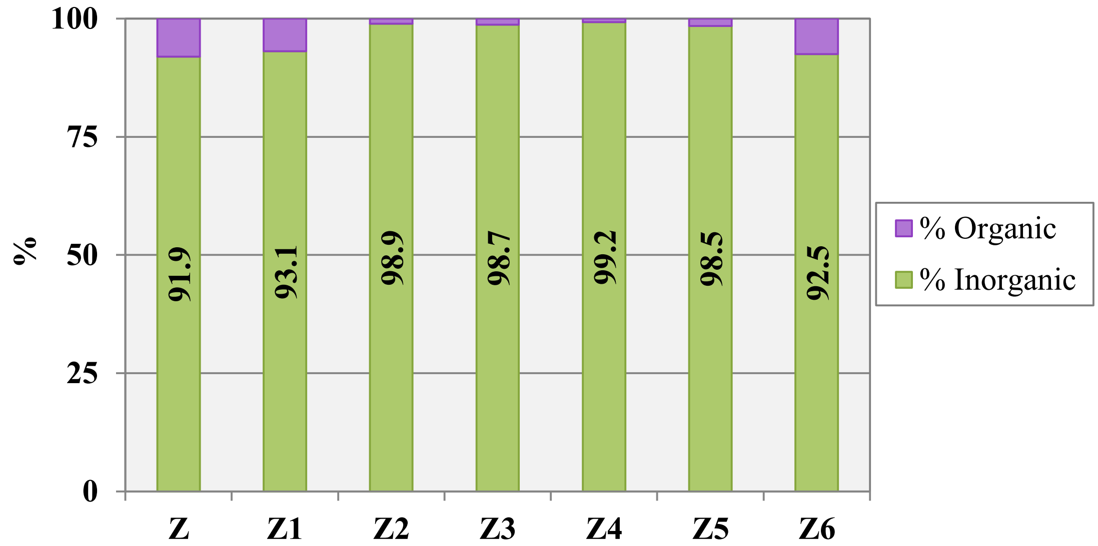

Figure 5.32: Percent organic vs. inorganic sedimentary particle composition for the Rapidan Reservoir: Transect Z.

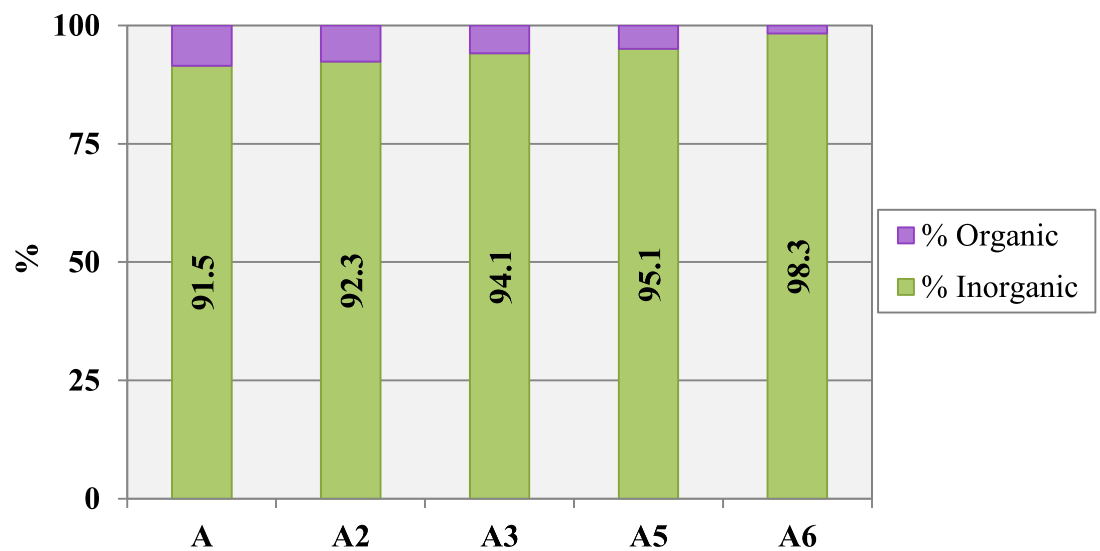

Figure 5.33: Percent organic vs. inorganic sedimentary particle composition for the Rapidan Reservoir: Transect A.

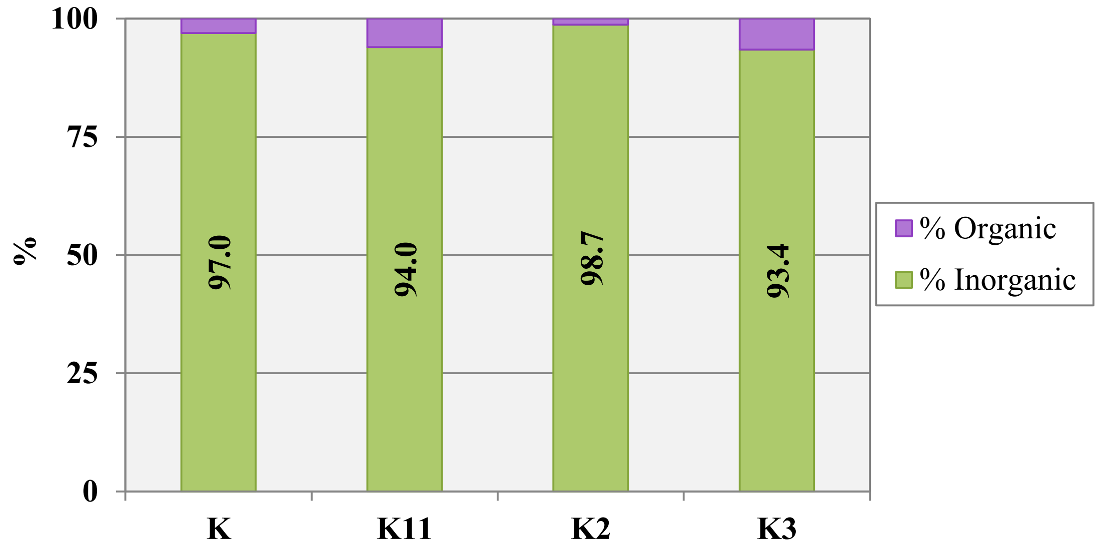

Figure 5.34: Percent organic vs. inorganic sedimentary particle composition for the Rapidan Reservoir: Transect K.

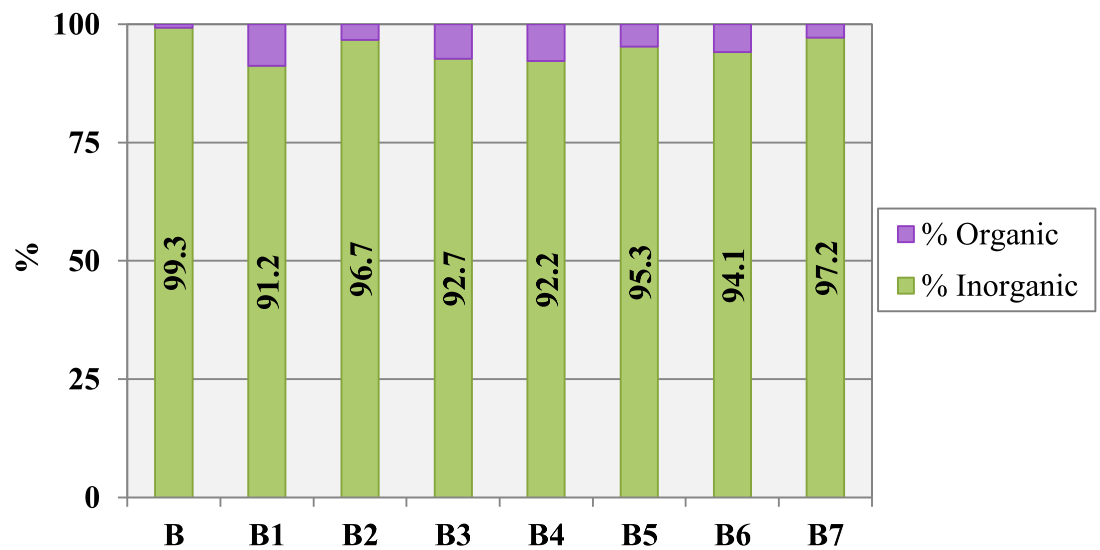

Figure 5.35: Percent organic vs. inorganic sedimentary particle composition for the Rapidan Reservoir: Transect B.

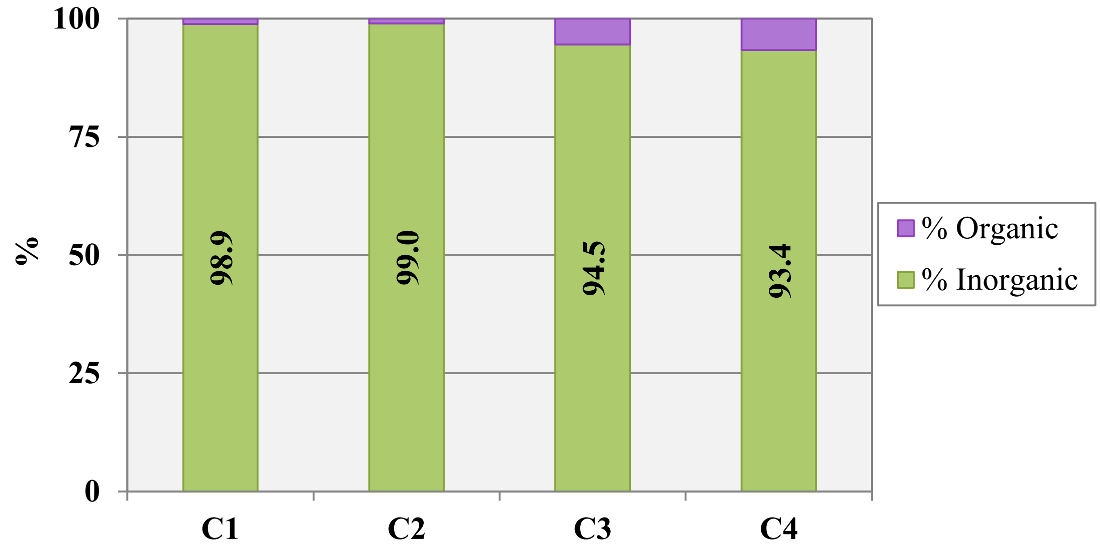

Figure 5.36: Percent organic vs. inorganic sedimentary particle composition for the Rapidan Reservoir: Transect C.

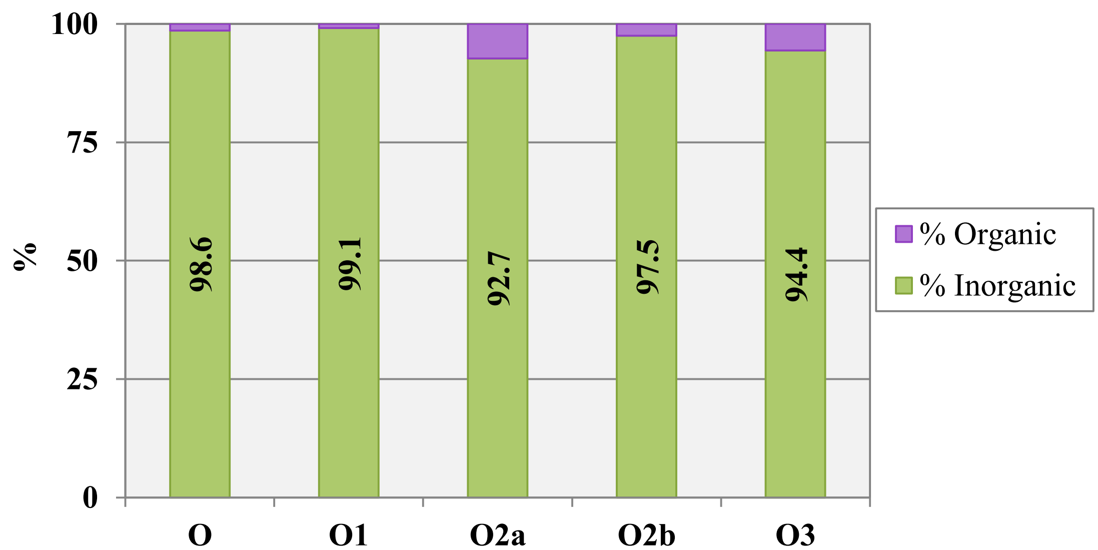

Figure 5.37: Percent organic vs. inorganic sedimentary particle composition for the Rapidan Reservoir: Transect O.

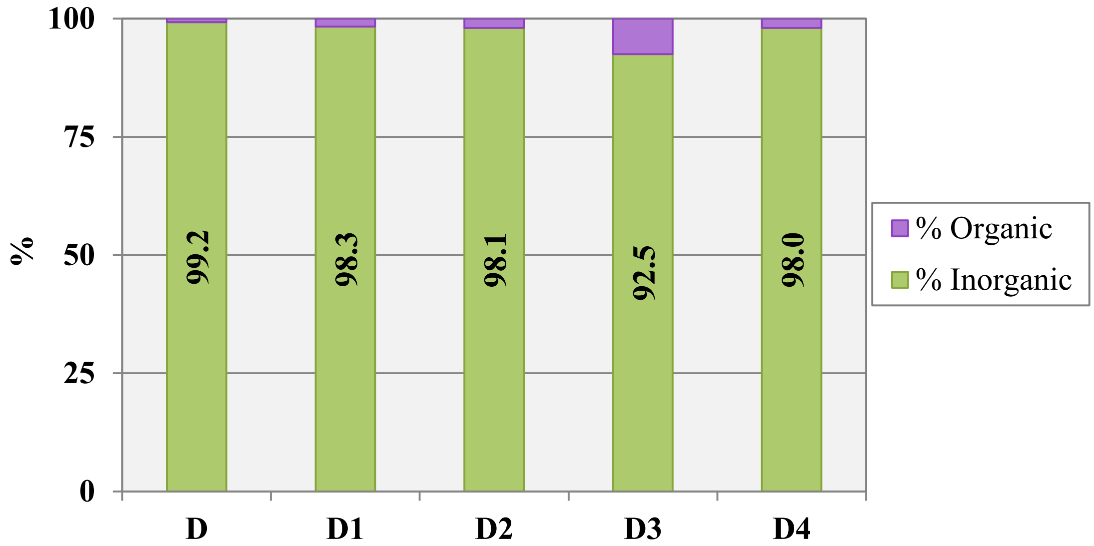

Figure 5.38: Percent organic vs. inorganic sedimentary particle composition for the Rapidan Reservoir: Transect D.

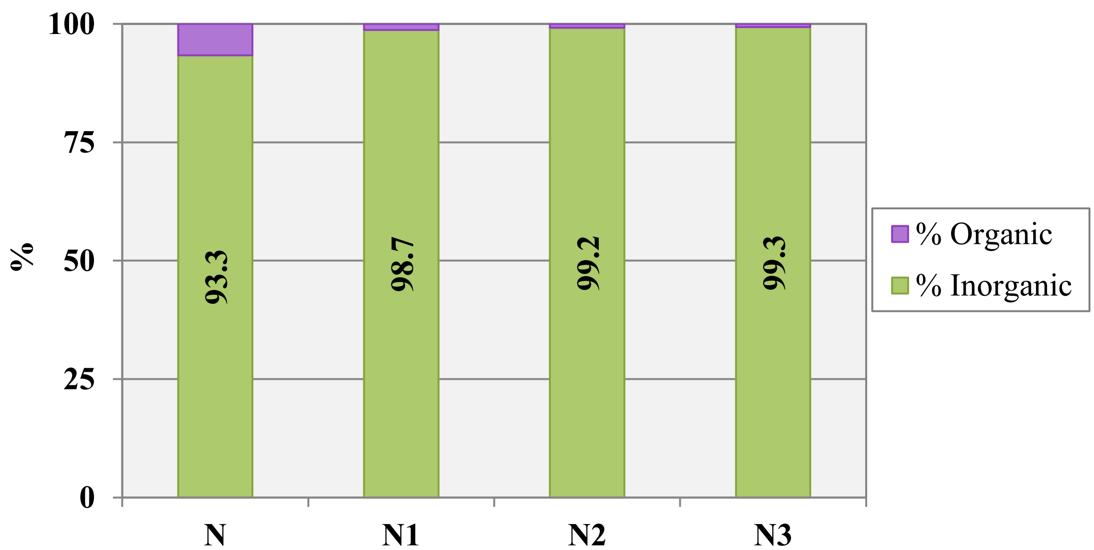

Figure 5.39: Percent organic vs. inorganic sedimentary particle composition for the Rapidan Reservoir: Transect N.

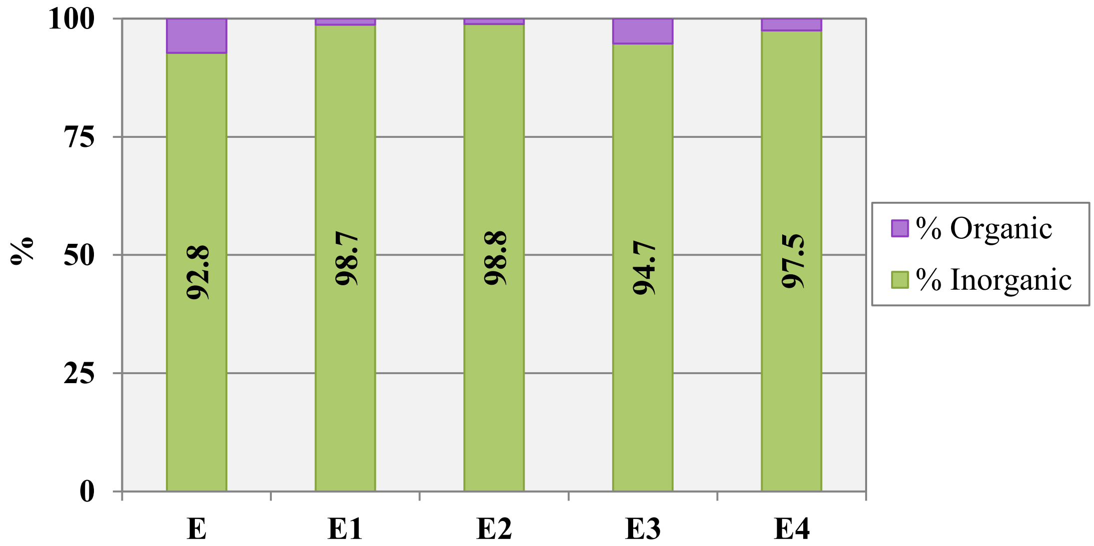

Figure 5.40: Percent organic vs. inorganic sedimentary particle composition for the Rapidan Reservoir: Transect E.

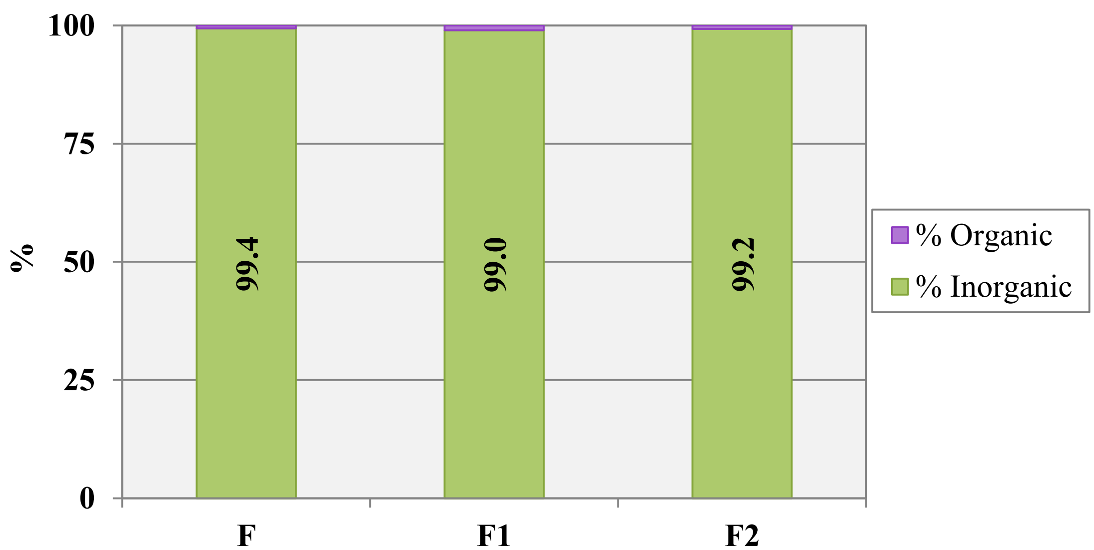

Figure 5.41: Percent organic vs. inorganic sedimentary particle composition for the Rapidan Reservoir: Transect F.

Table 5.13: Average % Inorganic Material by Transect, Rapidan Reservoir. Transect Z is furthest downstream. Transect F is furthest upstream.

TRANSECT	% INORGANIC	% ORGANIC
Z	96.12	3.88
A	94.27	5.73
K	95.79	4.21
B	94.83	5.17
C	96.44	3.56
O	96.46	3.54
D	97.23	2.77
N	97.64	2.36
E	96.50	3.50
F	99.21	0.79
Overall Average	**96.22**	**3.78**

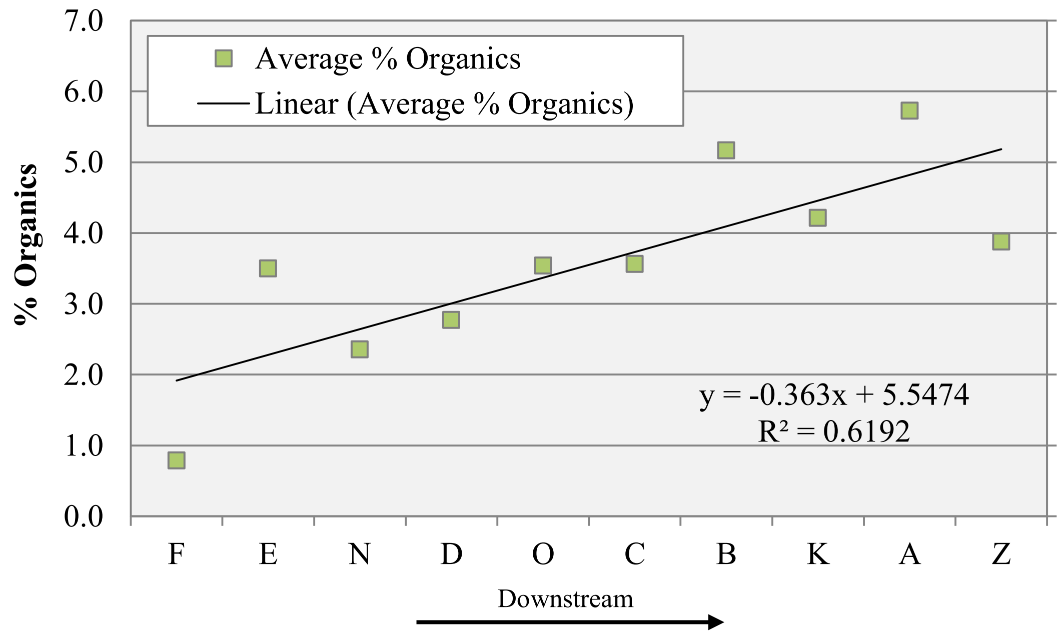

Figure 5.42: Correlation between the average % organics per transect from upstream to downstream through Rapidan Reservoir.

Sample B1 (Transect B) had the highest percentage of organics at 8.77%. Sample F (Transect F) had the lowest percent organics (0.58%), and is subsequently the sample located furthest upstream in the reservoir. All samples within a transect show that Transect A had the overall highest percentage of organics and Transect F had the lowest percentage of organic content. The average for all reservoir samples was 3.78% organics (96.22% inorganic). Appendix 3 provides detailed results for all samples. The low percentage of organics present in Rapidan Reservoir suggests that water likely does not have a significant residence time through the reservoir allowing for suspended materials to originate and settle.

LOI averages by transect were graphed from upstream to downstream (Figure 5.42). A trend line was added to the results which shows a loose trend (R^2 = 0.6192) signifying the percent organic matter within each sample increases from upstream to downstream (closest to the dam) in the reservoir. Downstream sediments both have been in the reservoir longer than upstream sediments and may be finer indicating easier transportability.

5.5 Particle Size Analyses

Fifty sediment samples were collected (Figure 5.43) and analyzed from ten different transects in Rapidan Reservoir, along with three duplicates. To illustrate the grain size distribution by weight percent, a histogram was created for each sample with weight percent on the Y-axis, and particle size (phi) on the X-axis. Results can be found in Figures 5.44-5.53.

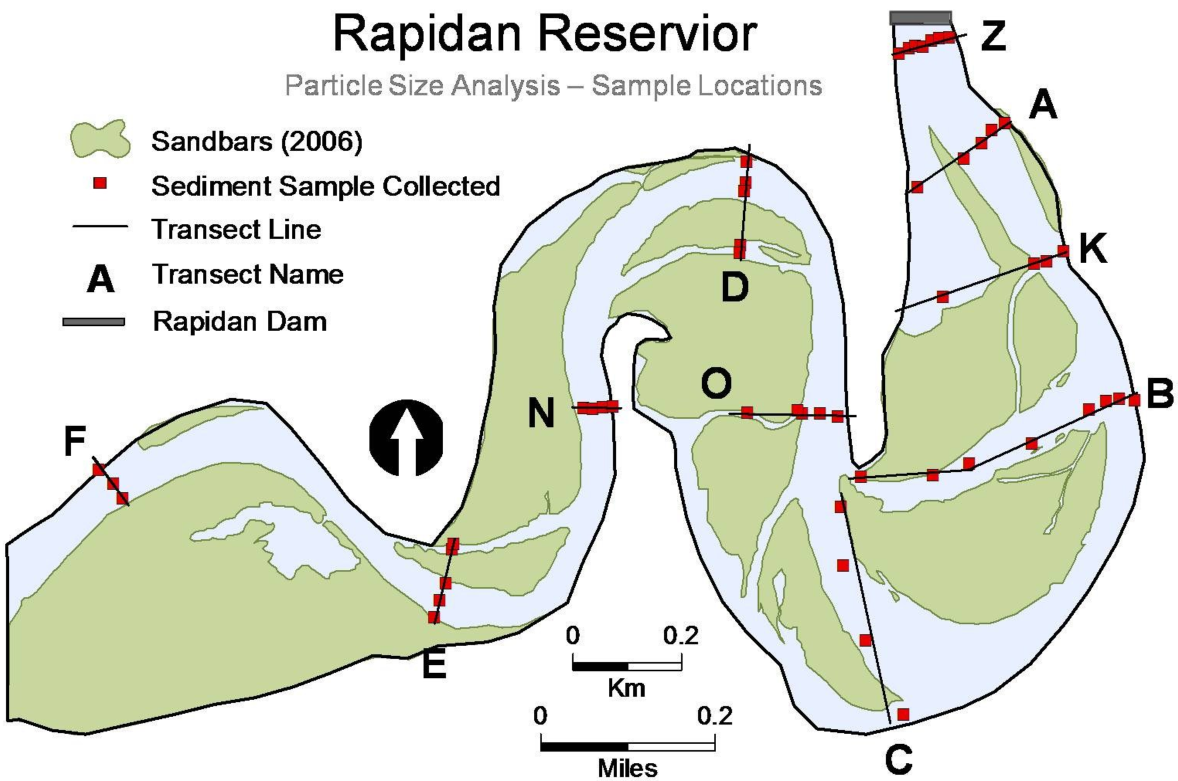

Figure 5.43: Transect locations throughout Rapidan Reservoir.

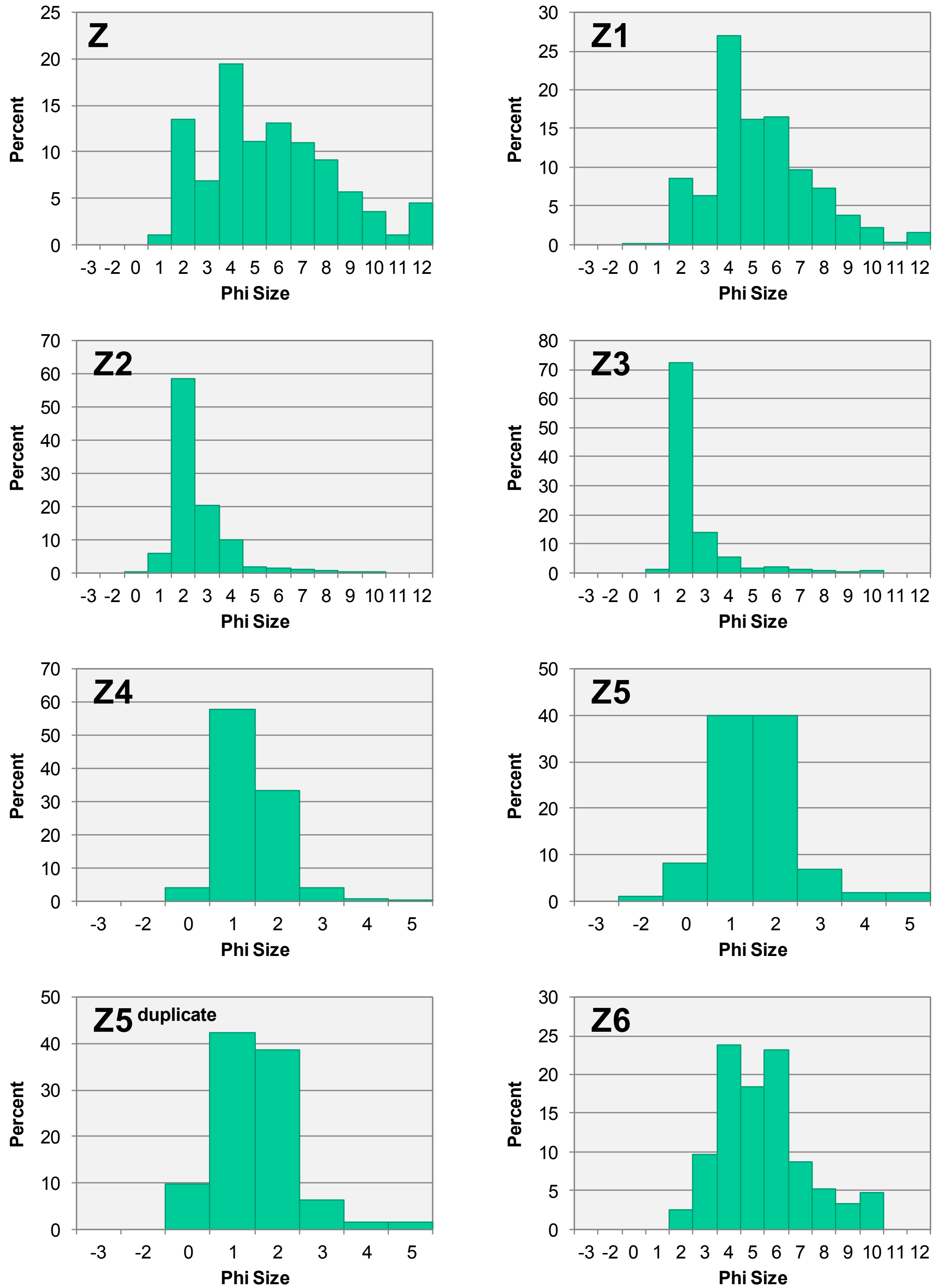

Figure 5.44: Particle class histogram: Transect Z.
Note: % scale changes by graph to best show the distribution between particle classes.

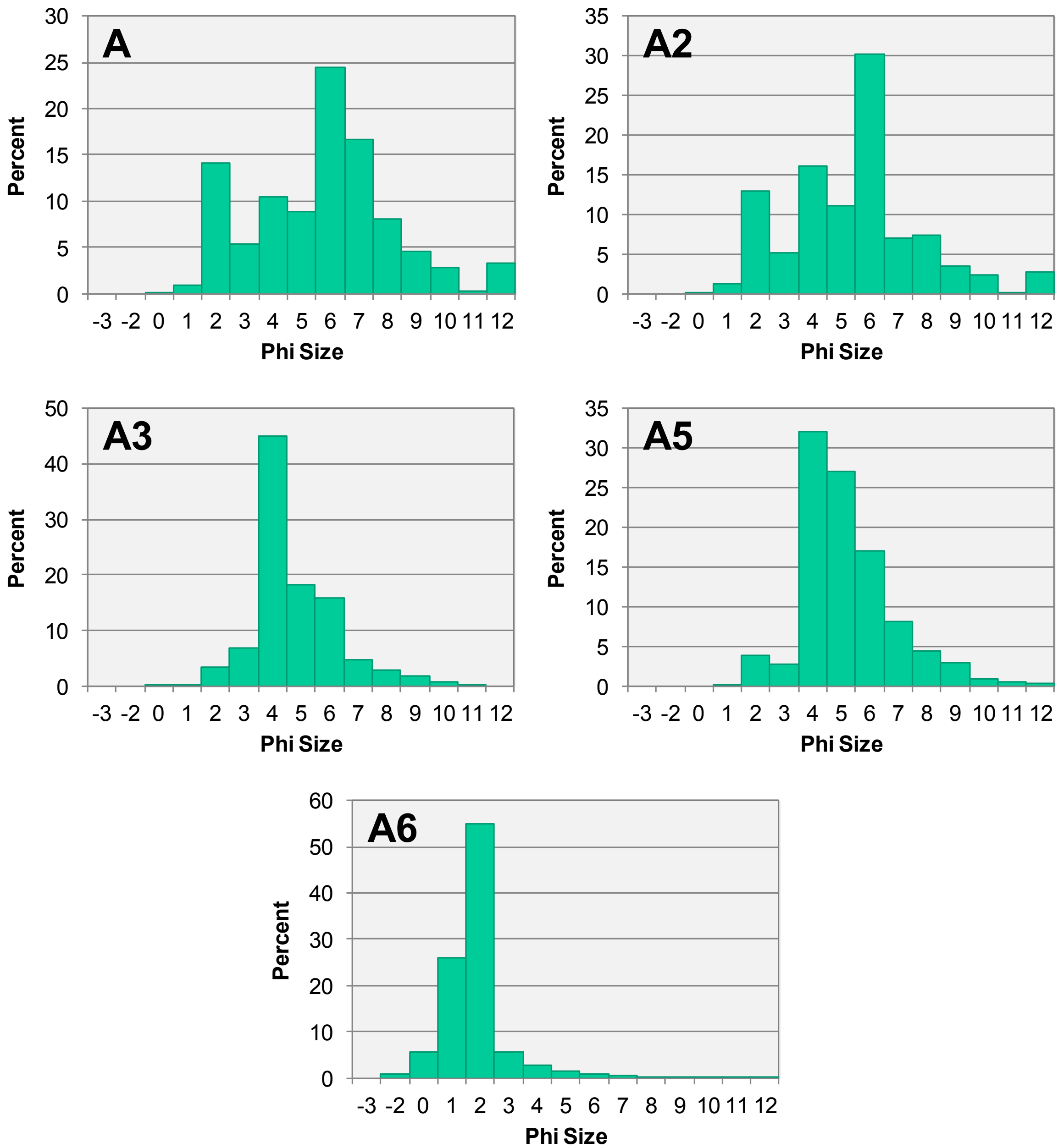

Figure 5.45: Particle class histogram: Transect A.
Note: % scale changes by graph to best show the distribution between particle classes.

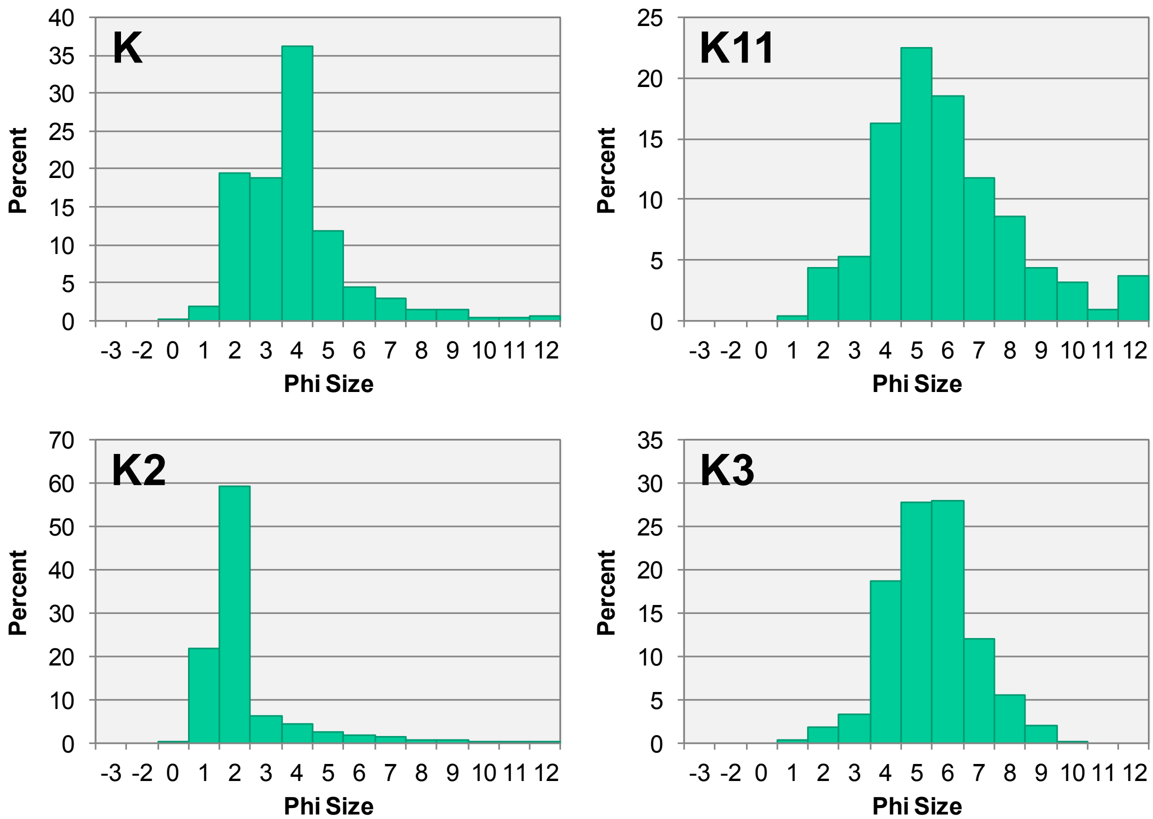

Figure 5.46: Particle class histogram: Transect K.
Note: % scale changes by graph to best show the distribution between particle classes.

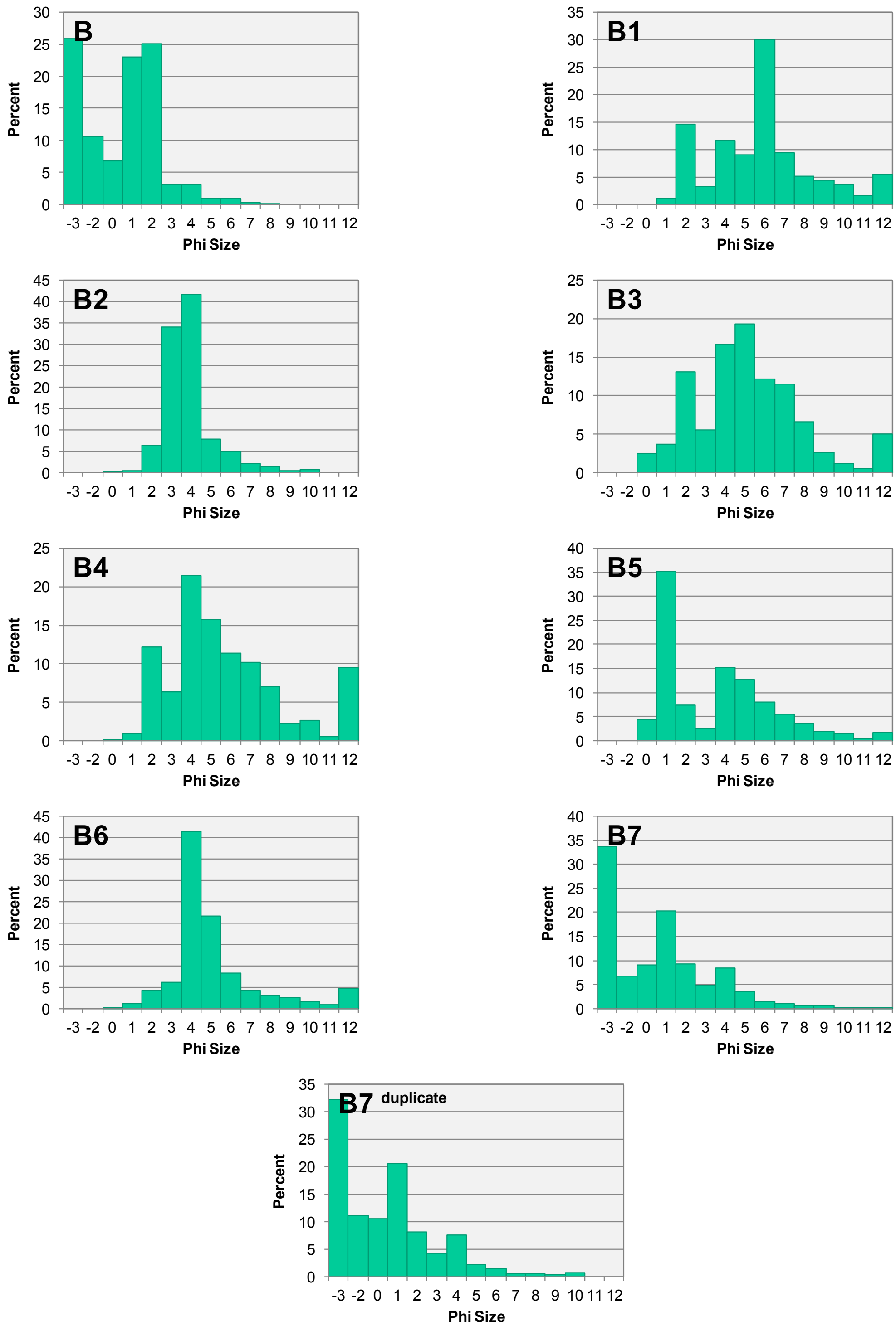

Figure 5.47: Particle class histogram: Transect B.
Note: % scale changes by graph to best show the distribution between particle classes.

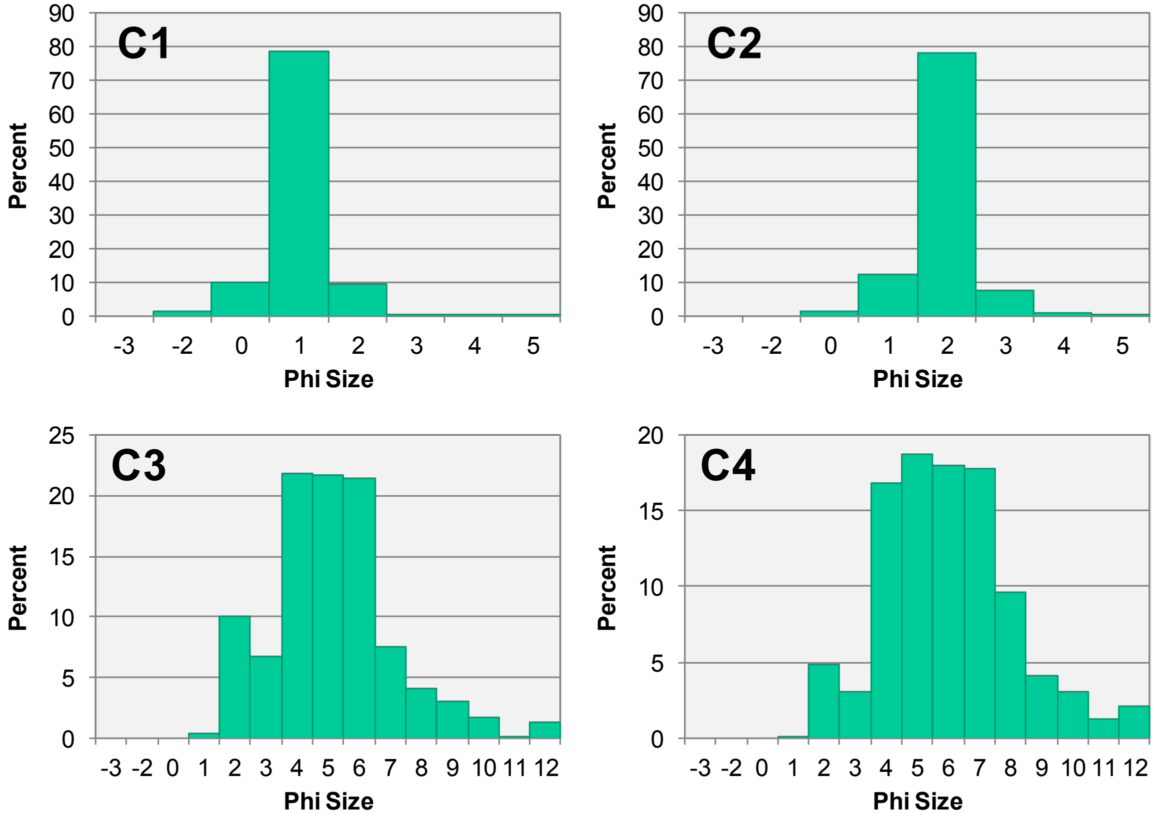

Figure 5.48: Particle class histogram: Transect C.
Note: % scale changes by graph to best show the distribution between particle classes.

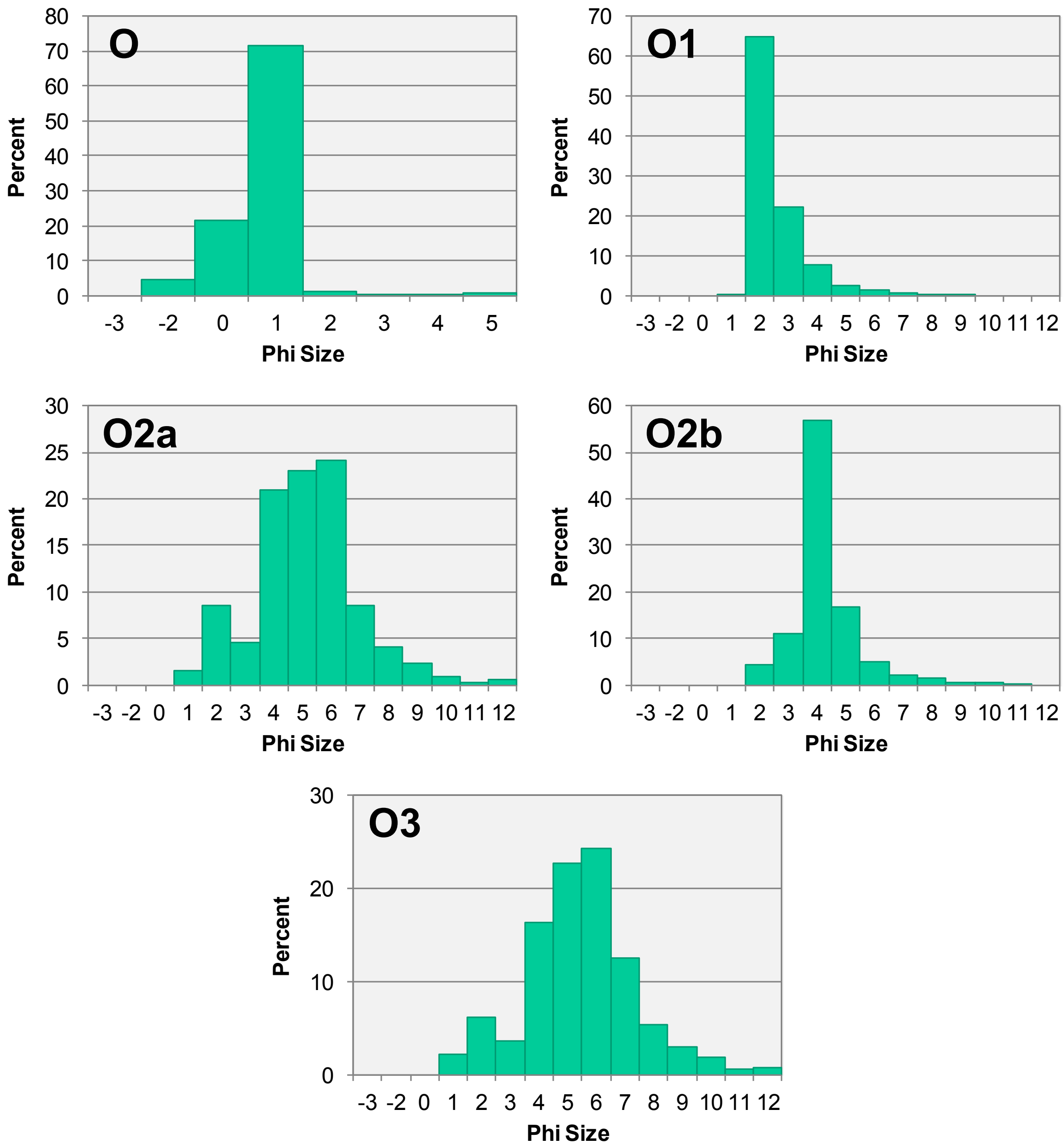

Figure 5.49: Particle class histogram: Transect O.
Note: % scale changes by graph to best show the distribution between particle classes.

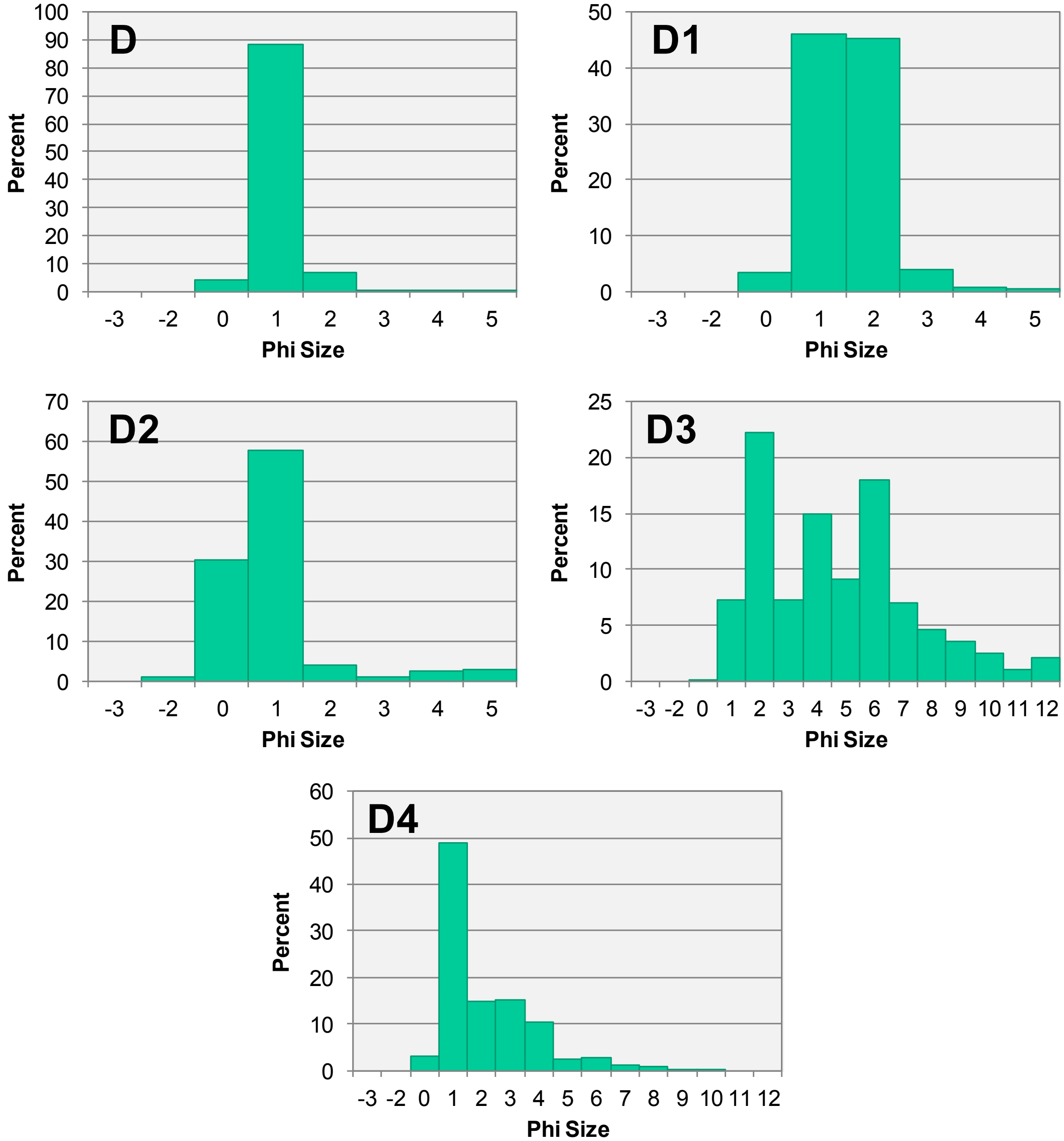

Figure 5.50: Particle class histogram: Transect D.
Note: % scale changes by graph to best show the distribution between particle classes.

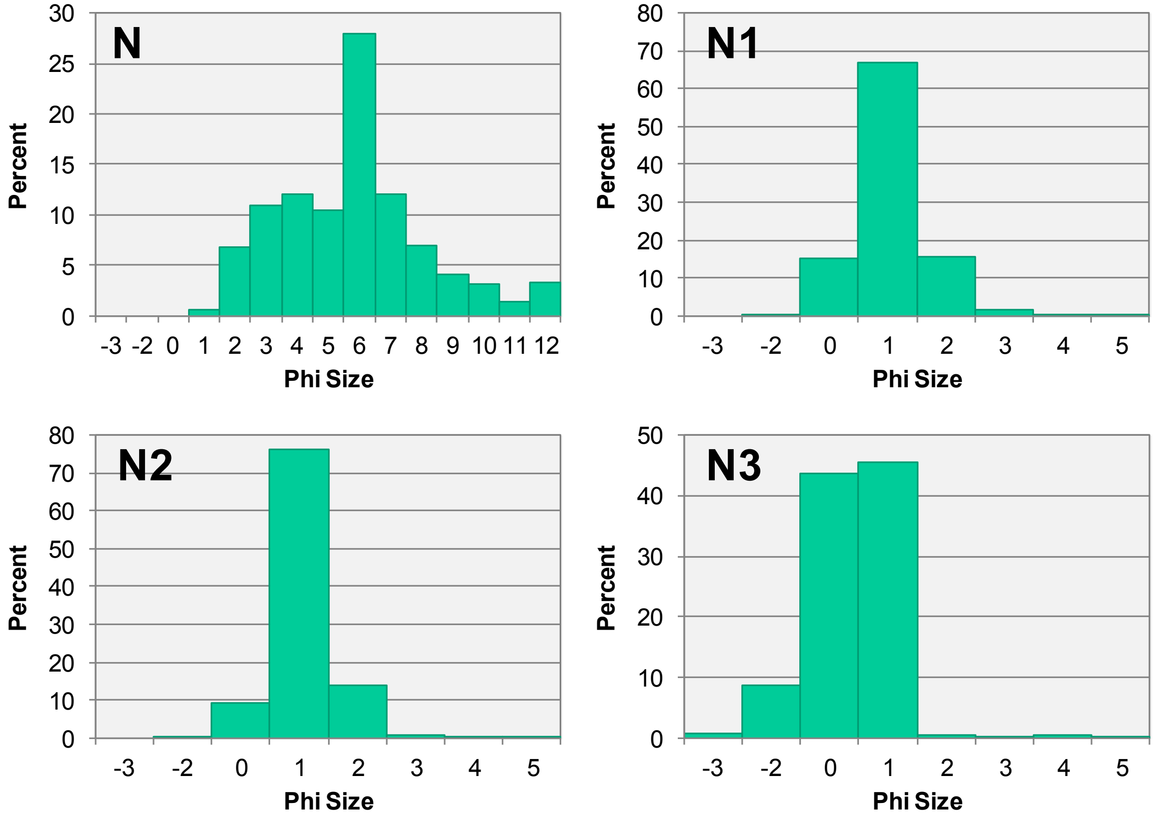

Figure 5.51: Particle class histogram: Transect N.
Note: % scale changes by graph to best show the distribution between particle classes.

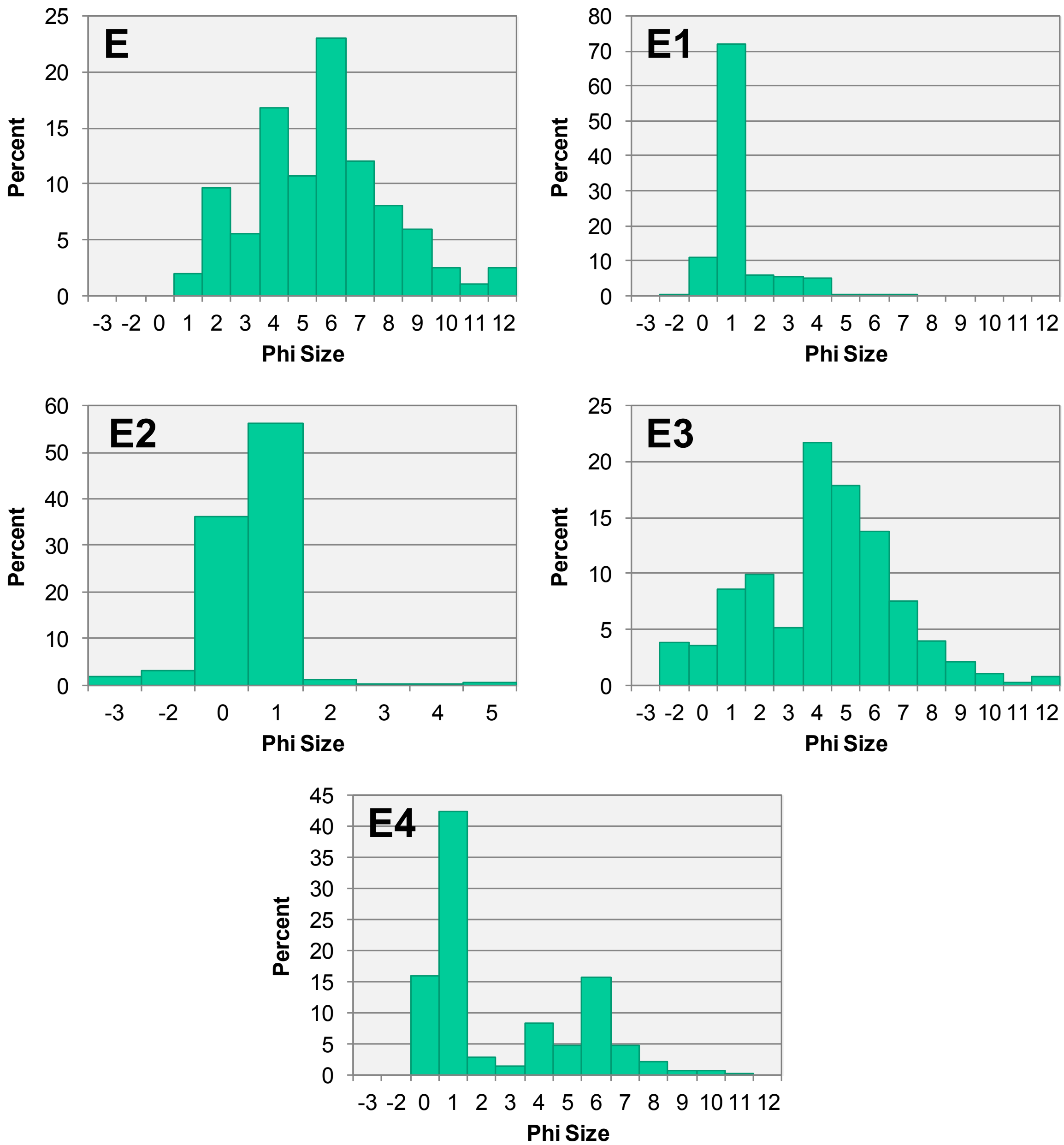

Figure 5.52: Particle class histogram: Transect E.
Note: % scale changes by graph to best show the distribution between particle classes.

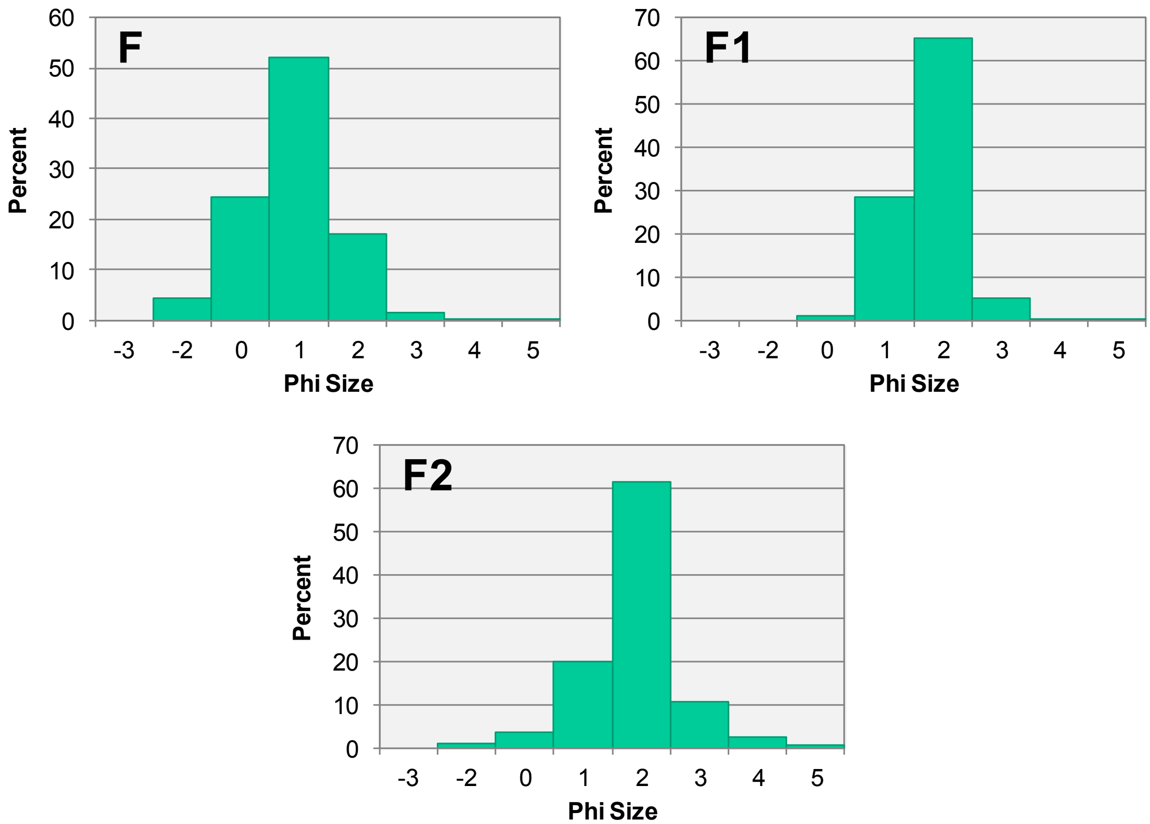

Figure 5.53: Particle class histogram: Transect F.
Note: % scale changes by graph to best show the distribution between particle classes.

Samples with one grain size representing a large percentage indicate that the sample is well sorted. From the distribution of the histograms, sample D appears to have the best sorting with almost 90% of the sample fraction in one grain size category. Other samples that are well sorted are C1, C2, O, N2, N3 and E2. All have at least one grain size that accounts for 70-90% of the total sample. Samples with a wide distribution and all grain sizes having lower percentages indicate that the sample is poorly sorted. A majority of the samples appear to be poorly sorted. Sample B3 shows no individual category accounting for over 20% of the total sample with thirteen of the fifteen grain size fractions having at least some weight percentage. Samples B, B5, B7, D3, E3 and E4 all show similar results with being poorly sorted samples.

5.5.1 2008-09 Statistics on Rapidan Reservoir Samples

Cumulative curves (S curves) of the percent coarser (or percent retained) grains were created for use in calculating percentiles as a procedure for statistical analyses. Cumulative curves grouped by 2008-09 transects are presented in Figures 5.54-5.63, from furthest downstream (transect Z) to furthest upstream (transect F).

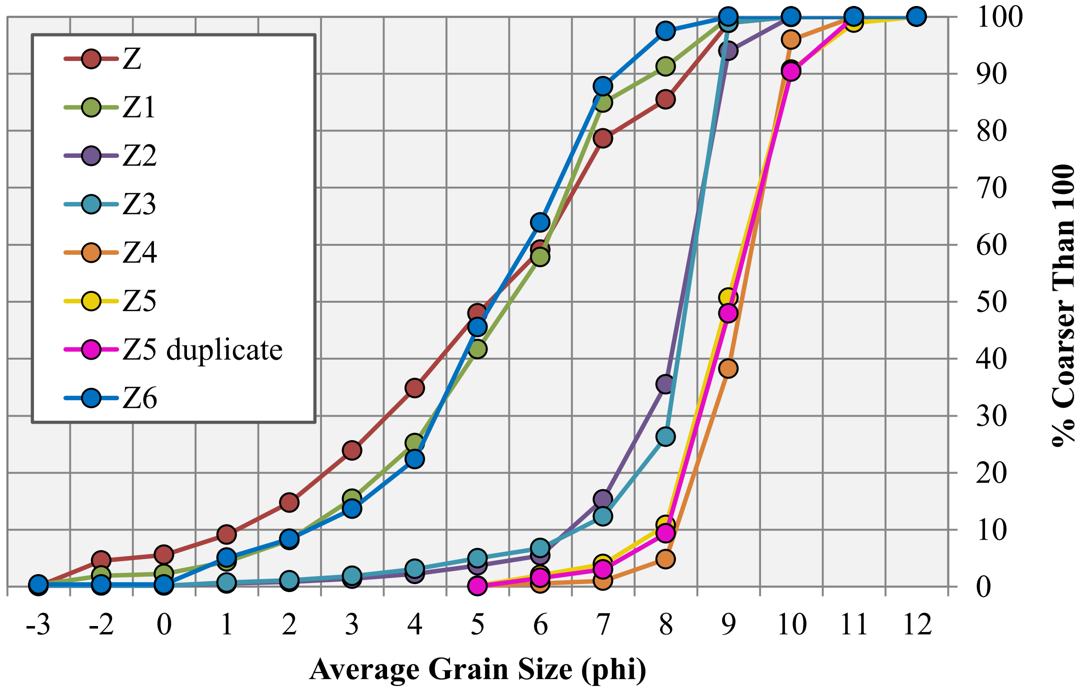

Figure 5.54: Cumulative weight percent, percent coarser, Transect Z

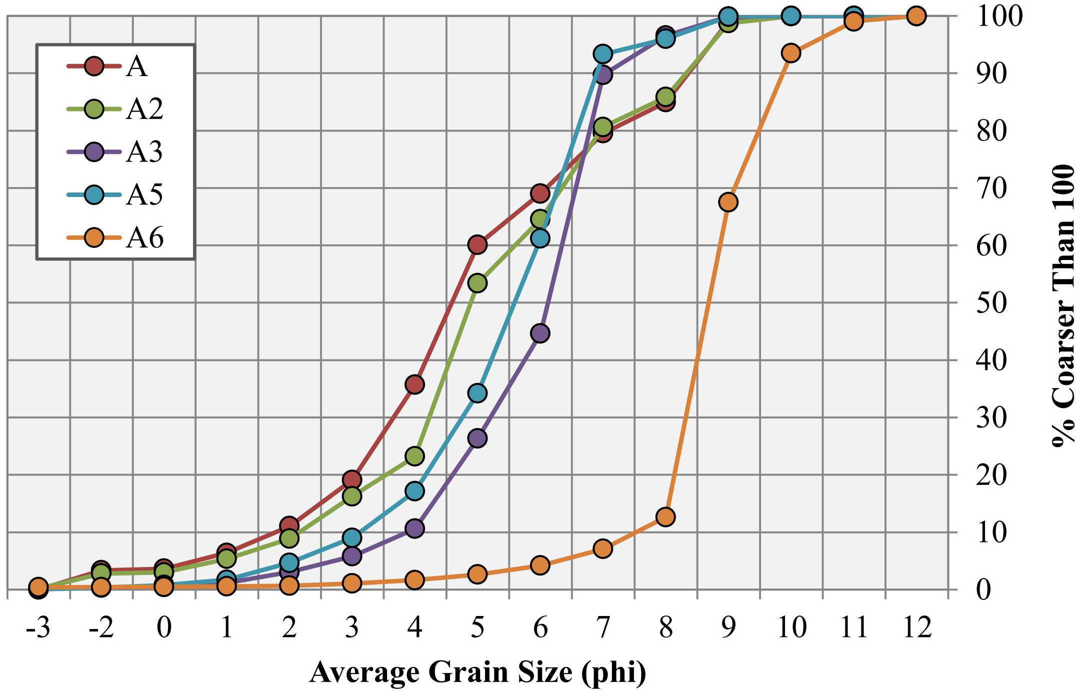

Figure 5.55: Cumulative weight percent, percent coarser, Transect A

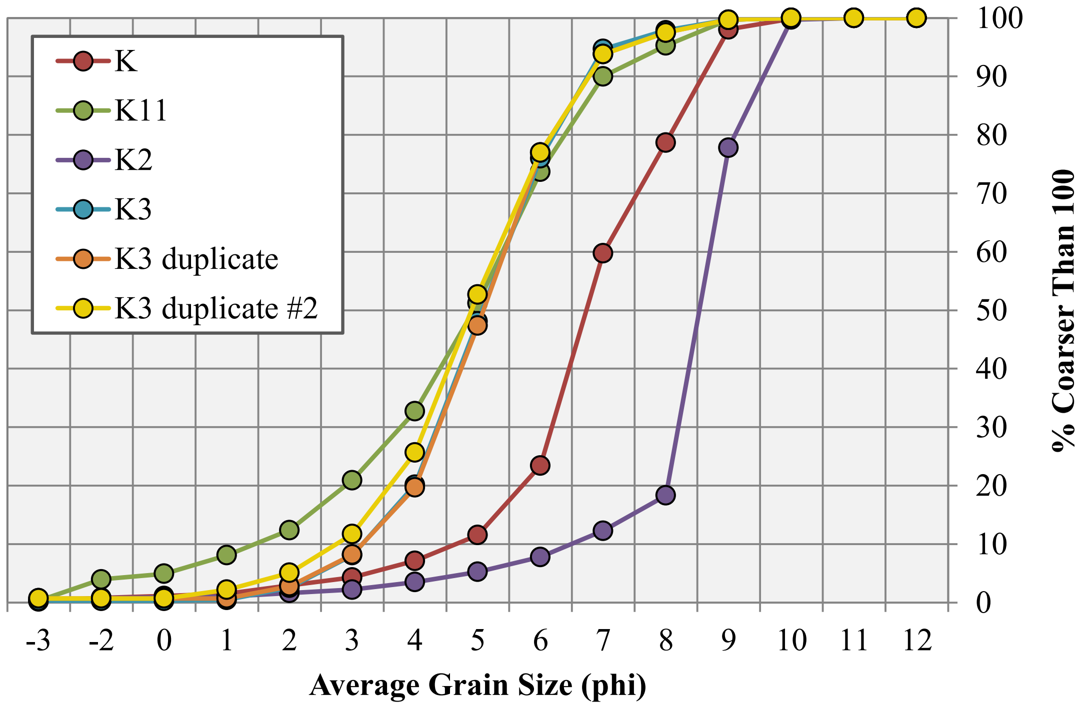

Figure 5.56: Cumulative weight percent, percent coarser, Transect K

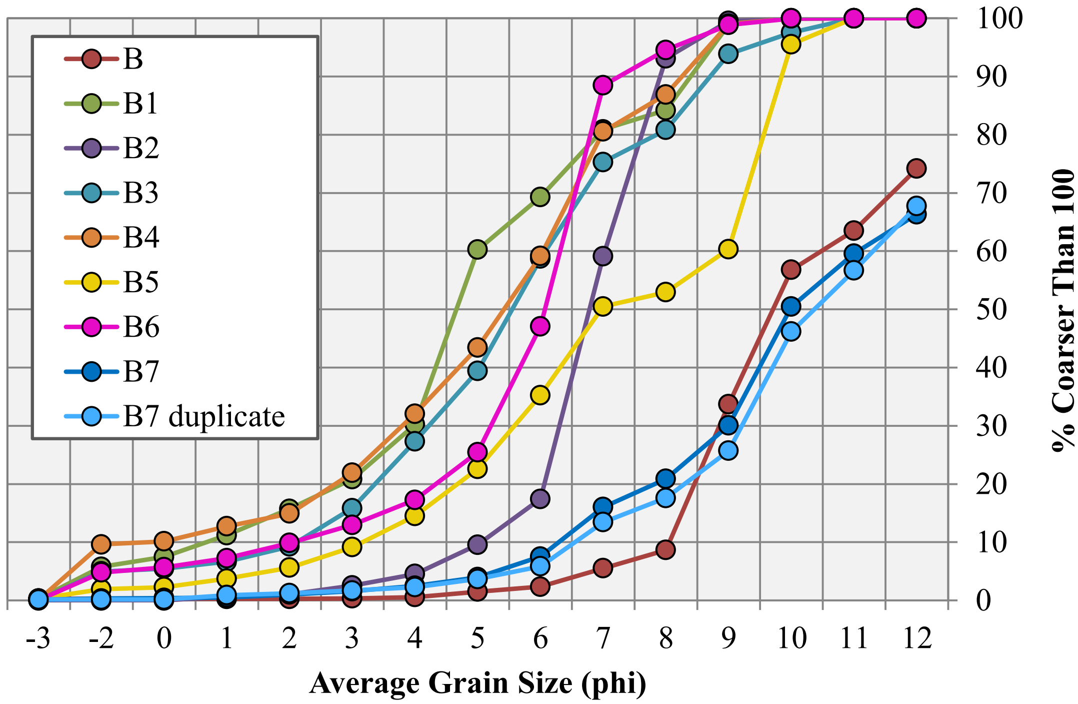

Figure 5.57: Cumulative weight percent, percent coarser, Transect B

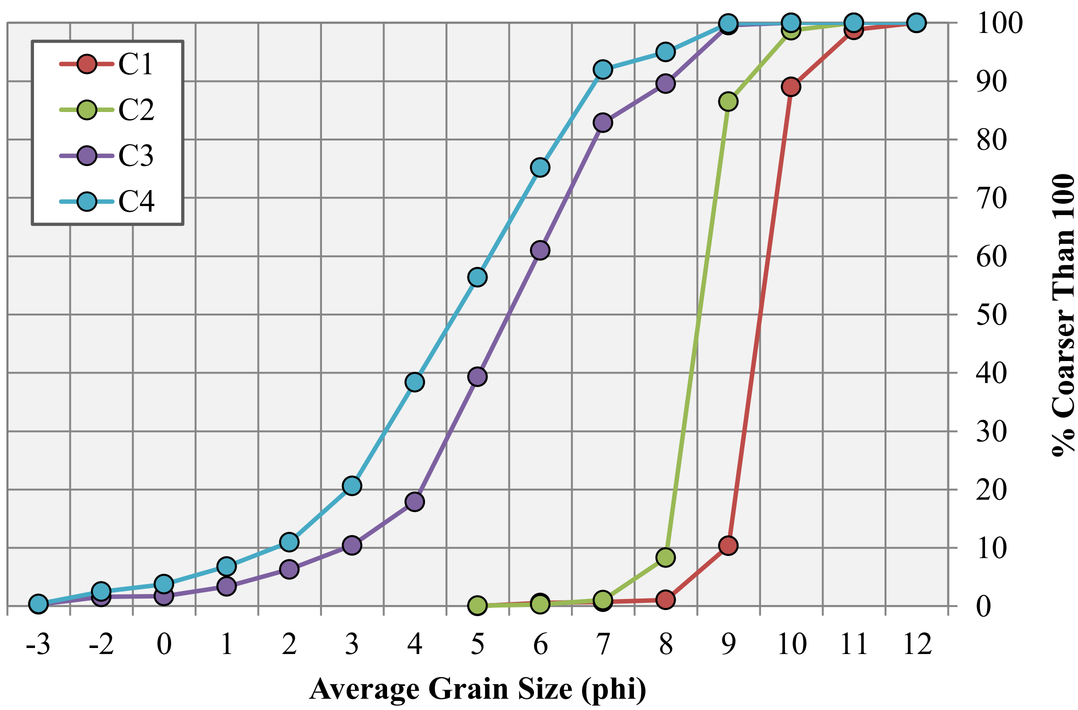

Figure 5.58: Cumulative weight percent, percent coarser, Transect C

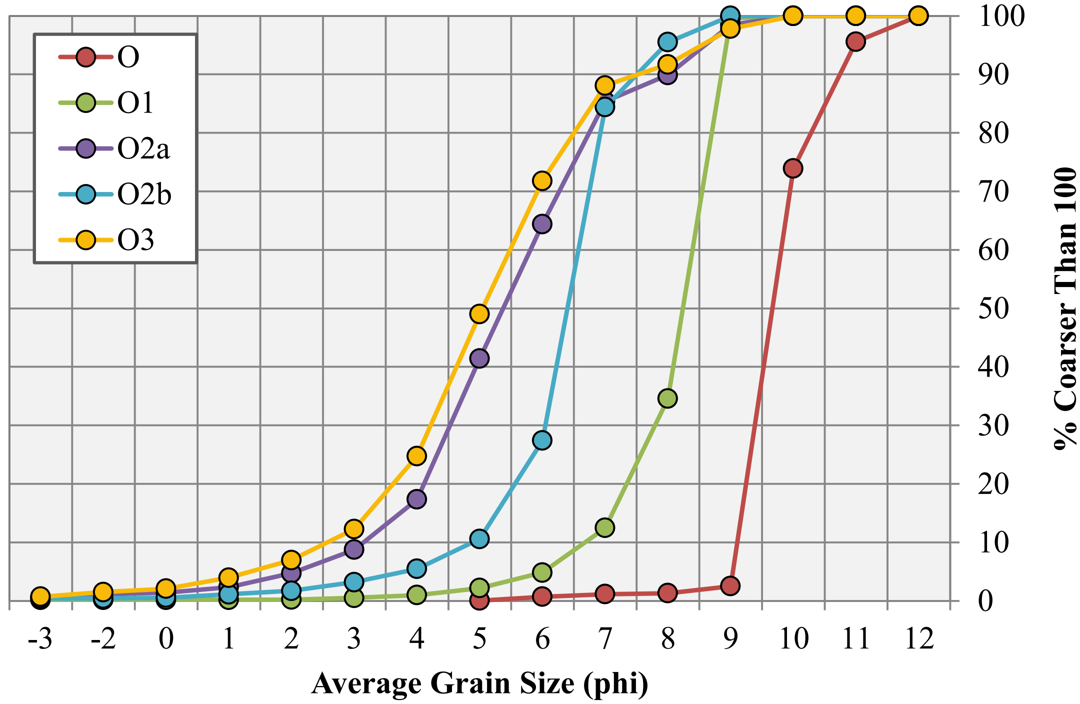

Figure 5.59: Cumulative weight percent, percent coarser, Transect O

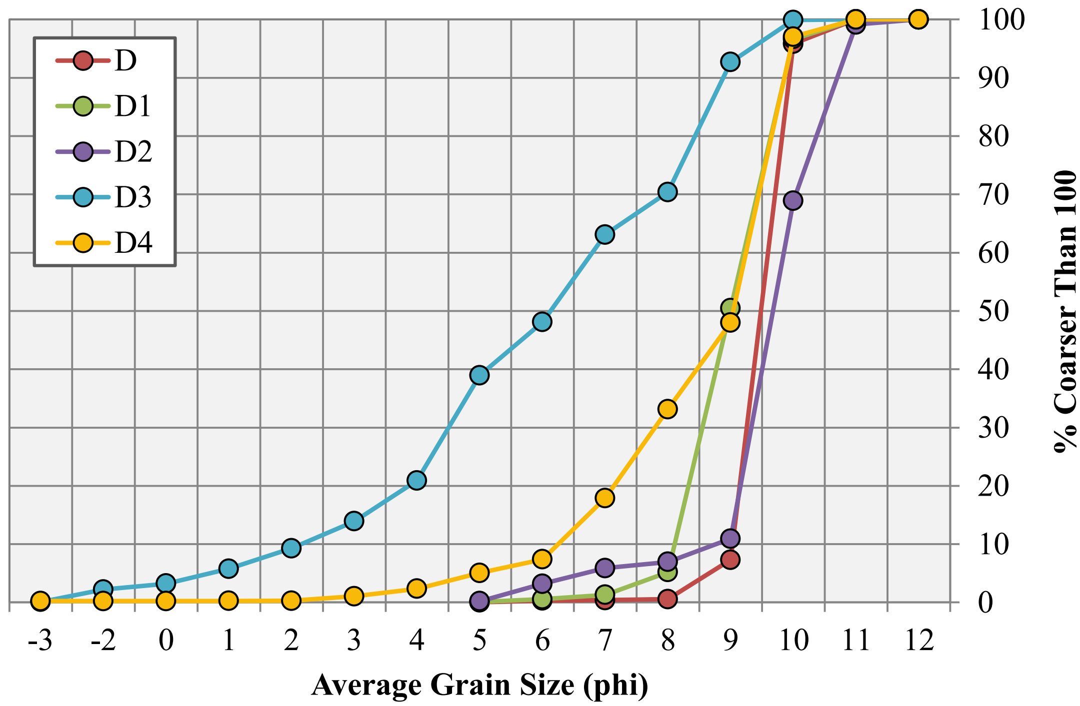

Figure 5.60: Cumulative weight percent, percent coarser, Transect D

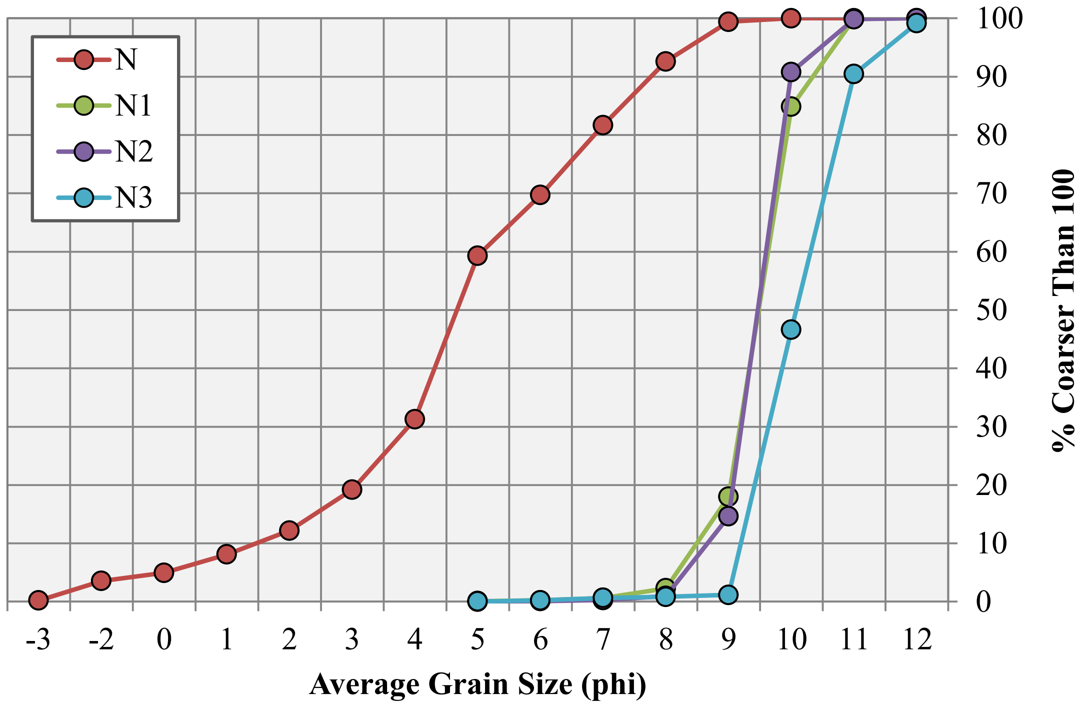

Figure 5.61: Cumulative weight percent, percent coarser, Transect N

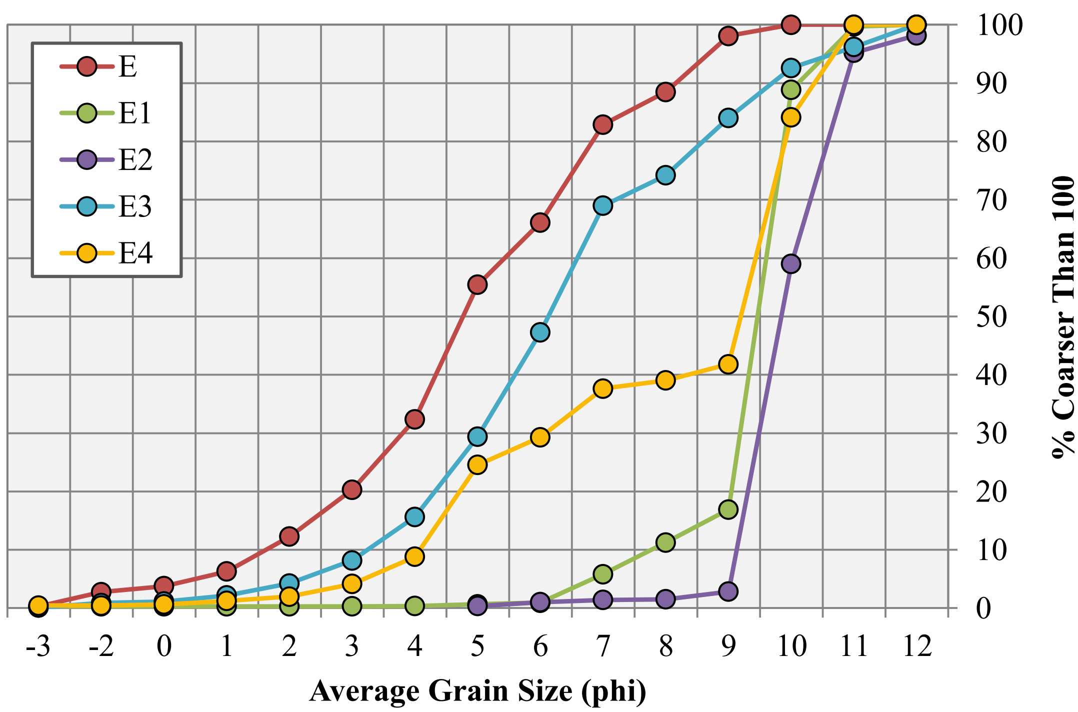

Figure 5.62: Cumulative weight percent, percent coarser, Transect E

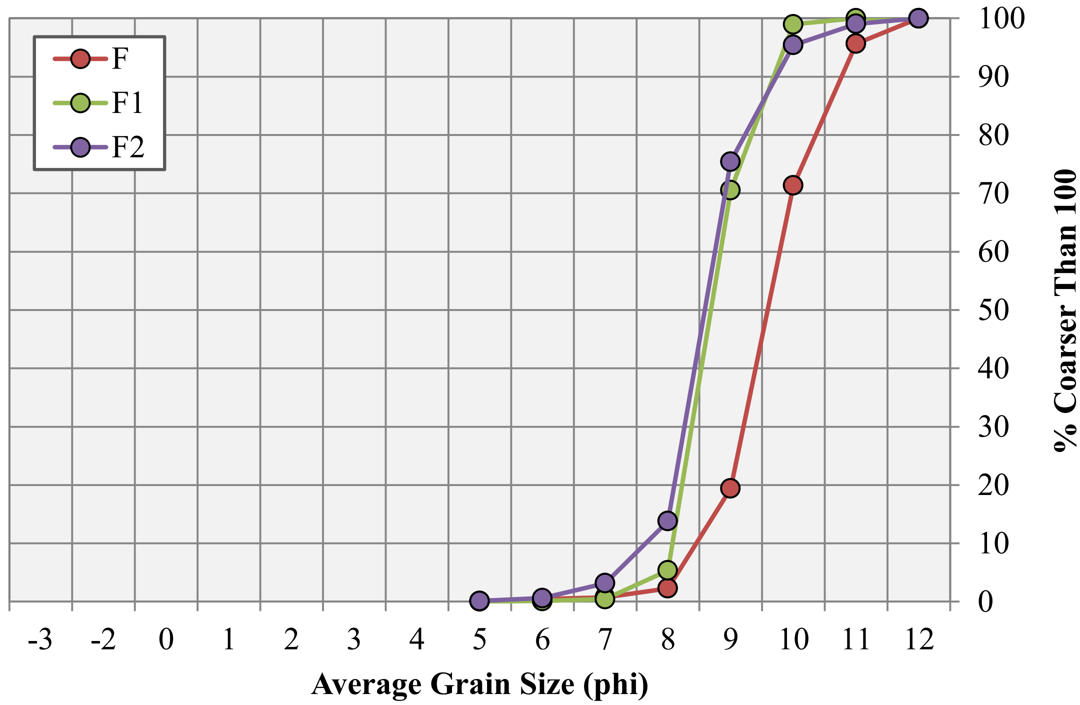

Figure 5.63: Cumulative weight percent, percent coarser, Transect F

Results from the cumulative S curves were taken for percentile analyses of each sample. Refer to Chapter 4.7 for descriptions of graphic mean, inclusive standard deviation, kurtosis and skewness. Table 5.14 provides the numerical value for each statistical measure as well as the category description for 2008-09 samples.

Table 5.14: 2008-09 statistical results for particle size analyses on collected reservoir bottom sediment from Rapidan Reservoir. Transect Z is furthest downstream, Transect F is furthest upstream. Table is continued on next page.

TRANSECT	SAMPLE ID	GRAPHIC MEAN		INCLUSIVE STANDARD DEVIATION		GRAPHIC KURTOSIS		INCLUSIVE GRAPHIC SKEWNESS	
Z	Z	3.252	Very Fine Sand	1.267	Poorly Sorted	1.460	Leptokurtic	-0.105	Negative Skewed
	Z1	3.687	Very Fine Sand	1.586	Poorly Sorted	1.476	Leptokurtic	0.157	Positive Skewed
	Z2	1.550	Medium Sand	1.227	Poorly Sorted	1.240	Leptokurtic	0.210	Positive Skewed
	Z3	1.326	Medium Sand	1.087	Poorly Sorted	1.117	Leptokurtic	0.442	Strongly Positive Skewed
	Z4	-0.189	Very Coarse Sand	1.130	Poorly Sorted	0.849	Platykurtic	0.170	Positive Skewed
	Z5 *	0.051	Coarse Sand	1.478	Poorly Sorted	1.025	Mesokurtic	-0.067	Near Symmetrical
	Z6	3.879	Very Fine Sand	1.400	Poorly Sorted	1.274	Leptokurtic	0.311	Strongly Positive Skewed
A	A	3.589	Very Fine Sand	1.718	Poorly Sorted	1.582	Very Leptokurtic	0.044	Near Symmetrical
	A2	3.601	Very Fine Sand	1.703	Poorly Sorted	1.580	Very Leptokurtic	0.064	Near Symmetrical
	A3	3.699	Very Fine Sand	1.425	Poorly Sorted	1.212	Leptokurtic	0.287	Positive Skewed
	A5	4.003	Silt	1.344	Poorly Sorted	1.289	Leptokurtic	0.343	Strongly Positive Skewed
	A6	0.371	Very Coarse Sand	1.526	Poorly Sorted	1.290	Leptokurtic	-0.138	Negative Skewed
K	K	2.916	Fine Sand	1.628	Poorly Sorted	1.251	Leptokurtic	0.144	Positive Skewed
	K2	0.787	Coarse Sand	1.502	Poorly Sorted	1.848	Very Leptokurtic	0.122	Positive Skewed
	K3 *	4.106	Silt	1.357	Poorly Sorted	1.280	Leptokurtic	0.368	Strongly Positive Skewed
	K11	4.034	Silt	1.369	Poorly Sorted	1.317	Leptokurtic	0.339	Strongly Positive Skewed
B	B	-1.331	Gravel	2.281	Very Poorly Sorted	0.646	Very Platykurtic	0.040	Near Symmetrical
	B1	3.584	Very Fine Sand	1.790	Poorly Sorted	1.645	Very Leptokurtic	0.020	Near Symmetrical
	B2	3.105	Very Fine Sand	1.316	Poorly Sorted	1.285	Leptokurtic	0.372	Strongly Positive Skewed
	B3	3.332	Very Fine Sand	2.020	Very Poorly Sorted	1.492	Leptokurtic	-0.107	Negative Skewed
	B4	3.595	Very Fine Sand	1.666	Poorly Sorted	1.464	Leptokurtic	0.086	Near Symmetrical
	B5	1.799	Medium Sand	2.680	Very Poorly Sorted	0.675	Platykurtic	-0.138	Negative Skewed
	B6	3.664	Very Fine Sand	1.471	Poorly Sorted	1.263	Leptokurtic	0.223	Positive Skewed
	B7 *	-1.350	Gravel	2.958	Very Poorly Sorted	0.778	Platykurtic	0.400	Strongly Positive Skewed

* Value is an average of sample and duplicate results.

Table 5.14 continued: 2008-09 statistical results for particle size analyses on collected reservoir bottom sediment from Rapidan Reservoir. Transect Z is furthest downstream, Transect F is furthest upstream.

TRANSECT	SAMPLE ID	GRAPHIC MEAN		INCLUSIVE STANDARD DEVIATION		GRAPHIC KURTOSIS		INCLUSIVE GRAPHIC SKEWNESS	
C	C1	-1.013	Gravel	0.907	Moderately Sorted	1.580	Very Leptokurtic	0.200	Positive Skewed
	C2	0.831	Coarse Sand	0.863	Moderately Sorted	1.813	Very Leptokurtic	-0.009	Near Symmetrical
	C3	3.703	Very Fine Sand	1.620	Poorly Sorted	1.518	Very Leptokurtic	0.129	Positive Skewed
	C4	4.068	Silt	1.393	Poorly Sorted	1.352	Leptokurtic	0.325	Strongly Positive Skewed
O	O	-1.506	Gravel	0.907	Moderately Sorted	1.189	Leptokurtic	-0.256	Negative Skewed
	O1	1.558	Medium Sand	1.015	Poorly Sorted	1.043	Mesokurtic	0.309	Strongly Positive Skewed
	O2a	3.797	Very Fine Sand	1.635	Poorly Sorted	1.564	Very Leptokurtic	0.142	Positive Skewed
	O2b	3.522	Very Fine Sand	1.404	Poorly Sorted	1.083	Mesokurtic	0.312	Strongly Positive Skewed
	O3	4.015	Silt	1.532	Poorly Sorted	1.567	Very Leptokurtic	0.249	Positive Skewed
D	D	-1.022	Gravel	0.646	Moderately Well	1.217	Leptokurtic	0.342	Strongly Positive Skewed
	D1	0.054	Coarse Sand	1.136	Poorly Sorted	0.833	Platykurtic	-0.094	Near Symmetrical
	D2	-1.406	Gravel	1.436	Poorly Sorted	1.741	Very Leptokurtic	0.195	Positive Skewed
	D3	2.937	Fine Sand	2.063	Very Poorly Sorted	1.077	Mesokurtic	-0.122	Negative Skewed
	D4	0.501	Coarse Sand	1.977	Poorly Sorted	0.754	Platykurtic	0.382	Strongly Positive Skewed
N	N	3.762	Very Fine Sand	1.552	Poorly Sorted	1.464	Leptokurtic	0.172	Positive Skewed
	N1	-0.856	Very Coarse Sand	1.160	Poorly Sorted	1.196	Leptokurtic	0.264	Positive Skewed
	N2	-0.884	Very Coarse Sand	0.992	Moderately Sorted	1.307	Leptokurtic	0.274	Positive Skewed
	N3	-1.930	Gravel	0.985	Moderately Sorted	0.824	Platykurtic	0.023	Near Symmetrical
E	E	3.691	Very Fine Sand	1.664	Poorly Sorted	1.573	Very Leptokurtic	0.100	Near Symmetrical
	E1	-0.799	Very Coarse Sand	1.326	Poorly Sorted	2.084	Very Leptokurtic	0.428	Strongly Positive Skewed
	E2	-1.679	Gravel	0.951	Moderately Sorted	0.848	Platykurtic	-0.132	Negative Skewed
	E3	2.798	Fine Sand	2.619	Very Poorly Sorted	1.517	Very Leptokurtic	-0.308	Strongly Negative Skewed
	E4	0.542	Coarse Sand	2.771	Very Poorly Sorted	0.716	Platykurtic	0.559	Strongly Positive Skewed
F	F	-1.088	Gravel	1.429	Poorly Sorted	0.969	Mesokurtic	0.069	Near Symmetrical
	F1	0.340	Coarse Sand	1.064	Poorly Sorted	1.071	Mesokurtic	-0.290	Negative Skewed
	F2	0.539	Coarse Sand	1.302	Poorly Sorted	1.443	Leptokurtic	-0.147	Negative Skewed

Calculated graphic mean results ranged from a minimum of -1.93 to a maximum of 4.106 for samples collected in 2008-09. 72% of the samples were sand (from very fine to very coarse sand), 18% were gravel and 10% were silt. Inclusive Standard Deviation results showed that 72% of samples were poorly sorted, 14% very poorly sorted, 12% moderately sorted and 2% moderately well sorted with a range of results from 0.646 on the low end up to 2.958. For kurtosis, 70% of samples were classified as either leptokurtic or very leptokurtic suggesting samples were more sorted towards the middle of the distribution curve (more peaked) rather than towards the edges. Kurtosis values ranges from 0.646 to 2.084. 58% of samples were either positively or strongly positively skewed, 22% were near symmetrical and 20% were negatively or strongly negatively skewed. Skewness values ranged from 0.308 to 0.559.

No strong correlations existed from upstream to downstream regarding sorting (inclusive standard deviation), kurtosis and skewness, however, all samples in the first four transects from downstream to upstream (Z, A, K, B) are all either very poorly sorted or poorly sorted. Figure 5.64 which will be discussed later visually suggests that grain sizes decrease slightly from upstream to downstream.

5.5.2 1985 Statistics on Rapidan Reservoir Samples

1985 sampling of sediments within Rapidan Reservoir was more extensive than sampling completed for this project in 2008-09. A total of 132 samples were collected and analyzed with enhanced coverage through the entire reservoir and into the upstream main channel of the Blue Earth River. Graphic mean, inclusive standard deviation, kurtosis and skewness results for 1985 can be found in Table 5.15.

Table 5.15: 1985 statistical results for particle size analyses on collected reservoir bottom sediment from Rapidan Reservoir. Transect C is furthest downstream, Transect W is furthest upstream. Table is continued on next page.

TRANSECT	SAMPLE ID	GRAPHIC MEAN		INCLUSIVE STANDARD DEVIATION		GRAPHIC KURTOSIS		INCLUSIVE GRAPHIC SKEWNESS	
C	P1C	4.02	Silt	3.54	Very Poorly Sorted	0.70	Platykurtic	-0.123	Negative Skewed
	P2C	4.22	Silt	2.68	Very Poorly Sorted	0.89	Platykurtic	0.207	Positive Skewed
	P3C	3.99	Very Fine Sand	3.35	Very Poorly Sorted	0.78	Platykurtic	-0.005	Near Symmetrical
	P4C	4.53	Silt	3.07	Very Poorly Sorted	0.82	Platykurtic	-0.045	Near Symmetrical
	P5C	4.99	Silt	3.03	Very Poorly Sorted	0.86	Platykurtic	0.106	Positive Skewed
	P6C	4.36	Silt	3.25	Very Poorly Sorted	1.07	Mesokurtic	-0.051	Near Symmetrical
	P7C	5.96	Silt	2.94	Very Poorly Sorted	0.69	Platykurtic	0.353	Strongly Positive Skewed
	P8C	5.97	Silt	2.08	Very Poorly Sorted	1.10	Mesokurtic	0.162	Positive Skewed
	P9C	4.20	Silt	2.51	Very Poorly Sorted	0.99	Mesokurtic	0.498	Strongly Positive Skewed
	P10C	6.95	Silt	2.14	Very Poorly Sorted	0.89	Platykurtic	0.138	Positive Skewed
	P11C	6.34	Silt	2.35	Very Poorly Sorted	0.86	Platykurtic	0.144	Positive Skewed
D	P1D	2.56	Fine Sand	0.94	Moderately Sorted	1.14	Leptokurtic	0.217	Positive Skewed
	P2D	6.00	Silt	2.58	Very Poorly Sorted	0.78	Platykurtic	0.300	Positive Skewed
	P3D	6.53	Silt	2.34	Very Poorly Sorted	0.82	Platykurtic	0.135	Positive Skewed
	P4D	6.01	Silt	2.40	Very Poorly Sorted	0.92	Mesokurtic	0.177	Positive Skewed
	P5D	6.02	Silt	2.21	Very Poorly Sorted	0.92	Mesokurtic	0.232	Positive Skewed
	P6D	4.70	Silt	2.96	Very Poorly Sorted	0.75	Platykurtic	0.459	Strongly Positive Skewed
	P7D	5.49	Silt	2.31	Very Poorly Sorted	1.02	Mesokurtic	0.259	Positive Skewed
	P8D	6.49	Silt	2.89	Very Poorly Sorted	0.60	Very Platykurtic	0.225	Positive Skewed
	P9D	7.27	Silt	2.23	Very Poorly Sorted	0.82	Platykurtic	0.021	Near Symmetrical
	P10D	1.71	Medium Sand	2.06	Very Poorly Sorted	1.91	Very Leptokurtic	0.192	Positive Skewed
	P11D	6.14	Silt	2.11	Very Poorly Sorted	1.00	Mesokurtic	0.198	Positive Skewed

Table 5.15 continued: 1985 statistical results for particle size analyses on collected reservoir bottom sediment from Rapidan Reservoir. Transect C is furthest downstream, Transect W is furthest upstream. Table is continued on next page.

TRANSECT	SAMPLE ID	GRAPHIC MEAN		INCLUSIVE STANDARD DEVIATION		GRAPHIC KURTOSIS		INCLUSIVE GRAPHIC SKEWNESS	
E	**P1E**	5.36	Silt	2.72	Very Poorly Sorted	0.85	Platykurtic	0.196	Positive Skewed
	P2E	3.64	Very Fine Sand	3.98	Very Poorly Sorted	0.65	Very Platykurtic	0.641	Strongly Positive Skewed
	P3E	5.07	Silt	2.81	Very Poorly Sorted	1.31	Leptokurtic	0.228	Positive Skewed
	P4E	6.12	Silt	2.45	Very Poorly Sorted	0.82	Platykurtic	0.210	Positive Skewed
	P5E	2.52	Fine Sand	1.40	Poorly Sorted	2.05	Very Leptokurtic	0.385	Strongly Positive Skewed
	P6E	5.84	Silt	2.34	Very Poorly Sorted	0.84	Platykurtic	0.373	Strongly Positive Skewed
	P7E	4.80	Silt	2.43	Very Poorly Sorted	0.96	Mesokurtic	0.178	Positive Skewed
	P8E	6.29	Silt	2.34	Very Poorly Sorted	0.81	Platykurtic	0.204	Positive Skewed
	P9E	2.82	Fine Sand	1.59	Poorly Sorted	1.86	Very Leptokurtic	0.494	Strongly Positive Skewed
	P10E	6.08	Silt	2.19	Very Poorly Sorted	0.97	Mesokurtic	0.185	Positive Skewed
	P11E	1.04	Medium Sand	1.47	Poorly Sorted	1.31	Leptokurtic	0.047	Near Symmetrical
F	**P1F**	5.84	Silt	1.86	Poorly Sorted	1.20	Leptokurtic	0.161	Positive Skewed
	P2F	4.24	Silt	2.75	Very Poorly Sorted	0.94	Mesokurtic	0.579	Strongly Positive Skewed
	P3F	5.81	Silt	2.37	Very Poorly Sorted	0.89	Platykurtic	0.301	Strongly Positive Skewed
	P4F	3.83	Very Fine Sand	2.27	Very Poorly Sorted	0.89	Platykurtic	0.541	Strongly Positive Skewed
	P5F	5.40	Silt	2.00	Very Poorly Sorted	1.05	Mesokurtic	0.391	Strongly Positive Skewed
	P6F	4.00	Silt	0.83	Moderately Sorted	1.18	Leptokurtic	0.038	Near Symmetrical
	P7F	5.81	Silt	2.27	Very Poorly Sorted	1.09	Mesokurtic	0.107	Positive Skewed
	P8F	5.89	Silt	2.35	Very Poorly Sorted	0.97	Mesokurtic	0.149	Positive Skewed
	P9F	5.93	Silt	2.54	Very Poorly Sorted	1.13	Leptokurtic	-0.021	Near Symmetrical
	P10F	5.13	Silt	2.65	Very Poorly Sorted	0.93	Mesokurtic	-0.013	Near Symmetrical
	P11F	2.33	Fine Sand	0.92	Moderately Sorted	1.86	Very Leptokurtic	0.269	Positive Skewed

Table 5.15 continued: 1985 statistical results for particle size analyses on collected reservoir bottom sediment from Rapidan Reservoir. Transect C is furthest downstream, Transect W is furthest upstream. Table is continued on next page.

TRANSECT	SAMPLE ID	GRAPHIC MEAN		INCLUSIVE STANDARD DEVIATION		GRAPHIC KURTOSIS		INCLUSIVE GRAPHIC SKEWNESS	
G	P3G	5.54	Silt	1.78	Poorly Sorted	1.18	Leptokurtic	0.111	Positive Skewed
	P4G	6.00	Silt	2.32	Very Poorly Sorted	0.89	Platykurtic	0.226	Positive Skewed
	P5G	7.35	Silt	1.95	Poorly Sorted	0.85	Platykurtic	0.161	Positive Skewed
	P6G	5.30	Silt	1.64	Poorly Sorted	1.07	Mesokurtic	0.127	Positive Skewed
	P7G	8.86	Clay	2.33	Very Poorly Sorted	1.61	Very Leptokurtic	-0.548	Strongly Negative Skewed
	P8G	5.42	Silt	2.80	Very Poorly Sorted	0.95	Mesokurtic	-0.068	Near Symmetrical
	P9G	Incomplete Results Reported							
	P10G	6.01	Silt	2.16	Very Poorly Sorted	0.99	Mesokurtic	0.194	Positive Skewed
	P11G	5.28	Silt	2.45	Very Poorly Sorted	1.03	Mesokurtic	0.147	Positive Skewed
	P12G	3.10	Very Fine Sand	3.02	Very Poorly Sorted	0.96	Mesokurtic	0.344	Strongly Positive Skewed
H	P1H	2.20	Fine Sand	1.68	Poorly Sorted	1.89	Very Leptokurtic	0.224	Positive Skewed
	P2H	6.18	Silt	2.19	Very Poorly Sorted	0.93	Mesokurtic	0.196	Positive Skewed
	P3H	4.78	Silt	2.46	Very Poorly Sorted	0.99	Mesokurtic	0.275	Positive Skewed
	P4H	6.09	Silt	2.29	Very Poorly Sorted	0.89	Platykurtic	0.200	Positive Skewed
	P5H	5.91	Silt	2.20	Very Poorly Sorted	0.92	Mesokurtic	0.277	Positive Skewed
	P6H	4.49	Silt	3.45	Very Poorly Sorted	0.91	Mesokurtic	0.343	Strongly Positive Skewed
	P7H	3.92	Very Fine Sand	2.87	Very Poorly Sorted	0.78	Platykurtic	0.112	Positive Skewed
	P8H	6.14	Silt	2.50	Very Poorly Sorted	1.00	Mesokurtic	0.085	Near Symmetrical
	P9H	6.19	Silt	2.43	Very Poorly Sorted	0.81	Platykurtic	0.203	Positive Skewed
	P10H	5.97	Silt	2.40	Very Poorly Sorted	0.92	Mesokurtic	0.163	Positive Skewed
	P11H	1.86	Medium Sand	2.24	Very Poorly Sorted	1.56	Very Leptokurtic	0.331	Strongly Positive Skewed
	P12H	3.03	Very Fine Sand	2.63	Very Poorly Sorted	0.96	Mesokurtic	0.562	Strongly Positive Skewed

Table 5.15 continued: 1985 statistical results for particle size analyses on collected reservoir bottom sediment from Rapidan Reservoir. Transect C is furthest downstream, Transect W is furthest upstream. Table is continued on next page.

TRANSECT	SAMPLE ID	GRAPHIC MEAN		INCLUSIVE STANDARD DEVIATION		GRAPHIC KURTOSIS		INCLUSIVE GRAPHIC SKEWNESS	
I	P1I	5.92	Silt	2.36	Very Poorly Sorted	0.79	Platykurtic	0.399	Strongly Positive Skewed
	P2I	5.73	Silt	2.29	Very Poorly Sorted	0.93	Mesokurtic	0.314	Strongly Positive Skewed
	P3I	6.08	Silt	2.41	Very Poorly Sorted	0.81	Platykurtic	0.257	Positive Skewed
	P4I	6.90	Silt	2.47	Very Poorly Sorted	0.73	Platykurtic	0.023	Near Symmetrical
	P5I	6.41	Silt	2.21	Very Poorly Sorted	0.91	Mesokurtic	0.177	Positive Skewed
	P6I	6.05	Silt	2.68	Very Poorly Sorted	1.01	Mesokurtic	0.058	Near Symmetrical
	P7I	5.08	Silt	1.96	Poorly Sorted	1.14	Leptokurtic	0.213	Positive Skewed
	P8I	5.11	Silt	2.94	Very Poorly Sorted	0.95	Mesokurtic	0.063	Near Symmetrical
	P9I	5.79	Silt	2.25	Very Poorly Sorted	0.90	Mesokurtic	0.325	Strongly Positive Skewed
	P10I	4.99	Silt	2.48	Very Poorly Sorted	0.96	Mesokurtic	0.166	Positive Skewed
	P11I	5.92	Silt	2.37	Very Poorly Sorted	0.90	Mesokurtic	0.217	Positive Skewed
	P12I	4.69	Silt	3.45	Very Poorly Sorted	1.05	Mesokurtic	0.396	Strongly Positive Skewed
J	P1J	5.76	Silt	2.66	Very Poorly Sorted	0.89	Platykurtic	0.102	Positive Skewed
	P2J	5.85	Silt	2.26	Very Poorly Sorted	0.89	Platykurtic	0.308	Strongly Positive Skewed
	P3J	5.83	Silt	2.52	Very Poorly Sorted	0.91	Mesokurtic	0.129	Positive Skewed
	P4J	3.09	Very Fine Sand	1.93	Poorly Sorted	1.84	Very Leptokurtic	0.571	Strongly Positive Skewed
	P5J	3.69	Very Fine Sand	2.15	Very Poorly Sorted	1.11	Leptokurtic	0.362	Strongly Positive Skewed
	P6J	5.52	Silt	2.53	Very Poorly Sorted	0.93	Mesokurtic	0.222	Positive Skewed
	P7J	1.90	Medium Sand	3.93	Very Poorly Sorted	0.70	Platykurtic	0.404	Strongly Positive Skewed
	P8J	4.15	Silt	2.20	Very Poorly Sorted	1.08	Mesokurtic	0.208	Positive Skewed
K	P1K	2.61	Fine Sand	2.46	Very Poorly Sorted	1.02	Mesokurtic	0.620	Strongly Positive Skewed
	P2K	3.52	Very Fine Sand	2.25	Very Poorly Sorted	1.27	Leptokurtic	0.429	Strongly Positive Skewed
	P3K	6.55	Silt	2.21	Very Poorly Sorted	0.89	Platykurtic	0.163	Positive Skewed
	P4K	5.91	Silt	2.28	Very Poorly Sorted	0.88	Platykurtic	0.285	Positive Skewed

Table 5.15 continued: 1985 statistical results for particle size analyses on collected reservoir bottom sediment from Rapidan Reservoir. Transect C is furthest downstream, Transect W is furthest upstream. Table is continued on next page.

TRANSECT	SAMPLE ID	GRAPHIC MEAN		INCLUSIVE STANDARD DEVIATION		GRAPHIC KURTOSIS		INCLUSIVE GRAPHIC SKEWNESS	
L	P1L	5.09	Silt	2.29	Very Poorly Sorted	1.07	Mesokurtic	0.273	Positive Skewed
	P2L	4.33	Silt	2.81	Very Poorly Sorted	0.94	Mesokurtic	0.517	Strongly Positive Skewed
	P3L	1.99	Medium Sand	1.26	Poorly Sorted	1.47	Leptokurtic	0.207	Positive Skewed
	P4L	6.17	Silt	2.49	Very Poorly Sorted	1.05	Mesokurtic	0.071	Near Symmetrical
	P5L	5.43	Silt	3.00	Very Poorly Sorted	0.70	Platykurtic	0.242	Positive Skewed
	P6L	5.90	Silt	2.51	Very Poorly Sorted	0.92	Mesokurtic	0.123	Positive Skewed
	P7L	3.43	Very Fine Sand	2.27	Very Poorly Sorted	1.12	Leptokurtic	0.521	Strongly Positive Skewed
M	P1M	6.20	Silt	2.32	Very Poorly Sorted	0.88	Platykurtic	0.172	Positive Skewed
	P2M	1.82	Medium Sand	2.84	Very Poorly Sorted	1.09	Mesokurtic	0.579	Strongly Positive Skewed
	P3M	5.13	Silt	2.94	Very Poorly Sorted	0.75	Platykurtic	0.388	Strongly Positive Skewed
	P4M	5.52	Silt	2.28	Very Poorly Sorted	0.99	Mesokurtic	0.333	Strongly Positive Skewed
	P5M	5.17	Silt	1.81	Poorly Sorted	1.12	Leptokurtic	0.264	Positive Skewed
N	P1N	5.45	Silt	2.83	Very Poorly Sorted	0.76	Platykurtic	0.059	Near Symmetrical
	P2N	4.29	Silt	2.52	Very Poorly Sorted	0.81	Platykurtic	0.415	Strongly Positive Skewed
	P3N	3.69	Very Fine Sand	2.36	Very Poorly Sorted	1.13	Leptokurtic	0.638	Strongly Positive Skewed
O	P1O	5.40	Silt	2.60	Very Poorly Sorted	0.91	Mesokurtic	0.235	Positive Skewed
	P2O	6.27	Silt	2.35	Very Poorly Sorted	1.07	Mesokurtic	0.092	Near Symmetrical
	P3O	5.83	Silt	3.11	Very Poorly Sorted	1.13	Leptokurtic	-0.036	Near Symmetrical
P	P1P	5.28	Silt	2.93	Very Poorly Sorted	1.06	Mesokurtic	0.158	Positive Skewed
	P2P	1.05	Medium Sand	2.17	Very Poorly Sorted	1.91	Very Leptokurtic	0.589	Strongly Positive Skewed
	P3P	4.33	Silt	3.09	Very Poorly Sorted	1.13	Leptokurtic	0.235	Positive Skewed

Table 5.15 continued: 1985 statistical results for particle size analyses on collected reservoir bottom sediment from Rapidan Reservoir. Transect C is furthest downstream, Transect W is furthest upstream.

TRANSECT	SAMPLE ID	GRAPHIC MEAN		INCLUSIVE STANDARD DEVIATION		GRAPHIC KURTOSIS		INCLUSIVE GRAPHIC SKEWNESS	
Q	P1Q	3.48	Very Fine Sand	3.06	Very Poorly Sorted	0.88	Platykurtic	-0.036	Near Symmetrical
	P2Q	1.29	Medium Sand	1.69	Poorly Sorted	1.71	Very Leptokurtic	0.292	Positive Skewed
	P3Q	4.12	Silt	2.77	Very Poorly Sorted	1.15	Leptokurtic	0.631	Strongly Positive Skewed
R	P1R	3.58	Very Fine Sand	3.45	Very Poorly Sorted	1.54	Very Leptokurtic	0.056	Near Symmetrical
	P2R	0.70	Coarse Sand	1.74	Poorly Sorted	2.21	Very Leptokurtic	0.232	Positive Skewed
	P3R	6.26	Silt	2.22	Very Poorly Sorted	0.91	Mesokurtic	0.188	Positive Skewed
S	P1S	6.05	Silt	2.46	Very Poorly Sorted	0.87	Platykurtic	0.159	Positive Skewed
	P2S	3.26	Very Fine Sand	2.29	Very Poorly Sorted	1.42	Leptokurtic	0.495	Strongly Positive Skewed
	P3S	1.63	Medium Sand	1.36	Poorly Sorted	1.76	Very Leptokurtic	0.388	Strongly Positive Skewed
T	P1T	5.66	Silt	2.44	Very Poorly Sorted	1.04	Mesokurtic	0.079	Near Symmetrical
	P2T	6.14	Silt	2.31	Very Poorly Sorted	0.83	Platykurtic	0.249	Positive Skewed
	P3T	5.95	Silt	2.17	Very Poorly Sorted	0.95	Mesokurtic	0.232	Positive Skewed
U	P1U	4.27	Silt	2.83	Very Poorly Sorted	0.96	Mesokurtic	0.212	Positive Skewed
	P2U	0.72	Coarse Sand	1.45	Poorly Sorted	1.92	Very Leptokurtic	0.216	Positive Skewed
	P3U	5.43	Silt	2.74	Very Poorly Sorted	1.08	Mesokurtic	0.013	Near Symmetrical
V	P1V	-1.00	Very Coarse Sand	2.71	Very Poorly Sorted	0.91	Mesokurtic	-0.081	Near Symmetrical
	P2V	Incomplete Results Reported							
	P3V	0.15	Coarse Sand	1.79	Poorly Sorted	0.84	Platykurtic	0.275	Positive Skewed
W	P1W	0.77	Coarse Sand	1.05	Poorly Sorted	1.11	Mesokurtic	0.004	Near Symmetrical
	P2W	-0.52	Very Coarse Sand	1.47	Poorly Sorted	0.91	Mesokurtic	-0.101	Negative Skewed
	P3W	1.54	Medium Sand	2.33	Very Poorly Sorted	1.74	Very Leptokurtic	0.303	Strongly Positive Skewed

Graphic mean results showed that 72% of samples in 1985 had a mean grain size in the "silt" category with a range of values from -1.00 to 8.86. 84% of samples were very poorly sorted, 15% were poorly sorted and less than 1% were moderately sorted. No samples were well sorted in 1985. Inclusive standard deviation results ranged from 0.83 to 3.98. Kurtosis results were somewhat equally distributed across the categories with 33% of samples being either platykurtic or very platykurtic (more sorted at the edges of the distribution), 42% mesokurtic (normal kurtosis) and 25% were leptokurtic or very leptokurtic (more sorted in the middle then edges). Kurtosis values ranged from 0.60 to 2.21. 81% of samples were either positively or strongly positively skewed indicating a larger proportion of fines within the sample. Skewness results ranged from -0.55 to0.64.

5.5.3 Comparison of 2008-09 to 1985 Particle Size Analyses Data

The sampling scope varied between samples collected in 1985 (132 samples) and those collected in 2008-09 (50 samples). 1985 samples covered the entire reservoir with more transects, and greater quantity of samples within transects. In addition, transect samples were also collected upstream from the reservoir in the main stem of the Blue Earth River channel where water levels and flow velocities were likely still influenced by the impoundment of water behind the dam. In contrast, visible sandbars were not sampled in 2008-09 and sampling focused only on exposed water which limited the sample area by 56% according to Table 5.12. Furthermore, sampling was not expanded upstream from the main reservoir area of interest to maintain consistency with the 1939 aerial photograph extent. Figures 5.64 to 5.67 show results from the IDW interpolation conducted using ArcGIS software.

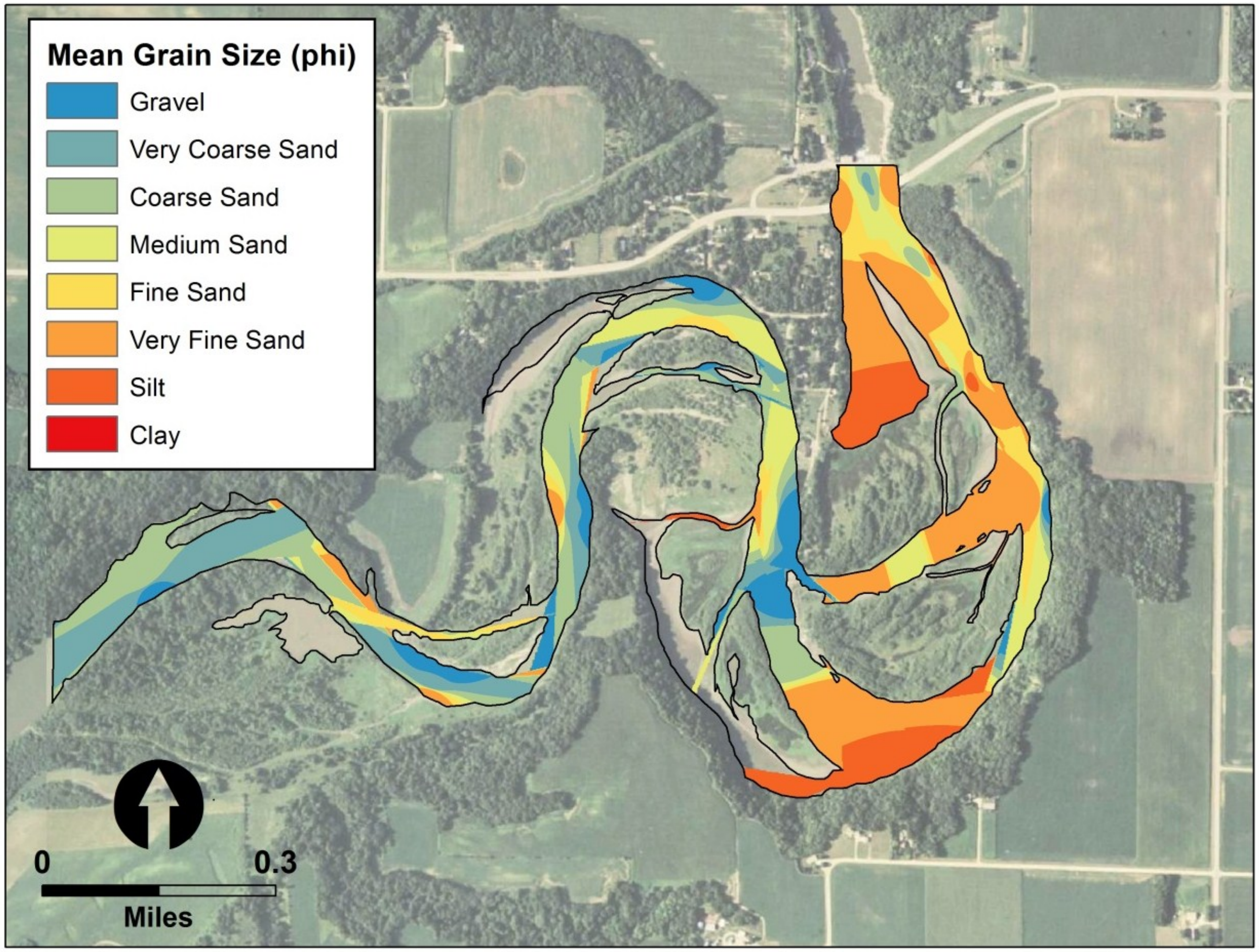

Figure 5.64: 2008-09 mean grain size (phi) within Rapidan Reservoir.

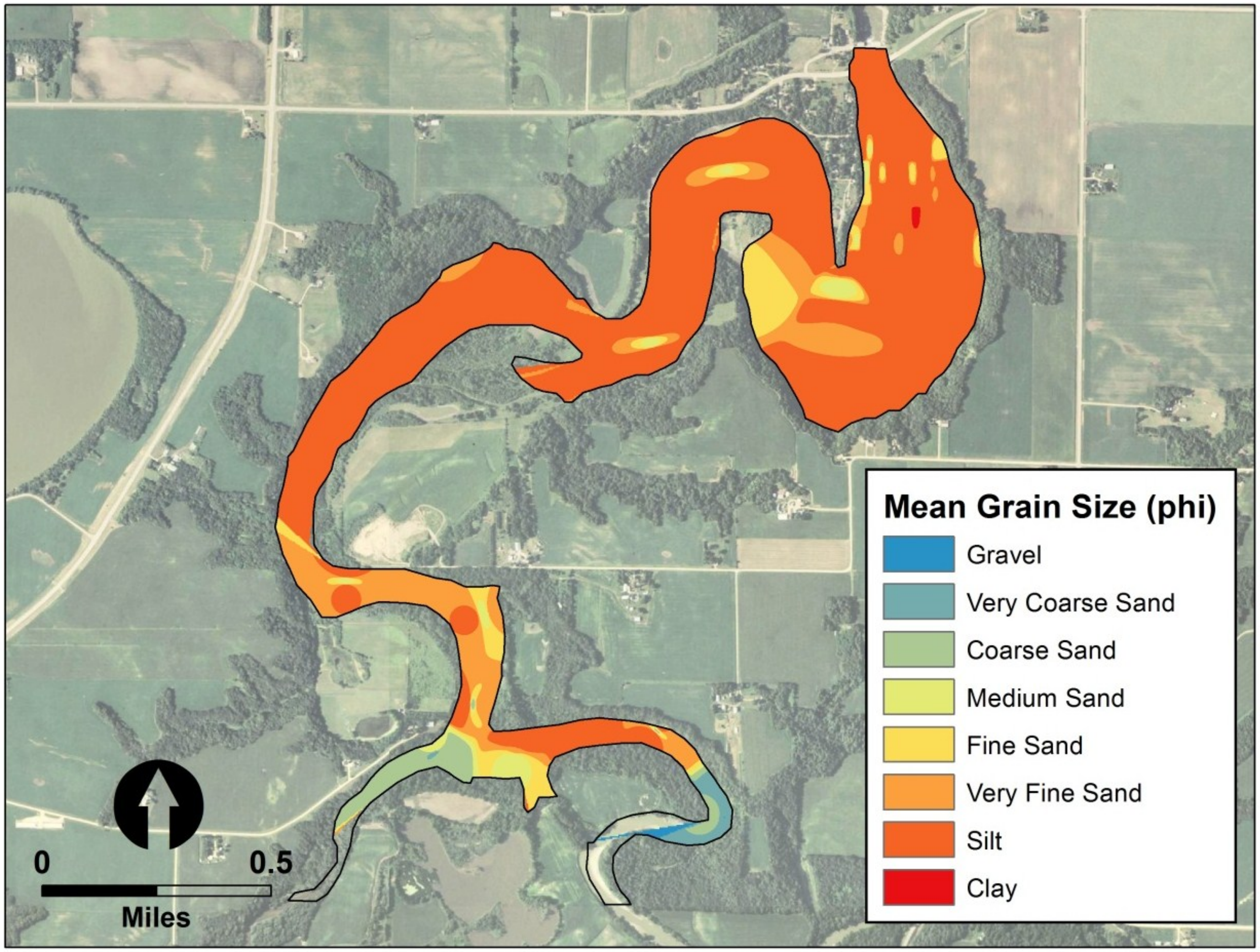

Figure 5.65: 1985 mean grain size (phi) within Rapidan Reservoir.

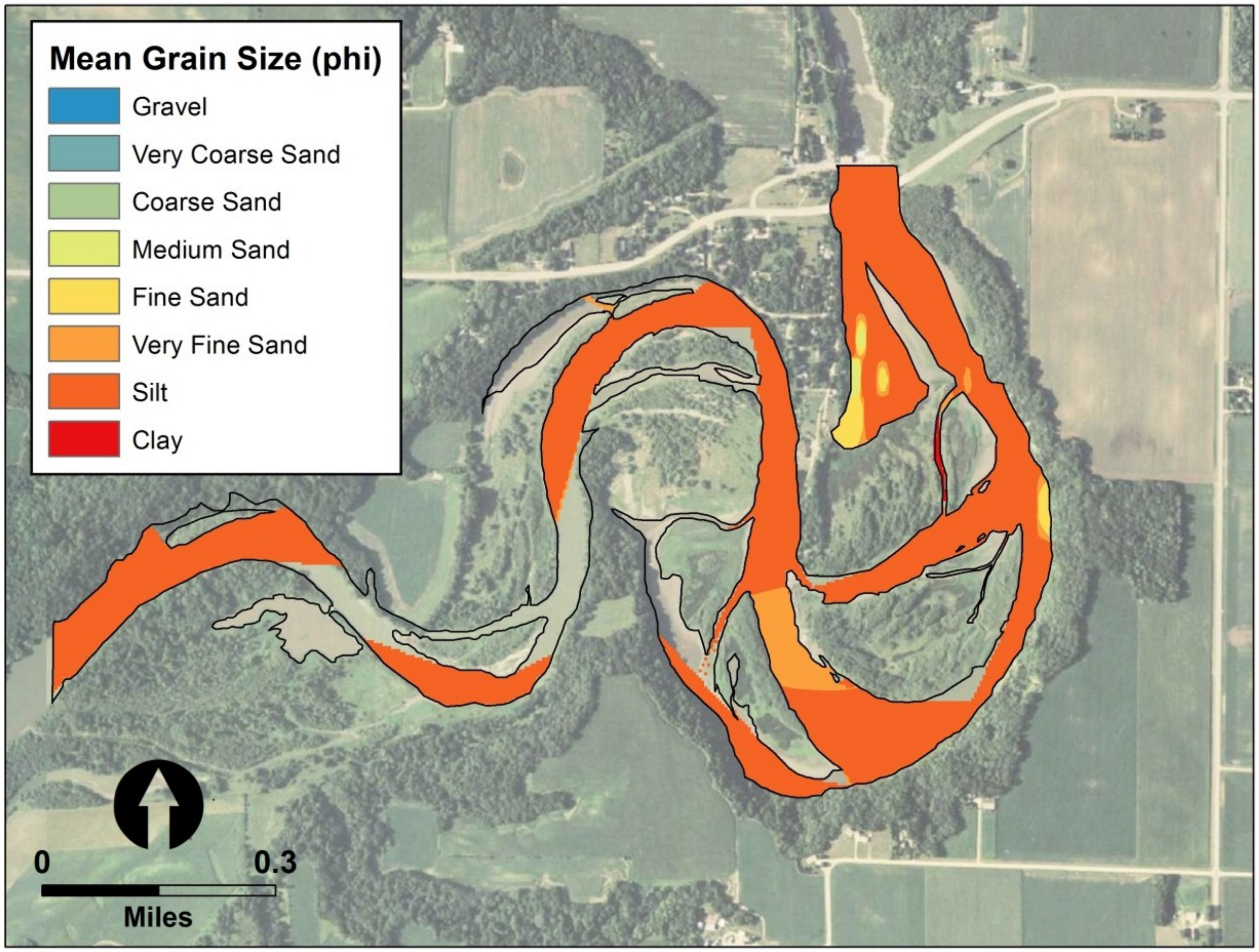

Figure 5.66: 1985 mean particle size (phi) within Rapidan Reservoir clipped to the extent of areas of the reservoir flooded during 2008-09.

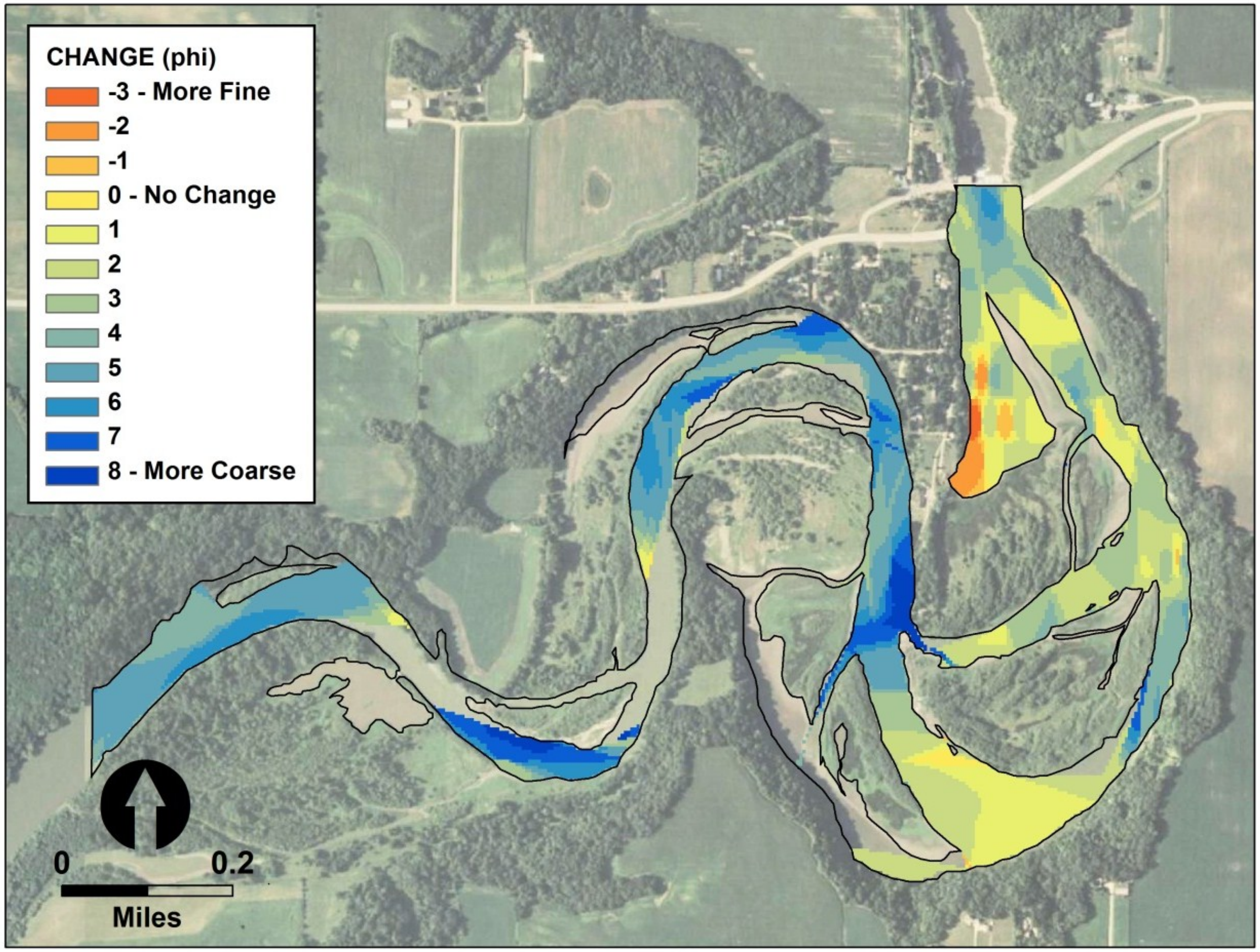

Figure 5.67: Change in grain size (phi) from 1985 sampling to 2008-09 sampling.

Table 5.16: Whole reservoir mean and median values, Rapidan Reservoir.

YEAR	MEAN	MEDIAN	VISUAL EQUIVALENT
	- phi -		
1985	4.537	4.903	Silt
1985*	5.346	5.666	Silt
2008-09	1.743	1.665	Medium Sand

*clipped to 2008-09 boundary extent

The most prominent change from 1985 to the current data from 2008-09 is the conversion and progression to coarser mean grain sizes. 72% of samples in 1985 fell in the silt category, while in 2008-09, 72% of sediments fell in the sand category (very fine to coarse sand). Additionally, 18% was classified as gravel for a total of 90% of the samples being coarser than the dominant silt of 1985. Furthermore, the whole reservoir mean grain size fell within the silt category in 1985 (5.346 Phi), and by 2008-09 had migrated to medium sand (1.743 Phi) within the natural river channel (Table 5.16).

Another strong point is that 84% of samples were very poorly sorted in 1985, whereas in 2008-09, 72% of samples were poorly sorted indicating winnowing of the smaller grains as samples became slightly more sorted through the years. The third notable point between the two datasets is that 81% of samples were either positively or strongly positively skewed in 1985 compared to 58% of samples in 2008-09. A positive skewness indicates that the distribution is skewed towards finer particle sizes. A decrease in the percentages of skewness would suggest a shift away from the finer grain sizes.

Generally, the 2008-09 mean grain size of particles increases longitudinally in the channel upstream from the dam (Figure 5.64), showing the progression of coarser materials within Rapidan Reservoir as compared to data in 1985 (Figures 5.65 and 5.66).

This is likely due to the more constricted flow from the narrowing of the natural channel by the migration and deposition of sandbars. Mid-channel grains coarsen immediately upstream from the dam intakes in the 2008-09 data. This could be attributed to suctioning of the fines before they are pulled through the intakes. Figures 5.64-5.66 are the output from the IDW interpolation using ArcMap 10.0. The reservoir boundary and sandbars were used as a polyline barrier to constrict the calculation to interpolate only within areas visible to the nearest result pixel. Figure 5.65 is the output of the 1985 interpolation using the full area of the sample distribution, and Figure 5.66 shows the 1985 results ran with the 2008-09 boundary extent. It is visually evident comparing Figure 5.64-5.66 that there was a dominance of silt in 1985 (orange) with a slight coarsening upstream in the main channel of the Blue Earth River and a scattered upstream to downstream progression from coarse sands to fine sands and silt in the 2008-09 output.

Figure 5.67 shows the differences (in phi) between the 1985 interpolation and the 2008-09 interpolation. Lower values indicate a progression to finer material and higher values indicate coarser mean grain sizes than what was found in 1985. One small area within the reservoir did move towards finer grain sizes from 1985 to 2008-09 though this area is now in a backwater pool that can become completely dry under persistent drought-like conditions) and is mostly standing water that does not receive any direct flow inputs. In 1985, this backwater area would have been open with no surrounding surface exposed sandbars. The remaining areas inundated by water in 2008-09 show a change to coarser sized grains.

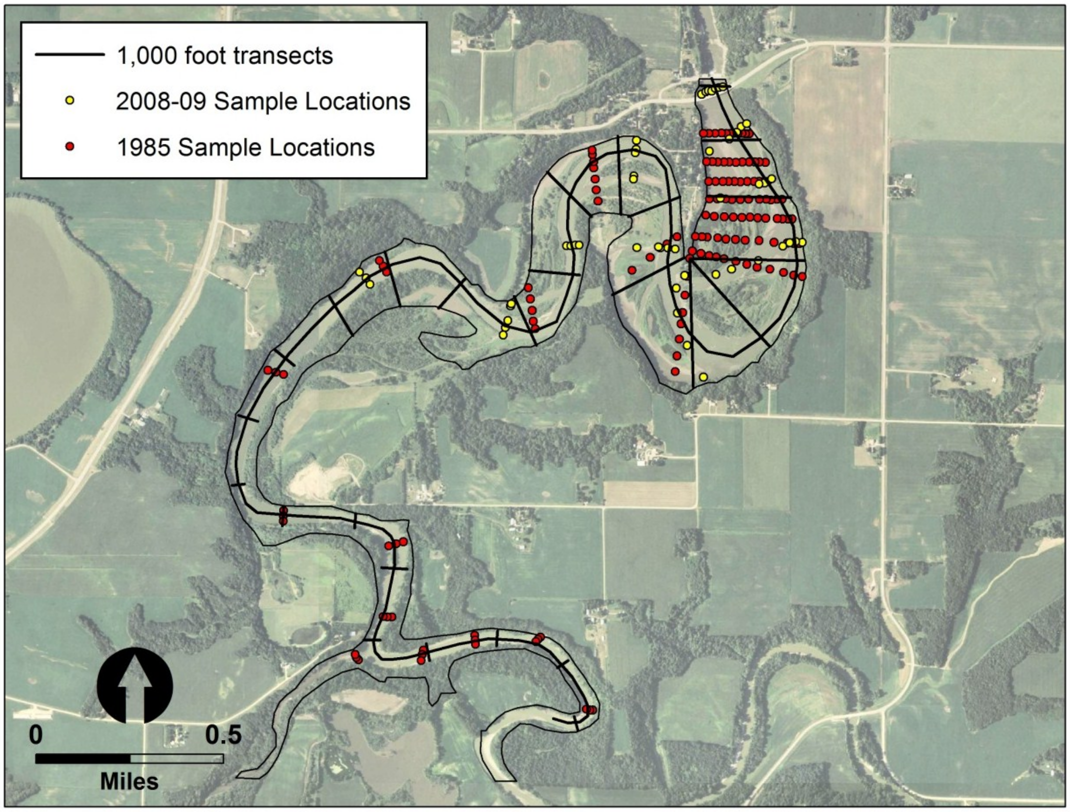

Figure 5.68: 1985 and 2008-09 sample locations along with the locations of 1,000-ft spaced transects for weighting mean particle size.

The GIS IDW interpolation results were segregated into fifteen evenly spaced transects, every 1,000 feet (Figure 5.68) to provide a longitudinal comparison of weighted mean grain size in Rapidan Reservoir. Results show a decrease in mean particle size from river mile 14.5 through mile 12.0 for 2008-09 (Figure 5.69). The 1985 data shows a fairly consistent grain size from mile 12 to 15 through the main body of the reservoir, with a slight coarsening of grain sizes from river mile 15 to mile 17 upstream from the reservoir (Figure 5.69). The stable mean grain size in 1985 correlates well with the dominance of silt within the reservoir.

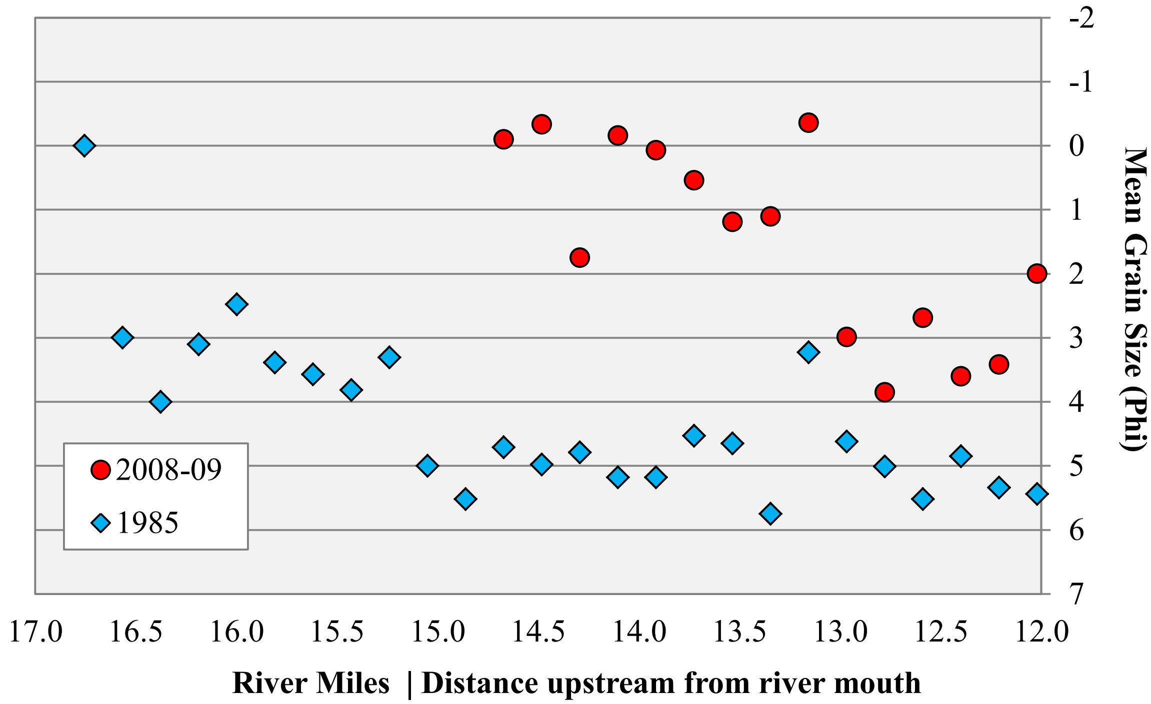

Figure 5.69: Longitudinal comparison of weighted mean sediment grain sizes in Rapidan Reservoir, 1985 and 2008-09. River miles are distances from the mouth of the Blue Earth River at Mankato, MN. Rapidan Dam is located at river mile 12.0.

Results presented from Gran et al. (2011) tell us that streams will incise naturally supplying a significant source (23-56%) of sediment to the Blue Earth River until a state of equilibrium is met. Over a 23-year period, Rapidan Reservoir morphed from a reservoir capable of trapping silt and fine grained particles to one only able to retain sand sized particles. Natural progression will continue to incise the thalweg through the reservoir which will erode previously deposited sediment and further disconnect the channel with the present floodplain.

Hjulstrom's Diagram (Figure 5.70) illustrates a line between transportation and deposition showing the velocities (dependent on particle size) at which sediment falls out of suspension and deposits on the channel bed. This velocity is known as the settling or fall velocity (Boggs 1987). The particles obtained and analyzed from 1985 and 2008-09 in Rapidan Reservoir were previously deposited sediments and therefore it can be assumed that the maximum velocity needed to deposit those particles had to be at or below the line represented in Hjulstrom's diagram. Results of weighted mean grain size from fifteen transects spaced approximately 1,000 feet apart throughout the reservoir (Figure 5.68) were paired with the average velocity (cm/sec) based on a more detailed version of Figure 5.70. Velocities for each 1,000 foot transect are shown in Table 5.17. Hjulstrom's Diagram was also annotated with the results from Table 5.17 to show the potential maximum velocities needed to deposit the samples collected (Figure 5.71 and 5.72).

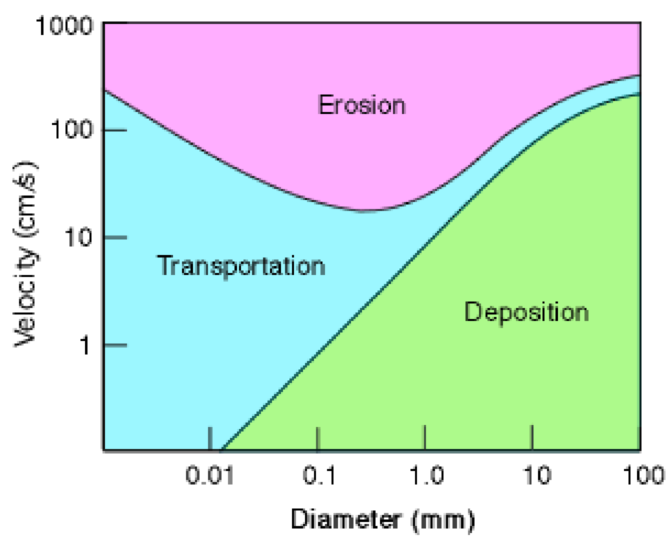

Figure 5.70: Hjulstrom's Diagram (simplified) showing mean particle sizes with velocities associated with erosion, transportation and deposition in open channels.

Table 5.17: Mean particle size, standard deviation and average depositional velocity based on Hjulstrom's Diagram for 1,000-foot transects spanning Rapidan Reservoir from Figure 5.68. River mile 12.02 is furthest downstream (nearest to Rapidan Dam); river mile 14.67 is furthest upstream.

River Miles	2008-09 Mean Grain Size		Standard Deviation	Average Velocity	1985 Mean Grain Size		Standard Deviation	Average Velocity
	Phi	mm		cm/sec	Phi	mm		cm/sec
12.02	2.00	0.25	1.65	1.50	5.44	0.02	0.19	0.15
12.21	3.42	0.09	0.31	0.60	5.34	0.02	1.02	0.15
12.40	3.60	0.08	0.82	0.55	4.85	0.03	1.12	0.24
12.59	2.69	0.15	1.01	0.90	5.52	0.02	0.59	0.15
12.78	3.85	0.07	0.17	0.50	5.01	0.03	0.99	0.24
12.97	2.99	0.13	1.59	0.85	4.62	0.04	1.40	0.30
13.16	-0.36	1.28	0.77	7.00	3.23	0.11	0.56	0.75
13.34	1.11	0.46	0.37	2.75	5.75	0.02	0.41	0.15
13.53	1.19	0.44	0.63	2.70	4.65	0.04	0.45	0.30
13.72	0.54	0.69	0.57	4.00	4.53	0.04	0.42	0.30
13.91	0.07	0.95	0.36	5.50	5.18	0.03	0.03	0.24
14.10	-0.16	1.11	0.81	6.30	5.18	0.03	0.03	0.24
14.29	1.75	0.30	1.25	2.00	4.79	0.04	0.17	0.30
14.48	-0.33	1.26	0.20	6.70	4.98	0.03	0.65	0.24
14.67	-0.10	1.07	0.17	6.10	4.71	0.04	0.16	0.30
AVERAGE				**3.20**				**0.27**

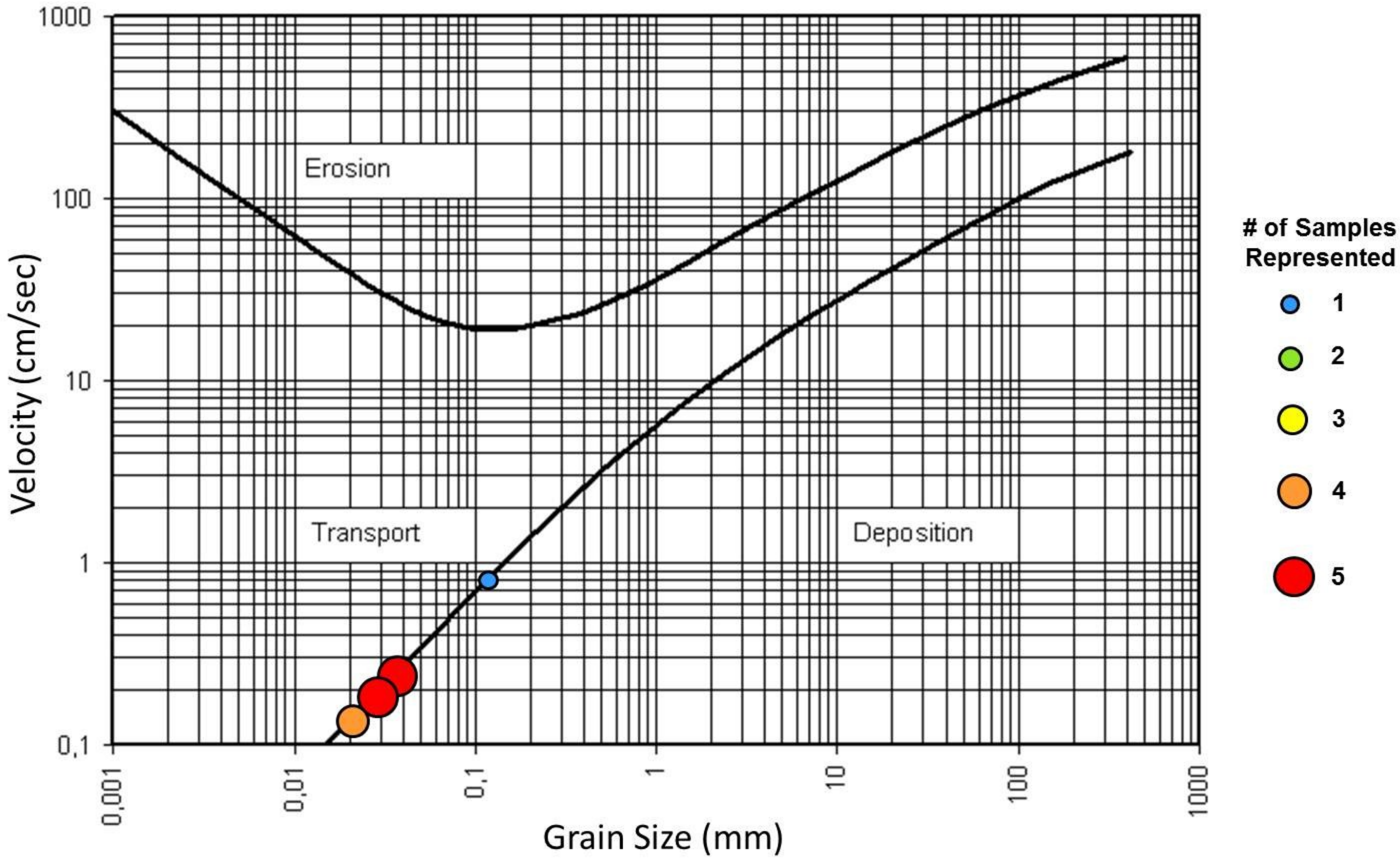

Figure 5.71: Annotated Hjulstrom Diagram with 1985 mean grain sizes (mm). Color and size of dot indicates number of samples represented.

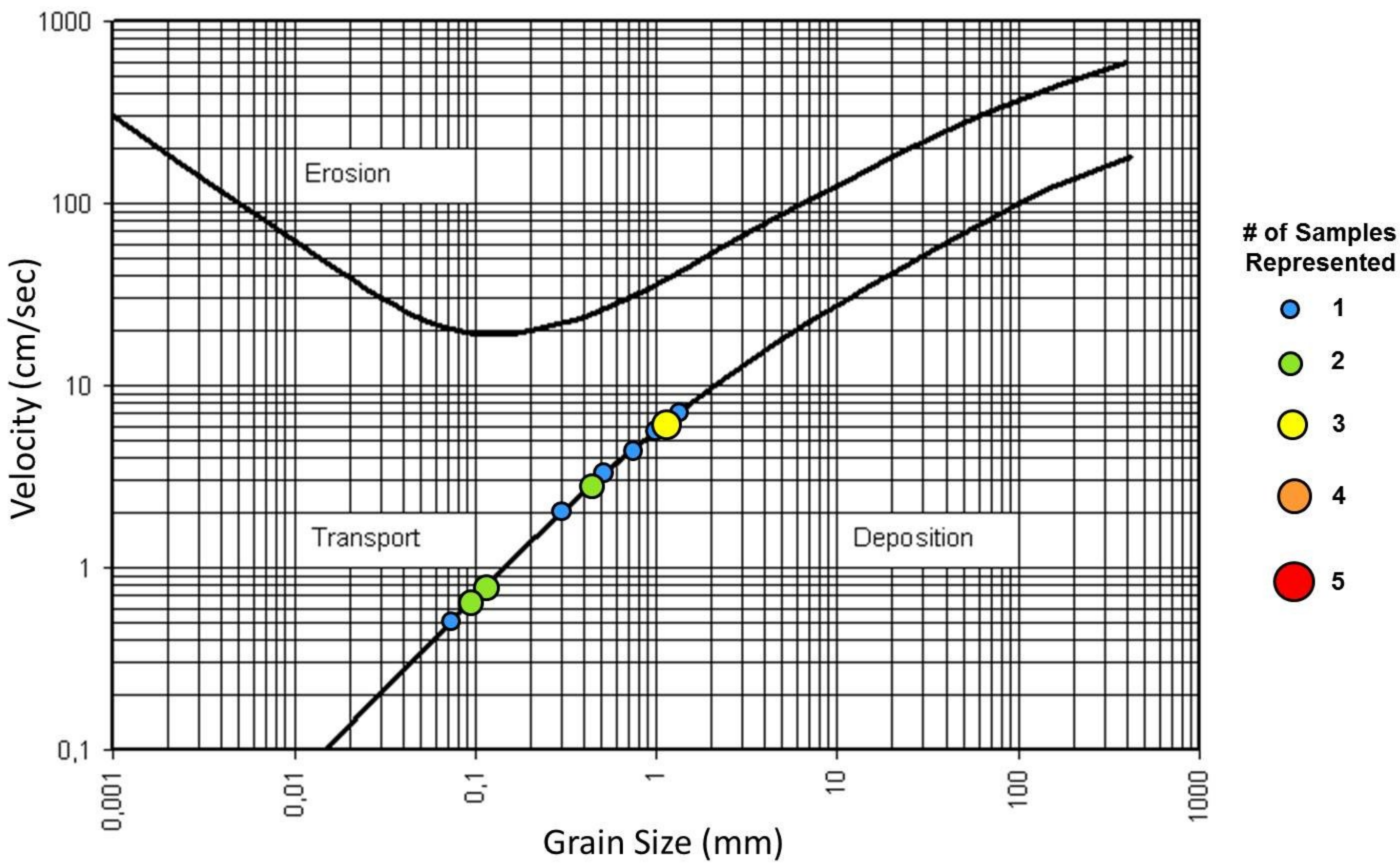

Figure 5.72: Annotated Hjulstrom Diagram with 2008-09 mean grain sizes (mm). Color and size of dot indicates number of samples represented.

The annotations presented in Figures 5.71 and 5.72 visually show that mean grain sizes for the depositing velocity maximum in 1985 was between 0.15 to 0.3 cm/sec, with one result of approximately 0.75 cm/sec which skews the data slightly higher. 2008-09 velocities ranged from 0.5 cm/sec up to 7 cm/sec.

The average velocity in 1985 was 0.27 cm/sec while the average velocity required to deposit the sediment in 2008-09 was 3.20 cm/sec. The increase by a factor of ten from 1985 to 2008-09 is an order of magnitude and suggests that with increased velocities, finer particles are being passed through to downstream reaches and are no longer being deposited in the main channel. As a result, the reservoir has coarsened over time. Backwater areas do still exist in the reservoir where water can be almost stagnant and certainly fines can be assumed to be deposited in those locations. The consequence of continued infilling of sediment through the reservoir has constricted the flow and deprived the reservoir of capacity, thus increasing velocities. With higher velocities during snowmelt runoff and after large runoff events, the reservoir could also see velocities falling in the erosion portion of Hjulstrom's Diagram which could remobilize deposited sediments and may be a partial explanation for why the reservoir served as a source for 150,909 tons of sediment in 2008 and 8,583 tons in 2009 to downstream reaches.

5.6 Synthesis

Since 1911, Rapidan Reservoir and the associated dam have artificially impounded water and segmented over 1,200 miles of tributary streams of the Blue Earth

River. Although many factors contribute to erosion and transport of sediment in the river's watershed, geomorphology and land use are among the most important. The watershed has easily erodible soils juxtaposed against steep bluffs and ravines. Land use is dominated by row crop agriculture that has altered the natural drainage network. Climate, with a penchant for saturating precipitation events that can last for several days and short, high intensity bursts of precipitation, can mobilize significant sediment and deliver vast loads of suspended solids through the system.

Throughout most of its life, the Rapidan Reservoir served as a catchment basin for sediment moving through the Blue Earth River. Water entering the reservoir spread out over a larger cross sectional area which in turn decreased water velocity. The diminished velocities allowed particles to fall out of suspension and deposit on the bed of the reservoir. Over time, sandbars accumulated and the reservoir volume slowly depleted. Sandbars channelized the river and created a natural thalweg. Currently 11 million cubic yards of sediment is deposited within Rapidan Reservoir. The narrowing of the channel increased water velocities and now restricts the ability of fines to fall out of suspension. Consequently, it is suspected that fines are moved downstream.

Historic analyses of sediment samples within Rapidan Reservoir show a vast inventory of silt in 1985. This is a logical outcome of the meteorological conditions prior to the sample collection. Specifically, the summer of 1985 was preceded by a wet fall (1984) and spring. Above normal flow and precipitation conditions were also observed in the spring and summer of 1984. The precipitation departure in October and December of 1984 was greater than 100% above normal. Precipitation totals for January, March and April of 1985 were also above normal, with above average monthly flows observed in March. The ensuing summer months (May through July) were exceptionally dry, 25 to 50% below normal. During prolonged periods of higher than normal precipitation, findings by the MPCA (2000, 2010) suggest that soils in the watershed have low infiltration capacities which could lead to considerable runoff. In addition, rivers have a natural tendency to incise their own channels (Gran et al. 2010, Magner 2004), which would remobilize sediments that make up the bedload (MPCA 2000). To further the point, Bauer (1998) and Thoma (2005) found that incision leads to stream bank erosion and sloughing which introduces large quantities of sediment to the system. This sequence of events (wet period followed by a dry period) should conceptually bring a coarser size fraction into the reservoir, and then create conditions that are incapable of remobilizing the deposited material downstream of the dam. As a result, one would expect that the particle sizes presented in Quade et al. (2004) would be biased towards a coarser fraction than what may have been found during normal or dry conditions.

Comparatively, samples from 2008-09 were collected over a prolonged period which may introduce some variability, mostly late fall and winter. This dataset shows a dominance of sand within the reservoir. Dry conditions persisted through summer 2007, but were truncated by a larger rainfall event in August (and subsequent increase in monthly average flows), followed by a wet fall. 2008 began with a dry spring, wet May and June and dry summer. Both 2007 and 2008 saw annual precipitation totals below the 30-year normal and had less precipitation and discharge than both 1984 and 1985.

Overall, precipitation and discharge tended to sway towards drier conditions which would theoretically introduce and move less coarse sediment into the reservoir relative to 1985.

Digitizing of sandbars from 1939 to 2006 illustrated a significant decrease in the percent surface area due to the accumulation of sediment within the reservoir. 1985 and 1992 showed the surface area of the reservoir decreased from 12 percent in 1985 and 29 percent in 1992 to 56 percent in 2006. Higher than expected percentages of surface area lost were tallied in 1949 and 1971 due to low water levels and the condition of the dam operation at that time. Despite these anomalies, the overall trend is observably increasing and the 2006 results are in accord with that trend.

Ruff (1987) suggested based on TSS concentration results upstream and downstream of the reservoir that Rapidan Reservoir was acting as a trap for sediment. Payne (1994) found in 1991 that the reservoir could act as a source for sediment during large runoff events but mostly served as a pass through neither trapping sediment nor sourcing it to downstream reaches. Current data suggests that the reservoir is serving as a source for sediment to downstream locations during the course of the ice-free monitoring season (March or April through October). The reservoir was a source for 136,878,755 kg (301,817,655 pounds) of suspended sediment in 2008 and 7,785,468 kg (17,166,956 pounds) in 2009 to the Blue Earth River downstream of the reservoir. Realistically, the reservoir could serve as a trap or pass-through during extremely low flow conditions, and a source during high flow conditions. The reservoir could also alter between source or sink dependent on flow and climactic variables throughout the year.

Rapidan Reservoir is not the same reservoir as it was when first constructed and even since the 1980s after the dam was rehabilitated and the reservoir partially dredged. The overall life of Rapidan Reservoir is in accordance with expectations of all reservoirs in general. Dependent on regional geomorphology, land use, soils, topography and climactic variables; all reservoirs have a limited life span which will be based on technology, economics and availability of funds for maintenance (Heintz Center 2002, Chanson and James 1998).

CHAPTER 6: CONCLUSION

This study provided a brief look into the sediment characteristics of Rapidan Reservoir over a 23 year period, by further exploring existing data from 1985 and comparing that dataset to more recent data collected in 2008 and 2009. The conclusive data suggest that due to the constant influx of sediment over the life span of the reservoir, the trap efficiency has been altered. Functioning reservoirs should be able to capture all grain size distributions. Currently Rapidan Dam cannot capture and maintain the silt and clay fraction which provides evidence indicating the loss of efficiency. Rapidan Reservoir is now less efficient at trapping sediment than it was in 1985 and the fingerprinting of deposited sediment within the reservoir expresses that story. In the 23 year period, the average grain size within the reservoir increased from silt to medium sand. The average maximum velocity required to deposit that sediment has also increased from 0.27 cm/sec to 3.20 cm/sec; an order of magnitude. The increase in velocity can be attributed to the deposition over time of numerous sandbars which decreases the area for water to spread out in the reservoir, slow down and deposit sediment. As a result, the reservoir can no longer trap the fine materials except in backwater areas created by sandbars. Increased velocities also provide the mechanism to remobilize already deposited sediment within the reservoir if velocities exceed the falling/settling velocity threshold presented in Hjulstrom's Diagram. Monitoring season results upstream and downstream from the reservoir in 2008 and 2009 show that the reservoir served as a source for suspended sediment to downstream reaches. A low percentage (0.58%-8.77%) of organic matter within the deposited sediments and a slight increase in organics from upstream to downstream also indicates that the residence time through the reservoir is not long enough to allow for the accumulation of organics. Furthermore, an analysis of eight aerial photographs dating from 1939 to 2006 show that the overall surface area in the reservoir has decreased by 56% since the late 1930's.

All results presented are based on two years of data (2008-09) paired with results from 1985. Ideally, more years of a data covering a broad range of climactic conditions would be preferred so "normal" conditions could be established for the current standing of the reservoir. We now know what is directly input to the reservoir and what is exiting. In addition, we can provide a limited view of the particle size distribution trapped by the dam. Combined, this serves as a benchmark for future studies to compare the progression of loss of the trap efficiency from Rapidan Reservoir.

The Blue Earth River below Rapidan Reservoir is a popular stretch for anglers and recreational boaters not only for the unique scenery to southern Minnesota but also due to the historic significance of Rapidan Dam and adjacent eatery, the Dam Store. Rapidan Dam has a finite life span. A study of this nature paired with follow up studies could inform decision making processes for either removal or further rehabilitation of the dam. Removal would provide an excellent opportunity for researchers to study a large scale experiment in river restoration, both the positive and negative effects from reopening a waterway that has been segmented for over a century.

LITERATURE CITED

Barr Engineering, Blue Earth County, MPCA, MDNR. 2000. Rapidan Dam Feasibility Study, Dam Removal Option. Report, 55 pp and Appendices.

Bauer, D. W., 1998. Stream Bank Erosion and Slumping along the Blue Earth River. M.S. thesis. University of Minnesota, St. Paul, MN, 77 pp.

Blann, Kristen, Anderson, James, Sands, Gary and Bruce Vondracek. 2009. Effects of Agricultural Drainage on Aquatic Ecosystems: A Review. Critical Review in Environmental Science and Technology. Volume 39, 11. Pages 909-1001.

Boggs, Sam Jr. 1987. Principles of Sedimentology and Stratigraphy. Macmillian Publishing Company, New York, New York. 784 pages.

Boggs, Sam Jr. 1992. Petrology of Sedimentary Rocks. Macmillan Publishing Company, New York, New York. 707 pages.

Boone, Hannah. 2000. The Minnesota River basin and its soil resources. [cited April 23, 2007]. Available from http://www.environmentaleducationohio.org/Site%20Archives/Case%20Studies/minnesota.html

Chanson, H. and P. James. 1998. Teaching Case Studies in Reservoir Siltation and Catchment Erosion. International Journal of Engineering Education. Volume 14, No. 4. Pages 265-275.

Crowder, Bradley M. 1987. Economic costs of reservoir sedimentation: a regional approach to estimation cropland erosion damage. Journal of Soil and Water Conservation. Volume 42, No. 3. Pages 194-197.

Dean, W.E. 1974. Determination of Carbonate and Organic Matter in Calcareous Sediments and Sedimentary Rocks by Loss on Ignition: Comparison with other Methods. Journal of Sedimentary Petrology. Volume 44. Pages 242-248.

Engstrom, Daniel R. and James E. Almendinger. 2000. Historical Changes in Sediment and Phosphorus Loading to the Upper Mississippi River: Mass-balance Reconstructions from the Sediments of Lake Pepin. Final Research Report prepared for the Metropolitan Council Environmental Services. St. Croix Watershed Research Station, Science Museum of Minnesota. Marine on St. Croix, Minnesota

Engstrom, DR, Almendinger, JE, Wolin, JA. 2008. Historical changes in sediment and phosphorus loading to the upper Mississippi River: mass-balance reconstructions from the sediments of Lake Pepin. Journal of Paleolimnology.

ESRI. 2007. How Inverse Distance Weighted (IDW) interpolation works. Environmental Systems Research Institute, Inc. Last modified August 7, 2007. Available from: http://webhelp.esri.com/arcgisdesktop/9.2/body.cfm?id=3304&pid=3302&topicname=How%20Inverse%20Distance%20Weighted%20(IDW)%20interpolation%20works&tocVisable=0

Fischenich, Mark. 2007. Dam hole to be repaired. Mankato Free Press, Mankato, Minnesota [cited February 18, 2008] Available from http://www.mankato-freepress.com/local/local_story_212001710.html

Friedman, Gerald M and Kenneth G. Johnson. 1982. Exercises in Sedimentology. John Wiley and Sons.

Friedman, G.M and J.E Sanders. 1978. Principles of Sedimentology. John Wiley & Sons. New York, NY.

Fu, K.D., He, D.M. and X.X. Lu. 2008. Sedimentation in the Manwan Reservoir in the Upper Mekong and its downstream impacts. Quaternary International. Volume 186-1. Pages 91-99.

Gran, Karen, Belmont, Patrick, Day, Stephanie, Jennings, Carrie, Lauer, J. Wesley, Viparelli, Enrica, Wilcock, Peter and Gary Parker. June 2011. An Integrated Sediment Budget for the Le Sueur River Basin. Report to the Minnesota Pollution Control Agency, St. Paul, MN

Gupta, Satish, Thoma, David and Marv Bauer. 2001. Sediment Origins: Agriculture's role in river water quality questioned by farmers. Resource: Engineering and Technology for a Sustainable World. December 1, 2001.

Guttman, N.B. 1989. Statistical descriptors of climate. Bulletin of the American Meteorological Society. Volume 70, No. 6, Pages 602-607.

Halacy, D.S. 1977. Earth, Water and Sun: Our Energy Alternatives. Harper and Row. New York, NY.

Heintz Center. 2002. Dam Removal: Science and Decision Making. The H. John Heinz III Center for Science, Economics and the Environment. Washington, D.C.

Kelley, D.W. and E.A. Nater. 2000. Historical sediment flux from three watersheds in Lake Pepin, Minnesota, USA. Journal of Environmental Quality, v. 29, pp.561–568.

(LPLA) Lake Pepin Legacy Alliance. 2009. "Site-specific" Water Standards for Lake Pepin and South Metro Mississippi. [cited January 2010] Available from http://www.lakepepinlegacyalliance.org/sitespecificstandards.html

Linehan, Dan. 2007. New stage for Rapidan Dam repair. Mankato Free Press, Mankato, Minnesota. [cited February 18, 2008] Available from http://www.mankato-freepress.com/local/local_story_305223302.html

Linehan, Dan. 2009. Rapidan Dam Breaking Even. Mankato Free Press. Mankato, Minnesota [cited January 2010].

Magdalene, Suzanne. 2004. From Field to Stream: Rapid Runoff through Agricultural Tile Drainage Systems within the Minnesota River Basin. Doctorate Thesis. University of Minnesota.

Magner, J.A, Payne, G.A and L.J. Steffen. 2004. Drainage Effects on Stream Nitrate-N and Hydrology in South-Central Minnesota (USA). Environmental Monitoring and Assessment. Volume 91. Pages 183-198.

Matsch, C.L. 1983. River Warren, the southern outlet of Lake Agassiz. Teller. Glacial Lake Agassiz: Geological Association of Canada. Special Paper 26. Pages 232-244.

Minnesota Pollution Control Agency (MPCA). 2000. CWP Project #1943 Blue Earth River major watershed diagnostic report. [cited April 23, 2007] Available from http://mrbdc.mnsu.edu/reports/bluearth/cwp30/cwp30.html

Minnesota Pollution Control Agency (MPCA). 2001. Minnesota River basin plan. [cited February 25 2007]. Available from http://www.pca.state.mn.us/water/basins/mnriver/mnbasinplan.pdf.

Minnesota Pollution Control Agency (MPCA). 2002. Minnesota River study shows reductions in key pollutants. [cited February 25 2007]. Available from http://www.pca.state.mn.us/publications/wq-b3-02.pdf.

Minnesota Pollution Control Agency (MPCA). 2005 (last updated). Overview: Blue Earth, Le Sueur and Watonwan Watersheds [cited December 2, 2008] Available from http://www.pca.state.mn.us/water/basins/mnriver/watersheds.html

Minnesota Pollution Control Agency (MPCA). 2006. Fecal coliform TMDL assessment for 21 impaired streams in the Blue Earth River basin. [cited March 13, 2007]. Available from http://www.pca.state.mn.us/publications/reports/tmdl-blueearth-fecal.pdf.

Minnesota Pollution Control Agency (MPCA). 2009. Identifying Sediment Sources in the Minnesota River Basin. Minnesota River Sediment Colloquium. [cited January 2010] Available from http://www.lakepepinlegacyalliance.org/SedSynth_FinalDraft-formatted.pdf

Minnesota Pollution Control Agency (MPCA). 2010. 2010 Draft TMDL list. [cited January 2010] Available from http://www.pca.state.mn.us/water/tmdl/tmdl-303dlist.html

Minnesota River Basin Joint Powers Board (MRBJPB). 2002. Minnesota River Basin Water Quality Overview. [cited February 18, 2008] Available from http://www.extension.umn.edu/distribution/naturalresources/DD7079.html

Mulla, David J. and Ananda Mallawatantri. 1999. Minnesota River basin water quality overview. Department of Soil, Water, and Climate [database online]. University of Minnesota, [cited April 23, 2007]. Available from http://www.soils.umn.edu/research/mn-river/doc/watqual.html.

Nagle, George N. 2002. The contribution of agricultural erosion to reservoir sedimentation in the Dominican Republic. Journal of Water Policy. Volume 3-6. Pages 491-505.

Payne, Gregory A. 1994. Sources and transport of sediment, nutrients, and oxygen-demanding substances in the Minnesota River Basin, 1989-92. United States Geological Survey. Water-Resources Investigations Report 93-4232.

Poff, Leroy and David Hart. 2002. How Dams Vary and Why it Matters for the Emerging Science of Dam Removal. BioScience. Vol. 52, No. 8. Pages 659-668.

Quade, Henry, Ruff, G., Danks, M., Fasching, P., Grutzner, F and Heidi Schreiner. 2004. The Rapidan Dam research project: environmental impacts of converting a run-of-the-river low head hydroelectric dam to a peaking operation. Water Resources Center, Minnesota State University, Mankato.

Quinn, Edward M. 1999. Dam removal: a tool for restoring riverine ecosystems. Restoration and Reclamation Review. Student On-Line Journal. Vol. 5, No. 1

Rantz, S.E. 1982. Measurement and Computation of Streamflow: Volume I. Measurement of Stage and Discharge. Geological Survey Water-Supply Paper 2175. U.S. Government Printing Office, Washington, D.C.

Ruff, Greg. 1987. The impact of a non-stratifying reservoir and its small, low-head, peaking hydroelectric dam on the water quality and POM transport of the Blue Earth River, south-central Minnesota. Master's thesis. Mankato State University, Mankato, Minnesota.

Sawaske, Spencer R. and David L. Freyberg. 2012. A comparison of past small dam removals in highly sediment-impacted systems in the U.S. Geomorphology. Volume 151-152. Pages 50-58.

Seeley, Mark. 2008. Understanding Earth's Climate and How It is Changing, First Lego League Climate Connections - October 16, 2008.

Sekely, Adam C. 2002. Streambank slumping and its contribution to the phosphorus and suspended sediment loads of the Blue Earth River. Minnesota. Journal of Soil and Water Conservation. 57(5), 243-250.

Senjem, Norman B., Moncrief, John F. and Randall, Gyles W. and Samuel D. Evans. 2002. Sediment problems and solutions for the Minnesota River. University of Minnesota Extension [database online]. Available from http://www.extension.umn.edu/distribution/naturalresources/DD6671.html.

Thoma, David P., Gupta, Satish C., Bauer, Marvin E. and C.E. Kirchoff. 2005. Airborne Laser Scanning for Riverbank Erosion Assessment. Remote Sensing of Environmental. Volume 95. Pages 493-501.

United States Army Corps of Engineers (USACOE). 2001. U.S. National Inventory of Dams. Report. Paper 672.

United States Army Corps of Engineers (USACOE). 2006. Feasibility study: Blue Earth River basin in Minnesota and Iowa. [database online]. St. Paul District. [cited April 23, 2007]. Available from http://www.mvp.usace.army.mil/environment/default.asp?pageid=1116.

United States Army Corps of Engineers (USACOE). 2009. Rapidan Dam Investigations: Blue Earth River Feasibility Study, Ecosystem Restoration. USACOE St. Paul District. St. Paul, Minnesota.

United States Department of the Interior (USDOI). 2003. Economic Analysis of Dam Decommissioning. Report Number: EC-2003-01, 61 pages.

Walker, William W. 1996. Simplified Procedures for Eutrophication Assessment and Prediction: User Manual. United States Army Corp of Engineers. Concord, MA.

Wang, Zaho-yin and Chunhong Hu. 2009. Strategies for Managing Reservoir Sedimentation. International Journal of Sediment Research. Volume 24-4, pages 369-384.

Waters, Thomas F. 1977. The streams and rivers of Minnesota. University of Minnesota. Minneapolis Press.

Water Resources Center (WRC). 2000. Diagnostic study of the Blue Earth River major watershed. Minnesota River Basin Data Center. [cited February 25 2007]. Available from http://mrbdc.mnsu.edu/reports/bluearth/cwp30/cwp30.html.

Water Resources Center (WRC), Minnesota State University. 2003. State of the Minnesota River: executive summary of surface water quality monitoring 2002. Minnesota River Basin Data Center. [cited February 25 2007]. Available from http://mrbdc.mnsu.edu/mnbasin/fact_sheets/stateofriver_2002.html.

Water Resources Center (WRC), Minnesota State University. 2004. State of the Minnesota River: executive summary of surface water quality monitoring 2003. Minnesota River Basin Data Center. [cited February 25 2007]. Available from http://mrbdc.mnsu.edu/mnbasin/fact_sheets/stateofriver_2003.html.

Water Resources Center (WRC), Minnesota State University. 2012. Turbidity Total Maximum Daily Load Greater Blue Earth River Basin. Minnesota Pollution Control Agency Report wq-iw7-29b.

APPENDIX 1: Water Chemistry Results

Table 7.01: BEC9 total suspended solids results, 2008.

2008 Blue Earth River main stem on at Rapidan Dam (BEC9) Total Suspended Solids					
Station	Date	Time	15 Minute Flow (cfs)	TSS (mg/L)	Lab
BEC9	4/2/2008	14:40	264	27	MCES
BEC9	4/9/2008	11:40	1260	26	MCES
BEC9	4/11/2008	13:15	1760	134	MCES
BEC9	4/14/2008	12:00	4190	364	MCES
BEC9	4/18/2008	11:30	2430	102	MCES
BEC9	4/18/2008	11:32	2430	90	MCES
BEC9	4/25/2008	10:50	2560	108	MCES
BEC9	4/28/2008	11:45	5840	386	MCES
BEC9	5/1/2008	11:23	4260	593	MCES
BEC9	5/6/2008	9:41	7710	784	MCES
BEC9	5/9/2008	11:20	5580	200	MCES
BEC9	5/20/2008	16:00	2640	48	MCES
BEC9	5/28/2008	11:00	1580	25	MCES
BEC9	5/30/2008	9:20	2190	648	MCES
BEC9	6/3/2008	12:15	5620	246	MCES
BEC9	6/5/2008	12:50	4510	206	MCES
BEC9	6/9/2008	14:15	6110	255	MCES
BEC9	6/17/2008	8:15	8110	330	MCES
BEC9	6/20/2008	12:45	4710	302	MCES
BEC9	6/23/2008	13:45	2930	164	MCES
BEC9	6/27/2008	14:40	2170	199	MCES
BEC9	7/1/2008	9:00	2530	5	MCES
BEC9	7/18/2008	11:10	635	52	MCES
BEC9	8/4/2008	10:40	647	44	MCES
BEC9	8/18/2008	10:45	142	28	MCES
BEC9	9/3/2008	12:20	102	37	MCES
BEC9	9/24/2008	12:35	56	26	MCES

Table 7.02: BEC9 total suspended solids results, 2009.

2009 Blue Earth River downstream from Rapidan Dam (BEC9) Total Suspended Solids					
Station	Date	Time	15 minute Flow (cfs)	TSS (mg/L)	Lab
BEC9	03/23/2009	16:22	1,470	143	MVTL
BEC9	03/24/2009	12:14	1,550	385	MVTL
BEC9	03/26/2009	11:24	2,060	515	MVTL
BEC9	04/03/2009	08:30	991	36	MVTL
BEC9	04/10/2009	13:05	686	51	MVTL
BEC9	04/14/2009	14:30	538	46	MVTL
BEC9	04/30/2009	11:15	1,230	48	MVTL
BEC9	05/07/2009	11:30	920	53	MVTL
BEC9	05/14/2009	10:30	1,220	34	MVTL
BEC9	05/19/2009	10:45	860	32	MVTL
BEC9	05/27/2009	12:10	504	35	MVTL
BEC9	06/02/2009	12:00	363	42	MVTL
BEC9	06/09/2009	09:00	338	41	MVTL
BEC9	06/15/2009	11:00	1,430	22	MVTL
BEC9	06/18/2009	14:15	1,250	47	MVTL
BEC9	06/23/2009	11:30	1,200	63	MVTL
BEC9	06/25/2009	14:02	983	85	MVTL
BEC9	07/06/2009	14:31	406	129	MVTL
BEC9	07/08/2009	12:11	379	47	MVTL
BEC9	07/14/2009	14:02	2,040	185	MVTL
BEC9	07/16/2009	09:10	1,790	118	MVTL
BEC9	07/28/2009	14:00	379	43	MVTL
BEC9	08/13/2009	12:35	146	50	MVTL
BEC9	08/20/2009	11:30	150	70	MVTL
BEC9	08/27/2009	11:50	127	70	MVTL
BEC9	09/17/2009	11:30	45	41	MVTL
BEC9	10/02/2009	11:55	49	19	MVTL
BEC9	10/07/2009	09:30	544	22	MVTL
BEC9	10/22/2009	12:00	831	13	MVTL
BEC9	10/26/2009	09:45	3,060	130	MVTL
BEC9	10/29/2009	12:45	2,520	45	MVTL

Table 7.03: BEC13W total suspended solids results, 2008.

2008 Watonwan River near Garden City, Minnesota (BEC13W) Total Suspended Solids					
Station	Date	Time	Hourly Flow cfs	TSS mg/L	Lab
BEC13W	4/1/2008	15:15	203 *	24	MVTL
BEC13W	4/4/2008	14:00	247 *	12	MVTL
BEC13W	4/10/2008	13:30	253	36	MVTL
BEC13W	4/11/2008	13:00	631	142	MVTL
BEC13W	4/14/2008	14:30	1,130	118	MVTL
BEC13W	4/17/2008	12:30	736	81	MVTL
BEC13W	4/22/2008	14:30	521	45	MVTL
BEC13W	4/25/2008	13:00	806	122	MVTL
BEC13W	4/27/2008	17:30	1,540	183	MVTL
BEC13W	4/29/2008	13:00	1,550	111	MVTL
BEC13W	5/2/2008	13:00	1,070	86	MVTL
BEC13W	5/5/2008	13:15	2,880	183	MVTL
BEC13W	5/7/2008	12:45	2,870	116	MVTL
BEC13W	5/9/2008	9:30	2,010	80	MVTL
BEC13W	5/14/2008	9:30	1,660	58	MVTL
BEC13W	5/19/2008	14:30	974	49	MVTL
BEC13W	5/22/2008	10:45	751	37	MVTL
BEC13W	5/29/2008	12:15	513	19	MVTL
BEC13W	5/30/2008	11:00	1,080	NA	MVTL
BEC13W	6/2/2008	9:30	1,750	91	MVTL
BEC13W	6/4/2008	9:30	1,540	97	MVTL
BEC13W	6/6/2008	NA	1,640	123	MVTL
BEC13W	6/9/2008	12:45	2,880	72	MVTL
BEC13W	6/10/2008	16:30	2,970	30	MVTL
BEC13W	6/11/2008	11:00	2,810	54	MVTL
BEC13W	6/13/2008	10:00	2,350	64	MVTL
BEC13W	6/16/2008	9:15	1,760	78	MVTL
BEC13W	6/18/2008	9:00	1,330	85	MVTL
BEC13W	6/20/2008	12:30	1,060	80	MVTL
BEC13W	6/26/2008	13:30	534	56	MVTL
BEC13W	7/2/2008	10:00	388	44	MVTL
BEC13W	7/7/2008	10:45	247	24	MVTL
BEC13W	7/16/2008	13:00	115	10	MVTL
BEC13W	7/17/2008	15:00	149	68	MVTL
BEC13W	7/18/2008	9:45	129	24	MVTL
BEC13W	7/25/2008	10:00	136	16	MVTL
BEC13W	8/1/2008	10:30	104	19	MVTL
BEC13W	8/13/2008	12:45	51	7	MVTL
BEC13W	9/2/2008	14:30	22	8	MVTL
BEC13W	9/23/2008	11:30	19	20	MVTL

* Instantaneous flow not available, Daily Average Flow value used | NA = data not available

Table 7.04: BEC13W total suspended solid results, 2009.

2009 Watonwan River near Garden City, Minnesota (BEC13W) Total Suspended Solids					
Station	**Date**	**Time**	**Hourly Flow** cfs	**TSS** mg/L	**Lab**
BEC13W	03/16/2009	13:30	-	78	MDH
BEC13W	03/17/2009	12:01	-	42	MVTL
BEC13W	03/24/2009	08:15	673	133	MVTL
BEC13W	03/26/2009	11:00	736	124	MVTL
BEC13W	04/29/2009	13:30	271	4.8	MDH
BEC13W	04/30/2009	10:45	277	15	MVTL
BEC13W	05/07/2009	11:50	222	18	MVTL
BEC13W	05/14/2009	10:55	287	20	MVTL
BEC13W	05/19/2009	10:25	205	19	MVTL
BEC13W	05/27/2009	11:30	124	16	MDH
BEC13W	06/02/2009	12:30	87	29	MVTL
BEC13W	06/03/2009	10:45	85	56	MDH
BEC13W	06/08/2009	14:15	97	24	MVTL
BEC13W	06/12/2009	14:00	573	123	MVTL
BEC13W	06/15/2009	11:45	449	124	MVTL
BEC13W	06/23/2009	11:15	268	80	MVTL
BEC13W	06/29/2009	11:00	219	77	MVTL
BEC13W	07/06/2009	12:00	110	27	MDH
BEC13W	07/08/2009	13:21	115	27	MVTL
BEC13W	07/14/2009	13:25	160	31	MVTL
BEC13W	07/16/2009	10:00	124	28	MVTL
BEC13W	07/28/2009	13:20	33	13	MVTL
BEC13W	08/03/2009	13:30	33	8.8	MDH
BEC13W	08/12/2009	10:20	15	15	MVTL
BEC13W	08/20/2009	11:10	20	13	MVTL
BEC13W	08/27/2009	11:30	17	6	MVTL
BEC13W	09/17/2009	11:05	10	27	MVTL
BEC13W	09/23/2009	13:00	9	26	MDH
BEC13W	10/02/2009	12:20	78	13	MVTL
BEC13W	10/07/2009	09:15	95	20	MVTL
BEC13W	10/22/2009	11:35	134	15	MVTL
BEC13W	10/26/2009	10:30	336	64	MVTL
BEC13W	10/28/2009	14:15	287	35	MVTL

Table 7.05: BEC34 total suspended solids results, 2008.

2008 Blue Earth River at Blue Earth CR 34 (BEC34) Total Suspended Solids					
Station	**Date**	**Time**	**15 Minute Flow** cfs	**TSS** mg/L	**Lab**
BEC34	4/4/2008	13:30	1,019	195	MSU
BEC34	4/11/2008	11:05	1,158	418	MSU
BEC34	4/15/2008	14:30	2,612	247	MSU
BEC34	4/27/2008	15:10	3,630	288	MSU
BEC34	5/4/2008	15:00	4,250	255	MSU
BEC34	5/11/2008	14:40	3,050	24	MSU
BEC34	5/21/2008	14:50	1,603	70	MSU
BEC34	5/31/2008	10:00	1,930	215	MSU
BEC34	6/2/2008	14:30	2,366	160	MSU
BEC34	6/7/2008	15:49	2,820	121	MSU
BEC34	6/14/2008	15:45	4,960	185	MSU
BEC34	6/21/2008	13:13	3,162	113	MSU
BEC34	6/30/2008	13:10	2,262	129	MSU
BEC34	7/9/2008	17:00	937	87	MSU
BEC34	7/22/2008	10:12	579	11	MSU
BEC34	8/2/2008	15:59	164	55	MSU
BEC34	8/10/2008	14:15	134	21	MSU
BEC34	8/28/2008	12:30	90	25	MSU
BEC34	9/17/2008	17:25	48	23	MSU
BEC34	10/17/2008	NA	41 *	10	MSU

* Instantaneous flow not available, Daily Average Flow value used | NA = data not available

Table 7.06: BEC34 total suspended solids results, 2009.

2009 Blue Earth River at Blue Earth CR 34 (BEC34) Total Suspended Solids					
Station	**Date**	**Time**	**15 Minute Flow** (cfs)	**TSS** (mg/L)	**Lab**
BEC34	03/25/2009	12:44	1,181	176	MSU
BEC34	04/07/2009	12:40	167	28	MSU
BEC34	04/19/2009	14:30	96	28	MSU
BEC34	04/28/2009	15:03	117	26	MSU
BEC34	05/08/2009	10:40	204	26	MSU
BEC34	05/17/2009	15:35	246	37	MSU
BEC34	05/30/2009	13:50	93	34	MSU
BEC34	06/10/2009	14:00	182	200	MSU
BEC34	06/22/2009	13:25	391	178	MSU
BEC34	07/06/2009	13:50	83	37	MSU
BEC34	07/18/2009	20:55	639	112	MSU
BEC34	07/29/2009	10:25	86	35	MSU
BEC34	08/12/2009	12:00	75	12	MSU
BEC34	09/03/2009	11:40	35	30	MSU
BEC34	09/25/2009	16:30	105	60	MSU
BEC34	10/08/2009	11:40	96	70	MSU
BEC34	10/23/2009	14:00	208	70	MSU

APPENDIX 2: Loss on Ignition Results

Table 7.07: Loss on Ignition results and percent inorganic vs. organic matter of Rapidan Reservoir river bottom sediment samples, at 550 degrees Celsius.

Transect	Sample ID	Weight Initial (g)	Weight Final (g)	% Solids	% Organics
Z	Z	10.0013	9.1943	91.93	8.07
	Z1	10.0027	9.3114	93.09	6.91
	Z2	10.0032	9.8929	98.90	1.10
	Z3	10.0009	9.8755	98.75	1.25
	Z4	10.0013	9.9239	99.23	0.77
	Z5	10.0013	9.8480	98.47	1.53
	Z6	10.0009	9.2494	92.49	7.51
A	A	10.0022	9.1530	91.51	8.49
	A2	10.0038	9.2370	92.33	7.67
	A3	10.0018	9.4144	94.13	5.87
	A5	10.0026	9.5085	95.06	4.94
	A6	10.0006	9.8339	98.33	1.67
K	K	10.0009	9.6987	96.98	3.02
	K11	10.0013	9.4011	94.00	6.00
	K2	10.0012	9.8743	98.73	1.27
	K3	10.0009	9.3450	93.44	6.56
B	B	10.0014	9.9304	99.29	0.71
	B1	10.0007	9.1240	91.23	8.77
	B2	10.0004	9.6698	96.69	3.31
	B3	10.0004	9.2692	92.69	7.31
	B4	10.0003	9.2215	92.21	7.79
	B5	10.0020	9.5302	95.28	4.72
	B6	10.0008	9.4107	94.10	5.90
	B7	10.0029	9.7186	97.16	2.84
C	C1	10.0017	9.8880	98.86	1.14
	C2	10.0002	9.9002	99.00	1.00
	C3	10.0026	9.4518	94.49	5.51
	C4	10.0017	9.3408	93.39	6.61
O	O	10.0004	9.8610	98.61	1.39
	O1	10.0013	9.9132	99.12	0.88
	O2a	10.0007	9.2683	92.68	7.32
	O2b	10.0020	9.7534	97.51	2.49
	O3	10.0007	9.4379	94.37	5.63
D	D	10.0010	9.9248	99.24	0.76
	D1	10.0013	9.8314	98.30	1.70
	D2	10.0012	9.8085	98.07	1.93
	D3	10.0015	9.2504	92.49	7.51
	D4	10.0007	9.8043	98.04	1.96
N	N	10.0027	9.3367	93.34	6.66
	N1	10.0003	9.8706	98.70	1.30
	N2	10.0015	9.9219	99.20	0.80
	N3	10.0020	9.9335	99.32	0.68
E	E	10.0011	9.2763	92.75	7.25
	E1	10.0014	9.8714	98.70	1.30
	E2	10.0021	9.8844	98.82	1.18
	E3	10.0014	9.4726	94.71	5.29
	E4	10.0007	9.7526	97.52	2.48
F	F	10.0007	9.9426	99.42	0.58
	F1	10.0011	9.8986	98.98	1.02
	F2	10.0016	9.9255	99.24	0.76
			Average	**96.22**	**3.78**

APPENDIX 3: Particle Size Sieve Weights

Table 7.08: Rapidan Reservoir sieve analyses weights for sediment samples.

Transect	Sample ID	Weight Initial	>12.7	>5.66	>1.4	>0.354	>0.180	>0.125	>0.063	<0.063	Loss	Total
		grams										
Z	Z	100.0	0.00	0.00	0.00	1.09	13.43	6.87	19.52	58.99	0.11	99.89
		% Mass	0.00	0.00	0.00	1.09	13.43	6.87	19.52	58.99	0.11	
	Z1	200.0	0.00	0.00	0.10	0.30	17.10	12.70	54.10	115.00	0.70	199.30
		% Mass	0.00	0.00	0.05	0.15	8.55	6.35	27.05	57.50	0.35	
	Z2	250.00	0.00	0.00	0.10	14.90	146.20	50.50	24.60	13.20	0.50	249.50
		% Mass	0.00	0.00	0.04	5.96	58.48	20.20	9.84	5.28	0.20	
	Z3	250.00	0.00	0.00	0.00	2.60	181.60	35.00	13.90	16.40	0.50	249.50
		% Mass	0.00	0.00	0.00	1.04	72.64	14.00	5.56	6.56	0.20	
	Z4 *	250.0	0.00	0.00	10.10	144.30	83.50	9.50	1.20	1.10	0.30	249.70
		% Mass	0.00	0.00	4.04	57.72	33.40	3.80	0.48	0.44	0.12	
	Z5 *	300.00	0.00	3.20	24.70	120.00	119.70	20.50	5.70	5.70	0.50	299.50
		% Mass	0.00	1.07	8.23	40.00	39.90	6.83	1.90	1.90	0.17	
	Z5 *	250.00	0.00	0.00	24.10	106.00	96.50	15.80	3.70	3.70	0.20	249.80
		% Mass	0.00	0.00	9.64	42.40	38.60	6.32	1.48	1.48	0.08	
	Z6	100.00	0.00	0.00	0.00	0.00	2.50	9.70	23.90	63.50	0.40	99.60
		% Mass	0.00	0.00	0.00	0.00	2.50	9.70	23.90	63.50	0.40	
A	A	250.0	0.00	0.00	0.10	2.10	35.40	13.50	26.30	172.60	0.00	250.00
		% Mass	0.00	0.00	0.04	0.84	14.16	5.40	10.52	69.04	0.00	
	A2	200.0	0.00	0.00	0.10	2.40	25.80	10.40	32.20	128.80	0.30	199.70
		% Mass	0.00	0.00	0.05	1.20	12.90	5.20	16.10	64.40	0.15	
	A3	250.0	0.00	0.00	0.10	0.20	8.30	17.10	112.70	110.70	0.90	249.10
		% Mass	0.00	0.00	0.04	0.08	3.32	6.84	45.08	44.28	0.36	
	A5	150.0	0.00	0.00	0.00	0.20	5.80	4.00	48.20	91.70	0.10	249.83
		% Mass	0.00	0.00	0.00	0.13	3.87	2.67	32.13	61.13	0.07	
	A6	250.0	0.00	2.40	13.90	64.90	137.20	13.90	7.20	9.50	1.00	249.00
		% Mass	0.00	0.96	5.56	25.96	54.88	5.56	2.88	3.80	0.40	
K	K	250.0	0.00	0.00	0.30	4.60	48.40	47.30	90.80	58.10	0.50	249.50
		% Mass	0.00	0.00	0.12	1.84	19.36	18.92	36.32	23.24	0.20	
	K11	100.00	0.00	0.00	0.00	0.30	4.40	5.30	16.30	73.40	0.30	99.70
		% Mass	0.00	0.00	0.00	0.30	4.40	5.30	16.30	73.40	0.30	
	K2	250.0	0.00	0.00	0.70	54.80	148.70	15.10	11.20	18.40	1.10	248.90
		% Mass	0.00	0.00	0.28	21.92	59.48	6.04	4.48	7.36	0.44	
	K3	100.0	0.00	0.00	0.00	0.30	1.80	3.20	18.70	75.70	0.30	99.70
		% Mass	0.00	0.00	0.00	0.30	1.80	3.20	18.70	75.70	0.30	
	K3	100.00	0.00	0.00	0.00	0.30	2.20	3.70	16.80	76.30	0.70	99.30
		% Mass	0.00	0.00	0.00	0.30	2.20	3.70	16.80	76.30	0.70	

* Settling tube analysis was not completed, not enough weight of fines.

K3 Sample IDs highlighted in red are sample duplicate results (Z5, K3, B7)

Table 7.08 continued: Rapidan Reservoir sieve analyses weights for sediment samples.

Transect	Sample ID	Weight Initial	>12.7	>5.66	>1.4	>0.354	>0.180	>0.125	>0.0625	<0.0625	Loss	Total
		grams										
B	B	300.0	77.50	31.90	20.20	69.30	75.10	9.40	9.50	6.30	0.80	299.20
		% Mass	25.83	10.63	6.73	23.10	25.03	3.13	3.17	2.10	0.27	
	B1	100.00	0.00	0.00	0.00	1.10	14.70	3.30	11.60	69.00	0.30	99.70
		% Mass	0.00	0.00	0.00	1.10	14.70	3.30	11.60	69.00	0.30	
	B2	250.0	0.00	0.00	0.30	0.90	16.00	85.00	104.20	43.60	0.00	250.00
		% Mass	0.00	0.00	0.12	0.36	6.40	34.00	41.68	17.44	0.00	
	B3	249.9	0.00	0.00	6.10	9.20	32.60	13.80	41.50	146.60	0.10	249.80
		% Mass	0.00	0.00	2.44	3.68	13.05	5.52	16.61	58.66	0.04	
	B4	249.9	0.00	0.00	0.10	2.30	30.30	15.90	53.50	147.50	0.30	249.60
		% Mass	0.00	0.00	0.04	0.92	12.12	6.36	21.41	59.02	0.12	
	B5	200.00	0.00	0.00	8.90	70.40	14.80	4.90	30.50	69.90	0.60	199.40
		% Mass	0.00	0.00	4.45	35.20	7.40	2.45	15.25	34.95	0.30	
	B6	250.0	0.00	0.00	0.10	2.70	10.80	15.20	103.50	117.60	0.10	249.90
		% Mass	0.00	0.00	0.04	1.08	4.32	6.08	41.40	47.04	0.04	
	B7	300.0	101.00	20.30	27.30	61.20	27.60	14.50	25.50	22.20	0.40	299.60
		% Mass	33.67	6.77	9.10	20.40	9.20	4.83	8.50	7.40	0.13	
	B7	300.00	96.80	33.20	31.50	61.40	24.30	12.50	22.70	17.10	0.50	299.50
		% Mass	32.27	11.07	10.50	20.47	8.10	4.17	7.57	5.70	0.17	
C	C1 *	250.00	0.00	3.00	24.50	196.60	23.20	0.80	0.50	1.30	0.10	249.90
		% Mass	0.00	1.20	9.80	78.64	9.28	0.32	0.20	0.52	0.04	
	C2 *	250.00	0.00	0.00	3.20	30.60	195.40	18.20	1.80	0.60	0.20	249.80
		% Mass	0.00	0.00	1.28	12.24	78.16	7.28	0.72	0.24	0.08	
	C3	100.00	0.00	0.00	0.00	0.40	10.00	6.70	21.90	60.70	0.30	99.70
		% Mass	0.00	0.00	0.00	0.40	10.00	6.70	21.90	60.70	0.30	
	C4	100.00	0.00	0.00	0.00	0.10	4.90	3.00	16.80	74.80	0.40	99.60
		% Mass	0.00	0.00	0.00	0.10	4.90	3.00	16.80	74.80	0.40	
O	O *	200.00	0.00	8.80	43.40	142.80	2.40	0.30	0.90	1.30	0.10	199.90
		% Mass	0.00	4.40	21.70	71.40	1.20	0.15	0.45	0.65	0.05	
	O1	250.0	0.00	0.00	0.00	1.00	162.60	55.20	19.10	11.60	0.50	249.50
		% Mass	0.00	0.00	0.00	0.40	65.04	22.08	7.64	4.64	0.20	
	O2a	100.00	0.00	0.00	0.00	1.50	8.60	4.50	21.00	63.80	0.60	99.40
		% Mass	0.00	0.00	0.00	1.50	8.60	4.50	21.00	63.80	0.60	
	O2b	100.00	0.00	0.00	0.00	0.00	4.50	11.10	57.00	27.00	0.40	99.60
		% Mass	0.00	0.00	0.00	0.00	4.50	11.10	57.00	27.00	0.40	
	O3	100.00	0.00	0.00	0.00	2.20	6.10	3.60	16.30	71.10	0.70	99.30
		% Mass	0.00	0.00	0.00	2.20	6.10	3.60	16.30	71.10	0.70	

* Settling tube analysis was not completed, not enough weight of fines.

K3 Sample IDs highlighted in red are sample duplicate results (Z5, K3, B7)

Table 7.08 continued: Rapidan Reservoir sieve analyses weights for sediment samples.

Transect	Sample ID	Weight Initial	>12.7	>5.66	>1.4	>0.354	>0.180	>0.125	>0.0625	<0.0625	Loss	Total
		grams										
D	D *	200.00	0.00	0.00	8.30	177.10	13.50	0.30	0.20	0.60	0.00	200.00
		% Mass	0.00	0.00	4.15	88.55	6.75	0.15	0.10	0.30	0.00	
	D1 *	200.00	0.00	0.00	6.70	92.40	90.50	7.80	1.50	0.90	0.20	199.80
		% Mass	0.00	0.00	3.35	46.20	45.25	3.90	0.75	0.45	0.10	
	D2 *	250.00	0.00	2.20	75.60	144.90	9.90	2.70	6.70	7.50	0.50	249.50
		% Mass	0.00	0.88	30.24	57.96	3.96	1.08	2.68	3.00	0.20	
	D3	100.0	0.00	0.00	0.10	7.20	22.30	7.30	15.00	48.00	0.10	99.90
		% Mass	0.00	0.00	0.10	7.20	22.30	7.30	15.00	48.00	0.10	
	D4	200.00	0.00	0.00	5.90	98.10	29.70	30.50	21.00	14.30	0.50	199.50
		% Mass	0.00	0.00	2.95	49.05	14.85	15.25	10.50	7.15	0.25	
N	N	100.00	0.00	0.00	0.00	0.60	6.80	10.90	12.00	69.50	0.20	99.80
		% Mass	0.00	0.00	0.00	0.60	6.80	10.90	12.00	69.50	0.20	
	N1 *	250.00	0.00	0.10	37.80	167.10	39.30	4.10	1.00	0.40	0.20	249.80
		% Mass	0.00	0.04	15.12	66.84	15.72	1.64	0.40	0.16	0.08	
	N2 *	250.00	0.00	0.40	22.60	190.40	34.20	1.70	0.50	0.20	0.00	250.00
		% Mass	0.00	0.16	9.04	76.16	13.68	0.68	0.20	0.08	0.00	
	N3 *	300.00	2.50	26.20	131.40	136.40	1.00	0.60	1.20	0.60	0.10	299.90
		% Mass	0.83	8.73	43.80	45.47	0.33	0.20	0.40	0.20	0.03	
E	E	100.00	0.00	0.00	0.00	1.90	9.60	5.60	16.80	65.80	0.30	99.70
		% Mass	0.00	0.00	0.00	1.90	9.60	5.60	16.80	65.80	0.30	
	E1	350.0	0.00	1.00	38.00	251.80	19.80	19.00	17.10	2.20	1.10	348.90
		% Mass	0.00	0.29	10.86	71.94	5.66	5.43	4.89	0.63	0.31	
	E2 *	350.0	6.30	10.50	126.70	196.60	4.60	0.40	1.30	2.30	1.30	348.70
		% Mass	1.80	3.00	36.20	56.17	1.31	0.11	0.37	0.66	0.37	
	E3	200.0	0.00	7.60	7.20	17.10	19.70	10.40	43.40	94.40	0.20	199.80
		% Mass	0.00	3.80	3.60	8.55	9.85	5.20	21.70	47.20	0.10	
	E4	200.00	0.00	0.00	31.70	84.70	5.50	2.80	16.70	57.70	0.90	199.10
		% Mass	0.00	0.00	15.85	42.35	2.75	1.40	8.35	28.85	0.45	
F	F *	250.00	0.00	10.90	60.70	129.90	42.80	3.80	0.80	0.80	0.30	249.70
		% Mass	0.00	4.36	24.28	51.96	17.12	1.52	0.32	0.32	0.12	
	F1 *	250.00	0.00	0.00	2.60	71.10	162.90	12.30	0.80	0.20	0.10	249.90
		% Mass	0.00	0.00	1.04	28.44	65.16	4.92	0.32	0.08	0.04	
	F2 *	250.00	0.00	2.40	9.00	50.00	154.10	26.60	6.40	1.20	0.30	249.70
		% Mass	0.00	0.96	3.60	20.00	61.64	10.64	2.56	0.48	0.12	

* Settling tube analysis was not completed, not enough weight of fines.

K3 Sample IDs highlighted in red are sample duplicate results (Z5, K3, B7)

APPENDIX 4: PARTICLE SIZE ANALYSIS SETTLING TUBE WEIGHTS

Table 7.09: Transect Z settling tube weights and analyses.

Sample ID	Beaker #	Representative Size Fraction (mm)	Original Sample Weight -- all size fractions (g)	Weight of FINES (g)	Weight of FINES per representative size fraction (g)	% of Original Sample Weight
Z	1	1/16	100.00	58.99	11.139	11.14%
	2	1/32			13.110	13.11%
	3	1/64			10.971	10.97%
	4	1/128			9.121	9.12%
	5	1/256			5.636	5.64%
	6	1/512			3.509	3.51%
	7	1/1024			1.033	1.03%
	8	1/2048			4.471	4.47%
Z1	1	1/16	200.00	115.00	32.395	16.20%
	2	1/32			32.988	16.49%
	3	1/64			19.472	9.74%
	4	1/128			14.456	7.23%
	5	1/256			7.586	3.79%
	6	1/512			4.300	2.15%
	7	1/1024			0.593	0.30%
	8	1/2048			3.210	1.61%
Z2	1	1/16	250.00	13.20	4.351	1.74%
	2	1/32			3.737	1.49%
	3	1/64			2.092	0.84%
	4	1/128			1.376	0.55%
	5	1/256			0.710	0.28%
	6	1/512			0.935	0.37%
	7	1/1024			0.000	0.00%
	8	1/2048			0.000	0.00%
Z3	1	1/16	250.00	16.40	4.381	1.75%
	2	1/32			4.710	1.88%
	3	1/64			3.107	1.24%
	4	1/128			1.924	0.77%
	5	1/256			0.965	0.39%
	6	1/512			1.312	0.52%
	7	1/1024			0.000	0.00%
	8	1/2048			0.000	0.00%
Z6	1	1/16	100.00	63.50	18.375	18.38%
	2	1/32			23.171	23.17%
	3	1/64			8.694	8.69%
	4	1/128			5.268	5.27%
	5	1/256			3.325	3.32%
	6	1/512			4.667	4.67%
	7	1/1024			0.000	0.00%
	8	1/2048			0.000	0.00%

Table 7.10: Transect A settling tube weights and analyses.

Sample ID	Beaker #	Representative Size Fraction (mm)	Original Sample Weight -- all size fractions (g)	Weight of FINES (g)	Weight of FINES per representative size fraction (g)	% of Original Sample Weight
A	1	1/16	250.00	172.60	22.355	8.94%
	2	1/32			60.980	24.39%
	3	1/64			41.476	16.59%
	4	1/128			20.209	8.08%
	5	1/256			11.594	4.64%
	6	1/512			6.950	2.78%
	7	1/1024			0.673	0.27%
	8	1/2048			8.363	3.35%
A2	1	1/16	200.00	128.80	22.317	11.16%
	2	1/32			60.381	30.19%
	3	1/64			13.856	6.93%
	4	1/128			14.750	7.38%
	5	1/256			7.030	3.52%
	6	1/512			4.755	2.38%
	7	1/1024			0.383	0.19%
	8	1/2048			5.327	2.66%
A3	1	1/16	250.00	110.70	45.780	18.31%
	2	1/32			39.336	15.73%
	3	1/64			11.958	4.78%
	4	1/128			6.893	2.76%
	5	1/256			4.681	1.87%
	6	1/512			1.795	0.72%
	7	1/1024			0.256	0.10%
	8	1/2048			0.000	0.00%
A5	1	1/16	150.00	91.70	40.471	26.98%
	2	1/32			25.645	17.10%
	3	1/64			12.161	8.11%
	4	1/128			6.521	4.35%
	5	1/256			4.412	2.94%
	6	1/512			1.381	0.92%
	7	1/1024			0.671	0.45%
	8	1/2048			0.438	0.29%
A6	1	1/16	250.00	9.50	3.893	1.56%
	2	1/32			2.457	0.98%
	3	1/64			1.445	0.58%
	4	1/128			0.973	0.39%
	5	1/256			0.333	0.13%
	6	1/512			0.218	0.09%
	7	1/1024			0.091	0.04%
	8	1/2048			0.089	0.04%

Table 7.11: Transect K settling tube weights and analyses.

Sample ID	Beaker #	Representative Size Fraction (mm)	Original Sample Weight -- all size fractions (g)	Weight of FINES (g)	Weight of FINES per representative size fraction (g)	% of Original Sample Weight
K	1	1/16	250.00	58.10	29.726	11.89%
	2	1/32			11.023	4.41%
	3	1/64			7.094	2.84%
	4	1/128			3.360	1.34%
	5	1/256			3.538	1.42%
	6	1/512			1.049	0.42%
	7	1/1024			0.764	0.31%
	8	1/2048			1.546	0.62%
K2	1	1/16	250.00	18.40	6.408	2.56%
	2	1/32			4.367	1.75%
	3	1/64			3.195	1.28%
	4	1/128			1.392	0.56%
	5	1/256			1.561	0.62%
	6	1/512			0.337	0.13%
	7	1/1024			0.393	0.16%
	8	1/2048			0.746	0.30%
K3	1	1/16	100.00	75.70	27.882	27.88%
	2	1/32			27.973	27.97%
	3	1/64			12.068	12.07%
	4	1/128			5.543	5.54%
	5	1/256			2.069	2.07%
	6	1/512			0.165	0.16%
	7	1/1024			0.000	0.00%
	8	1/2048			0.000	0.00%
K11	1	1/16	100.00	73.40	22.499	22.50%
	2	1/32			18.505	18.50%
	3	1/64			11.785	11.79%
	4	1/128			8.518	8.52%
	5	1/256			4.312	4.31%
	6	1/512			3.161	3.16%
	7	1/1024			0.952	0.95%
	8	1/2048			3.667	3.67%

Table 7.12: Transect B settling tube weights and analyses.

Sample ID	Beaker #	Representative Size Fraction (mm)	Original Sample Weight -- all size fractions (g)	Weight of FINES (g)	Weight of FINES per representative size fraction (g)	% of Original Sample Weight
B	1	1/16	300.00	6.30	2.566	0.86%
	2	1/32			2.753	0.92%
	3	1/64			0.654	0.22%
	4	1/128			0.326	0.11%
	5	1/256			0.000	0.00%
	6	1/512			0.000	0.00%
	7	1/1024			0.000	0.00%
	8	1/2048			0.000	0.00%
B1	1	1/16	100.00	69.00	9.048	9.05%
	2	1/32			30.019	30.02%
	3	1/64			9.377	9.38%
	4	1/128			5.140	5.14%
	5	1/256			4.495	4.49%
	6	1/512			3.732	3.73%
	7	1/1024			1.713	1.71%
	8	1/2048			5.476	5.48%
B2	1	1/16	250.00	43.60	19.707	7.88%
	2	1/32			12.570	5.03%
	3	1/64			4.978	1.99%
	4	1/128			3.705	1.48%
	5	1/256			1.000	0.40%
	6	1/512			1.639	0.66%
	7	1/1024			0.000	0.00%
	8	1/2048			0.000	0.00%
B3	1	1/16	249.90	146.60	48.137	19.26%
	2	1/32			30.261	12.11%
	3	1/64			28.742	11.50%
	4	1/128			16.416	6.57%
	5	1/256			6.543	2.62%
	6	1/512			2.921	1.17%
	7	1/1024			1.227	0.49%
	8	1/2048			12.354	4.94%
B4	1	1/16	249.90	147.50	39.239	15.70%
	2	1/32			28.429	11.38%
	3	1/64			25.372	10.15%
	4	1/128			17.424	6.97%
	5	1/256			5.530	2.21%
	6	1/512			6.447	2.58%
	7	1/1024			1.362	0.54%
	8	1/2048			23.697	9.48%

Table 7.12 continued: Transect B settling tube weights and analyses.

Sample ID	Beaker #	Representative Size Fraction (mm)	Original Sample Weight -- all size fractions (g)	Weight of FINES (g)	Weight of FINES per representative size fraction (g)	% of Original Sample Weight
B5	1	1/16	200.00	69.90	25.269	12.63%
	2	1/32			16.168	8.08%
	3	1/64			10.728	5.36%
	4	1/128			7.067	3.53%
	5	1/256			3.775	1.89%
	6	1/512			2.923	1.46%
	7	1/1024			0.750	0.37%
	8	1/2048			3.219	1.61%
B6	1	1/16	250.00	117.60	54.048	21.62%
	2	1/32			20.497	8.20%
	3	1/64			10.736	4.29%
	4	1/128			7.747	3.10%
	5	1/256			6.527	2.61%
	6	1/512			3.935	1.57%
	7	1/1024			2.227	0.89%
	8	1/2048			11.883	4.75%
B7	1	1/16	300.00	22.20	10.650	3.55%
	2	1/32			4.442	1.48%
	3	1/64			2.695	0.90%
	4	1/128			1.747	0.58%
	5	1/256			1.515	0.50%
	6	1/512			0.374	0.12%
	7	1/1024			0.245	0.08%
	8	1/2048			0.533	0.18%
B7 QA/QC	1	1/16	300.00	17.10	6.555	2.18%
	2	1/32			4.235	1.41%
	3	1/64			1.705	0.57%
	4	1/128			1.381	0.46%
	5	1/256			1.047	0.35%
	6	1/512			2.178	0.73%
	7	1/1024			0.000	0.00%
	8	1/2048			0.000	0.00%

Table 7.13: Transect C settling tube weights and analyses.

Sample ID	Beaker #	Representative Size Fraction (mm)	Original Sample Weight -- all size fractions (g)	Weight of FINES (g)	Weight of FINES per representative size fraction (g)	% of Original Sample Weight
C3	1	1/16	100.00	60.70	21.683	21.68%
	2	1/32			21.418	21.42%
	3	1/64			7.459	7.46%
	4	1/128			4.110	4.11%
	5	1/256			2.953	2.95%
	6	1/512			1.631	1.63%
	7	1/1024			0.143	0.14%
	8	1/2048			1.304	1.30%
C4	1	1/16	100.00	74.80	18.801	18.80%
	2	1/32			17.990	17.99%
	3	1/64			17.788	17.79%
	4	1/128			9.643	9.64%
	5	1/256			4.160	4.16%
	6	1/512			3.052	3.05%
	7	1/1024			1.256	1.26%
	8	1/2048			2.109	2.11%

Table 7.14: Transect O settling tube weights and analyses.

Sample ID	Beaker #	Representative Size Fraction (mm)	Original Sample Weight -- all size fractions (g)	Weight of FINES (g)	Weight of FINES per representative size fraction (g)	% of Original Sample Weight
O1	1	1/16	250.00	11.60	6.625	2.65%
	2	1/32			3.002	1.20%
	3	1/64			1.155	0.46%
	4	1/128			0.773	0.31%
	5	1/256			0.045	0.02%
	6	1/512			0.000	0.00%
	7	1/1024			0.000	0.00%
	8	1/2048			0.000	0.00%
O2a	1	1/16	100.00	63.80	22.954	22.95%
	2	1/32			24.096	24.10%
	3	1/64			8.601	8.60%
	4	1/128			4.024	4.02%
	5	1/256			2.387	2.39%
	6	1/512			0.911	0.91%
	7	1/1024			0.288	0.29%
	8	1/2048			0.540	0.54%
O2b	1	1/16	100.00	27.00	16.805	16.81%
	2	1/32			5.117	5.12%
	3	1/64			2.293	2.29%
	4	1/128			1.471	1.47%
	5	1/256			0.590	0.59%
	6	1/512			0.568	0.57%
	7	1/1024			0.156	0.16%
	8	1/2048			0.000	0.00%
O3	1	1/16	100.00	71.10	22.791	22.79%
	2	1/32			24.247	24.25%
	3	1/64			12.472	12.47%
	4	1/128			5.318	5.32%
	5	1/256			3.001	3.00%
	6	1/512			1.887	1.89%
	7	1/1024			0.595	0.60%
	8	1/2048			0.790	0.79%

Table 7.15: Transect D settling tube weights and analyses.

Sample ID	Beaker #	Representative Size Fraction (mm)	Original Sample Weight -- all size fractions (g)	Weight of FINES (g)	Weight of FINES per representative size fraction (g)	% of Original Sample Weight
D3	1	1/16	100.00	48.00	9.150	9.15%
	2	1/32			18.048	18.05%
	3	1/64			6.984	6.98%
	4	1/128			4.638	4.64%
	5	1/256			3.523	3.52%
	6	1/512			2.544	2.54%
	7	1/1024			1.007	1.01%
	8	1/2048			2.106	2.11%
D4	1	1/16	200.00	14.30	4.688	2.34%
	2	1/32			5.405	2.70%
	3	1/64			2.604	1.30%
	4	1/128			1.549	0.77%
	5	1/256			0.016	0.01%
	6	1/512			0.070	0.03%
	7	1/1024			0.000	0.00%
	8	1/2048			0.000	0.00%

Table 7.16: Transect N settling tube weights and analyses.

Sample ID	Beaker #	Representative Size Fraction (mm)	Original Sample Weight -- all size fractions (g)	Weight of FINES (g)	Weight of FINES per representative size fraction (g)	% of Original Sample Weight
N	1	1/16	100.00	69.50	10.390	10.39%
	2	1/32			28.031	28.03%
	3	1/64			12.061	12.06%
	4	1/128			7.035	7.03%
	5	1/256			4.089	4.09%
	6	1/512			3.151	3.15%
	7	1/1024			1.395	1.39%
	8	1/2048			3.350	3.35%

Table 7.17: Transect E settling tube weights and analyses.

Sample ID	Beaker #	Representative Size Fraction (mm)	Original Sample Weight -- all size fractions (g)	Weight of FINES (g)	Weight of FINES per representative size fraction (g)	% of Original Sample Weight
E1	1	1/16	350.00	2.20	0.969	0.28%
	2	1/32			1.032	0.29%
	3	1/64			0.199	0.06%
	4	1/128			0.000	0.00%
	5	1/256			0.000	0.00%
	6	1/512			0.000	0.00%
	7	1/1024			0.000	0.00%
	8	1/2048			0.000	0.00%
E3	1	1/16	200.00	94.40	35.793	17.90%
	2	1/32			27.529	13.76%
	3	1/64			14.915	7.46%
	4	1/128			7.884	3.94%
	5	1/256			4.114	2.06%
	6	1/512			2.102	1.05%
	7	1/1024			0.489	0.24%
	8	1/2048			1.574	0.79%
E	1	1/16	100.00	65.80	10.652	10.65%
	2	1/32			23.082	23.08%
	3	1/64			12.066	12.07%
	4	1/128			8.044	8.04%
	5	1/256			5.968	5.97%
	6	1/512			2.530	2.53%
	7	1/1024			0.999	1.00%
	8	1/2048			2.457	2.46%
E4	1	1/16	200.00	57.70	9.474	4.74%
	2	1/32			31.516	15.76%
	3	1/64			9.291	4.65%
	4	1/128			4.355	2.18%
	5	1/256			1.465	0.73%
	6	1/512			1.242	0.62%
	7	1/1024			0.356	0.18%
	8	1/2048			0.000	0.00%

APPENDIX 5: 2008-09 PERCENTILES

Table 7.18: Rapidan Reservoir Phi Percentiles (2008-09).

RAPIDAN RESERVOIR SEDIMENT SAMPLE PERCENTILES							
SAMPLE ID	Φ 5	Φ 16	Φ 25	Φ 50	Φ 75	Φ 84	Φ 95
A	0.740	2.005	2.986	3.568	4.560	5.194	6.817
A2	0.748	2.066	2.968	3.551	4.547	5.187	6.838
A3	1.998	2.414	2.875	3.517	4.520	5.166	6.860
A5	2.011	2.963	3.126	3.708	4.701	5.337	6.967
A6	-2.234	-1.136	-0.528	0.596	1.211	1.652	3.238
B	-4.034	-3.906	-3.689	-1.193	0.618	1.106	2.754
B1	0.552	1.929	3.004	3.589	4.589	5.233	6.913
B2	1.240	2.089	2.246	2.801	3.786	4.425	6.070
B3	-0.590	1.444	2.445	3.461	4.454	5.091	6.725
B4	0.838	2.109	2.847	3.522	4.517	5.156	6.803
B5	-1.782	-1.393	-0.996	2.295	3.846	4.494	6.197
B6	1.635	2.357	2.831	3.502	4.495	5.132	6.764
B7	-4.735	-4.412	-4.080	-1.750	1.030	2.472	4.348
B7 QAQC	-4.301	-4.077	-3.865	-2.445	0.291	2.111	4.088
C1	-2.726	-1.669	-1.523	-1.146	-0.589	-0.223	0.877
C2	-1.337	0.218	0.416	0.762	1.220	1.513	2.222
C3	1.032	2.304	2.996	3.581	4.581	5.225	6.904
C4	1.872	3.019	3.183	3.768	4.770	5.416	7.108
D	-1.769	-1.562	-1.444	-1.118	-0.662	-0.387	0.553
D1	-1.652	-1.199	-0.885	0.182	0.875	1.178	1.925
D2	-2.943	-2.516	-2.133	-1.354	-0.744	-0.347	2.954
D3	-0.619	0.841	1.471	3.167	4.163	4.803	6.458
D4	-1.694	-1.354	-1.076	0.046	2.282	2.812	4.482
E	0.824	2.260	2.999	3.584	4.584	5.228	6.908
E1	-2.660	-1.657	-1.496	-1.089	-0.427	0.350	2.779
E2	-3.175	-2.736	-2.442	-1.559	-0.999	-0.742	-0.189
E3	-2.907	0.189	1.721	3.285	4.281	4.921	6.572
E4	-2.742	-1.808	-1.477	-0.649	3.427	4.082	5.826
F	-3.141	-2.556	-2.060	-1.117	-0.141	0.409	1.395
F1	-1.488	-0.879	-0.247	0.601	1.065	1.298	1.940
F2	-1.738	-0.836	0.148	0.684	1.367	1.769	2.556
K	0.571	1.410	2.026	2.824	3.869	4.514	6.196
K2	-1.385	-0.542	0.251	0.762	1.469	2.139	4.107
K3	2.241	3.057	3.221	3.805	4.804	5.446	7.116
K3 QAQC	2.192	3.050	3.214	3.803	4.813	5.469	7.222
K3 QAQC1	2.193	3.050	3.215	3.803	4.813	5.469	7.223
K11	1.963	2.988	3.152	3.736	4.736	5.379	7.052
N	1.246	2.452	3.015	3.599	4.596	5.237	6.895
N1	-2.761	-1.796	-1.634	-1.089	-0.205	0.318	1.409
N2	-2.546	-1.658	-1.518	-1.086	-0.371	0.093	1.111
N3	-3.447	-2.960	-2.705	-1.945	-1.174	-0.885	-0.367

Table 7.18 continued: Rapidan Reservoir Phi Percentiles (2008-09).

RAPIDAN RESERVOIR SEDIMENT SAMPLE PERCENTILES							
SAMPLE ID	Φ 5	Φ 16	Φ 25	Φ 50	Φ 75	Φ 84	Φ 95
O	-3.145	-2.512	-1.910	-1.332	-0.893	-0.673	-0.195
O1	0.394	0.655	0.839	1.424	2.214	2.595	3.891
O2a	0.948	2.452	3.050	3.638	4.646	5.300	7.040
O2b	1.943	2.249	2.538	3.332	4.337	4.986	6.695
O3	1.018	2.956	3.121	3.710	4.721	5.378	7.136
Z	0.775	2.022	2.811	3.298	4.039	4.438	5.150
Z1	1.171	2.317	2.962	3.548	4.550	5.196	6.887
Z2	-0.355	0.546	0.767	1.410	2.272	2.695	4.198
Z3	0.222	0.415	0.564	1.090	1.951	2.473	3.999
Z4	-1.716	-1.312	-1.059	-0.294	0.669	1.038	1.864
Z5	-2.582	-1.393	-1.018	0.185	1.023	1.495	2.577
Z5 QAQC	-2.526	-1.425	-1.064	0.061	0.937	1.382	2.422
Z6	2.058	2.692	3.062	3.648	4.651	5.298	6.995

APPENDIX 6: 1985 PERCENTILES

Table 7.19: Rapidan Reservoir Phi Percentiles (1985).

RAPIDAN RESERVOIR SEDIMENT SAMPLE PERCENTILES							
SAMPLE ID	Φ 5	Φ 16	Φ 25	Φ 50	Φ 75	Φ 84	Φ 95
P1C	-0.801	-0.165	0.388	4.595	6.593	7.617	9.744
P2C	0.687	1.654	2.168	3.933	6.190	7.063	9.424
P3C	-0.674	0.339	0.962	4.169	6.393	7.472	9.679
P4C	0.321	1.103	1.962	4.831	6.664	7.668	9.766
P5C	0.746	1.850	2.691	4.811	7.146	8.316	10.070
P6C	-0.389	0.804	2.633	4.622	6.540	7.648	9.764
P7C	2.003	3.134	3.656	5.053	8.803	9.690	10.622
P8C	3.070	3.985	4.539	5.810	7.106	8.126	9.974
P9C	1.523	2.031	2.342	3.408	5.680	7.154	9.612
P10C	3.719	4.829	5.427	6.707	8.508	9.323	10.438
P11C	3.039	3.948	4.547	6.114	8.003	8.955	10.304
P1D	1.219	1.715	1.938	2.439	3.086	3.515	4.422
P2D	2.579	3.503	3.940	5.400	8.066	9.095	10.393
P3D	3.278	4.110	4.707	6.319	8.270	9.163	10.386
P4D	2.565	3.676	4.208	5.711	7.602	8.640	10.181
P5D	3.171	3.855	4.337	5.716	7.440	8.491	10.118
P6D	1.339	1.962	2.295	3.719	7.093	8.433	10.171
P7D	2.302	3.367	3.830	5.098	6.879	8.001	9.919
P8D	2.543	3.489	3.913	5.899	9.469	10.087	10.738
P9D	3.746	4.909	5.571	7.189	9.000	9.698	10.583
P10D	-0.995	0.252	0.748	1.708	2.636	3.156	7.821
P11D	3.311	4.084	4.609	5.902	7.379	8.420	10.088
P1E	1.748	2.634	3.270	5.025	7.282	8.428	10.113
P2E	-0.628	0.092	0.518	1.572	7.501	9.250	10.532
P3E	-0.052	2.791	3.462	4.458	6.594	7.972	9.965
P4E	2.815	3.684	4.185	5.761	7.933	8.926	10.304
P5E	0.991	1.579	1.835	2.358	3.003	3.624	6.828
P6E	3.003	3.645	4.015	5.233	7.541	8.645	10.203
P7E	1.641	2.436	3.004	4.626	6.411	7.342	9.599
P8E	3.214	3.920	4.426	5.976	8.013	8.974	10.316
P9E	1.132	1.682	1.920	2.450	3.261	4.334	7.225
P10E	3.107	3.929	4.468	5.845	7.416	8.457	10.103
P11E	-1.388	-0.266	0.211	1.048	1.898	2.350	4.020
P1F	3.348	4.113	4.617	5.757	6.821	7.652	9.778
P2F	1.330	1.904	2.199	3.131	5.950	7.687	9.932
P3F	2.711	3.578	4.001	5.311	7.431	8.531	10.148
P4F	1.460	1.941	2.205	3.056	5.614	6.507	8.895
P5F	3.104	3.640	3.969	4.953	6.554	7.610	9.743
P6F	2.629	3.244	3.489	4.001	4.515	4.769	5.575

Table 7.19 continued: Rapidan Reservoir Phi Percentiles (1985).

RAPIDAN RESERVOIR SEDIMENT SAMPLE PERCENTILES							
SAMPLE ID	Φ 5	Φ 16	Φ 25	Φ 50	Φ 75	Φ 84	Φ 95
P7F	2.420	3.615	4.251	5.693	7.094	8.131	9.973
P8F	2.538	3.587	4.171	5.677	7.344	8.398	10.080
P9F	1.974	3.269	4.502	6.014	7.455	8.495	10.119
P10F	1.333	2.328	3.044	5.301	6.788	7.776	9.820
P11F	1.270	1.691	1.882	2.298	2.741	2.988	5.176
P3G	3.118	3.900	4.388	5.555	6.589	7.179	9.463
P4G	2.935	3.729	4.221	5.667	7.566	8.613	10.171
P5G	4.414	5.433	5.866	7.078	8.791	9.526	10.511
P6G	3.123	3.755	4.179	5.289	6.380	6.847	8.872
P7G	2.074	6.574	8.062	9.423	10.302	10.571	10.872
P8G	1.177	2.374	3.329	5.655	7.155	8.220	10.008
P10G	3.127	3.909	4.430	5.782	7.296	8.340	10.056
P11G	1.734	2.928	3.558	5.083	6.787	7.829	9.841
P12G	-1.299	0.553	1.063	2.325	5.405	6.431	8.918
P1H	0.004	0.950	1.372	2.141	2.868	3.502	6.904
P2H	3.253	4.013	4.541	5.927	7.579	8.602	10.161
P3H	1.698	2.459	2.989	4.399	6.301	7.473	9.691
P4H	3.030	3.808	4.331	5.802	7.620	8.647	10.182
P5H	3.165	3.796	4.228	5.543	7.322	8.402	10.083
P6H	0.494	1.027	1.431	3.656	5.885	8.795	10.425
P7H	0.347	0.925	1.271	3.898	5.990	6.942	9.364
P8H	1.987	3.749	4.369	5.932	7.749	8.752	10.223
P9H	2.901	3.740	4.246	5.842	8.004	8.979	10.324
P10H	2.567	3.591	4.160	5.709	7.554	8.595	10.163
P11H	-1.506	0.057	0.557	1.341	2.659	4.172	6.477
P12H	0.282	0.837	1.126	2.063	4.779	6.193	8.820
P1I	3.145	3.700	4.049	5.257	7.727	8.812	10.277
P2I	2.813	3.586	3.999	5.253	7.204	8.339	10.099
P3I	2.957	3.707	4.159	5.651	7.874	8.887	10.291
P4I	3.311	4.178	4.845	6.861	8.921	9.667	10.582
P5I	3.373	4.205	4.777	6.156	7.893	8.858	10.261
P6I	1.262	3.530	4.156	5.821	7.801	8.807	10.250
P7I	2.396	3.356	3.784	4.905	6.280	6.986	9.350
P8I	0.846	2.043	3.156	5.030	7.117	8.252	10.032
P9I	3.001	3.667	4.064	5.313	7.282	8.393	10.085
P10I	1.688	2.561	3.174	4.807	6.592	7.594	9.731
P11I	2.684	3.610	4.111	5.575	7.514	8.574	10.157
P12I	0.563	1.324	1.936	3.627	5.830	9.106	10.509
P1J	1.875	3.051	3.757	5.578	7.586	8.637	10.185
P2J	3.029	3.694	4.104	5.396	7.352	8.447	10.107
P3J	2.219	3.297	3.938	5.626	7.524	8.573	10.156
P4J	1.199	1.733	1.974	2.537	3.610	4.993	8.546
P5J	1.118	1.842	2.206	3.272	4.949	5.961	8.516
P6J	2.047	3.088	3.661	5.143	7.200	8.334	10.065
P7J	-2.587	-1.835	-1.158	0.808	5.730	6.721	9.223

Table 7.19 continued: Rapidan Reservoir Phi Percentiles (1985).

RAPIDAN RESERVOIR SEDIMENT SAMPLE PERCENTILES							
SAMPLE ID	Φ 5	Φ 16	Φ 25	Φ 50	Φ 75	Φ 84	Φ 95
P8J	1.283	2.123	2.640	3.969	5.500	6.359	8.828
P1K	0.155	0.689	0.921	1.652	4.258	5.496	8.488
P2K	0.952	1.683	2.043	2.996	4.605	5.866	8.907
P3K	3.442	4.328	4.929	6.301	8.090	9.010	10.321
P4K	3.017	3.709	4.140	5.483	7.447	8.525	10.138
P1L	2.054	3.006	3.521	4.723	6.463	7.544	9.713
P2L	1.181	1.884	2.223	3.308	6.062	7.796	9.981
P3L	0.478	0.979	1.281	1.981	2.669	3.019	5.459
P4L	1.859	3.830	4.458	5.963	7.705	8.712	10.206
P5L	1.661	2.331	2.840	4.914	7.933	9.037	10.387
P6L	2.197	3.400	4.032	5.689	7.576	8.615	10.172
P7L	0.910	1.592	1.921	2.687	4.740	6.008	8.602
P1M	3.051	3.868	4.426	5.952	7.784	8.778	10.234
P2M	-1.100	-0.562	-0.229	0.726	3.199	5.291	7.996
P3M	1.651	2.287	2.749	4.291	7.491	8.801	10.329
P4M	2.555	3.457	3.862	5.014	6.941	8.102	9.967
P5M	2.929	3.574	3.942	4.977	6.281	6.952	9.316
P1N	1.700	2.354	2.891	5.439	7.462	8.544	10.149
P2N	1.505	2.001	2.291	3.655	6.354	7.220	9.531
P3N	1.354	1.841	2.084	2.721	4.952	6.496	9.243
P1O	1.901	2.884	3.489	4.989	7.162	8.322	10.067
P2O	2.375	4.041	4.701	6.067	7.686	8.691	10.195
P3O	-0.722	3.017	3.821	5.658	7.792	8.816	10.261
P1P	0.467	2.575	3.500	4.847	7.237	8.427	10.126
P2P	-1.026	-0.612	-0.353	0.333	1.288	3.443	6.615
P3P	-1.092	1.777	2.245	3.667	6.189	7.561	9.776
P1Q	-0.691	0.155	0.908	3.799	5.461	6.483	9.068
P2Q	-0.630	0.057	0.441	1.196	2.103	2.617	6.304
P3Q	1.276	1.845	2.122	2.903	5.257	7.618	10.035
P1R	-3.253	0.723	1.509	3.323	4.942	6.709	9.647
P2R	-1.256	-0.473	-0.068	0.717	1.355	1.856	6.408
P3R	3.277	4.056	4.598	6.008	7.721	8.722	10.209
P1S	2.582	3.596	4.175	5.787	7.767	8.779	10.239
P2S	0.479	1.494	1.848	2.554	4.204	5.728	8.619
P3S	0.263	0.717	0.930	1.499	2.266	2.689	5.999
P1T	2.002	3.242	3.959	5.574	7.109	8.165	9.985
P2T	3.193	3.850	4.309	5.764	7.792	8.802	10.249
P3T	3.159	3.842	4.319	5.667	7.292	8.348	10.060
P1U	0.456	1.567	2.198	3.927	6.107	7.327	9.632
P2U	-0.948	-0.321	0.022	0.735	1.340	1.743	5.214
P3U	0.917	2.710	3.672	5.404	7.103	8.176	9.990
P1V	-4.935	-3.880	-3.017	-0.633	1.028	1.527	4.010
P3V	-2.045	-1.595	-1.220	-0.146	1.501	2.195	3.500

Table 7.19 continued: Rapidan Reservoir Phi Percentiles (1985).

RAPIDAN RESERVOIR SEDIMENT SAMPLE PERCENTILES							
SAMPLE ID	Φ 5	Φ 16	Φ 25	Φ 50	Φ 75	Φ 84	Φ 95
P1W	-0.904	-0.261	0.087	0.799	1.408	1.777	2.674
P2W	-2.897	-2.126	-1.522	-0.395	0.564	0.962	1.731
P3W	-1.505	-0.203	0.330	1.276	2.486	3.552	7.650

APPENDIX 7: SITE PHOTOS

Figure 7.1: Looking upstream to Rapidan Dam from BEC9.
Photo by author, 2007

Figure 7.2: USGS gauging station at BEC9.
Photo by author, 2007

Figure 7.3: Looking downstream at BEC13 on the Watonwan River.
Photo by author, 2007.

Figure 7.4: Looking downstream at BEC34 on the Blue Earth River.
Photo by author, 2007